Expanding the Scope of Phenanthroline-Based Copper(I) Complexes in Photoredox Catalysis

by
Thomas P. Nicholls, BSc (Hons)
School of Natural Sciences – Chemistry

Submitted in fulfilment of the requirements for the Doctor of Philosophy
University of Tasmania
October 2018

This thesis contains no material which has been accepted for a degree or diploma by the University or any other institution, except by way of background information and duly acknowledged in the thesis, and to the best of my knowledge and belief no material previously published or written by another person except where due acknowledgement is made in the text of the thesis, nor does the thesis contain any material that infringes copyright.

Thomas P. Nicholls

12 October 2018

Acknowledgement

Many people need to be thanked for all the help I received during my PhD candidature. First of all, to my supervisors Dr. Alex Bissember and Assoc. Prof. Michael Gardiner. I owe a lot to both for leading and mentoring me throughout. I have gained a lot throughout this experience and this is largely attributed to their depth of experience and capacity to impart knowledge. To all the other PhD and Honours students as well as other academics and postdocs within the synthesis group for all their help in many aspects of research, coursework, presentations and companionship. Special thanks to Assoc. Prof. Max Massi for allowing me to visit his laboratory at Curtin University and collect valuable data that was essential for my research project. And finally, to my friends and family for their unconditional love and support.

Publications and Presentations

The following list details the publications[1] and presentations that have resulted from research performed during the candidature of the Doctor of Philosophy.

Publications Resulting from Research Described in this Thesis:

Peer-Reviewed Journals:

1. A. Olding; **T. P. Nicholls**; A. C. Bissember,
   Recent Applications of [Cu(dap)$_2$]Cl in Visible Light-Mediated Photoredox Catalysis,
   Australian Journal of Chemistry **2018**, *71*, 547–548.

2. **T. P. Nicholls**; J. C. Robertson; M. G. Gardiner; A. C. Bissember,
   Identifying the Potential of Pulsed LED Irradiation in Synthesis: Copper-Photocatalysed C–F Functionalisation,
   Chemical Communications **2018**, *54*, 4589–4592.

3. **T. P. Nicholls**; D. Leonori; A. C. Bissember,
   Applications of Visible Light Photoredox Catalysis to the Synthesis of Natural Products and Related Compounds,
   Natural Product Reports **2016**, *33*, 1248–1254.

4. **T. P. Nicholls**; G. E. Constable; J. C. Robertson; M. G. Gardiner; A. C. Bissember,
   Brønsted Acid Cocatalysis in Copper(I)-Photocatalyzed α-Amino C–H Bond Functionalization,
   ACS Catalysis **2016**, *6*, 451–457.

[1] Reprints of the publications are contained within Appendix A.2.

Publications Resulting from Research Not Described in this Thesis:

Peer-Reviewed Journals:

1. **T. P. Nicholls**; L. C. Henderson; A. C. Bissember, *Brønsted Acid-Mediated Radical Processes in Organic Synthesis*, *Australian Journal of Chemistry* **2015**, *68*, 1791–1795.

Book Chapters:

1. '**Seven-Membered Rings**' A. G. Meyer; J. A. Smith; C. Hyland; C. C. Williams; A. C. Bissember; T. P. Nicholls, In *Progress in Heterocyclic Chemistry, Vol. 28*; G. W. Gribble, J. A. Joule, Eds.; Elsevier: Amsterdam, 2016.

Presentations:

1. **T. P. Nicholls**; G. E. Constable; J. C. Robertson; M. Massi; M. G. Gardiner; A. C. Bissember, *Extending the Scope of Copper(I) Complexes in Visible-Light-Mediated Photoredox Catalysis*, **Southern Highlands Conference on Heterocyclic Chemistry**, Moss Vale, NSW, 2018 (Oral presentation).

2. **T. P. Nicholls**; G. E. Constable, J; C. Robertson; M. Massi; M. G. Gardiner; A. C. Bissember, *Phenanthroline-Based Cu(I) Complexes: Fundamental Properties & Applications in Photoredox Catalysis*, **The Many Dimensions of Stereochemistry: Catalysis, Chemical Biology, Macromolecules, and Synthesis**, Rhode Island, USA, 2018 (Poster Presentation).

3. **T. P. Nicholls**; J. C. Robertson; M. G. Gardiner; A. C. Bissember, *Investigating the Potential of Copper(I) Complexes in Visible Light-Mediated Photoredox Catalysis*, **The 11th Australasian Organometallics Symposium**, Perth, WA, 2018 (Oral presentation).

4. **T. P. Nicholls**; J. C. Robertson; M. G. Gardiner; A. C. Bissember, *Investigating the Potential of Copper(I) Complexes in Visible Light-Mediated Photoredox Catalysis*, **42nd Annual Synthesis Symposium**, Melbourne, VIC, 2017 (Oral presentation).

5. **T. P. Nicholls**; C. C. Ho; A. C. Bissember; M. G. Gardiner, *Design and Synthesis of a Novel Abnormal* N*–Heterocyclic Carbene Complex*, **41st Annual Synthesis Symposium**, Melbourne, VIC, 2016 (Poster presentation).

6. **T. P. Nicholls**; C. C. Ho; A. C. Bissember; M. G. Gardiner, *Design and Synthesis of a Novel Abnormal* N*–Heterocyclic Carbene Complex*, **The 27th International Conference on Organometallic Chemistry**, Melbourne, VIC, 2016 (Poster presentation).

7. **T. P. Nicholls**; C. C. Ho; A. C. Bissember; M. G. Gardiner, *Design and Synthesis of a Novel Abnormal N–Heterocyclic Carbene Complex*, **The 9th Australasian Organometallics Symposium**, Sydney, NSW, 2015 (Oral presentation).

Abstract

Recently, research concerning photoredox catalysis has enjoyed renewed interest. Photoredox catalysis provides a mode of small molecule activation that takes advantage of the ability of several transition metal complexes to absorb visible light which facilitates single electron transfer (SET) processes with organic substrates. This mild approach has broad applicability across a vast range of chemical transformations. While ruthenium- and iridium-based photoredox-catalysed transformations have received considerable attention, copper-based complexes remain underexplored in this area.

This thesis reports on the development of new synthetic methodology with the broad objective of exploring the scope, limitations, and reactivity of copper-based complexes in photoredox catalysis. In particular, the preparation and study of a library of novel and previously reported copper complexes was conducted. This involved an investigation into the synthesis of homoleptic bis(phenanthroline)copper(I) complexes and heteroleptic phenanthroline-containing copper(I) complexes. Extensive characterisation of their structural, photophysical and electrochemical properties was conducted. Both direct and indirect methods were utilised to characterise the fundamental properties of these complexes including an examination of their reactivity in distinctive atom-transfer radical addition (ATRA) processes.

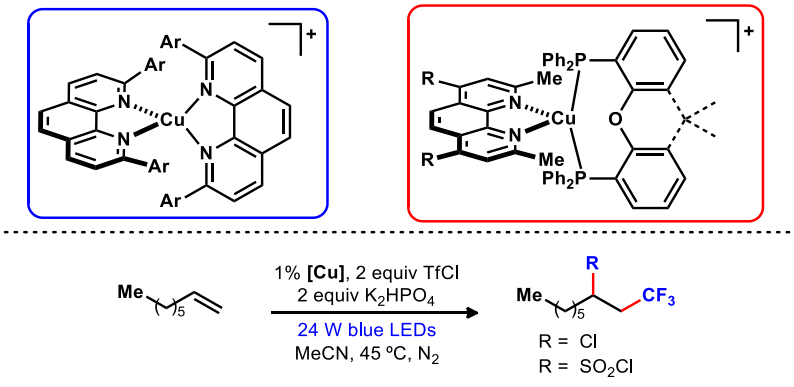

The development of new synthetic methodology began with a proof of concept study in which the weak oxidising power of the prototypical copper-based photoredox catalyst, [Cu(dap)$_2$]Cl, was utilised to catalyse Povarov-type reactions of *N*,*N*-

dialkylanilines/ *N*-aryltetrahydroisoquinolines with electron deficient olefins to produce a range of annulated products. This transformation represents the first example of the weak oxidising power of a copper-based photoredox catalyst being exploited to facilitate the oxidation of amines that are ultimately incorporated into synthetic targets. Intriguingly, the presence of trifluoroacetic acid (TFA) in the reaction was found to be essential to facilitate an efficient reaction. An investigation into the role of TFA suggested that the aerobic quenching of putative photoexcited copper(I) species is mediated by TFA.

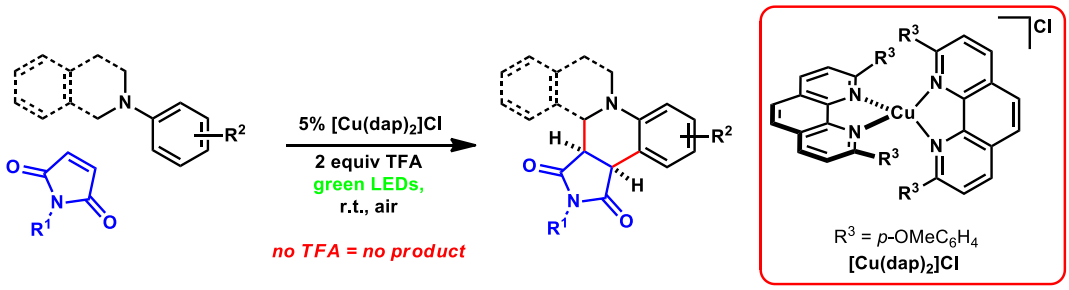

A copper photoredox catalysed dual α-amino C–H/ C–F bond functionalisation reaction was subsequently developed to enable the synthesis of a library of perfluorinated aromatic compounds. During the development of this protocol it was found that a pulsed irradiation strategy provided enhanced yields and significant rate increases when compared to continuous irradiation. This methodology allows for the rapid synthesis of a broad range of fluorinated arenes under mild conditions. This is the first study identifying the potential of pulsed irradiation in photoredox-catalysis.

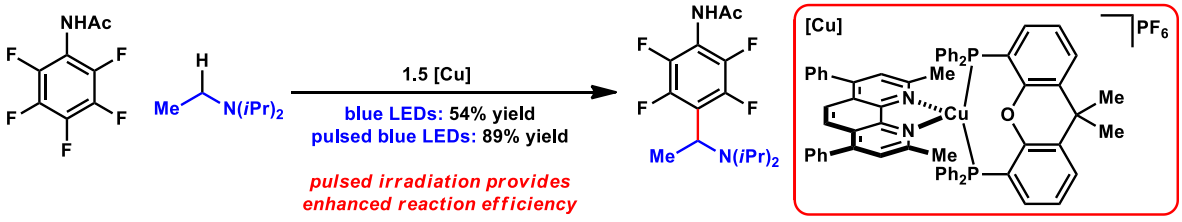

Glossary

The following abbreviations have been used throughout this thesis:

°	degree(s)
°C	degrees Celsius
δ	chemical shift (parts per million)
ε	molar absorptivity (M^{-1} cm^{-1})
λ	wavelength (nm)
τ_0	excited state lifetime
ϕ_{em}	emission quantum yield
μg	microgram(s)
μL	microlitre(s)
μs	microsecond(s)
Å	Ångstrom
Ac	acetyl
AIBN	azobisisobutyronitrile
aq.	aqueous
Ar	unspecified aryl group
Ar_F	unspecified perfluorinated aryl group
ATRA	atom-transfer radical addition
ATRP	atom-transfer radical polymerisation
bcp	4,7-diphenyl-2,9-dimethyl-1,10-phenanthroline (bathocuproine)
BDE	bond dissociation energy
binc	bis(2-isocyanophenyl)phenylphosphonate
Bn	benzyl
Boc	*tertiary* butoxycarbonyl
bpy	2,2-bipyridine
br	broad
Bu	butyl
^{t}Bu	*tertiary* butyl

CFL	compact fluorescent lamp
cm	centimetre(s)
Cy	cyclohexyl
p-cymene	*para*-isopropyltoluene
d	doublet
dap	2,9-di-*para*-anisyl-1,10-phenanthroline
dba	dibenzylideneacetone
DBU	1,8-diazabicyclo[5.4.0]undec-7-ene
dF(CF_3)ppy	2-(2,4-difluorophenyl)-5-(trifluoromethyl)pyridine
DMAP	4-(*N*,*N*-dimethylamino)pyridine
DMF	*N*,*N*-dimethylformamide
dmp	2,9-dimethyl-1,10-phenanthroline
DMPU	1,3-dimethyl-3,4,5,6-tetrahydro-2(1*H*)-pyrimidinone
DMSO	dimethyl sulfoxide
DNA	deoxyribonucleic acid
DPEphos	Bis{(2-diphenylphosphino)phenyl} ether
dpp	2,9-diphenyl-1,10-phenanthroline
dppf	1,1'-bis(diphenylphosphino)ferrocene
dppm	diphenylphosphinomethane
dtbbpy	4,4'-di-*tertiary*-butyl-2,2'-bipyridine
dtbp	2,9-di-*tertiary*-butyl-1,10-phenanthroline
$E_{1/2}$	half wave potential
EDCI	1-ethyl-3-(3-dimethylaminopropyl)carbodiimide
EDG	electron donating group
EI	electron impact (mass spectrometry)
equiv.	equivalent(s)
ESI	electrospray (mass spectrometry)
Et	ethyl
Et_2O	diethyl ether
EtOAc	ethyl acetate
EtOH	ethanol

EWG	electron withdrawing group
g	gram(s)
GC	gas chromatograpy
gem	geminal
glyme	dimethoxyethane
h	hour(s)
HDF	hydrodefluorination
HETPHEN	heteroleptic bisphenanthroline complexes
HLF	Hofmann–Löffler–Freytag
HMPA	hexamethylphosphoramide
HOMO	highest occupied molecular orbital
HRMS	high resolution mass spectrometry
Hz	Hertz
IR	infrared
ISC	intersystem crossing
J	coupling constant
K	Kelvin
kHz	kilo-Hertz
L	ligand
lux	luminous emittance
LED	light emitting diode
LUMO	lowest unoccupied molecular orbital
m	multiplet
m	*meta*
M	molar
M^+	molecular ion
Me	methyl
MeCN	acetonitrile
MeOH	methanol
MHz	mega-Hertz
min	minute(s)

mL	millilitre(s)
MLCT	metal to ligand charge transfer
^{1}MLCT	singlet metal to ligand charge transfer
^{3}MLCT	triplet metal to ligand charge transfer
MMA	methyl methacrylate
mmol	millimole(s)
mol	mole(s)
MS	mass spectrometry
m/*z*	mass to charge ratio
nm	nanometer(s)
NMR	nuclear magnetic resonance
ns	nanoseconds
o	*ortho*
ORTEP	Oak Ridge Thermal-Ellipsoid Plot Program
p	*para*
PC	photoredox catalyst
PEGMA	poly(ethyleneglycol) methyl ether methacrylate
Ph	phenyl
PhMe	toluene
pin	pinacolato
pK_a	acid dissociation constant
ppm	parts per million
ppy	2-phenylpyridine
Pr	propyl
*i*Pr	isopropyl
q	quartet
R	unspecified alkyl group
R_f	unspecified perfluorinated alkyl group
r.t.	room temperature
s	singlet
SCE	saturated calomel electrode

SET	single electron transfer
t	triplet
TEMPO	2,2,6,6-tetramethyl-1-piperidinyloxy free radical
Tf	trifluoromethanesulfonyl
TFA	trifluoroacetic acid
THF	tetrahydrofuran
TLC	thin layer chromatography
TMEDA	*N*,*N*,*N*,*N*-tetramethylethylenediamine
TMS	trimethylsilyl
Ts	*para*-toluenesulfonyl
UV	ultra violet
V	volt(s)
vs.	versus
v/v	unit volume per unit volume (ratio)
W	watt(s)
XP	4,5-bis(diphenylphosphino)-9,9-dimethylxanthene (xantphos)

Table of Contents

Chapter One

Applications of Visible-Light-Mediated Copper Photoredox Catalysts in Synthesis

This chapter provides an overview of applications of copper-based complexes in visible-light-mediated photoredox catalysis. In recent years, these processes have re-emerged as a viable technology that enables the selective formation of chemical bonds under mild reaction conditions. This chapter showcases a broad range of powerful chemical transformations catalysed by copper-based complexes including: atom-transfer radical addition reactions, C–H bond functionalisation processes, reductive couplings, fragmentations, cyclisations and polymerisations.

1.1 Overview of Visible-Light-Mediated Photoredox Catalysis

1.1.1 Transition metal-based visible-light-mediated photoredox catalysis

The development of new modes of small molecule activation is of fundamental importance in catalysis and organic synthesis, more generally. The activation of small molecules by irradiating with light was achieved as early as the 1800s,[1] and the far-reaching consequences of photochemical methods to drive global industry were envisioned by the famous Italian chemist Ciamician in the early 20th century.[2] Since 2008, one area that has received significant, and renewed interest is the development of visible-light-mediated chemical transformations by employing transition metal-based photoredox catalysts that harness energy from visible light (Figure 1.1.1).[3] These complexes can absorb photons from simple household light bulbs, light-emitting diodes (LEDs), or even sunlight. In this way, these catalysts can mediate a broad range of chemical transformations that typically require much harsher conditions or simply cannot occur at all. There are many organic dyes that are also capable of mediating chemical transformations in similar ways.[4]

Visible-light-mediated photoredox catalysis has developed into a powerful strategy for performing single-electron transfer (SET) processes under mild reaction conditions.[3]

Typically, organic molecules do not absorb light in the visible range.[5] In contrast, transition metal-based photoredox catalysts do absorb such wavelengths of light. These complexes can subsequently transfer this energy, via SET (or energy transfer), to organic molecules in a controlled fashion (Figure 1.1.2).

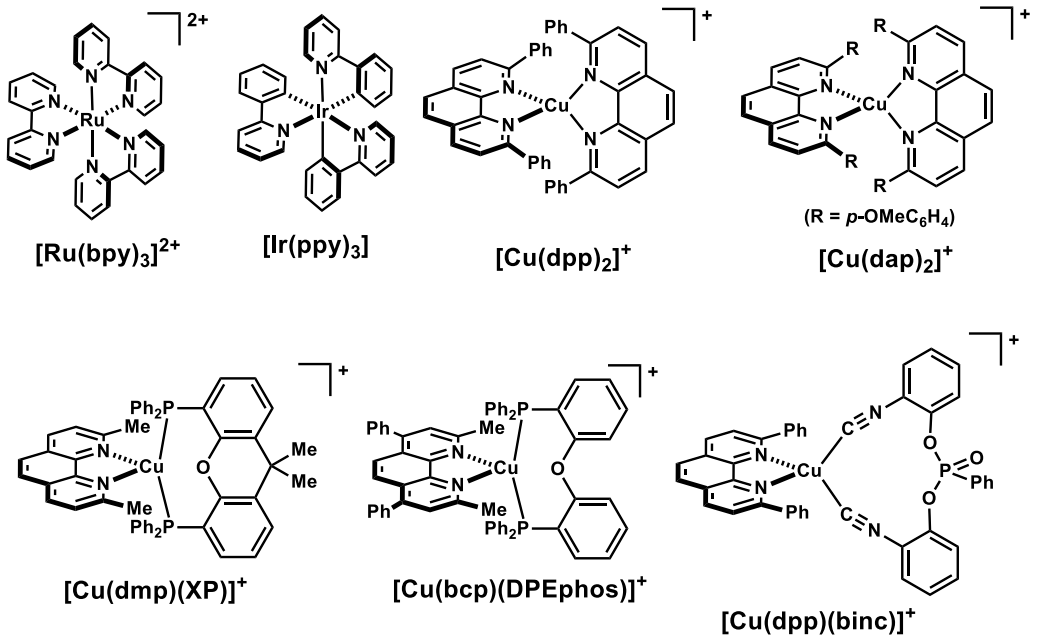

Figure 1.1.1: Typical transition metal-based photoredox catalysts.

The ability of many transition metal-based photoredox catalysts to mediate SET processes derives from the remarkable property that they are both more strongly oxidising and reducing when in their photoexcited state (Figure 1.1.2).[3e] This allows most complexes to operate through both oxidative and reductive quenching cycles to facilitate chemical transformations. For example, upon absorbing a photon, the prototypical photoredox catalyst, $[Ru(bpy)_3]^{2+}$ undergoes a metal-to-ligand charge transfer (MLCT) followed by rapid intersystem crossing (ISC) which populates the lowest energy, triplet MLCT excited state.[3e] This triplet MLCT excited state is typically long lived (1100 ns for $[Ru(bpy)_3]^{2+}$)[6] because decay to the singlet ground state is spin forbidden.[7] It is this triplet MLCT excited state that participates in intermolecular SET processes. When $[Ru(bpy)_3]^{2+}$ is photoexcited it can interact with an organic acceptor molecule, **A**, which oxidises the complex to $[Ru(bpy)_3]^{3+}$ and produces a radical anion, $\mathbf{A}^{\bullet-}$. This oxidised complex, $[Ru(bpy)_3]^{3+}$, is a strong oxidant and can

be easily reduced by an organic donor species, **D**, to close the catalytic cycle and produce a radical cation, $\mathbf{D}^{\bullet+}$. This represents an oxidative quenching cycle. By analogy, $[Ru(bpy)_3]^{2+}$ can also operate through a reductive quenching cycle which also produces reactive organic radicals. In essence, the photoredox catalyst typically acts as an electron shuttle.[3e] This fundamental reactivity can be exploited in diverse applications.[3]

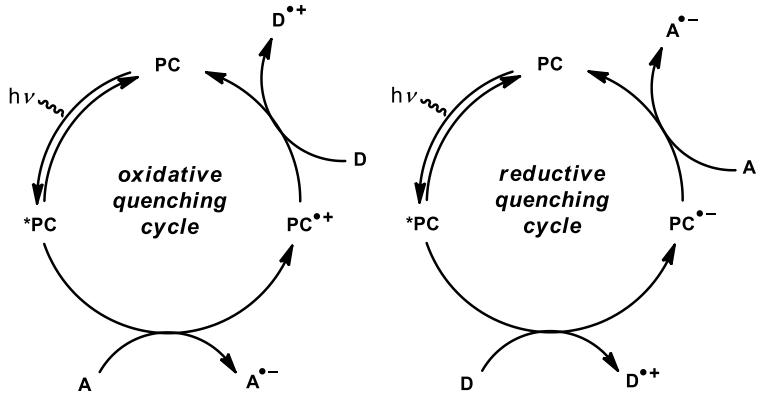

Figure 1.1.2: General photoredox catalytic cycle.[3ar] PC = photoredox catalyst.

1.1.2 Applications of visible-light-mediated photoredox catalysis

The applications of photoredox catalysis to organic synthesis are many and varied.[3] Since 2008, synthetic chemists have redirected significant attention to employing visible light as a reagent in tandem with catalysts as an attractive way to perform chemical transformations. In many cases, visible-light-mediated photoredox catalysis provides benefits derived from the mild conditions typical of photoredox catalysis, when compared to the physical parameters of established protocols for a given transformation.[8] Perhaps more importantly, several visible-light-mediated photoredox transformations have been developed that do not have an existing thermal counterpart. Thus, new approaches to organic synthesis have been developed using this methodology.[3]

There are several general categories for which most visible-light-mediated photoredox protocols fall within. These include, carbon–carbon and carbon–heteroatom bond formation, α-amino C–H oxidation, decarboxylative coupling, cycloaddition and atom-transfer radical addition (ATRA) reactions account for the most well developed areas of

visible light-mediated photoredox catalysis. A brief overview of these protocols is given below.

There are many reports of carbon–carbon and carbon–heteroatom bond forming processes utilising visible-light-mediated photoredox protocols. C–C bond formation of Csp^3, Csp^2 and Csp hybridised carbon atoms have been developed, as well as C–N, C–O, C–S, C–P, and C–Cl bond forming processes.[9] In addition, co-operative catalysis has also been utilised in this manifold. For example, an elegant protocol developed for such transformations implements a dual transition metal/ photoredox catalysis methodology.[10] A nickel-catalysed cross-coupling reaction enabled by photoredox catalysis reported by MacMillan and co-workers is an illustrative example (Scheme 1.1.1).[11] The coupling of aryl bromides with simple alcohols is difficult because C–O reductive elimination from Ni(II) is predicted to be endergonic. However, an iridium-based photoredox catalyst can oxidise this complex to Ni(III), from which reductive elimination is energetically favourable. In addition, Lewis and Brønsted acid dual catalysis strategies are common throughout photoredox catalysis.[3n]

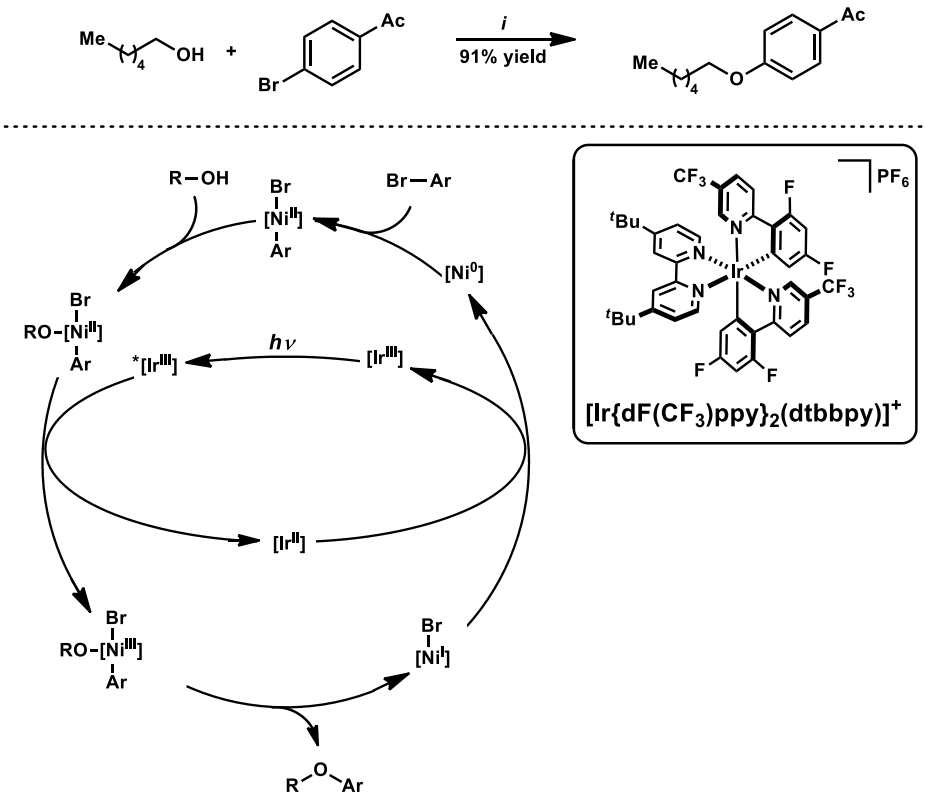

Scheme 1.1.1: Photoredox-enabled, nickel-catalysed cross-coupling reaction.[11] Reagents and conditions: (*i*) 1% [Ir], 5% $NiCl_2$•glyme, 5% dtbbpy, 10% quinuclidine, K_2CO_3, blue LEDs, MeOH.

Visible light-mediated photoredox-catalysed α-amino functionalisation can occur either via an iminium ion or α-amino radical intermediate (Scheme 1.1.2).[12] This dichotomy allows reactions with either nucleophiles, or electrophiles. Thus, aza-Henry reactions,[13] α-alkylations and α-alkynylations of tetrahydroisoquinolines have been achieved,[14] as well as α-arylation of α-amino carbonyl compounds though putative iminium species.[15] A range of additions to Michael acceptors via putative α-amino radical intermediates have also been reported.[16]

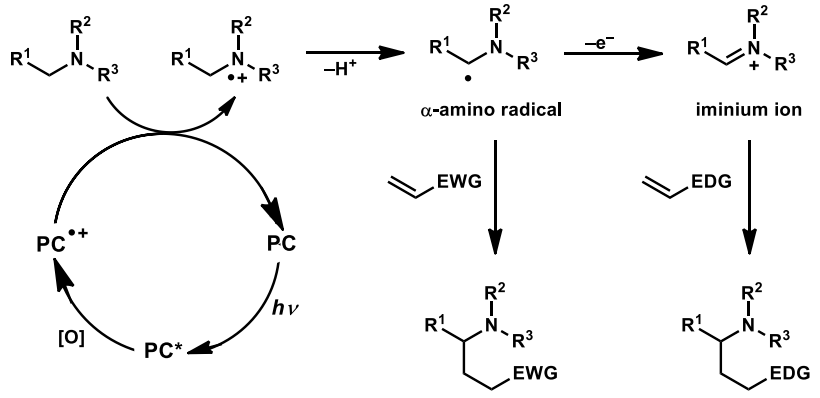

Scheme 1.1.2: Visible-light-mediated photoredox-catalysed α-amino functionalisation reactions via both α-amino radicals and iminium ion intermediates. PC = photoredox catalyst.

Photocatalytic decarboxylative coupling reactions typically proceed through either an alkyl or acyl radical intermediate generated from a carboxylic acid or their derivatives such as esters.[17] These highly reactive intermediates can facilitate numerous C–C and C–N bond-forming processes. Numerous photocycloadditions have also been developed including formal [4 + 2]-, [3 + 2]-, and [2 + 2]-variants.[18] Often, Lewis or Brønsted acids are required to overcome large energy gaps to allow such reactions to proceed.[3n,19] However, this can also be achieved by oxidising the diene or dienophile to a radical cation in the absence of additives.[20] Photoredox catalysis is particularly well suited to this class of chemistry due to its ability to facilitate SET processes. Radical cation Diels–Alder reactions, the synthesis of pyrrole and pyrazole derivatives and "click" reactions are all viable through visible-light-mediated photocatalytic methods.[18]

Atom-transfer radical additions (ATRA) are typically redox neutral reactions in which a reactant undergoes σ-bond cleavage and adds across an alkene (π-bond), thus forming two new σ-bonds.[21] In these reactions, the substrate undergoes both single electron oxidation and reduction during the transformation and there is no net change in oxidation state. Visible-light-mediated photoredox-catalysed ATRA reactions commonly employ haloalkanes or alkylsulfonylchlorides as the atom-transfer reagents that can add to both alkenes or alkynes.

Finally, fluorinations and fluoroalkylations are specific but important classes of reactions that can be achieved through visible-light-mediated photoredox catalysis.[22] Fluorinated compounds are important due to their use as pharmaceuticals, agrochemicals

and other organic materials (Scheme 1.1.3A).[23] A good example is the direct trifluoromethylation of arene C–H bonds developed by MacMillan and co-workers (Scheme 1.1.3B).[24] The use of triflyl chloride as a precursor to the trifluoromethyl radical allows the introduction of the trifluoromethyl group to a range of (hetero)arene compounds and is amenable to the late stage functionalisation of complex molecules which is useful for library synthesis.

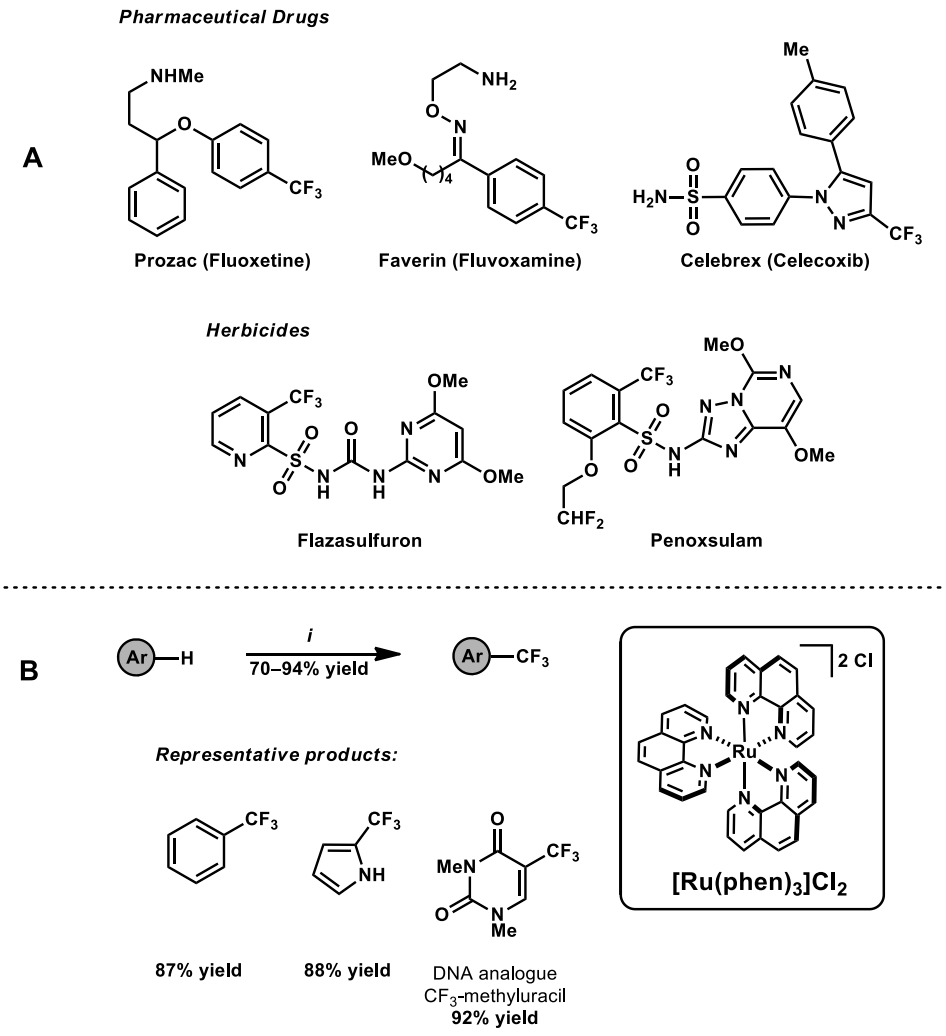

Scheme 1.1.3: (a) Examples of pharmaceutical drugs and agrochemicals containing aryl–CF_3 substituents. (b) Visible-light-mediated photoredox-catalysed direct trifluoromethylation of arenes. Reagents and conditions: (*i*) 1–2% [Ru], 1–4 equiv CF_3SO_2Cl, 1 equiv K_2HPO_4, hv, MeCN.

1.2 Copper(I) Complexes in Visible-Light-Mediated Photoredox Catalysis

1.2.1 Homoleptic and heteroleptic copper(I) complexes

The most common transition metal-based photoredox catalysts are typically based on polypyridyl complexes of ruthenium or iridium (Figure 1.1.1).[3] These second and third row transition metal complexes feature octahedral geometries and provide good structural, photophysical and electrochemical properties. However, examples of visible-light-mediated photoredox catalysis utilising cheap, earth abundant base metals, such as copper, are far less common.

In 1977, McMillin reported the preparation of a class of photoactive, bis(2,9-disubstituted-1,10-phenanthroline)copper(I) complexes featuring distorted tetrahedral geometries.[25] While these complexes exhibited similar quantum yields to that of $[Ru(bpy)_3]^{2+}$ (2.8%),[26] the excited state lifetimes were significantly shorter (~100–300 ns). Ten years later, Sauvage and co-workers disclosed the first synthesis of $[Cu(dap)_2]Cl$ (Figure 1.1.1).[27] This work demonstrated that a copper-based complex was able to catalyse a visible-light-mediated photoredox transformation for the first time. Specifically, they demonstrated the reductive coupling of *p*-nitrobenzylbromide (**1.1**) to deliver bis-(*p*-nitro)dibenzyl (**1.2**) under an inert atmosphere, or oxidation to *p*-nitrobenzaldehyde (**1.3**) under air (Scheme 1.2.1). Importantly, it was demonstrated that both visible light and $[Cu(dap)_2]Cl$ were necessary for the reaction to proceed. Interestingly, despite this proof of concept, the synthetic applications of copper complexes in photoredox catalysis were not further explored until 2012.

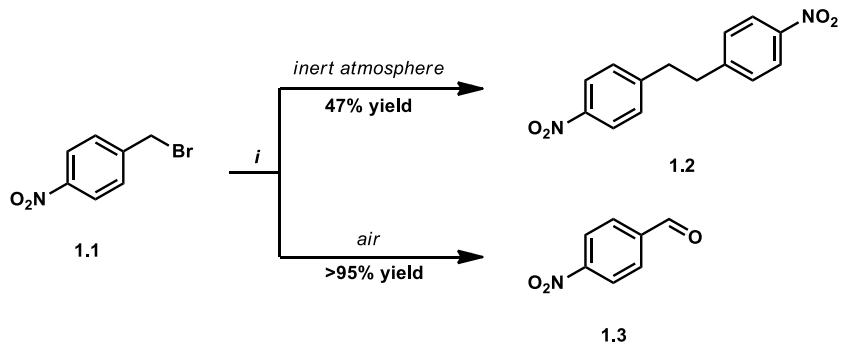

Scheme 1.2.1: Seminal report of a photoredox transformation catalysed by a copper complex. Reagents and conditions: (*i*) 0.02% $[Cu(dap)_2]Cl$, 1.8 equiv NEt_3, CH_2Cl_2, hv.[26]

The poor synthetic utility of coordinatively unsaturated copper-based photoredox catalysts may derive from unfavourable structural reorganisations that occur upon photoexcitation.[28] The ground state copper(I) centre is oxidised as a result of the MLCT and this is accompanied by a flattening distortion that shortens the excited state lifetime and lowers the emission quantum yield. This will be discussed in detail in Chapter Two. Importantly, this structural rearrangement does not occur with coordinatively saturated, octahedral ruthenium- and iridium-based photoredox catalysts that have longer lifetimes.[3n] In addition, unlike ruthenium- and iridium-based systems, bis(phenanthroline)copper(I) complexes cannot mediate photoredox-catalysed processes via a reductive quenching cycle.[29] While this last feature may be regarded as a limitation, this property can potentially facilitate more tractable mechanistic investigations as the involvement of a reductive quenching cycle can be eliminated.[30]

Another class of photoactive copper-based complexes that have been utilised to mediate photoredox-catalysed transformations are heteroleptic copper(I) complexes (Figure 1.1.1). Many of these complexes have enhanced structural, photophysical and electrochemical properties to those of their homoleptic bis(phenanthroline) analogues.[31] As such, they have the potential to expand the synthetic applications of copper-based visible-light-mediated photoredox catalysis beyond what is possible with homoleptic bis(phenanthroline)copper(I) complexes.

1.2.2 Copper(I) photoredox-catalysed ATRA processes

Following Sauvage's pioneering 1987 study,[27] the applications of copper photoredox-catalysed transformations were revisited by Reiser and co-workers after 25 years.[32] Reiser has contributed many of the most significant applications in this field, including the development of reactions involving proposed inner sphere processes which are not possible when utilising ruthenium- or iridium-based photoredox catalysts.[32,33] The initial report featured the $[Cu(dap)_2]Cl$-catalysed ATRA of activated halides such as, CBr_4, α-halocarbonyl compounds or electron deficient benzyl halides to a broad range of alkenes (Scheme 1.2.2).[27] No sacrificial electron donor was required as the reaction is redox neutral. The reaction proceeds through the oxidative quenching cycle, presumably with the photoexcited state of $[Cu(dap)_2]^+$ oxidised by the alkyl halide **1.4** to produce a Cu(II) species, alkyl radical anion **1.6** and a halide. The alkyl radical anion **1.6** adds to the alkene and the ensuing alkyl radical **1.7**, reduces the Cu(II) species to close the catalytic cycle with concomitant formation of carbocation **1.8**. Nucleophilic attack by the halide anion completes the synthesis (Scheme 1.2.2). The related ATRA reaction between styrene and tetrabromomethane was also investigated by Mayer and co-workers who established that several bis(phenanthroline)copper(I) complexes could catalyse this transformation.[34]

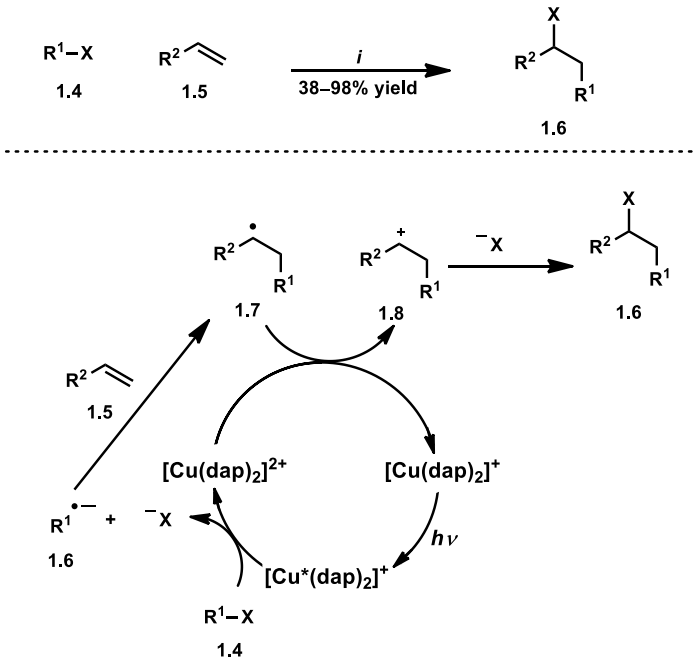

Scheme 1.2.2: Typical catalytic cycle of ATRA reactions catalysed by copper-based photoredox catalysts. Reagents and conditions: (*i*) 0.3% $[Cu(dap)_2)]Cl$, 1 equiv **1.4**, 1 equiv **1.5**, green LEDs, CH_2Cl_2.[31]

A radical addition/ oxidation/ cyclisation reaction of unactivated alkenes containing sulfonamides **1.9**, was developed by Dolbier and co-workers (Scheme 1.2.3).[35] The production of pyrrolidines **1.13** was achieved, in moderate to excellent yield, utilising sulfonyl chloride **1.10** as a source of HCF_2 radicals. However, during optimisation of the reaction the authors discovered another competing ATRA process in which the carbocation intermediate **1.11** was trapped by chloride before cyclisation could occur. This chlorination process could be suppressed by addition of silver carbonate. Finally, intramolecular, nucleophilic attack by the sulphonamide group led to compound **1.13**.

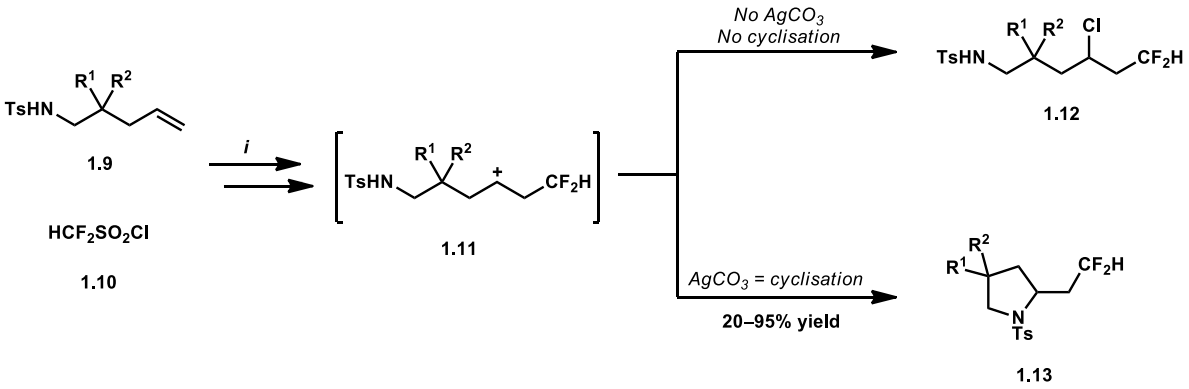

Scheme 1.2.3: [Cu(dap)$_2$]Cl catalysed cyclisation of sulfonamides. Reagents and conditions: (*i*) 1% [Cu(dap)$_2$]Cl, hv, Cl(CH$_2$)$_2$Cl, 70 °C.[34]

Dolbier and co-workers described another ATRA process involving fluoroalkylsulfonyl chlorides **1.15** as a source of fluoroalkyl radicals.[36] This study illustrated that [Cu(dap)$_2$]Cl was capable of catalysing the addition of fluoroalkyl groups to electron-deficient, unsaturated carbonyl compounds **1.14**. Chloride was also added across the double bond, and thus, SO_2 extrusion occurs (Scheme 1.2.4). [Cu(dap)$_2$]Cl was superior to several known ruthenium- and iridium-based photoredox catalysts. Ultimately, the fluoroalkylchlorination protocol proved to be general and efficient. The presence of an α-C–Cl bond in the α-chloro-β-fluoroalkylcarbonyl products **1.16** provided access to amino acids, alkenes and other useful derivatives.

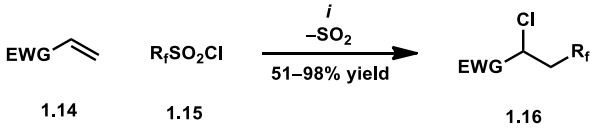

Scheme 1.2.4: [Cu(dap)$_2$]Cl-catalysed cyclisation of sulfonamides. Reagents and conditions: (*i*) 1% [Cu(dap)$_2$]Cl, 1 equiv **1.14**, 2 equiv **1.15**, 20% K$_2$HPO$_4$, hv, Cl(CH$_2$)$_2$Cl, 25 °C.[35]

In complementary work, Reiser and co-workers reported the trifluoromethylchlorosulfonylation of unactivated alkenes (Scheme 1.2.5).[33a] Previously, it had been reported that ruthenium- or iridium-based photoredox catalysts afforded the

trifluoromethylchlorination product only.[37] However, coordinatively unsaturated copper-based complexes which undergo structural rearrangement upon photoexcitation, delivered the trifluoromethylchlorosulfonylation product, and thus, SO_2 extrusion does not occur. This interesting complementary reactivity is suggested to be the result of inner sphere processes in which the photoexcited copper(I) species is oxidised by triflyl chloride to produce the trifluoromethyl radical with concomitant coordination of SO_2Cl to the metal centre. After the trifluoromethyl radical adds to the alkene to produce an alkyl radical, this Cu–SO_2Cl complex delivers SO_2Cl to the alkyl radical to furnish trifluoromethylchlorosulfonylation product. This is supported by different product distributions depending on the steric environment of the substrate and catalyst. When branched alkene **1.17** and [Cu(dap)$_2$]Cl are used, a 3:1 distribution of chlorosulfonylation product **1.19**, and chlorination product **1.20**, is observed (Scheme 1.2.5). The steric bulk provided by branched alkene **1.17** disfavours the chlorosulfonylation pathway and SO_2 extrusion occurs more readily, but this can be biased by a decrease in the bulk of the catalyst. Consistent with this, when [Cu(dap)$_2$]Cl is substituted for the sterically less bulky [Cu(dpp)(binc)]Cl (Scheme 1.2.5), a product distribution of 9:1 is observed with a similar yield (Scheme 1.2.5). This unique feature of copper-based photoredox catalysts to enable inner sphere processes augments the ability of most photoredox catalysts to simply engage in SET. This is in good agreement with their coordinatively unsaturated nature. The ability to transiently coordinate Lewis basic species and subsequently deliver them to organic intermediates allows access to new modes of activation and unprecedented reactivity within the class of photoredox catalysis

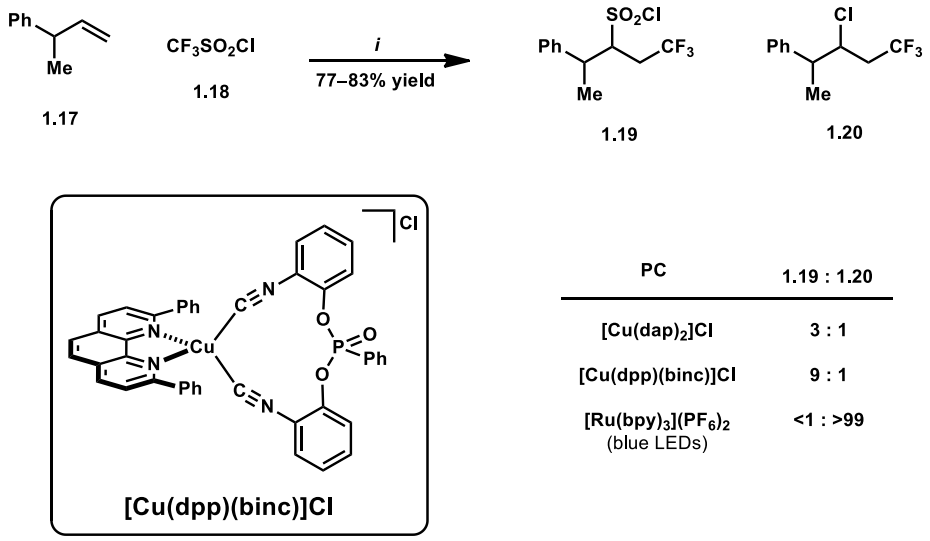

Scheme 1.2.5: Trifluoromethylation reactions with increased steric bulk in the substrate. Reagents and conditions: (*i*) 1% PC, 1 equiv **1.17**, 2 equiv **1.18**, 2 equiv K_2HPO_4, green LEDs, MeCN. PC = photocatalyst.[32a]

This inner sphere process has been exploited with several extensions of this general strategy being developed. Firstly, a two-step, iterative photoredox catalysis sequence was developed to further functionalise trifluoromethylchlorosulfonylation products **1.22** (Scheme 1.2.6A).[33b] The alkylsulfonylchlorides **1.22**, that were produced utilising the copper-catalysed protocol described above, do not engage further in electron transfer processes mediated by [Cu(dap)2]Cl. However, they were activated by [*fac*-Ir(ppy)3] to produce sulfonyl radicals that were trapped by styrenes. This allowed the production of β-hydroxysulfones **1.23**, in a one-pot, two stage reaction. Secondly, the synthesis of trifluoromethylated sultones **1.26**, from alkenols **1.24**, was reported by Reiser and co-workers (Scheme1.2.6B).[33c] Presumably, an analogous inner sphere mechanism is also operative leading to trifluoromethylchlorosulfonylation intermediate **1.25**. Intramolecular nucleophilic attack from the pendant alcohol creates a new S–O bond and delivers fluorinated cyclic sultones **1.26**.

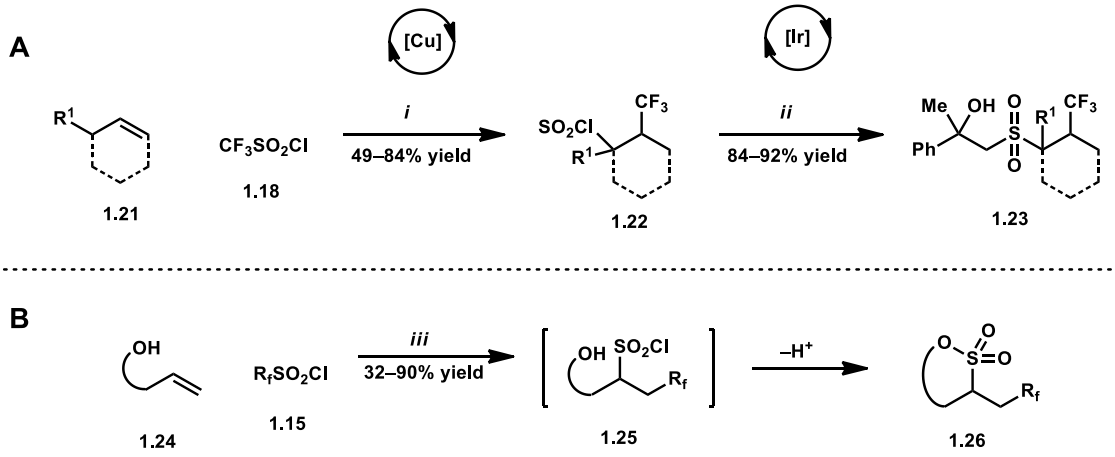

Scheme 1.2.6: Extensions of inner-sphere trifluorofluoromethylchlorosulfonylation reaction. Reagents and conditions: (*i*) 1% $[Cu(dap)_2]Cl$, 2 equiv K_2HPO_4, blue LEDs, MeCN;[32b] (*ii*) 1% [*fac*-$Ir(ppy)_3$)], α-methylstyrene, blue LEDs, MeCN:H_2O (5:1); (*iii*) 1% $[Cu(dap)_2]Cl$, 2 equiv K_2HPO_4, green LEDs, MeCN.[32c]

Further evidence of inner sphere processes with $[Cu(dap)_2)]Cl$ was reported by Reiser and co-workers when they investigated the iodoperfluorination of alkenes and alkynes.[33d] Several methods have been developed for this transformation, including thermal initiation using a radical starter such as azobisisobutyronitrile (AIBN) and a photoredox-catalysed protocol using Eosin Y.[38] However, styrenes are not reported to participate in either of these processes. Fortunately, styrenes and phenylacetylenes were found to be viable reactants when $[Cu(dap)_2]Cl$ was used to catalyse the transformation. A detailed mechanistic investigation suggested inner sphere processes that are consistent with the divergent reactivity observed employing styrene and $[Cu(dap)_2]Cl$. The failure of $[Ru(bpy)_3]Cl_2$ and AIBN to effect this transformation suggests that neither classical photoredox nor radical chain mechanisms are feasible. However, a ligand transfer cycle or a rebound cycle, both involving inner sphere processes could explain the divergent reactivity featuring $[Cu(dap)_2]Cl$ (Scheme 1.2.7). The ligand transfer cycle involves SET from photoexcited $[Cu(dap)_2]^+$ to produce a fluoroalkyl radical **1.30**, which adds to the styrene **1.28** as per the conventional ATRA mechanism to produce alkyl radical **1.32**. However, it is suggested that decoordination of a dap ligand also occurs upon production of the fluoroalkyl radical **1.30**, to produce a copper(II)–iodo species **1.31**, that subsequently oxidises the alkyl radical **1.32**, as well as transferring the iodo ligand to deliver the formal ATRA product **1.29**.[33d] Alternatively, a

rebound cycle may be operative in which the copper(II)–iodo species **1.31** coordinates the alkyl radical **1.32** to produce a copper(III) species **1.33** which reductively eliminates the ATRA product **1.29**. Both these mechanisms are consistent with the divergent reactivity when a copper-based photoredox catalyst is used in place of $[Ru(bpy)_3]Cl_2$ or AIBN. The ATRA product can only be formed when a copper-based catalyst is used that can deliver iodide to form the product and close the catalytic cycle.

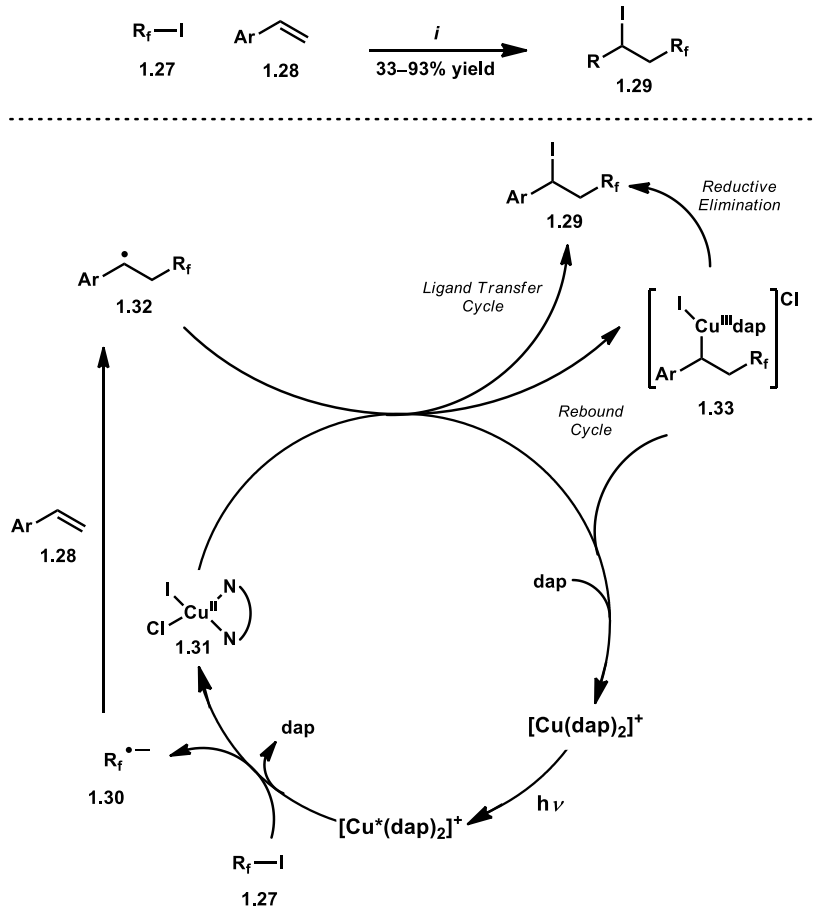

Scheme 1.2.7: Proposed mechanism for the ATRA of fluoroalkyl iodides with styrenes catalysed by $[Cu(dap)_2]Cl$.[33d] Reagents and conditions: (*i*) 1% $[Cu(dap)_2]Cl$, 1 equiv **1.27**, 2 equiv **1.28**, green LEDs, MeCN, 25 °C.

Another example of inner sphere processes when using a copper-based photoredox catalyst is the oxo-azidation of vinyl arenes reported by Reiser and co-workers (Scheme 1.2.8).[33e] It is proposed that a copper(II) species **1.37**, formed by oxidation of photoexcited

$[Cu(dap)_2]^+$ by O_2 and subsequent ligand exchange is the catalytically active species. This complex undergoes visible-light-mediated homolysis which reduces the complex and produces an azide radical which can add to the double bond of the styrene. Incorporation of O_2 to the ensuing azidoalkyl radical **1.41**, produces a peroxy radical species **1.42**, which can subsequently oxidise the copper(I) species **1.39**, and ultimately form oxo-azidation products **1.36**. This represents the first example of a copper(II) complex as the catalytically active species in a visible-light-mediated photoredox-catalysed transformation, made possible by structural rearrangement of the copper complex upon photoexcitation and the lability firstly of a single phenanthroline-based ligand.

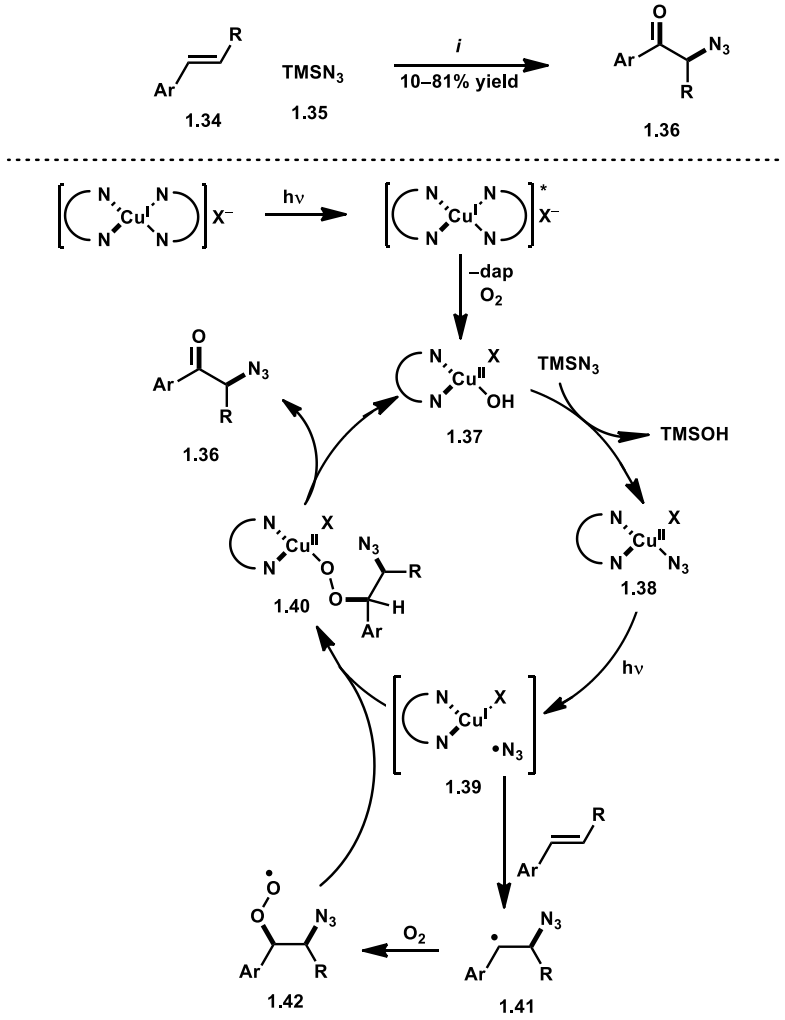

Scheme 1.2.8: Proposed mechanism for the oxo-azidation of styrenes which exhibit a copper(II) species as the active catalyst.[33f] Reagents and conditions: (i) 1% $[Cu(dap)_2]Cl$, 1 equiv **1.34**, 2 equiv **1.35**, air, green LEDs, MeCN 25 °C.

Finally, many methods for the installation of an azide group require highly toxic and/ or potentially explosive materials which are usually nucleophilic sources of azide. The mild conditions typical of photoredox catalysis are particularly suited to the installation of such a highly reactive, and useful functional group. The Zhdankin reagent (**1.43**), a hypervalent iodine reagent, was first reported in 1994 as an electrophilic source of azide (Scheme 1.2.9).[39] Greaney and co-workers reported that the Zhdankin reagent (**1.43**) could be reduced by $[Cu(dap)_2]Cl$ to produce an azide radical that could subsequently be trapped by activated alkenes in an ATRA process.[40] This was followed by addition of a nucleophile, such as methanol, to the ensuing alkyl radical to deliver azidomethoxylation products (Scheme 1.2.9). Alternatively, if the reaction were performed in the dark, double azidation products were produced. The light switchable behaviour provides divergent reactivity of either double C–N bond formation in the dark or C–N/ C–O bond formation under visible light irradiation.

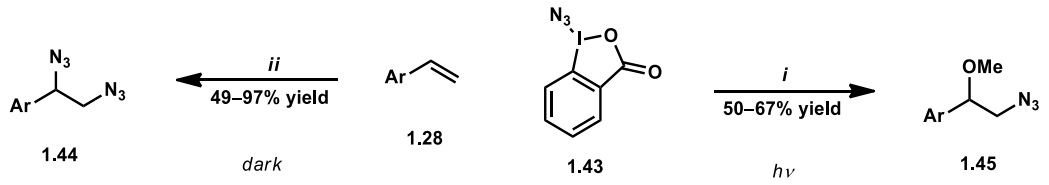

Scheme 1.2.9: $[Cu(dap)_2]Cl$-catalysed azidation and double azidation of styrenes. Reagents and conditions: (*i*) 1% $[Cu(dap)_2]Cl$, visible light, MeOH; (*ii*) 1% $[Cu(dap)_2]Cl$, dark, MeOH.[41]

1.2.3 Copper(I) photoredox-catalysed C–H functionalisation reactions

A C–H activation reaction featuring the Zhdankin reagent (**1.43**), was developed for benzylic azidation (Scheme 1.2.10).[41] The proposed mechanism involves initiation and chain propagation steps. The reduction of the Zhdankin reagent (**1.43**) by photoexcited $[Cu(dap)_2]^+$ releases an azide radical which subsequently abstracts a hydrogen atom from the benzylic position of the substrate to produce alkyl radical **1.49**. In the chain propagation step, alkyl radical **1.49** abstracts the azide group from another molecule of electrophilic Zhdankin reagent (**1.43**) to furnish the azidated product **1.47**. The ensuing iodane radical **1.50**, can then abstract a hydrogen atom from the benzylic substrate, thus propagating the chain. Primary, secondary and tertiary azides were produced in generally good yield.

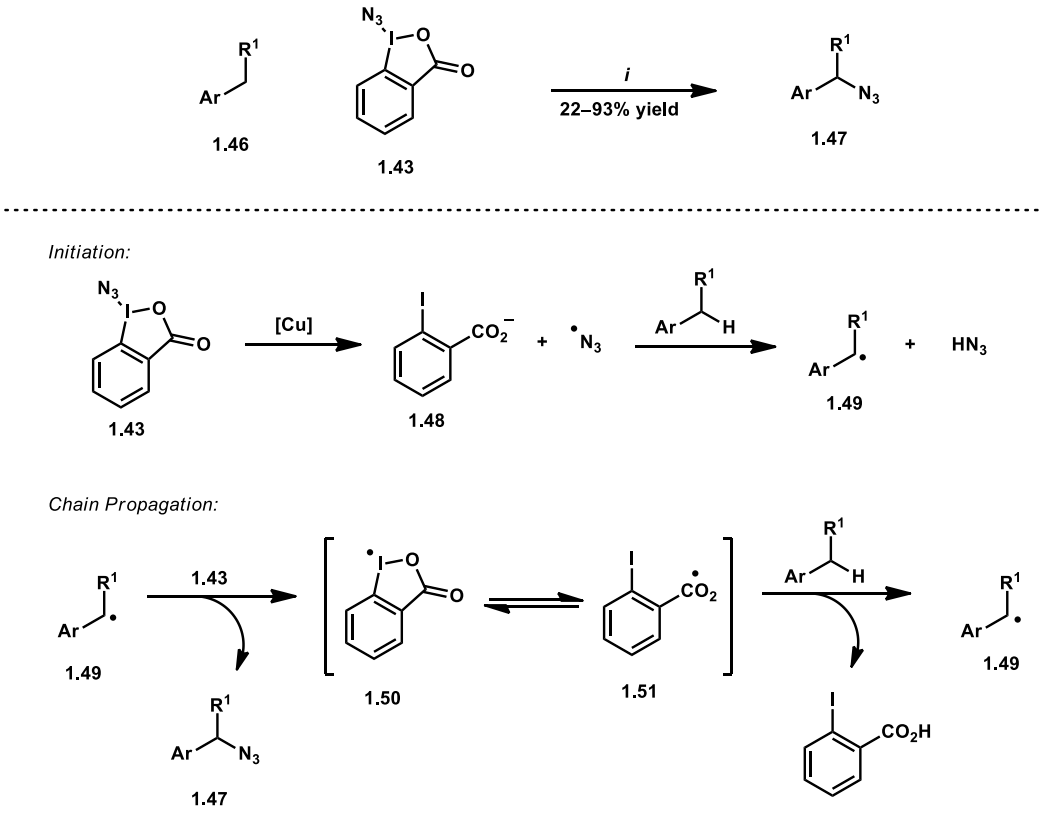

Scheme 1.2.10: Proposed mechanism for the benzylic C–H azidation using a copper photoredox catalyst. [Cu] = $[Cu(dap)_2]Cl$.[41]

The first visible-light-mediated photoredox process catalysed by a heteroleptic copper(I) complex was reported by Collins and co-workers in 2012.[42] This study featured a photocyclodehydrogenation reaction for the synthesis of [5]helicene (**1.53**) from stilbene precursor **1.52** (Scheme 1.2.11A). While established methodology relied on UV light to mediate this transformation,[43] the addition of a copper-based photoredox catalyst allowed the reaction to proceed under visible light. The use of visible light in this process has several advantages. UV light irradiation produced overoxidation products and lacked regiocontrol. This resulted in the formation of [5]helicene (**1.53**) as only the minor product. However, both these issues were avoided in the visible-light-mediated protocol and [5]helicene (**1.53**) was prepared efficiently. Generating the heteroleptic copper-based complexes *in situ* enabled the rapid screening of several related heteroleptic copper(I) complexes featuring diphosphine and diimine ligands. Ultimately, the most efficient complex for this transformation was identified as $[Cu(dmp)(XP)]BF_4$ (Scheme 1.2.11A).

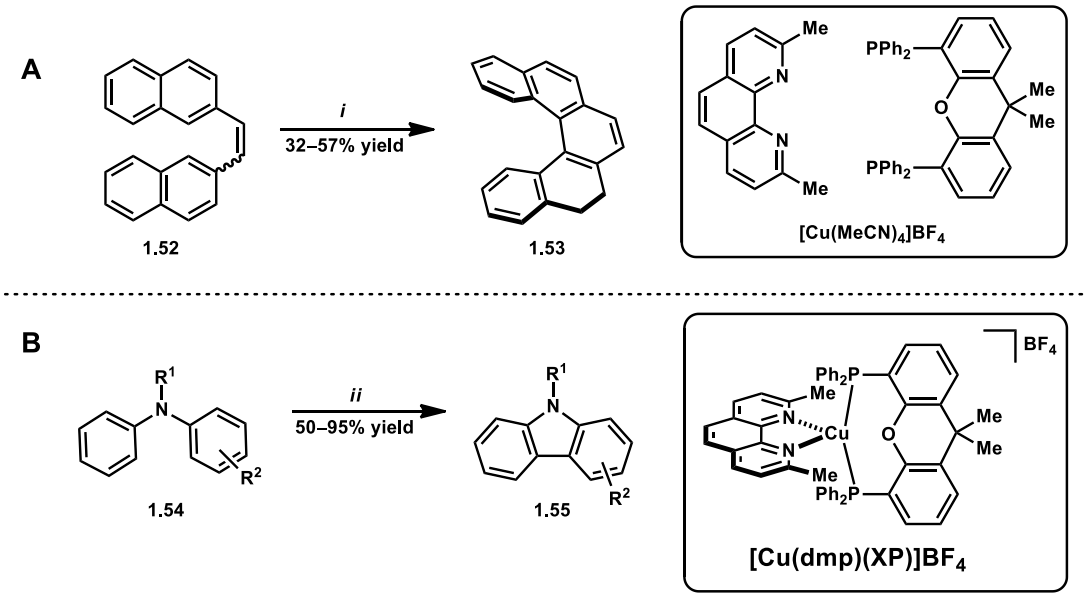

Scheme 1.2.11: Cyclisation reactions featuring C–H activation. Reagents and conditions: (*i*) 10% $[Cu(MeCN)]BF_4$, 10% diphosphine ligand, 10% diimine ligand, 1 equiv I_2, 50 equiv propylene oxide, hv, THF;[41] (*ii*) 5% [Cu], 1 equiv I_2, hv, THF/propylene oxide (~56:1).[43]

A similar protocol for the synthesis of carbazoles from di- or triaryl amines **1.54** was developed by the same researchers shortly after (Scheme 1.2.11B).[44] This cyclisation protocol also involved an oxidative C–C bond formation step and was catalysed by $[Cu(dmp)(XP)]BF_4$ (Scheme 1.2.11B). Established methods for the oxidative C–C coupling of diarylamines to produce carbazoles typically require harsh conditions including high temperatures.[45] In contrast, this transformation proceeded at room temperature using only O_2 or I_2 as sacrificial oxidants.

1.2.4 Heteroleptic copper(I) photoredox-catalysed reactions

Recently, heteroleptic copper-based complexes have been used to catalyse a range of visible-light-mediated chemical transformations. The increased excited state lifetimes of these complexes, as well as favourable redox properties allow the scope of copper-based photoredox catalysis to be extended beyond ATRA and other limited classes of reactivity. This is exemplified by photoredox-catalysed allylations (Scheme 1.2.12). While $[Cu(dap)_2]Cl$ has been shown to be an efficient catalyst for allylation reactions using allyltributyltin as reactant,[32a] many allylsilanes do not participate. However, the heteroleptic complex

[Cu(dpp)(binc)]BF_4 can effect such transformations using the more environmentally benign allylsilanes (Scheme 1.2.12A).[33f] This potentially derives from the significantly increased excited state lifetime (17 μs) or stronger reductive power of the heteroleptic species. The allylation of α-halocarbonyl compounds using allyltributyltin or allyltrimethylsilane was also reported by Reiser and co-workers.[32a,33f]

In related work, a reductive coupling reaction between hypervalent iodine species and allylsulfonamides was developed by Ollivier in 2013 (Scheme 1.2.12B).[46] Aryl radicals are produced by reduction of the corresponding hypervalent iodine reagents catalysed by either [Cu(dap)$_2$]PF_6 or [Cu(dpp)$_2$]PF_6. The aryl radical then adds to the alkene moiety of the allyl tosylates in an anti-Markovnikov manner that is typical of transformations involving radical processes, and the ensuing alkyl radical then eliminates a sulphonamide radical to furnish the allylated products. NMR studies were consistent with a Cu^I/ Cu^{II} mechanism in which the diamagnetic Cu(I) species is oxidised to the paramagnetic Cu(II) species in the presence of [Ph_2I][PF_6]. Subsequently, resonances in the NMR spectrum consistent with the Cu(I) species returned upon addition of the sacrificial reductant diisopropylethylamine. This C–C bond-forming reaction had broad scope and was equally as efficient as ruthenium- and iridium-based photoredox catalysts.

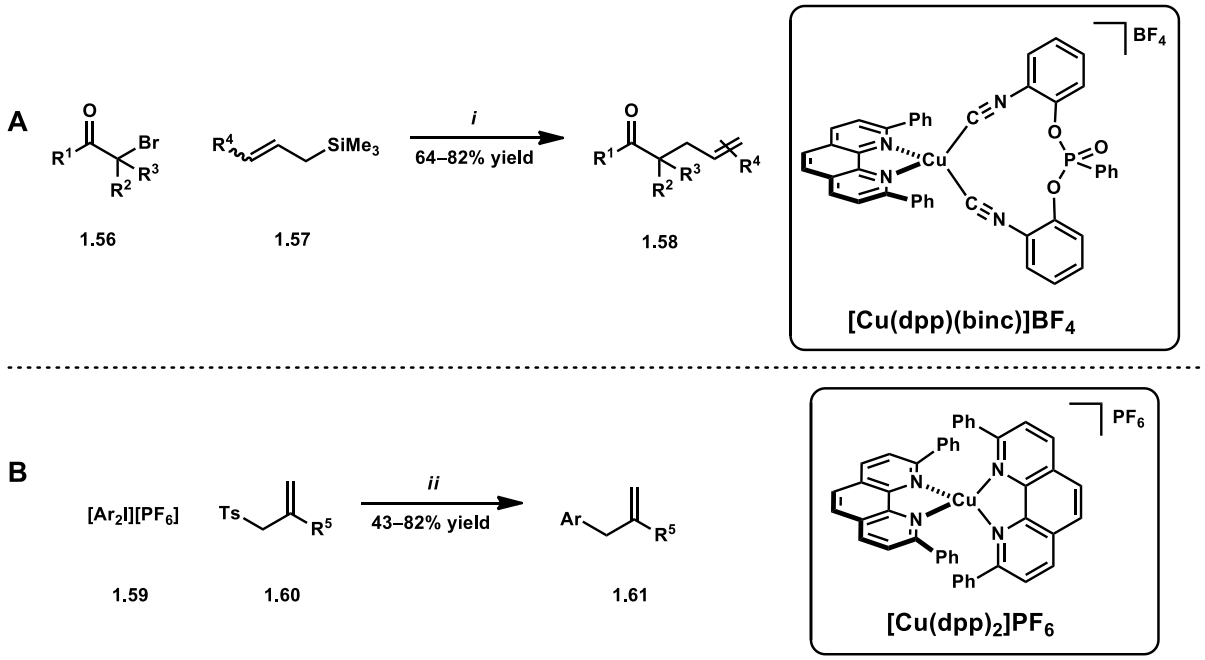

Scheme 1.2.12: Visible-light-mediated copper-catalysed allylation reactions. Reagents and conditions: (*i*) 1% [Cu], blue LEDs, MeCN;[32f] (*ii*) 0.5% [Cu], 2 equiv *i*Pr$_2$NEt, green LEDs, MeCN.[45]

Another example of a heteroleptic copper(I) complex being used as a photoredox catalyst is the decarboxylative C–N coupling of a range of *N*-hydroxyphthalimide esters **1.62** to produce protected amines **1.63** reported by Fu and co-workers (Scheme 1.2.13A).[47] This alternative to the powerful Curtius rearrangement dispenses with the need to handle azides and proceeds under mild conditions.[48] The reaction was found to be general, with primary and secondary alkyl groups engaging efficiently in the reaction and a wide variety of functional groups were tolerated. The proposed mechanism involved reduction of the *N*-hydroxyphthalimide ester by photoexcited copper(I) complex to produce a carboxyl radical, with concomitant coordination of phthalimide to the oxidised copper(II) species.[47] The carboxyl radical eliminates CO_2 and the ensuing alkyl radical abstracts phthalimide from the copper(II) complex to furnish the protected amines and close the catalytic cycle. This is another example in which inner sphere processes allow reactivity that is unprecedented with more common photoredox catalysts featuring saturated octahedral coordination geometries.

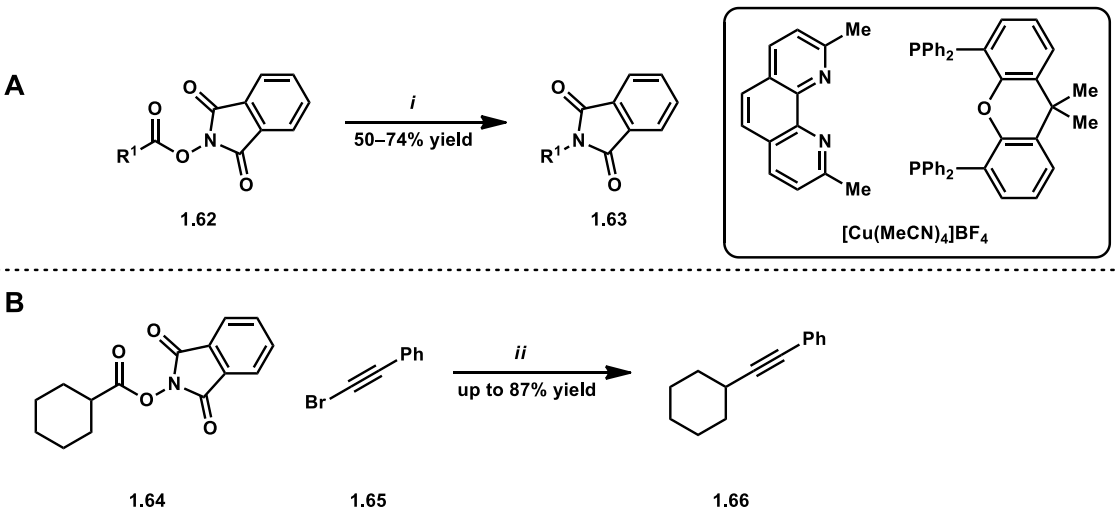

Scheme 1.2.13: Visible-light-mediated, copper-catalysed decarboxylative fragmentation reactions. Reagents and conditions: (*i*) 10% CuCN, 5% dmp, 15% xantphos, blue LEDs, $Cl(CH_2)_2Cl$, 5–10 °C;[46] (*ii*) 1% $[Cu(NN)(PP)]BF_4$, 2 equiv iPr_2NEt, 1.5 equiv Hantzsch ester, blue LEDs, THF.[48]

In 2018, the generality of heteroleptic copper-based complexes in photoredox catalysis was further demonstrated by a study in which fifty copper-based complexes featuring various diphosphine and diimine ligands were tested against the decarboxylative fragmentation of *N*-(acyloxy)phthalimides **1.64** and subsequent coupling with alkynylbromides **1.65** (Scheme1.2.13B).[49] Many of these complexes efficiently catalysed the transformation to deliver good yields of the substituted alkyne product **1.66**. The ability to generate such a large range of heteroleptic copper-based complexes derives from their simple one step synthesis from, generally, commercially available materials.

Evano and co-workers reported a heteroleptic copper complex that can catalyse several visible-light-mediated photoredox transformations (Scheme 1.2.14).[50] Several heteroleptic copper-based complexes featuring phenanthroline and diphosphine ligands were screened in an aryl halide reduction reaction. A system featuring $[Cu(dmp)(DPEphos)]PF_6$ and diisopropylethylamine as terminal reductant was found to be the most efficient and this complex was chosen to test the generality of such heteroleptic complexes in a range of transformations. The reduction of both activated and unactivated aryl iodides proceeded in good yields, activated aryl bromides and even an activated aryl chloride also participated in the reduction reaction (Scheme 1.2.14A). A cyclisation reaction of aryl iodides with pendant

alkenes **1.66** was discovered to be efficient and general, with a wide range of *N*- and *O*-heterocycles, as well as carbocycles produced in modest to good yield (Scheme 1.2.14B). Finally, the direct arylation of (hetero)arenes with aryl iodides or bromides was achieved with 20 examples reported in generally good yield (Scheme 1.2.14C). This demonstrates the generality of heteroleptic copper-based complexes in photoredox catalysis and exploits the significant reducing power of heteroleptic copper(I) complexes.

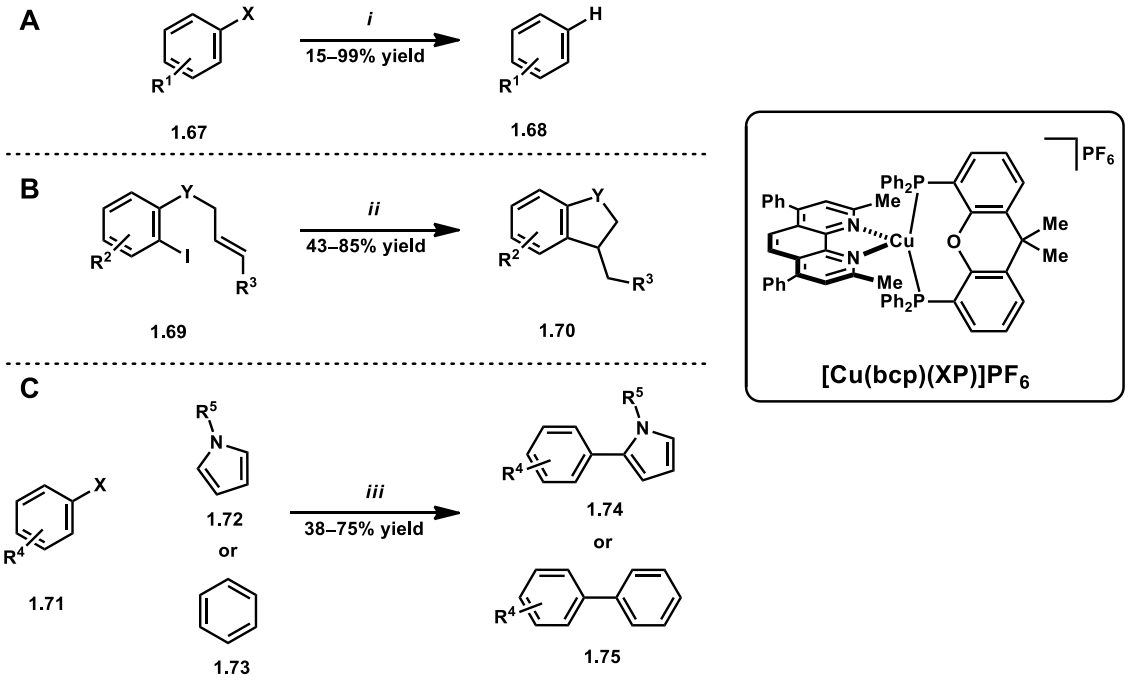

Scheme 1.2.14:[49] Reduction, ATRA and direct arylation reactions catalysed by a heteroleptic copper-based photoredox catalyst. Reagents and conditions: (*i*) 5% [Cu], 10 equiv *i*Pr$_2$NEt, blue LEDs, MeCN; (*ii*) 10% [Cu], 10 equiv *i*Pr$_2$NEt, blue LEDs, MeCN; (*iii*) 10% [Cu], 10 equiv *i*Pr$_2$NEt, blue LEDs, MeCN.

Finally, an atom-transfer radical polymerisation (ATRP) reaction between poly(ethyleneglycol) methyl ether methacrylate (PEGMA) and methyl methacrylate (MMA) was developed using [Cu(dap)$_2$]Cl as the photoredox catalyst.[51] The reaction mixture was irradiated at 420 nm and required the use of an initiator, ethyl-α-bromophenylacetate, and a tertiary amine, such as dimethylaniline, as sacrificial reductant. Polymer was obtained with polydispersity index as low as 1.15. The living nature of the system was verified by the preparation of block copolymers of PPEGMA-*b*-PMMA with high molecular weights and

narrow molecular weight distributions.

1.3 Summary and Project Aims

Despite numerous reports of visible light-mediated photoredox transformations featuring ruthenium- or iridium-based complexes since 2008,[3] reports of such transformations featuring copper-based complexes are conspicuously absent from the literature. In early 2015, when this project commenced, there were only six reports of copper-based complexes being used in photoredox catalysis.[27,32,41,44.,46] Apart from the seminal report by Sauvage and co-workers published in 1987, all these reports appeared after 2012. The scope of copper-based photoredox catalysis was limited in reaction scope, with most reports confined to ATRA reactions. Despite many reports of ruthenium- and iridium-based complexes catalysing photoredox α-amino C–H functionalisation processes, there were no reports utilising a copper-based photoredox catalyst. As of this date, there are now twenty-one studies published, including reports described within this thesis.[30,52]

The limited applications of visible-light-mediated photoredox-catalysed transformations employing earth abundant copper-based complexes potentially derives from less desirable photophysical properties when compared to the established ruthenium- and iridium-based complexes. Shorter excited state lifetimes of homoleptic, coordinatively unsaturated, distorted tetrahedral copper(I) complexes result from structural rearrangements that occur upon photoexcitation. These structural rearrangements are not apparent for coordinatively saturated, octahedral ruthenium- or iridium-based complexes.[28b]

With this context, the project has two key aims:

1. To prepare a range of new homoleptic phenanthroline-based copper(I) complexes to study their structural, photophysical and electrochemical properties to inform the use of these complexes in synthesis;
2. To exploit the intrinsic properties of these complexes to create novel copper photoredox-catalysed reactions.

1.4 References

(1) L. H. Friedburg, *J. Am. Chem. Soc.* **1899**, *21*, 445–454.

(2) G. Ciamician, *Science* **1912**, *36*, 385–394.

(3) For reviews on visible light photoredox catalysis published since 2012, see: (a) J. W. Tucker; C. R. J. Stephenson, *J. Org. Chem.* **2012**, *77*, 1617–1622; (b) J. Xuan; W.-J. Xiao, *Angew. Chem., Int. Ed.* **2012**, *51*, 6828–6838; (c) S. Maity; N. Zheng, *Synlett* **2012**, *23*, 1851–1856; (d) L. Shi; W. Xia, *Chem. Soc. Rev.* **2012**, *41*, 7687–7697; (e) C. K. Prier; D. A. Rankic; D. W. C. MacMillan, *Chem. Rev.* **2013**, *113*, 5322–5363; (f) M. Reckenthäler; A. G. Griesbeck, *Adv. Synth. Catal*. **2013**, *355*, 2727–2744; (g) T. Koike; M. Akita, *Synlett* **2013**, *24*, 2492–2505; (h) D. M. Schultz; T. P. Yoon. *Science* **2014**, *343*, 1239176; (i) J. W. Beatty; C. R. J. Stephenson, *Acc. Chem. Res.* **2015**, *48*, 1471–1484; (j) F. Tan; W. Xiao, *Acta Chim. Sinica*, **2015**, *73*, 85–89; (k) M. D. Kärkäs, J. A. Porco Jr., C. R. J. Stephenson, *Chem. Rev.* **2016**, *116*, 9683-9747; (l) A. Studer; D. P. Curran, *Angew. Chem., Int. Ed.* **2016**, *55*, 58–102; (m) N. A. Romero; D. A. Nicewicz, *Chem. Rev.* **2016**, *116*, 10075–10166; (n) K. L. Skubi; T. R. Blum; T. P. Yoon, *Chem. Rev.* **2016**, *116*, 10035–10074; (o) T. P. Nicholls; D. Leonori; A. C. Bissember, *Nat. Prod. Rep.* **2016**, *33*, 1248–1254; (p) M. Chen; M. Zhong; J. A. Johnson, *Chem. Rev.* **2016**, *116*, 10167–10211; (q) F. Teplý, In *Visible light photoredox Catalysis with* $[Ru(bpy)_3]^{2+}$*: General principles and the twentieth century roots*; B. König, Eds.; De Gruyter: Berlin, Germany, **2013**; Chemical Photocatalysis, pp 111–138; (r) D. W. Manley; J. C. Walton, *Beilstein J. Org. Chem.* **2015**, *11*, 1570–1582; (s) T. McCallum; S. Rohe; L. Barriault, *Synlett* **2017**, *28*, 289–305; (t) J. Z. Bloh; R. Marschall, *Eur. J. Org. Chem.* **2017**, 2085–2094; (u) W. Huang; X. Cheng, *Synlett* **2017**, *28*, 148–158; (v) Y. Fang; Y. Ma; M. Zheng; P. Yang; A. M. Asiri; X. Wang, *Coord. Chem. Rev.* **2017**, *373*, 83–115; (w) Z. Garlets; J. D. Nguyen; C. R. J. Stephenson, *Isr. J. Chem.* **2014**, *54*, 351–360; (x) T. Koike; M. Akita, *Synlett* **2013**, *24*, 2492–2505; (y) J. Lalevée; M.-A. Tehfe; F. Morlet-Savary; B. Graff; F. Dumur; D. Gigmes; N. Blanchard; J.-P. Fouassier, *Chimica* **2012**, *66*, 439–441; (z) M. Recjenthäler; A. G. Griesbeck, *Adv. Synth. Catal.* **2013**, *355*, 2727–2744; (aa) S. Telitel; F. Dumur; M. Lepeltier; D. Gigmes; J.-P. Fouassier; J. Lalevée, *C. R. Chim.* **2016**, *19*, 71–78; (ab) V. Srivastava; P. P. Singh, *RSC Adv.* **2017**, *7*, 31377–31392; (ac) J. K. Matsui; S. B. Lang; D. R. Heitz; G. A. Molander, *ACS Catal.* **2017**,

7, 2563–2575; (ad) M. Majek; A. J. von Wangelin, *Acc. Chem. Res.* **2016**, *49*, 2316–2327; (ae) D. M. Arias-Rotondo; J. K. McCusker, *Chem. Soc. Rev.* **2016**, *45*, 5803–5820; (af) K. A. Margrey; D. A. Nicewicz, *Acc. Chem. Res.* **2016**, *49*, 1997–2006; (ag) M. H. Shaw; J. Twilton; D. W. C. MacMillan, *J. Org. Chem.* **2016**, *81*, 6898–6926; (ah) N. Corrigan; S. Shanmugam; J. Xu; C. Boyer, *Chem. Soc. Rev.* **2016**, *45*, 6165–6212; 9 (ai) R. A. Angnes; Zhou Li; C. R. D. Correia; G. B. Hammond, *Org. Biomol. Chem.* **2015**, *13*, 9152–9167; (aj) S. Fukuzumi; K. Ohkubo, *Org. Biomol. Chem.* **2014**, *12*, 6059–6071; (ak) T. Koike; M. Akita, *Inorg. Chem. Front.* **2014**, *1*, 562–576; (al) D. P. Hari; B. König, *Chem. Commun.* **2014**, *50*, 6688–6699; (am) D. A. Nicewicz; T. M. Nguyen, *ACS Catal.* **2014**, *4*, 355–360; (an) Y. Xi; H. Yi; A. Lei, *Org. Biomol. Chem.* **2013**, *11*, 2387–2403; (ao) K. Zeitler, *Angew. Chem., Int. Ed.* **2009**, *48*, 9785–9789; (ap) G. Zhang; C. Bian; A. Lei, *Chin. J. Catal.* **2015**, *36*, 1428–1439; (aq) Y.-Q. Zou; J.-R. Chen; W.-J. Xiao, *Angew. Chem., Int. Ed.* **2013**, *52*11701–11703; (ar) T.P. Nicholls; D. Leonori; A. C. Bissember, *Nat. Prod. Rep.* **2016**, *33*, 1248–1254.

(4) N. A. Romero; D. A. Nicewicz, *Chem. Rev.* **2016**, *116*, 10075–10166.

(5) D. Hristova; D. Neshchadin; G. Gescheidt, *J. Phys. Chem. B* **2015**, *119*, 13883–13887.

(6) V. Balzani; G. Bergamini; F. Marchioni; P. Ceroni, *Coord. Chem. Rev.* **2006**, *250*, 1254–1266.

(7) Despite this transition being spin forbidden there remains a small possibility that it will occur. R. Englman; J. Jortner, *Mol. Phys.* **1970**, *18*, 145–164.

(8) L. Marzo; S. K. Pagire; O. Reiser; B. König, *Angew. Chem., Int. Ed.* **2018**, *57*, 10034–10072.

(9) (a) P. Rebaud; P. Leong, *Science* **2008**, *322*, 55–56; (b) M. N. Hopkinson; B. Sahoo; J.-L. Li; F. Glorius, *Chem. Eur. J.* **2014**, *20*, 3874–3886; (c) H. Huo; E. Meggers, *Chimia* **2016**, *70*, 186–191; (d) E. Jahn; U. Jahn, *Angew. Chem., Int. Ed.* **2014**, *53*, 13326–13328; (e) T. Koike; M. Akita, *Org. Biomol. Chem.* **2016**,*14*, 6886-6890; (f) Y. Liu; W. Dong, *Chin. J. Chem.* **2017**, *35*, 1491–1500; (g) K. Luo; W.-C. Yang; L. Wu, *Asian, J. Org. Chem.* **2017**, *6*, 350–367; (h) M. Peña-López; A. Rosas-Hernández; M. Beller, *Angew. Chem., Int. Ed.* **2015**, *54*, 5006–5008; (i)X.-D. An; S. Yu, *Tettrahedron Lett.* **2018**, *59*, 1605–1613; (j) K. N. Lee; M.-Y. Ngai, *Chem. Commun.* **2017**, *53*, 13093–13112; (k) J.-P. Goddard; C. Ollivier; L. Fensterbank, *Acc. Chem. Res.* **2016**, 19, 24–1936; (l) C.-J. Wallentin; J. D. Nguyen; C.

R. J. Stephenson, *Chimia* **2012**, *66*, 394–398; (m) J. Xie; H. Jin; C. Zhu, *Tetrahedron Lett.* **2014**, *55*, 36–48; (n) X. Sun; S. Yu, *Synlett* **2016**, *27*, 2659–2675; (o) J. Zhu; W.-C. Yang; X.-D. Wang; L. Wu, *Adv. Synth. Catal.* **2018**, *360*, 386–400.

(10) (a) B. Tóth; O. Tischler; Z. Novák, *Tetrahedron Lett.* **2016**, *57*, 4505–4513; (b) Z. Zuo; D. T. Ahneman; L. Chu; J. A. Terrett; A. G. Doyle; D. W. C. MacMillan, *Science* **2014**, *345*, 437–440; (c) O. Boubertakh; J.-P. Goddard, *Eur. J. Org. Chem.* **2017**, 2072–2084; (d) N. Hoffman, *ChemCatChem* **2015**, *7*, 393–394; (e) L. N. Cavalcanti; G. A. Molander, *Top. Curr. Chem.* **2016**, *374*, 1–23; (f) M. N. Hopkinson; A. Tlahuext-Aca; F. Glorius, *Acc. Chem. Res.* **2016**, *49*, 2261–2272; (g) J. C. Tellis; C. B. Kelly; D. N. Primer; M. Jouffroy; N. R. Patel; G. A. Molander, *Acc. Chem. Res.* **2016**, *49*, 1429–1439; (h) M. D. Levin; S. Kim; F. D. Toste, *ACS Cent. Sci.* **2016**, *2*, 293–301; (i) X. Lang; J. Zhao; X. Chen, *Chem. Soc. Rev.* **2016**, *45*, 3026–3038; (j) Y.-Y.Gui; L. Sun; Z.-P. Lu; D.-G. Yu, *Org. Chem. Front.* **2016**, *3*, 522–526; (k) C. Vila, *ChemCatChem* **2015**, *7*, 1790–1793; (l) M. Zhang; C. Zhu; L.-W. Ye, *Synthesis* **2016**, *48*, 1150–1157.

(11) J. A. Terrett; J. D. Cuthbertson; V.W. Shurtleff; D. W. C. MacMillan, *Nature* **2015**, *524*, 330−334.

(12) (a) M. Rüping; R. M. Königs; L. Atodiresei, In *Photoredox catalysed α-functionalisation of amines – Visible light mediated carbon–carbon and carbon–heteroatom bond forming reactions*; B. König, Eds.; De Gruyter: Berlin, Germany, **2013**; Chemical Photocatalysis, pp 169–184; (b) K. Zeitler; M. Neumann, In *Synergistic Visible light photoredox Catalysis*; B. König, Eds.; De Gruyter: Berlin, Germany, **2013**; Chemical Photocatalysis, pp 151–168; (c) K. Nakajima; Y. Miyake; Y. Nishibayashi, *Acc. Chem. Res.* **2016**, *49*, 1946–1956; (d) J. W. Beatty; C. R. J. Stephenson, *Acc. Chem. Res.* **2015**, *48*, 1474–1484.

(13) A. G. Condie; J. C. Gonzalez-Gomez; C. R. J. Stephenson, *J. Am. Chem. Soc.* **2010**, *132*, 1464–1465.

(14) (a) D. P. Hari; B. König, *Org.Lett.* **2011**, *13*, 3852–3855; (b) M. Reuping; R. M. Koenigs; K. Poscharny; D. C. Fabry; D. Leonori; C. Vila, *Chem. Eur. J.* **2012**, *18*, 5170–5174.

(15) (a) Z.-Q. Wang; M. Hu; X.-C. Huang; L.-B. Gong; Y.-X. Xie; J.-H. Li, *J. Org. Chem.* **2012**, *77*, 8705–8711; (b) S. Zhu; M. Reuping, *Chem. Commun.* **2012**, *48*, 11960–11962.

(16) (a) P. Kohls; D. Jadhav; G. Pandey; O. Reiser, *Org. Lett.* **2012**, *14*, 672–675; (b) L. Ruiz Espelt; E. M. Wiensch; T. P. Yoon; *J. Org. Chem.* **2013**, *78*, 4107–4114; (c) Y. Miyake; K.

Nakajima; Y. Nishibayashi, *J. Am. Chem. Soc.* **2012**, *134*, 3338–3341; (d) S. Zhu; A. Das; L. Bui; H. Zhou; D. P. Curran; M. Reuping, *J. Am. Chem. Soc.* **2013**, *135*, 1823–1829.

(17) (a) F. Le Vaillant; J. Waser, *Chimia* **2017**, *71*, 226–230; (b) H. Huang; K. Jia; Y. Chen, *ACS Catal.* **2016**, *6*, 4983–4988.

(18) (a) Y. Liu; R. Song; J. Li, *Sci. China Chem.* **2016**, *59*, 161–170; (b) J. Xuan; L.-Q. Lu; J.-R. Chen; W.-J. Xiao, *Eur. J. Org. Chem.* **2013**, 6755–6770.

(19) F. Mayr; R. Brimioulle; T. Bach, *J. Org. Chem.* **2016**, *81*, 6965–6971.

(20) D. W. Reynolds; N. L. Bauld, *Tetrahedron* **1986**, *42*, 6189–6194.

(21) (a) M.-Y. Cao; X. Ren; Z. Lu, *Tetrahedron Lett.* **2015**, *56*, 3732–3742; (b) T. Koike; M. Akita, *Org. Chem. Front.* **2016**, *3*, 1345–1349.

(22) (a) M. Akita; T. Koike, *C. R. Chim.* **2015**, *18*, 742–751; (b) R. Chaudhary; P. Natarajan, *ChismistrySelect* **2017**, *2*, 6458–6479; (c) T. Koike; M. Akita, *Top. Catal.* **2014**, *57*, 967–974; (d) T. Chatterjee; N. Iqbal; Y. You; E. J. Cho, *Acc. Chem. Res.* **2016**, *49*, 2284–2294.

(23) (a) O. A. Tomashenko; V. V. Grushin, *Chem. Rev.* **2011**, *111*, 4475–4521; (b) S. Purser; P. R. Moore; S. Swallow; V. Gouverneur, *Chem. Soc. Rev.* **2008**, *37*, 320–330; (c) K. Müller; C. Faeh; F. Diederich, *Science* **2007**, *317*, 1881–1886; (d) M. Schlosser, *Angew. Chem., Int Ed.* **2006**, *45*, 5432–5446.

(24) D. A. Nagib; D. W. C. MacMillan, *Nature* **2011**, *480*, 224–228.

(25) D. R. McMillin; M. T. Buckner; B. T. Ahn, *Inorg. Chem*. **1977**, *16*, 943–945.

(26) N. Armaroli, *Chem. Soc. Rev.* **2001**, *30*, 113–124.

(27) J.-M. Kern; J.-P. Sauvage, *J. Chem. Soc., Chem. Commun.* **1987**, 546–548.

(28) (a) N. Armaroli, *Chem. Soc. Rev.* **2001**, *30*, 113–124. (b) N. Armaroli; G. Accorsi; F. Cardinali; A. Listorti, In *Photochemistry and Photophysics of Coordination Compounds: Copper*; V. Balzani; S. Campagna, Eds.; Springer: Berlin, Germany, **2007**; Topics in Current Chemistry *280*, pp 69–116.

(29) S. Paria; O. Reiser, *ChemCatChem* **2014**, *6*, 477–2483.

(30) T. P. Nicholls; G. E. Constable; J. C. Robertson; M. G. Gardiner; A. C. Bissember, *ACS Catal.* **2016**, *6*, 451–457.

(31) (a) S.-P. Luo; E. Mejía; A. Friedrich; A. Pazidis; H. Junge; A.-E. Surkus; R. Jackstell; S. Denurra; S. Gladiali; S. Lochbrunner; M. Beller, *Angew. Chem., Int. Ed.* **2013**, *52*, 419–

423; (b) E. Mejía; S.-P. Luo; M. Karnahl; A. Friedrich; S. Tschierlei; A.-E. Surkus; H. Junge; S. Gladiali; S. Lochbrunner; M. Beller, *Chem. Eur. J.* **2013**, *19*, 15972–15978.

(32) (a) M. Pirtsch; S. Paria; T. Matsuno; H. Isobe; O. Reiser, *Chem. Eur. J.* **2012**, *18*, 7336–7340; (b) S. Paria; M. Pirtsch; V. Kais; O. Reiser, *Synthesis* **2013**, *45*, 2689–2689.

(33) (a) D. B. Bagal; G. Kachkovskyi; M. Knorn; T. Rawner; B. M. Bhanage; O. Reiser, *Angew. Chem., Int. Ed.* **2015**, *54*, 6999–7002; (b) S. K. Pagire; S. Paria; O. Reiser, *Org. Lett.* **2016**, *18*, 2106–2109; (c) T. Rawner; M. Knorn; E. Lutsker; A. Hossain; O. Reiser, *J. Org. Chem.* **2016**, *81*, 7139–7147; (d) T. Rawner; E. Lutsker; C. A. Kaiser; O. Reiser, *ACS Catal.* **2018**, *8*, 3950–3956; (e) A. Hossain; A. Vidyasagar; C. Eichinger; C. Lankes; J. Phan; J. Rehbein; O. Reiser, *Angew. Chem., Int. Ed.* **2018**, *57*, 8288–8292; (f) M. Knorn; T. Rawner; R. Czerwieniec; O. Reiser, *ACS Catal.* **2015**, *5*, 5186–5193.

(34) M. M. Cetin; R. T. Hodson; C. R. Hart; D. B. Cordes; M. Findlater; D. J. Casadonte Jr.; A. F. Cozzolino; M. F. Mayer, *Dalton Trans.* **2017**, *46*, 6553–6569.

(35) Z. Zhang; X. Tang; C. S. Thomoson; W. R. Dolbier Jr., *Org. Lett.* **2015**, *17*, 3528–3531.

(36) X.-J. Tang; W. R. Dolbier Jr., *Angew. Chem., Int. Ed.* **2015**, *54*, 4246–4249.

(37) S. H. Oh; Y. R. Malpani; N. Ha; Y.-S. Jung; S. B. Han, *Org. Lett.* **2014**, *16*, 1310–1313.

(38) (a) J.-M. Vincent; A. Rabion; V. K. Yachandra; R. H. Fish, *Can. J. Chem.* **2001**, *79*, 888–895; (b) T. Yajima; M. Ikegami, *Eur. J. Org. Chem.* **2017**, 2126–2129.

(39) V. V. Ahdankin; C. J. Kuehl; A. P. Krasutsky; M. S. Formaneck; J. T. Bolz, *Tetrahedron Lett.* **1994**, *42*, 47–51.

(40) G. Fumagalli; P. T. G. Rabet; S. Boyd; M. F. Greaney, *Angew. Chem., Int. Ed.* **2015**, *54*, 11481–11484.

(41) P. T. G. Rabet; G. Fumagalli; S. Boyd; M. F. Greaney, *Org. Lett.* **2016**, *18*, 1646–1649.

(42) A. C. Hernandez-Perez; A. Vlassova; S. K. Collins, *Org. Lett.* **2012**, *14*, 2988–2991.

(43) K. B. Joergensen, *Molecules* **2010**, *15*, 4334–4358.

(44) A. C. Hernandez-Perez; S. K. Collins, *Angew. Chem., Int. Ed.* **2013**, *52*, 12696–12700.

(45) B. Liégault; D. Lee; M. P. Huetis; D. R. Stuart; K. Fagnou, *J. Org. Chem.* **2008**, *73*, 5022–5028.

(46) A. Baralle; L. Fensterbank; J.-P. Goddard; C. Olivier, *Chem. Eur. J.* **2013**, *19*, 10809–10813.

(47) W. Zhao; R. P. Wurz; J. C. Peters; G. C. Fu, *J. Am. Chem. Soc.* **2017**, *139*, 12153–12156.

(48) N. M. Ahmad, *Name Reactions for Functional Group Transformations*; J. J. Li; E. J. Corey, Eds.; John Wiley & Sons: Hoboken, USA, **2007**; pp 438–450;

(49) C. Minozzi; A. Caron; J.-C. Grenier-Petel; J. Santandrea; S. K. Collins, *Angew. Chem., Int. Ed.* **2018**, *57*, 5477–5481.

(50) B. Michelet; C. Deldaele; S. Kajouj; C. Moucheron; G. Evano, *Org. Lett.* **2017**, *19*, 3576–3579.

(51) W. Ma; D. Chen; Y. Ma; L. Wang; C. Zhao; W. Yang, *Polym. Chem.* **2016**, *7*, 4226–4236.

(52) T. P. Nicholls; J. C. Robertson; M. G. Gardiner; A. C. Bissember, *Chem. Commun.* **2018**, *54*, 4589–4592.

Chapter Two

Synthesis and Characterisation of Copper(I) Complexes

This chapter describes the synthesis and characterisation of novel and known homoleptic and heteroleptic phenanthroline-based copper(I) complexes. Extensive characterisation of their structural, photophysical and electrochemical properties is discussed in the context of their viability as potential visible light photoredox catalysts. These complexes were screened in a notable ATRA reaction which is suggested to proceed through an inner sphere mechanism. This allows the properties of the complexes to be examined through an indirect method.

2.1 Introduction

Several homoleptic copper(I) complexes featuring phenanthroline ligands have been used in the past to catalyse highly efficient, visible-light-mediated, photoredox-catalysed transformations.[1] While the prototypical copper-based photoredox catalyst, $[Cu(dap)_2]^+$ (**2.1**) was first synthesised and used as a photoredox catalyst only 9 years after $[Ru(bpy)_3]^{2+}$,[2] its application in synthesis is far more limited (Figure 2.1.1A).[3] This may derive, in part, from pronounced structural rearrangements that occur upon photoexcitation for homoleptic bis(phenanthroline)copper(I) complexes.[1b] When the ground state copper(I) species absorbs a photon of visible light, a metal to ligand charge transfer (MLCT) occurs. This effectively oxidises the copper(I) metal centre from a d^{10} complex which displays a distorted tetrahedral coordination geometry to a copper(II), d^9 complex which adopts a more square planar coordination geometry. This pronounced structural rearrangement typically results in shorter excited state lifetimes for this class of complexes. Additionally, bimolecular quenching of the excited state by anions or solvent molecules is more prevalent due to the axial coordination sites that become available (Figure 2.1.1B). Interligand π-stacking interactions between the aryl group(s) on one ligand with the phenanthroline backbone of the other also results in significant distortion in the coordination geometry.[4] This structural

rearrangement is not observed for octahedral ruthenium and iridium complexes that are more commonly used as visible light photoredox catalysts (Figure 2.1.1A).[3e,i,k]

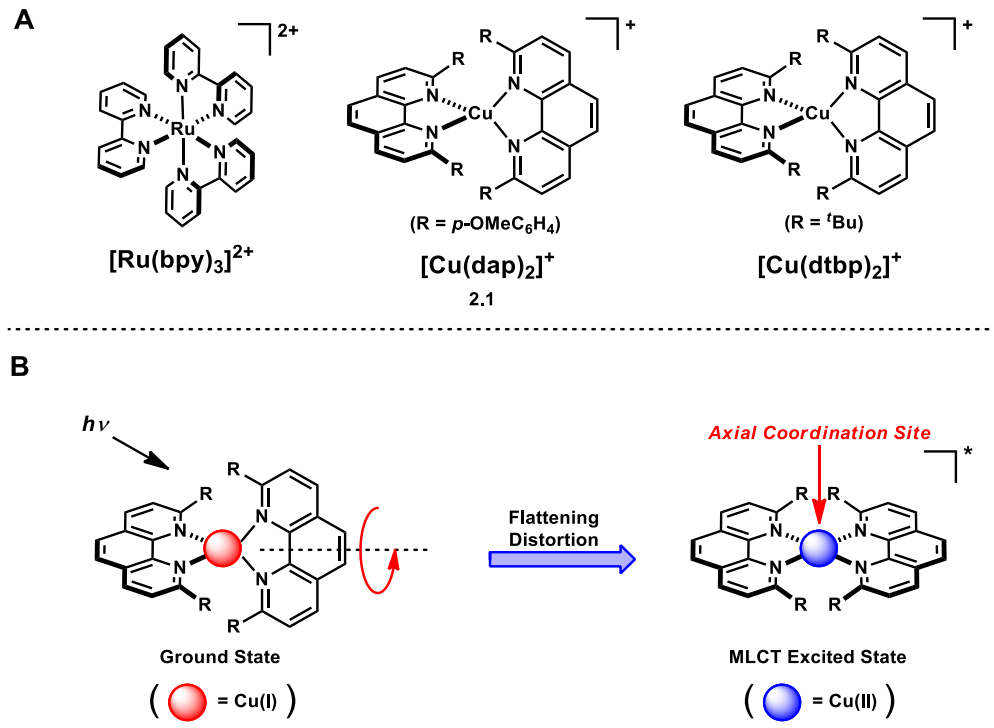

Figure 2.1.1: (A) The prototypical photoredox catalyst $[Ru(bpy_3]^{2+}$ and copper(I) complexes $[Cu(dap)_2]^+$ (**2.1**) and $[Cu(dtbp)_2]^+$. (B) Structural rearrangement that occurs upon photoexcitation for homoleptic bis(phenanthroline)copper(I) complexes.

Significant research has focused on tuning the photophysical properties of bis(phenanthroline)copper(I) complexes.[1] Complex molecular architectures based on bis(phenanthroline)copper(I) complexes have been studied including catenanes,[5] rotaxanes,[6] and dendrimers.[7] While these studies provide useful insights into the photophysics and photochemistry of this class of complexes, their use in photoredox catalysis is more limited. The coordination geometry of both the ground and excited states of bis(phenanthroline)copper(I) complexes has a profound impact on their photophysical and electrochemical properties.[1] A simple strategy to control the coordination geometry is to increase the steric bulk of the ligand. This is typically achieved by modification at the 2- and 9-positions of the phenanthroline backbone. Bis(phenanthroline)copper(I) complexes featuring unsubstituted phenanthroline ligands typically exhibit poor photophysical properties. Within this class, substituents at the 2- and 9-positions are generally accepted to

be requisite components of complexes that display significant luminescence.[1] Substituents in these positions will have a greater steric effect on the metal centre as they point toward it. This is exemplified by the bulky bis(2,9-di-*tert*-butylphenanthroline)copper(I) complex, $[Cu(dtbp)_2]^+$, reported by Burstyn and co-workers (Figure 2.1.1A).[8] Due to the extreme steric bulk of the *tert*-butyl groups, this complex features a tetrahedral coordination geometry in the ground state with very little distortion and has an increased excited state lifetime (1.9 μs). A detailed investigation of the photophysical properties of this complex revealed that the increased excited state lifetime derives from the absence of a flattening distortion presumably derived from the increased steric bulk.[9] The Cu–N bond lengths are the longest reported for this class of complex presumably due to the extreme steric crowding. This is exemplified by its coordinative instability in solution. Specifically, when the complex is dissolved in many common polar solvents that are typically utilised in photoredox catalysis, one of the ligands decoordinates resulting in a monophenanthroline complex. This instability limits its application in photoredox catalysis and suggests that 2,9-substituents of moderate steric bulk may be better suited to maintain coordinative stability while still providing desirable photophysical properties.

While several bis(phenanthroline)copper(I) complexes featuring 2,9-diaryl substituents have been synthesised in the past,[1,10] there has not been a systematic study of the effects of the 2,9-diaryl substituents on the structural, photophysical and electrochemical properties of their related complexes. It is possible that this class of complexes was not initially targeted as they typically exhibit shorter excited state lifetimes when compared to ruthenium- and iridium-based complexes. One contributing factor is the extensive π-stacking between an aryl substituent on one ligand with the phenanthroline backbone of the other. This interligand π-stacking interaction contributes to distortion in the tetrahedral coordination geometry away from the ideal D_{2d} symmetry.[1] However, phenanthroline ligands bearing 2,9-diaryl substituents provide enhanced steric shielding of the metal centre, which may limit nucleophilic attack that results in quenching of the excited state (Figure 2.1.2).[1] With this in mind, it was determined that the synthesis and characterisation of a library of homoleptic bis(2,9-diarylphenanthroline)copper(I) complexes would be valuable to contributing to the understanding of substituent effects in this class of complexes.

Furthermore, it was anticipated that this research would inform the application of these potential photoredox catalysts in synthesis.

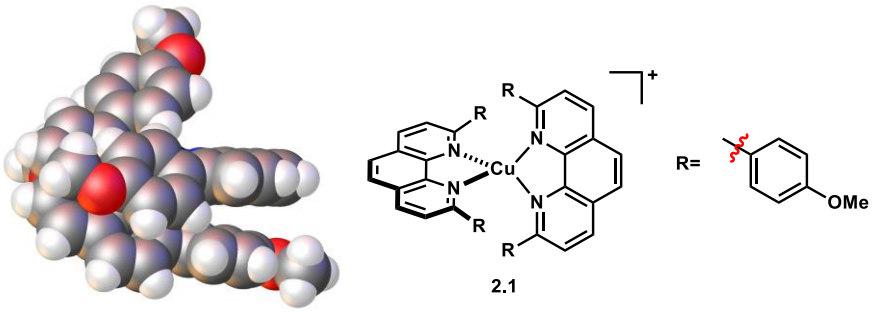

Figure 2.1.2: Space filling diagram of parent complex, $[Cu(dap)_2]^+$ (**2.1**) depicting the steric crowding of the metal centre provided by the 2,9-diaryl substituents.

In addition to homoleptic copper(I) complexes, a range of photoactive, phenanthroline-containing, heteroleptic derivatives have been used to mediate visible light photoredox-catalysed synthetic processes.[11] Several complexes within this class feature extended excited state lifetimes and significant redox potentials which highlight their capacity as photoredox catalysts. Heteroleptic copper(I) complexes featuring phenanthroline derivatives and phosphine ligands have been known since the early 1980s.[12] However, it was not until very recently that the utility of this class of complexes in synthesis was clearly demonstrated.[11] This derives from several factors including difficulties in their preparation or isolation and unsatisfactory photophysical properties associated with simple mono- or bidentate phosphine ligands featuring small bite angles.[12–14]

In 1981, McMillan and co-workers attempted to synthesise a heteroleptic copper(I) complex featuring phenanthroline derivatives and monodentate triphenylphosphine ligands. This resulted in a complex mixture of complexes being formed involving the phenanthroline ligand and varying degrees of phosphine incorporation and that these complexes exist in dynamic equilibrium.[13] Photophysical and electrochemical data for these systems were obtained with the complex $[Cu(dmp)(PPh_3)_2]^+$,[a] displaying an excited state lifetime of 330 ns and a reduction potential for the Cu^{I*}/Cu^{II} couple of –0.9 V vs. SCE. Unfortunately, the

[a] dmp = 2,9-dimethyl-1,10-phenanthroiline

difficulty in isolating the poorly defined complexes and the requirement of excess triphenylphosphine in the system to supress ligand dissociation, did not elicit any attempts to utilise these complexes as photoredox catalysts. Furthermore, the reduction potential of the Cu^{I*}/Cu^{II} couple is significantly lowered in comparison to complex **2.1** (–1.43 V vs. SCE).

The use of bidentate diphosphine ligands in these systems partially simplifies the dynamic equilibrium and results in a more well defined system.[14] However, a disproportionation reaction of heteroleptic $[Cu(N\hat{}N)(P\hat{}P)]^+$ complexes to form their homoleptic analogues occurs (Figure 2.1.3). The ratio of heteroleptic complex to homoleptic complexes can be influenced by the nature of the diphosphine ligand. The use of bidentate diphosphine ligands with small P–Cu–P bite angles, such as diphenylphosphinomethane (dppm), results in more of the homoleptic complexes being formed. As the bite angle of the diphosphine ligand increases, the ratio of heteroleptic to homoleptic complexes becomes more favourable and with sufficiently large bite angles the heteroleptic complex can be simply prepared and isolated. This can be explained by a destabilisation of the homoleptic bis(diphosphine) complex **2.3** with increasing bite angle as steric factors preclude its formation.

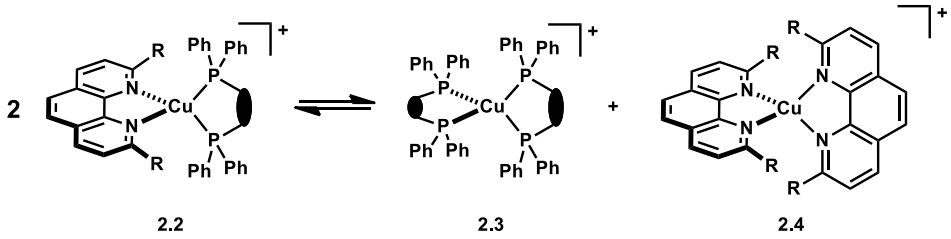

Figure 2.1.3: Dynamic equilibrium in solution between heteroleptic complexes and their homoleptic analogues.

The use of bidentate diphosphine ligands also improves the photophysical properties of this class of complexes. Within the series of copper(I) complexes featuring dmp and simple diphosphine ligands with the structure $Ph_2P(CH_2)_nPPh_2$ **2.5** (Figure 2.1.4), as the bite angle of the diphosphine ligand increases, a trend of longer excited state lifetimes is observed.[14] The complex with the largest P–Cu–P bite angle, which features a 1,4-diphenylphosphinobutane ligand, exhibits an impressive excited state lifetime of 10.8 μs. This is almost an order of magnitude longer than that of the prototypical photoredox catalyst $[Ru(bpy)_3]^{2+}$ (1100 ns).

Unfortunately, this complex still exists in dynamic equilibrium with its respective homoleptic complexes and thus features poor coordinative stability.

In 2002, McMillin and co-workers reported a photoactive, phenanthroline-based heteroleptic copper(I) complex containing a diphosphine ligand, $[Cu(dmp)(DPEPhos)]^+$ (**2.6**).[15] This complex exists in solution without any dynamic equilibrium observed. The use of the ligand DPEPhos, which has a natural bite angle of 102°,[b] sufficiently destabilises the homoleptic bis(diphosphine) complex and the desired heteroleptic complex **2.6** is formed in isolation. A further improvement in the excited state lifetime is observed (14.3 μs) and this complex exhibits a reduction potential for the Cu^{I*}/Cu^{II} couple of –1.64 V vs. SCE which is also an improvement on parent complex **2.1** (–1.43 V vs. SCE).

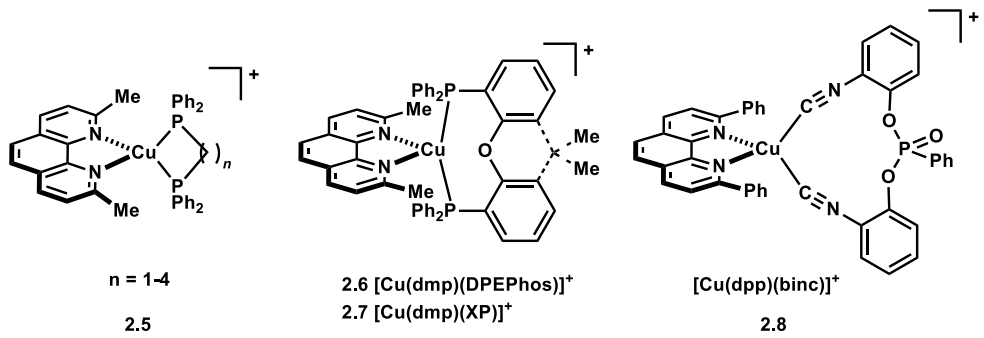

Figure 2.1.4: Examples of known phenanthroline-containing, heteroleptic copper(I) complexes.

The first example of a heteroleptic copper(I)-based complex used in photoredox catalysis was reported in 2012 with complex **2.6** used to catalyse the synthesis of [5]helicene.[11a] This complex was found to be superior to both $[Ru(bpy)_3]^{2+}$ and $[Ir(ppy)_2(dtbppy)]^+$ in this process. Since then, heteroleptic copper(I) complexes have been used to catalyse a range of chemical transformations including the synthesis of carbazoles,[11b] reduction of water to produce hydrogen,[11c,d] trifluromethylchlorosulfonylation of alkenes,[11e] and more recently, reduction of aryl halides,[11f] atom-transfer radical additions (ATRA),[11f] direct arylations, α-amino C–H finctionalisations,[11g] and decarboxylative couplings.[11j] This broad applicability showcases this classes significant redox potentials as well as its greatly improved

[b] The natural bite angle is defined as the preferred chelation angle determined by ligand backbone constraints only.[25]

photophysical properties.

While the heteroleptic diphosphine complexes can be synthesised and isolated, these species still suffer from disproportionation over long reaction times in polar solvents.[11f,g,j] For example, small quantities of the related homoleptic complexes have been observed in reaction mixtures at their completion.[11f] This derives from the lability of the diphosphine and phenanthroline-based ligands. In 2015, Reiser and co-workers developed several novel phenanthroline-based heteroleptic copper(I) complexes **2.8** featuring bis(isonitrile) ligands in place of diphosphine ligands (Figure 2.1.4).[11e] Importantly, the use of the bis(isonitrile) ligand overcomes the issue of disproportionation and extends the excited state lifetime (17 μs) while maintaining desirable electrochemical properties.

At the beginning of 2015, when this project was initiated, most of the synthetic applications of copper-based visible light photoredox catalysts involved homoleptic bis(phenanthroline)copper(I) complexes. As such, the synthesis of homoleptic copper(I) complexes was initially prioritised. As the project progressed, an increasing number of synthetic applications featuring heteroleptic copper(I) complexes were reported. Today, there are a similar number of reports between the two classes of complexes.

2.2 Preparation of 2,9-Diaryl-1,10-phenanthroline Ligands

2.2.1 Synthetic approaches to 2,9-diaryl-1,10-phenanthroline ligands

Methods for the installation of various alkyl and aryl groups to the 2- and 9-positions of 1,10-phenanthroline (**2.9**) are well established (Scheme 2.2.1).[16] There are two general strategies used to achieve this. The first involves deprotonation of both the 2- and 9-positions of 1,10-phenanthroline (**2.9**) which are both adjacent to an electronegative nitrogen atom.[16a] Deprotonation at this position is favourable due to the inductive electron-withdrawing effect of the electronegative nitrogen atom which increases the acidity of the α-protons in the 2- and 9- positions. Typically, alkyl/ aryllithium nucleophiles are used, and this alkyl/ aryl group is installed at both the 2- and 9-positions. This is followed by oxidation/ rearomatisation using MnO_2 to complete the synthesis (Scheme 2.2.1). While this one pot synthesis is attractive for some compounds, it is limited in scope and typically low yielding due to numerous

side products that complicate purification. Furthermore, aryllithium compounds are inherently reactive and depending on the position and properties of the functional groups required, production of the requisite substituted aryllithium may, in many cases, be particularly difficult. Indeed, when this procedure was attempted using *tert*-butyllithium, the disubstituted product was isolated in only 8% yield following multiple chromatographic steps and recrystallisations.

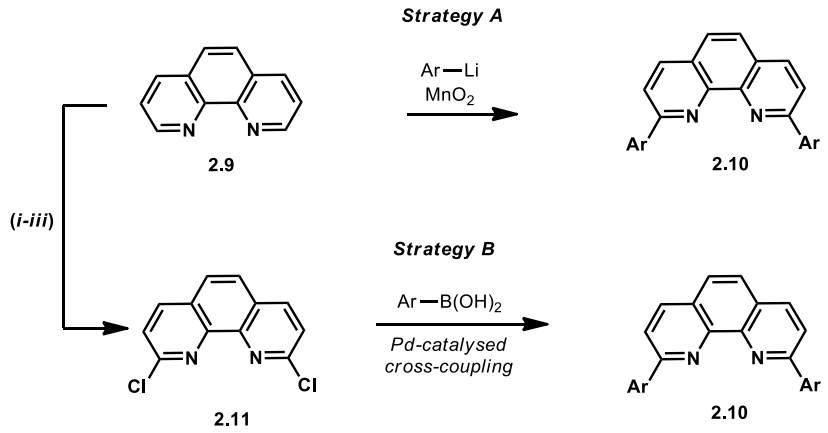

Scheme 2.2.1: Known synthetic routes to 2,9-diaryl-1,10-phenanthrolines. Reagents and conditions: (*i*) 1,3-diiodopropane, PhMe, 110 °C; (*ii*) ^{t}BuOK, ^{t}BuOH, air, 40°C; (*iii*) PCl_5, $POCl_3$, 110 °C.

An alternative to the above mentioned strategy involves the synthesis of key intermediate dichloride **2.11.**[16b] This compound is known to participate in cross-coupling reactions such as the Suzuki-Miyaura and Stille reactions.[16c] While bromides are typically more reactive than the equivalent chlorides under standard cross-coupling conditions derived from their lower bond dissociation energies,[17] α-nitrogen atoms activate the 2- and 9-positions of dichloride **2.11**. Furthermore, the synthesis of the analogous bromide would require the use of the far more expensive phosphoryl bromide. This alternative, and more modular, cross-coupling strategy offered a more viable and reliable approach for the synthesis of a library of related compounds that are directly accessible from key intermediate **2.11** using a range of commercially available boronic acids. Alternatively, boronate esters or organostannanes can be readily synthesised from commercially available aryl halides.

Employing boronic acids offered significant advantages relative to other nucleophiles in this protocol. There are a diverse range of boronic acids available from commercial vendors and their low toxicity and ease of handling compares favourably.[18]

2.2.2 Preparation of key intermediate 2,9-dichloro-1,10-phenanthroline (2.11)

The synthesis of key intermediate **2.11** was achieved in three steps, using previously reported chemical transformations on a multi-gram scale (Scheme 2.2.2).[16b] The first step in the synthesis was the protection of the basic nitrogen atoms of phenanthroline **2.9** using 1,3-diiodopropane. Precipitation of dication **2.12** using a non-polar solvent such as hexane allowed this material to be used in the next step without further purification. A base-mediated, autoxidation at the 2- and 9-positions of dication **2.12** delivered the oxidised product **2.13**. Finally, dichlorination at the 2- and 9-positions was achieved using phosphorous pentachloride and phosphoryl chloride as solvent. The use of phosphoryl chloride as solvent is not common due to several factors including its violent reaction with water. This incompatibility necessitates a complicated work-up and purification procedure, involving quenching of the phosphoryl chloride with large quantities of cracked ice that resulted in an amine hydrochloride salt that was difficult to extract into organic solvents and this resulted in yield losses. Ultimately, this three step sequence afforded the key intermediate, dichloride **2.11**, in 46% overall yield and each step could be performed on a multi-gram scale.

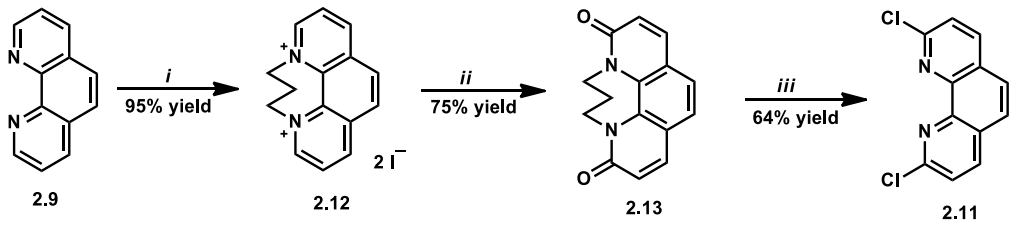

Scheme 2.2.2: Synthetic route to key intermediate phenanthroline **2.11**. Reagents and conditions: (*i*) 1,3-diiodopropane, PhMe, 110 °C; (*ii*) ^{t}BuOK, ^{t}BuOH, air, 40°C; (*iii*) PCl_5, $POCl_3$, 110 °C.[16b]

2.2.3 *Preparation of aryl nucleophiles for cross-coupling reactions*

While many aryl boronic acids are commercially available, a small number of the required aryl nucleophiles had to be synthesised. In all cases, this was achieved by adapting established methodology and making minor modifications (Scheme 2.2.3). For example, an Ullmann C–N coupling procedure was used to install an aryl group to the 1-position of carbazole (**2.14**).[19] This copper-catalysed C–N bond forming reaction required the use of only a catalytic amount of copper(I) iodide but also required an elevated temperature (180 °C) and the polar, aprotic solvent DMPU. Halogen–lithium exchange reactions were used to transform organic halides to organostannanes employing the strong base *n*-butyllithium.[20] Reacting the resultant aryllithium with tributylstannyl chloride at –78 °C afforded the required organostannanes. Finally, the production of boronate ester **2.20** involved a two step procedure in which phenol **2.18** was first methylated using sodium hydride and methyl iodide.[21] The resulting ether **2.19** was subjected to a palladium-catalysed Miyaura borylation reaction to furnish the boronate ester **2.20**.[22]

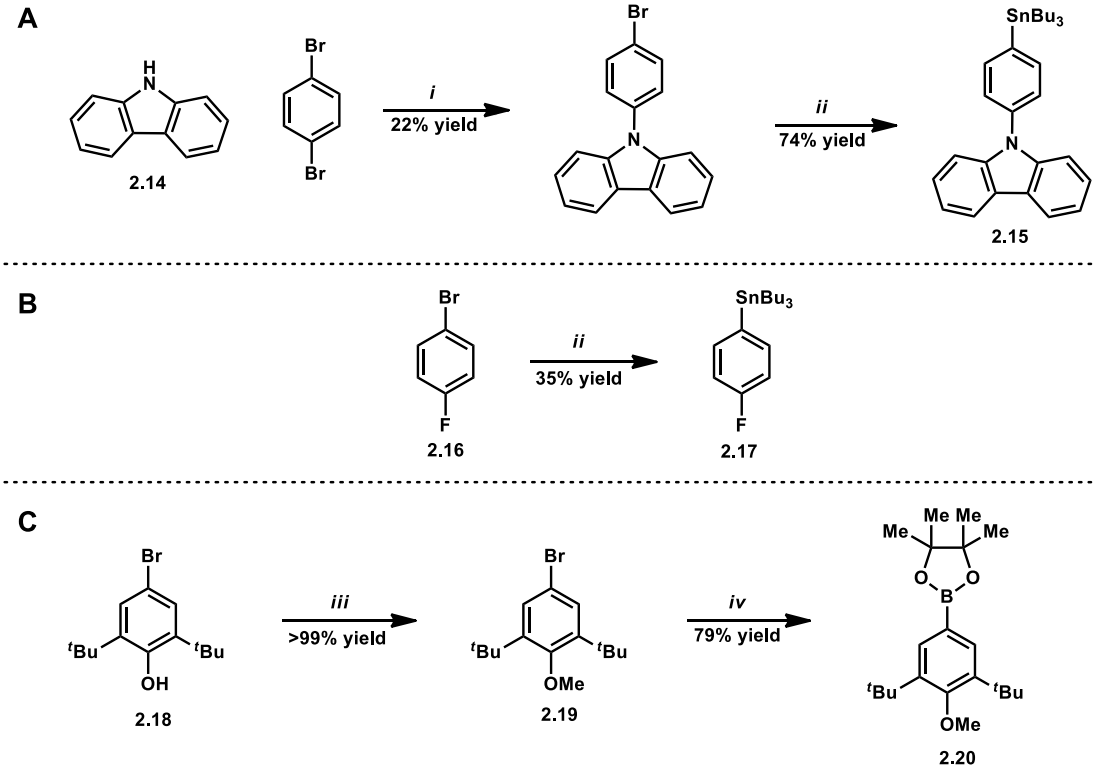

Scheme 2.2.3: Synthesis of aryl nucleophiles used in subsequent cross-coupling reactions. Reagents and conditions: (*i*) CuI, K_2CO_3, 18-crown-6, DMPU, 180 °C; (*ii*) *n*-BuLi, Bu_3SnCl, THF, –78-25 °C; (*iii*) NaH, MeI, 0–25 °C; (*iv*) B_2pin_2, $[Pd(PCy_3)_2Cl_2]$, KOAc, DMF, 150 °C.

2.2.4 Preparation of 2,9-diaryl-1,10-phenanthroline ligands

With key phenanthroline **2.11** in hand, it was possible to begin the synthesis of a library of 2,9-diaryl-1,10-phenanthroline ligands. A protocol developed by Sauvage and co-workers used to install a *p*-anisyl group at the 2- and 9-positions of dichloride **2.11** employed two equivalents of *p*-anisylboronic acid (**2.21**) and was completed in 18 h (Scheme 2.2.4).[16c] Under these conditions the desired diarylated product **2.23** was formed**,** however, a significant amount of monoarylated product **2.22** was also observed (15%). To overcome this, the amount of boronic acid **2.21** added to the reaction mixture was increased from two equivalents to four and after a 16 h reaction time the only product isolated was the diarylated product **2.23**.

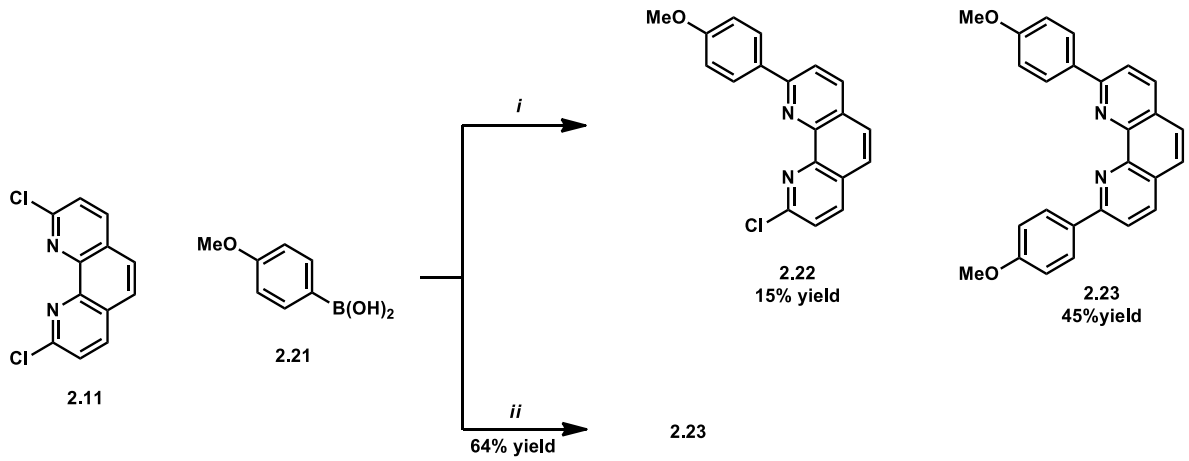

Scheme 2.2.4: Synthetic route to 2,9-di-*p*-anisyl-1,10-phenanthroline (**2.23**). Reagents and conditions: (*i*) 2 equiv **2.21**, $[Pd(PPh_3)_4]$, Na_2CO_3, PhMe:H_2O (2:1), 95 °C; (*ii*) 4 equiv **2.21**, $[Pd(PPh_3)_4]$, Na_2CO_3, PhMe:H_2O (2:1), 95 °C.

Utilising this modified protocol, a small library of novel and known 2,9-diaryl-1,10-phenanthroline ligands was prepared (Table 2.2.1). These ligands were designed to incorporate aryl substituents with varying electron withdrawing or donating groups and varying steric bulk so that the effect of these parameters on the properties of the complexes ultimately formed could be investigated. In addition, aryl groups such as *N*-phenylcarbazole and 9,9-dimethyl-9*H*-fluorene, which feature extended conjugation were also investigated, as this is a common feature in many photoactive compounds.[23]

Table 2.2.1: Library of 2,9-diaryl-1,10-phenanthroline ligands prepared via palladium catalysed cross-coupling reactions.

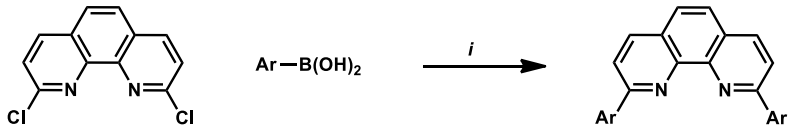

Ar	Yield (%)	Ar	Yield (%)
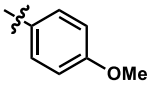 2.23	64	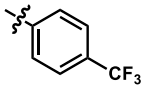 2.29	48
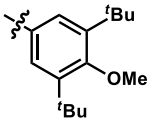 2.24	34[a]	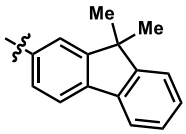 2.30	17
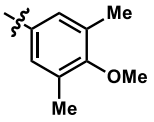 2.25	38	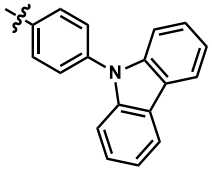 2.31	53[c]
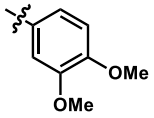 2.26	55	 2.32	56
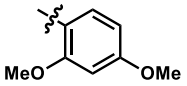 2.27	31	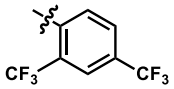 2.33	33
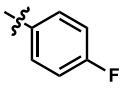 2.28	16[b]		

Procedure: (*i*) 1 equiv **2.11**, 4 equiv boronic acid, 10 mol % [$Pd(PPh_3)_4$], (2:1) PhMe:H_2O, 95 °C. [a]4 equiv of boronate ester **2.20** used instead of boronic acid. [b]4 equiv stannane **2.17** used instead of boronic acid. [c]4 equiv of stannane **2.15** used instead of boronic acid.

The modified protocol was successfully applied to the synthesis of eleven 2,9-diaryl-1,10-phenanthroline ligands. It should be noted that Suzuki–Miyaura couplings gave yields ranging from 31–64%. Stille couplings proceeded with similar efficiency (10–53% yield). No general trends associated with the electronic or steric nature of the aryl nucleophiles were identified in these coupling reactions. All of these reactions were unoptimised. Processes which do not rely on expensive transition metals should be sought if these ligands are highly

sought after in the future.

2.3 Preparation of Copper(I) Complexes

2.3.1 Preparation of homoleptic copper(I) complexes

With a library of ligands in hand, the final step in the synthesis of the homoleptic copper(I) complexes was the complexation. This was a very simple process, which is likely due to the strong affinity of the phenanthroline moiety for the copper(I) metal centre. This affinity is enhanced due to the chelate effect and the ligand forming a stable five-membered chelate ring with the metal centre.[1] The formation of these complexes was achieved by simply stirring the ligand and copper source in dichloromethane (Scheme 2.3.1A).[16c] In most cases, the formation of the bis(phenanthroline)copper(I) complex was accompanied by a rapid colour change from a colourless to deep red solution. However, the sterically bulky ligand **2.24** did not undergo this colour change immediately. The solution rapidly turned an orange colour before gradually changing to the deep red colour typical of bis(phenanthroline)copper(I) complexes, over several days. Similar observations have been reported.[8] This is likely due to the rapid formation of the monoligated complex **2.34** which exhibits the orange colour followed by slow formation of the bisligated complex **2.35** which is deep red. This hypothesis is supported by the appearances of isolated crystals of both mono- and bisligated species, which featured these respective colours (Scheme 2.3.1B).

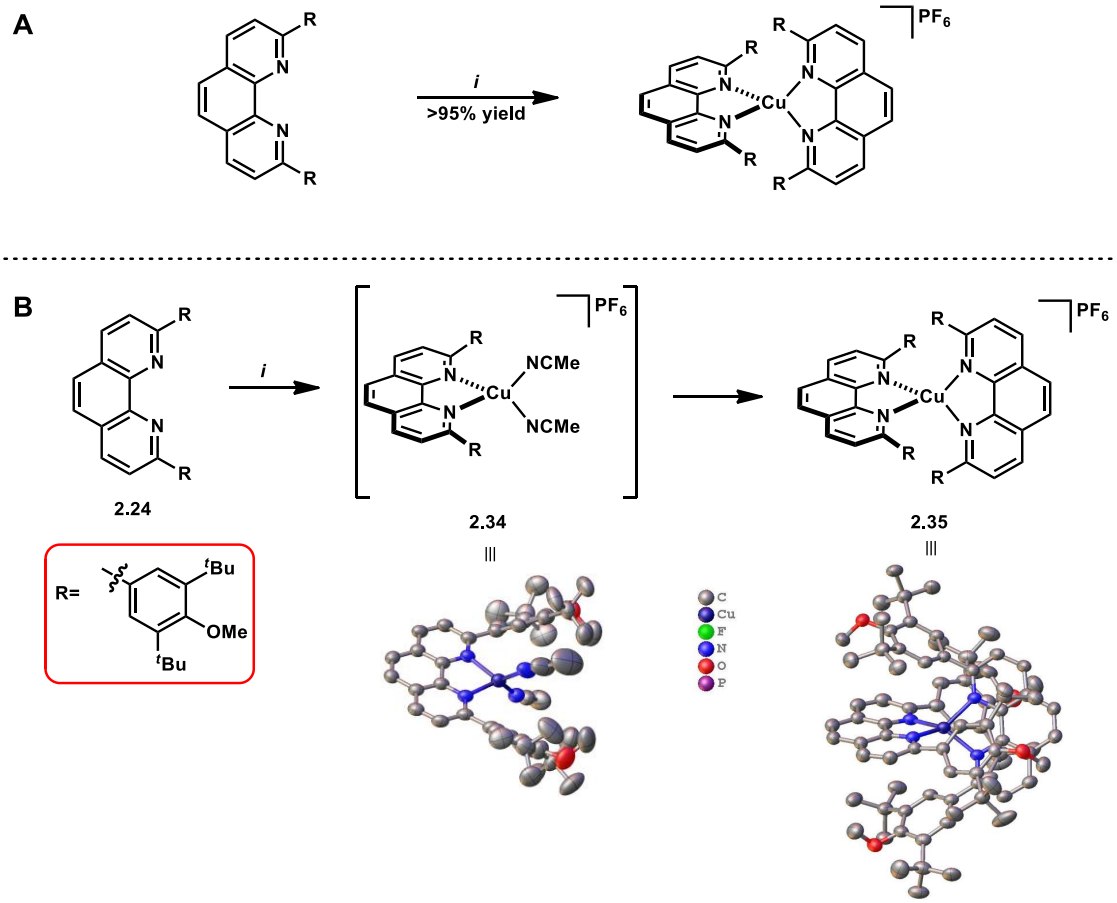

Scheme 2.3.1: General strategy for the synthesis of homoleptic copper(I) complexes. Reagents and conditions: (*i*) $[Cu(MeCN)_4]PF_6$, CH_2Cl_2, 25 °C. ORTEP representations of copper(I) complexes **2.34**, and **2.35**. Thermal ellipsoids are drawn at the 50% probability level. The residue containing a complete CuL_2 unit was chosen to display for complex **2.35**. Hexafluorophosphate anions, solvent molecules, hydrogen atoms and disorder have been omitted for clarity.

In most cases, the complexation step was simple, however, there were some challenges encountered. The difuryl ligand **2.32** gave a complex mixture of products when subjected to the reaction conditions outlined in Scheme 2.3.1A. While the production of the bisligated complex was evident, as judged by mass spectrometry, there was at least one other major product formed. The difficulty in separating the two species by crystallisation precluded its identification. It is possible that the Lewis basic oxygen atom present in the furyl rings are interacting in some way with the metal centre which may account for the unidentified product. Additionally, when ligand **2.33** was subjected to the reaction conditions for 2 h an inseparable complex mixture was obtained, and extended reaction times delivered similar results. It is possible that the steric bulk of the 2,4-bis(trifluoromethyl)phenyl group

disfavours formation of the bisligated complex and this is consistent with results published by Sadighi and co-workers who found that, when using the related bulkier 2,4,6-tris(trifluoromethyl)phenyl-1,10-phenanthroline ligand, only the monoligated complex was formed and the bisligated complex was not observed.[24] Ultimately, a range of ten homoleptic bis(phenanthroline)copper(I) complexes were successfully prepared and isolated (Figure 2.3.1). These species were then extensively characterised.

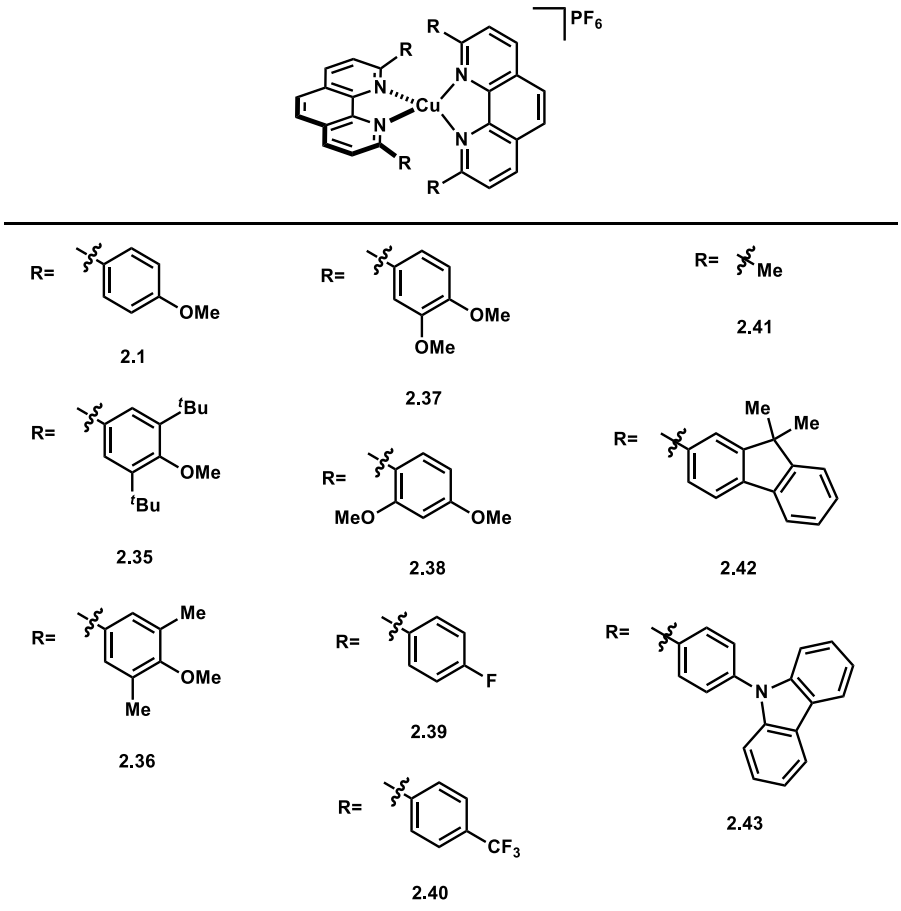

Figure 2.3.1: Homoleptic copper(I) complexes synthesised.

2.3.2 *Preparation of heteroleptic copper(I) complexes*

As noted earlier, statistical mixtures of homo- and heteroleptic complexes are formed when using diphosphine ligands with small bite angles.[14] Thus, only diphosphine ligands with large bite angles were selected in this study as the formation of well defined complexes is required to enable extensive and meaningful characterisation. The two diphosphine ligands selected were DPEphos (**2.44**) and xantphos (**2.45**) which feature natural bite angles

of 102° and 112° respectively (Figure 2.3.2).[c] In addition to large bite angles, the ether linkage present in both ligands allows the possibility of weak bonding interactions between the oxygen atom and the metal centre (Cu–O distance ~3.2 Å) that may contribute to higher thermal stabilities of the respective complexes.[25] Both these diphosphine ligands feature in known heteroleptic copper(I) photoredox catalysts.[11a-d,f-j]

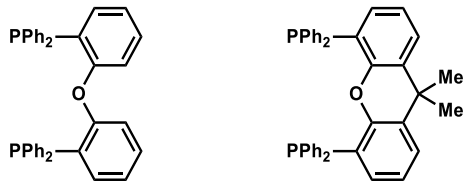

2.44 2.45

Figure 2.3.2: Diphosphine ligands used to form heteroleptic copper(I) complexes.

The synthesis of the heteroleptic complexes involved a two stage, one pot reaction (Scheme 2.3.2). In the first stage, the diphosphine ligand **2.44** or **2.45** was reacted with the copper source to form the diphosphinocopper(I) complex **2.46**. This complex presumably maintains a four coordinate structure with the remainder of the coordination sphere being filled by labile solvent molecules or the acetonitrile ligand present in the copper source. After formation of the chelating diphosphine complex **2.46** is complete, as judged by TLC, a dilute solution of a phenanthroline derivative was slowly added which rapidly complexes the diphosphinocopper(I) species **2.46**. This completed the synthesis of the heteroleptic complexes **2.47**. In total, four known heteroleptic copper(I) complexes were synthesised using this approach, all in >70% yields (Figure 2.3.3).

[c] The natural bite angle is defined as the preferred chelation angle determined by ligand backbone constraints only.[25]

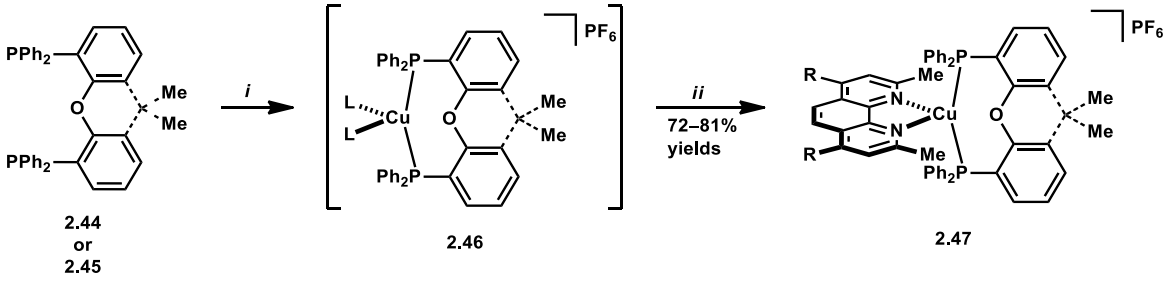

Scheme 2.3.2: Two stage, one pot synthesis of heteroleptic copper(I) complexes. Reagents and conditions: (*i*) $[Cu(MeCN)_4]PF_6$, CH_2Cl_2, 25 °C; (*ii*) 2,9-dimethylphenanthroline (dmp) or bathocuproine (bcp), CH_2Cl_2, 25 °C.

2.3.3 Summary

In total, a library of fourteen phenanthroline-containing copper(I) complexes were synthesised featuring both homo- and heteroleptic copper(I) complexes (Figure 2.3.1 and Figure 2.3.3). The range of homoleptic complexes synthesised allowed the investigation of the effect of varying steric and electronic parameters of the 2,9-diaryl substituents on the properties of the complexes as well as the effect of extended conjugation (*vide infra*). The heteroleptic complexes allowed comparisons to also be made between the two major classes of potential copper(I) photoredox catalysts.

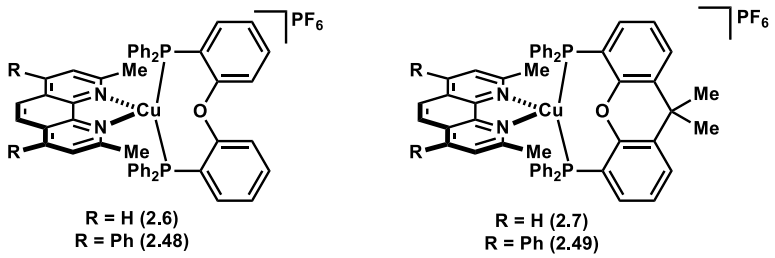

Figure 2.3.3: Heteroleptic copper(I) complexes synthesised.

2.4 Characterisation of Copper(I) Complexes

2.4.1 Introduction

The ability of a metal complex or organic dye to efficiently catalyse a visible light photoredox-catalysed process is predominately dependent on its physical and chemical properties.[26] The structural, photophysical and electrochemical properties of these

complexes, in both the ground and excited states, will largely determine their viability as photoredox catalysts. While these properties can be examined in isolation, it is essentially impossible to disentangle their effects because of two competing rate influences. For example, a copper(I) complex featuring bulky ligands will likely resist the structural rearrangement that occurs upon photoexcitation. This may lead to a longer excited state lifetime as is the case of the very bulky bis(2,9-di-*tert*-butyl-1,10-phenanthroline copper(I) complex ($[Cu(dtbp)_2]^+$) (Figure 2.1.1). However, the increased bulk leads to coordinative instability in a range of polar solvents making the complex less applicable to visible light photoredox catalysis. As such, these properties typically cannot be tuned orthogonally. While these distinct properties are discussed below in isolation, the interplay of these variables is certainly important to consider.

2.4.2 Structural characterisation of copper(I) complexes

Vapour diffusion of diethyl ether into saturated acetonitrile solutions of complexes **2.1**, **2.35**, **2.40**, and **2.42** provided dark red single crystals of these complexes (Figure 2.4.1). Complexes **2.40** and **2.42** belong to the monoclinic space group *C*2/*c* and complex **2.35** to the monoclinic space group *P*2/*c* while complex **2.1** belongs to the triclinic space group *P*–1. The asymmetric unit for complex **2.1** comprises a single CuL_2 unit and an anion residue. Both complexes **2.40** and **2.42** have crystallographic C_2 symmetry and each feature an acetonitrile solvent molecule and an anion residue that also resides on a crystallographic C_2 axis. The asymmetric unit for complex **2.35** includes one complete CuL_2 unit and two others residing on crystallographic C_2 axes, three diethyl ether and two acetonitrile solvent molecules and two complete anion residues. The Cu–N bond lengths were typical of related bis(2,9-diarylphenanthroline)copper(I) complexes. For example, Cu–N bond lengths of 2.032(3)–2.112(3) Å have been reported for [bis(2,9-diphenyl-1,10-phenanthroline)copper(I)] tetrafluoroborate (Table 2.4.1).[27]

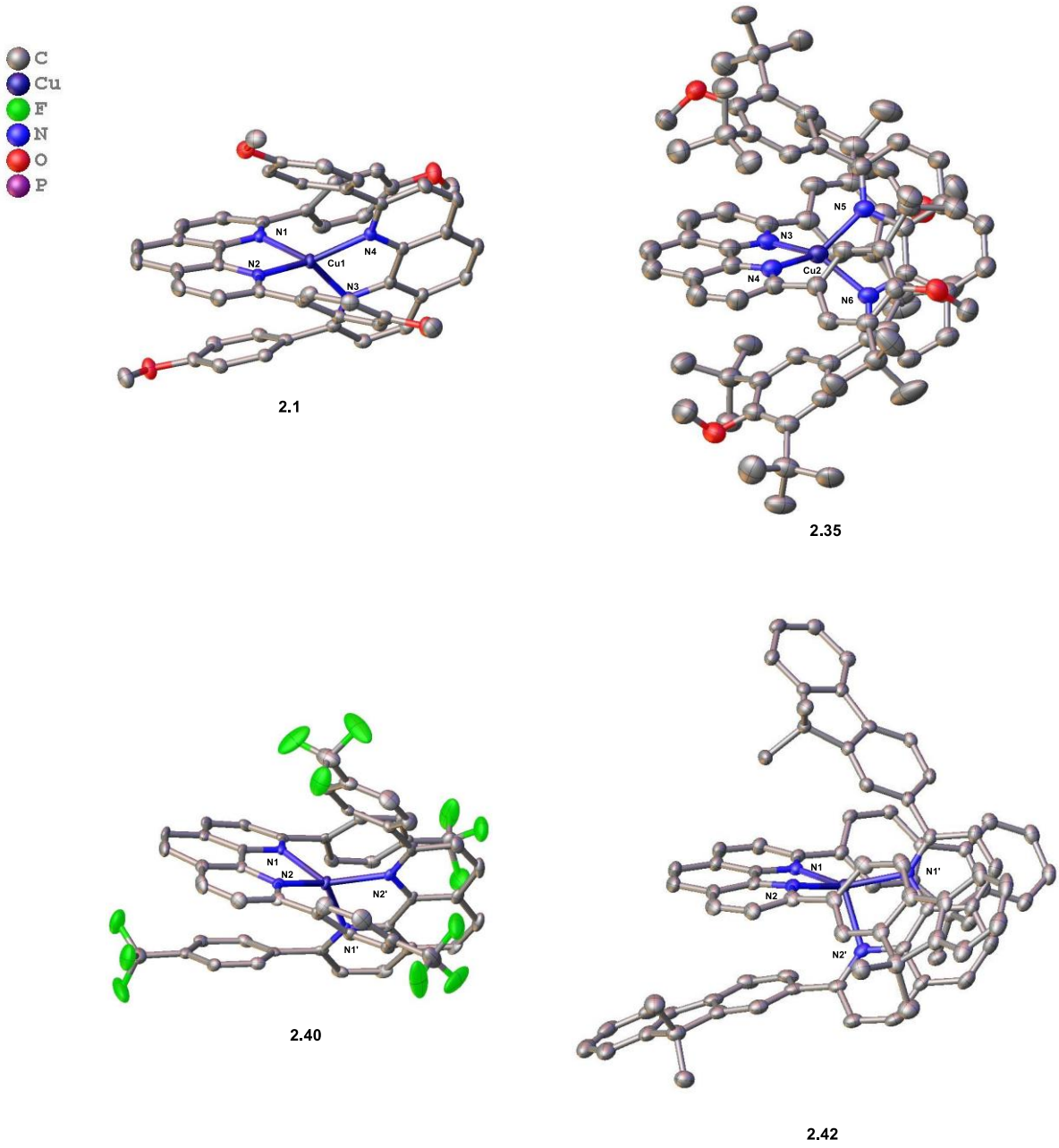

Figure 2.4.1: ORTEP representations of copper(I) complexes **2.1**, **2.35**, **2.40**, and **2.42**. Thermal ellipsoids are drawn at the 50% probability level. The residue containing a complete CuL_2 unit was chosen to display for complex **2.35**. Hexafluorophosphate anions, solvent molecules, hydrogen atoms and disorder have been omitted for clarity. Key bond lengths (Å) and angles (°): **2.1**; Cu–N1 2.045(2), Cu–N2 2.030(2), Cu–N3 2.055(2), Cu–N4 2.027(2), N1–Cu–N2 83.23(8), N3–Cu–N4 83.10(9), **2.35**; Cu1–N1 2.028(3), Cu1–N2 2.025(3), Cu2–N3 2.030(2), Cu2–N4 2.022(2), Cu2–N5 2.016(2), Cu2–N6 2.034(2), Cu3–N7 2.015(3), Cu3–N8 2.006(2), N1–Cu1–N2 84.68(18), N3–Cu2–N4 84.63(9), N5–Cu2–N6 84.34(9), N7–Cu3–N8 83.73(13), **2.40**; Cu–N1 2.055(3), Cu–N2 2.026(3), N1–Cu–N2 83.11(11), **2.42**; Cu–N1 2.000(2), Cu–N2 2.112(2), N1–Cu–N2 82.88(8).

There is significant distortion from the ideal D_{2d} symmetry in each of the complexes **2.1**, **2.35**, **2.40**, and **2.42** consistent with most previously reported

bis(phenanthroline)copper(I) species.[1a,3l,28] The distortions can be defined by three key components; flattening, rocking and wagging distortions (Table 2.4.1).[1a] Psuedo-tetrahedral copper(I) complexes commonly have the overall distortion in the coordination geometry quantified by examination of flattening, rocking and wagging distortions.[1a,29] Flattening distortions were quantified by measuring the interplanar angle between least squares planes of the coordination ring of each ligand. For an ideal tetrahedral structure, the angle would be 90° and an ideal square planar structure would be 0°. Rocking distortions were quantified by production of a vector between the metal centre and a centroid between C5 and C6 on the phenanthroline backbone of one ligand and measuring the obtuse angles to both nitrogen atoms of the other ligand from this vector. In an ideal tetrahedral structure these angles would be equal. The wagging distortion is defined as the distance between a least squares plane of the phenanthroline backbone of one ligand and the nitrogen atoms of the other ligand. In the absence of wagging these would be equal in absolute value.

Table 2.4.1: Quantification of the distortions within the coordination sphere of complexes **2.1(PF$_6$)**, **2.35**, **2.40**, and **2.42** and related complexes. The flattening distortion is defined by the interplanar angle between coordination planes for each ligand. The rocking distortion is defined by the angle between a centroid between C5 and C6, the metal centre and the nitrogen atoms on the other ligand. The wagging distortion is defined as the distance between a least squares plane of the phenanthroline backbone of one ligand and the nitrogen atoms of the other ligand. The π-stacking distance refers to the distance between a ring centroid of the aryl substituent on one ligand and the least squares plane of the phenanthroline backbone of the other.

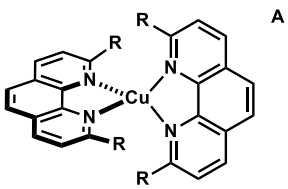

2.50: R = *t*Bu, A = B(C$_6$F$_5$)$_4$
2.51: R = 1-napthyl, A = CuBr$_2$

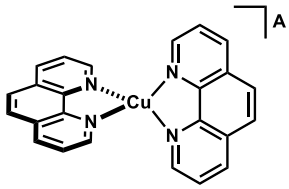

2.52(ClO$_4$): A = ClO$_4$
2.52(CuBr$_2$): A = CuBr$_2$

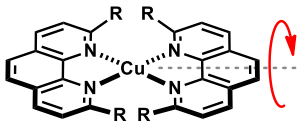

flattening distortion

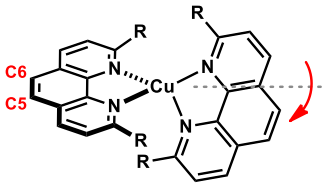

rocking distortion

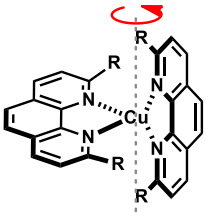

wagging distortion

[Cu]	flattening distortion (°)	rocking distortion (°)	wagging distortion (Å)	π-stacking distance (Å)
2.50	88.92(5)	136.26(4) & 138.90(3)	–1.322(2) & 1.519(2)	–
		133.19(3) & 142.38(4)	–1.076(2) & 1.7371(19)	
2.51	73.70(17)	113.57(13) & 158.59(13)	–0.134(8) & 2.365(6)	3.463(3) & 3.639(3)
		110.29(13) & 164.29(13)	–0.147(8) & 2.228(7)	
2.52(ClO$_4$)	54.4(5)	139.6(2) & 139.6(2)	–1.058(8) & 1.058(8)	–
		139.3(2) & 139.3(2)	–1.060(8) & 1.060(8)	
2.52(CuBr$_2$)	78.8(3)	123.9(2) & 149.88(16)	–0.560(10) & 1.925(9)	–
2.1(PF$_6$)	69.326(2)	119.537(2) & 157.0082(9)	–0.416046(13) & 1.93495(6)	3.41379(10) & 3.4001(1)
		124.569(3) & 150.259(1)	–0.80242(3) & 1.61656(6)	–
2.1(BF$_4$)	69.3(4)	121.5(2) & 155.22(18)	–0.495(12) & 1.879(11)	1.396(15)
2.35	64.567(11)–66.94(3)	137.21(7) & 137.21(7)	–1.220(2) &1.220(2)	3.5862(6)–3.8021(9)
		138.14(6) & 138.14(6)	–1.215(3) & 1.215(3)	
		137.37(2) & 138.259(11)	–1.0427(2) & 1.3268(3)	
		135.987(16) & 139.278(8)	–1.115031(18) & 1.20839(18)	
		137.77(8) & 137.77(8)	–1.194(3) & 1.194(3)	
		137.66(9) & 137.66(9)	–1.182(3) & 1.182(3)	
2.40	69.081(4)	119.737(2) & 155.445(1)	–0.61598(2) & 1.76772(7)	3.3836(1)
2.42	64.195(8)	109.364(7) & 162.497(3)	–0.150878(11) & 2.00949(14)	3.5378(3)

Bis(phenanthroline)copper(I) complexes **2.50** and **2.51** are shown for comparative purposes. Complex **2.51** arguably displays the least distortion from an ideal tetrahedral coordination geometry out of the series of 2,9-disubstituted bis(1,10-phenanthroline)copper(I) complexes.[8] The steric bulk of the *tert*-butyl groups and the absence

of π-stacking interactions presumably force the complex to adopt a more ideal tetrahedral geometry and all three flattening, rocking and wagging distortions remain minimal. Conversely, complex **2.51** displays one of the most distorted tetrahedral coordination geometries of the series reported.[30] This potentially stems from enhanced π-stacking interactions as a result of extended conjugation of the 1-napthyl groups.

Flattening distortions were prevalent in all complexes **2.1(PF$_6$)**, **2.35**, **2.40**, and **2.42** and likely originate from π-stacking interactions that become available with significant flattening. Furthermore, it has previously been suggested that the flattening distortion derives from more efficient packing in the crystal lattice.[28] The complex [bis(1,10-phenanthroline)copper(I)]$^+$ (**2.52**) displays significant variability in coordination geometry depending on the counter anion.[31] Complex **2.52(ClO$_4$)** exhibits a pronounced flattening distortion {54.5(5)°} but no rocking or wagging distortion is observed. In contrast, complex **2.52(CuBr$_2$)** displays only a modest flattening distortion {78.8(3)°} and significant rocking and wagging distortions. However, when comparing complexes **2.1(PF$_6$)** and **2.1(BF$_4$)** only small differences in each of the flattening, rocking and wagging distortions are observed.[32] It is possible that the strong π-stacking interaction that arises only when 2,9-diaryl substituents are present, increases the effect of intramolecular interactions such that intermolecular forces do not have a strong influence on the coordination geometry. Stronger intramolecular interactions derived from π-stacking may also explain the increased photoexcited state lifetimes observed for several [bis(2,9-diaryl-1,10-phenanthroline)copper(I)]$^+$ complexes when compared with related complexes that do not feature 2,9-diaryl substituents. The excited state lifetimes for the previously prepared and studied complex **2.1** (270 ns)[2] and [bis(2,9-diphenyl-1,10-phenanthroline)copper(I)] tetrafluoroborate (310 ns)[10a] which both feature 2,9-diaryl substituents are significantly increased compared to [bis(2,9-dimethyl-1,10-phenanthroline)copper(I)] chloride (90 ns)[33] which features 2,9-dimethyl substituents that are incapable of participating in π-stacking. The flattening distortion in complex **2.40** is similar to that of complex **2.1(PF$_6$)** (Table 2.4.1). Both of these complexes feature aryl substituents with similar steric bulk (*p*-OMeC$_6$H$_4$ and *p*-CF$_3$C$_6$H$_4$). Due to their low steric bulk both these substituents allow efficient π-stacking interactions. The flattening distortion was more pronounced in complexes **2.35** and **2.42**. Whilst this is associated with the increased steric bulk on the 2,9-diaryl substituents the intra- and intermolecular influences are complex.

The rocking distortion for complex **2.40** was also similar to that of complex **2.1(PF$_6$)** and these complexes also exhibit similar π-stacking distances to each other (Table 2.4.1). In contrast, the rocking distortion is increased in complex **2.42**. The *gem*-dimethyl groups present in complex **2.42** provide an increase in the π-stacking distance, however, a more pronounced rocking distortion is observed. The rocking distortion in complex **2.35** is significantly reduced and a longer π-stacking distance is observed. Potentially, the greater steric bulk, particularly of the di-*m*-(^{t}Bu) groups and the symmetrical distribution of the bulk almost completely prevents the rocking distortion in **2.35**.

Wagging distortions follow a similar trend with the extent of the distortion for complex **2.40** remaining similar to that of complex **2.1(PF$_6$)** and complex **2.35** displays more limited distortion. This potentially derives from the steric parameters of the respective aryl substituents. Interestingly, complex **2.42** features the most significant distortion. This potentially originates from the unsymmetrical steric bulk of the 2,9-diaryl substituents with the orientation of the *gem*-dimethyl group forcing a more significant wagging distortion.

Armaroli and co-workers previously reported complex **2.35** and demonstrated its kinetic inertness to ligand dissociation.[9] These researchers demonstrated that the complex was inert to ligand exchange even in the presence of excess 1,10-phenanthroline, over extended time frames and at reflux in dichloromethane or acetonitrile despite the lack of steric bulk in unsubstituted 1,10-phenanthroline. This contrasts with related homoleptic bis(phenanthroline)copper(I) complexes that feature less bulky ligands than **2.24**. Such complexes typically participate in ligand substitution reactions in the presence of even less bulky 1,10-phenanthroline-based ligands according to the HETPHEN (heteroleptic bisphenanthroline complexes) principle.[34] Armaroli and co-workers also reported extended timeframes for the synthesis of complex **2.35** and suggested that these observations derive from the steric bulk of the ligand, however, the solid state structure was not reported in that study. Notably, the solid state structure reported here suggests that the bulk of the 2,9-diaryl substituents in complex **2.35** may be responsible for the kinetic locking of the ligands within the complex. The high steric congestion in this complex **2.35**, discussed above, supports this.

The use of 2,9-diaryl substituents that allow π-stacking interactions results in significant distortion in the ground state coordination geometry of the complexes. This distortion can be minimised by the use of sterically bulky substituents which make the π-

stacking interactions less efficient and force the complexes to adopt more ideal tetrahedral geometries as in the case for complex **2.35**. Furthermore, variation of the steric properties of the complexes has broader implications within photoredox catalysis (*vide infra).*

Crystal structures of heteroleptic complexes **2.6**, **2.7**, and **2.49** were also obtained. Vapour diffusion of diethyl ether into saturated solutions of either dichloromethane (**2.6**) or acetonitrile (**2.7** and **2.49**) provided pale yellow single crystals of these complexes (Figure 2.4.2). Complexes **2.7** and **2.49** belong to the triclinic space group *P*–1 and complex **2.6** to the triclinic space group *P*1. The asymmetric unit for complex **2.6** features two complete CuL_2 units, two anion residues and two dichloromethane solvent molecules. The asymmetric unit for complex **2.7** simply features a complete CuL_2 unit and anion residue and complex **2.49** features a complete CuL_2 unit two anion residues that lie on crystallographic C_2 axes and a diethyl ether solvent molecule. Solid state structures of complexes **2.6**, **2.7** and **2.49** have previously been reported. However, in each case these complexes feature either different anions or solvent molecules.[15,11i,35] All Cu–N and Cu–P bond lengths and N–Cu–N and P–Cu–P bond angles are typical of this class of complexes (Figure 2.4.2).

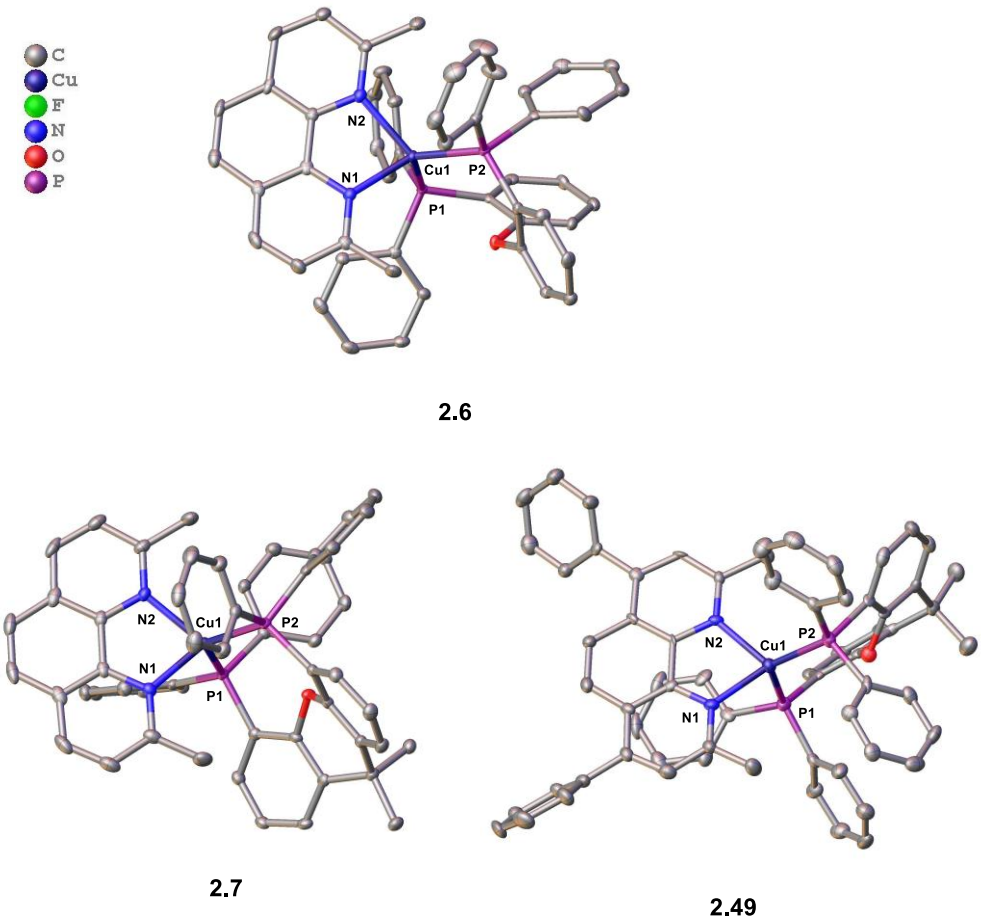

Figure 2.4.2: ORTEP representations of heteroleptic copper(I) complexes **2.6**, **2.7**, and **2.49**. Thermal ellipsoids are drawn at the 50% probability level. Hexafluorophosphate anions, solvent molecules, hydrogen atoms and disorder have been omitted for clarity. Key bond lengths (Å) and angles (°): **2.6** Cu1–N1 2.077(4), Cu1–N2 2.124(4), Cu1–P1 2.2489(12), Cu1–P2 2.3063(12), N1–Cu1–N2 80.54(14), P1–Cu1–P2, 113.85(5); **2.7** Cu1–N1 2.0881(15), Cu1–N2, 2.0960(15), Cu1–P1 2.2854(5), Cu1–P2 2.2638(5), N1–Cu1–N2 115.33(4), P1–Cu1–P2 120.303(19); **2.49** Cu1–N1 2.0703(16), Cu1–N2 2.1028(16), Cu1–P1 2.2432(5), Cu1–P2 2.2998(6), N1–Cu1–N2 80.48(6), P1–Cu1–P2 119.71(2).

The heteroleptic copper(I) complexes **2.6**, **2.7**, and **2.49** display similar distorted tetrahedral coordination geometries to the homoleptic copper(I) complexes, however, the overall distortion is reduced (Table 2.4.2). This likely derives from the absence of interligand π-stacking interactions. In all cases, the flattening distortion is less than 10° away from the ideal 90° that would be expected for an ideal tetrahedral coordination geometry. Rocking distortions remain significant in all complexes **2.6**, **2.7**, and **2.49**, however, it is moderately reduced in complex **2.7**. Wagging distortions are also prevalent in each of the complexes **2.6**, **2.7**, and **2.49**. Given the reduced number of crystal structures reported for this class of

heteroleptic copper(I) complexes it is not possible to perform an extensive analysis of these distortions as was the case for the homoleptic copper(I) complexes.

Other interesting aspects of the solid state structures of the heteroleptic complexes **2.6**, **2.7**, and **2.49** are that the diphosphine ligands are distinctly less flat when compared to a phenanthroline ligand which features an almost perfectly planar backbone due to uninterrupted conjugation. The xantphos ligand (**2.45**) displays a V-shaped geometry in both complexes **2.7** and **2.49** and the DPEphos ligand (**2.44**), which features only a single ether linkage between phenyl rings, has almost a 90° angle between these two rings in complex **2.6**. The respective bite angles of the diphosphine ligands remain large with complexes **2.6**, **2.7** and **2.49** featuring P–Cu–P bite angles of 113.85(5)°, 120.30319)° and 119.71(2)°, respectively (Figure 2.4.2). The Cu–O distance between the metal centre and the oxygen atom in the diphosphine ligand is within 3.1663(12)-3.21232(5) Å in all cases, which is indicative of a weak interaction. Potentially, if this interaction is maintained in the photoexcited state, one of the axial coordination sites that becomes available with significant flattening of the coordination geometry may be blocked.

Table 2.4.2: Quantification of the distortions within the coordination sphere of complexes **2.6**, **2.7** and **2.49**. The flattening distortion is defined by the interplanar angle between coordination planes for each ligand. The rocking distortion is defined by the angle between a centroid between C5 and C6, the metal centre and the phosphorous atoms on the other ligand. The wagging distortion is defined as the distance between a least squares plane of the phenanthroline backbone of one ligand and the phosphorous atoms of the other ligand.

[Cu]	flattening distortion (°)	rocking distortion (°)	wagging distortion (Å)
2.6	82.1306(18)	101.0711(16) &148.8928(7)	–0.467358(9) & 2.87602(5)
	84.0897(18)	101.7899(16) & 144.2553(8)	–0.339420(6) & 2.87736(5)
2.7	87.37(4)	106.911(18) & 132.592(18)	–1.1216(18) & 2.6361(14)
2.49	85.7603(13)	96.8790(15) & 143.1026(7)	–0.919385(16) & 2.57591(5)

2.4.3 Photophysical characterisation of copper(I) complexes

The photophysical properties of the copper(I) complexes are perhaps the most important factor in determining their efficiency as photoredox catalysts.[3,11] Thus, properties such as molar absorptivity, emission quantum yield and excited state lifetime are of particular interest when designing or identifying potential photoredox catalysts.[36] The molar absorptivity of the complex, especially at the excitation wavelength, is important as this will

have a direct impact on the amount of catalyst in its active, excited state at any given time. The emission quantum yield describes how likely emission from the complex is, given a set number of photons being introduced into the system. While emission itself is not required to turn over the catalyst, this provides a measure of the likelihood of the catalyst to absorb a photon and subsequently oxidise/ reduce an organic donor/ acceptor. Finally, the length of the excited state lifetime is important, as longer lifetimes result in the catalyst spending more time in its active state. While these properties will have the most significant impact on the efficiency of the copper(I) complexes as photoredox catalysts, there are also several other interesting photophysical properties that can be examined. The collection of extensive photophysical data required specialised equipment and these experiments were performed by the author in Professor Max Massi's laboratory at Curtin University.

The absorption spectra of the homoleptic copper(I) complexes were typically quite similar with most complexes exhibiting strong absorption bands between 220 nm and 400 nm which are attributed to π–π^* transitions within the ligands. Given the high degree of conjugation within the ligands themselves, this result is expected. Many complexes also exhibited a weaker, but significant, absorption band between 420–460 nm (Figure 2.4.3). This band is attributed to the MLCT excitation.[1] Fortunately, this broad absorption band falls within the visible spectrum and shows that these complexes could likely be excited by irradiating with visible light. The MLCT absorption band is most prominent in complexes **2.36**, **2.38**, **2.39**, **2.40** and **2.41** as is reflected by their molar absorptivities at their respective λ_{max} (Table 2.4.1). Both complexes **2.39** and **2.40** feature electron withdrawing groups whereas **2.36** and **2.38** feature electron donating groups. As such, these results suggest tuning the electronic parameters of the ligand does not significantly influence the proficiency of the MLCT excitation process. Varying steric factors do not provide a discernible trend either and both complexes featuring extended conjugation (**2.42** and **2.43**) do not improve the efficiency of the MLCT band. However, the intensity of the π–π^* transitions in complex **2.43** are greatly increased. While it is difficult to ascertain the reasoning behind such varying absorption properties it is worth noting that many of these complexes display a more prominent MLCT absorption band than the parent complex **2.1**, suggesting that they may perform well as photoredox catalysts.[2]

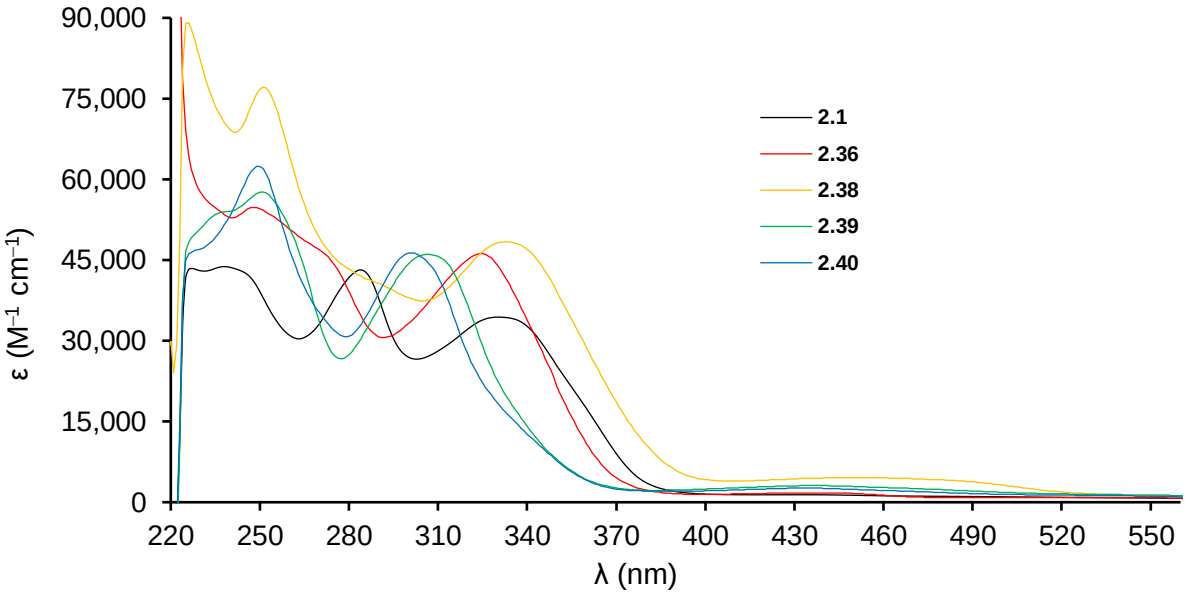

Figure 2.4.3: Absorption spectra of selected homoleptic copper(I) complexes depicting the MLCT absorption band.

The emission spectra of the homoleptic copper(I) complexes were also obtained. When employing excitation wavelengths between 300–330 nm, these complexes typically exhibit relatively sharp emission bands centred around 360-400 nm. This is attributed to the π–π* transitions within the phenanthroline-derived ligands and this assignment is supported by short excited state lifetimes as well as small Stokes shifts. The Stokes shift is the difference between the absorption and emission λ_{max} of the same electronic transition.[37] π–π* transitions are typically characterised by small Stokes shifts while MLCT transitions typically display large Stokes shifts. The small variation in λ_{max} for the π–π* transitions in homoleptic copper(I) complexes is likely derived from differing electronic environments within the ligand due to the various 2,9-diaryl substituents. A significant red shift is observed for complex **2.43** with λ_{max} centered at 444 nm. Complex **2.43** features a carbazole group which extends the conjugation beyond the phenanthroline backbone. Carbazole-containing compounds are known to have distinctive photophysical properties and as such this variation is not unexpected.[38]

A broad emission profile from ~600–800 nm and beyond, attributed to the MLCT emission, is also observed for many of the complexes (Figure 2.4.4).[d] The assignment of MLCT

[d] Detection beyond 800 nm was not performed as this requires a near infrared detector.

emission is based on large Stokes shifts and long excited state lifetimes which are indicative of phosphorescence, as well as comparison to known related complexes.[1] The emission profile of the parent complex **2.1** did not exhibit an MLCT band. This suggests that the efficiency of emission from the MLCT excited complex is increased in many of the new complexes and this is reflected in their greater emission quantum yield.

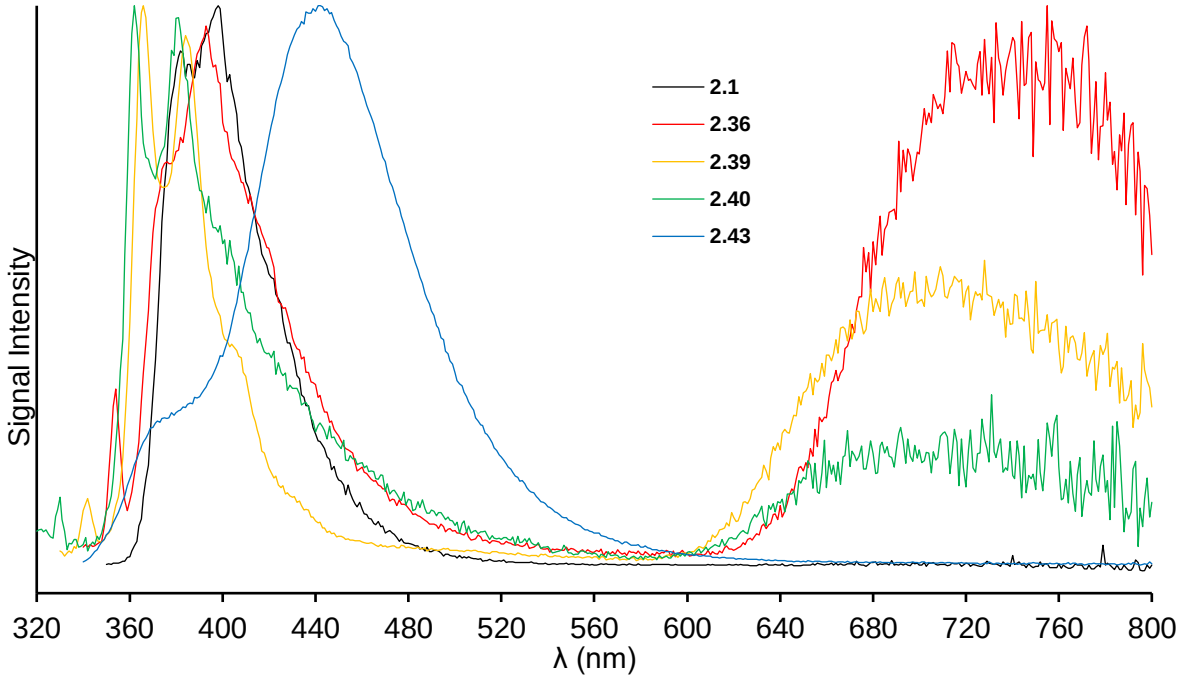

Figure 2.4.4: Emission spectra of selected homoleptic copper(I) complexes.

Measuring the emission spectra at 77 K gave further information about the electronic parameters of the complexes. The observation of a red shift of the λ_{max} in emission spectra when recorded at 77 K as opposed to 298 K, is a well known phenomenon for photoactive copper(I) complexes.[36a] This red shift derives from the similarity in energy between the singlet and triplet MLCT excited states. At higher temperatures thermal repopulation of the ^{1}MLCT from the ^{3}MLCT can occur and emission from this higher energy excited state is prevalent. Conversely, at lower temperature this repopulation of the higher energy ^{1}MLCT is less prevalent so emission from the lower energy ^{3}MLCT predominates. This results in a red shift of the emission λ_{max} at lower temperature due to the larger energy gap (Figure 2.4.5).

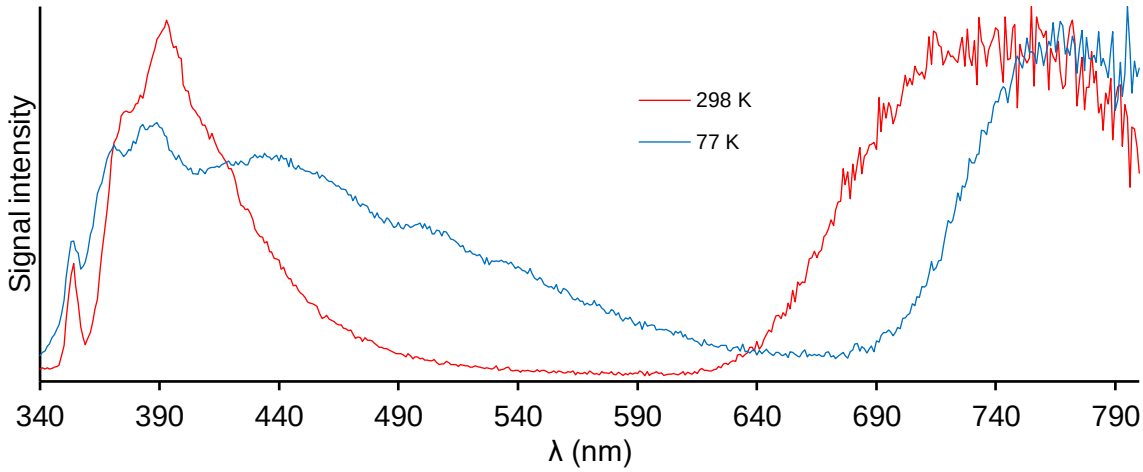

Figure 2.4.5: Red shift of the MLCT λ_{max} in the emission spectrum for complex **2.36** at 77 K.

Excited state lifetimes for several complexes were recorded at 77 K. Attempts to obtain these data at 298 K were impeded by the weak emission profiles and low quantum yields observed for several of these complexes. Although equivalent data for the excited state lifetime of the parent complex **2.1** at 298 K is reported in the literature,[2] the absence of sufficient experimental information did not enable this result to be reproduced.[e] Excited state lifetimes for all complexes that exhibited efficient MLCT emission at 77 K were recorded. Excited state lifetimes are often highly dependent on the solvent used for a variety of reasons including bimolecular quenching by solvent molecules.[1] Conducting experiments at 77 K allows the solvent to be frozen which limits non-radiative relaxation of the excited state. This typically results in greater emission intensity and extended excited state lifetimes. Excited state lifetimes obtained for complexes **2.36** (1602 ns), **2.38** (1563 ns), **2.39** (1098 ns), and **2.40** (1697 ns) suggest phosphorescence derived from a ^{3}MLCT transition. The excited state lifetimes for several other transitions are short (<10 ns) which suggest π–π^* transitions. The observation of small Stokes shifts supports this. A summary of photophysical data obtained is given in Table 2.4.3.

[e] This issue has been noted in the literature.[11e]

Table 2.4.3: Electronic absorption and luminescence data for copper(I) complexes **2.1**, **2.35-2.43**, **2.6-2.7** and **2.48-2.49** Measurements were performed in air equilibrated CH_2Cl_2 at 298 K unless otherwise noted. The excitation wavelength used to record the emission spectra was 320 nm except for **2.1** (330 nm), **2.40** (330 nm) **2.7** (280 nm) and **2.49** (390 nm).

		ABSORPTION		EMISSION		
entry	[Cu]	λ_{max} (nm)	ε ($M^{-1}cm^{-1}$)	λ_{max} (nm)	Φ_{em}	τ_0 (ns)
1	**2.1**	287 337 426 (MLCT)	42500 34100 1390	339 670 (MLCT)	0.22×10^{-4}	3.3 (398 nm)[a,c] 270[5,b]
2	**2.35**	335 340 (MLCT)	49500 6988	391 540 (MLCT)	0.034	87[17,b]
3	**2.36**	250 328 440 (MLCT)	53000 44700 1738	394 750 (MLCT)	0.071	1602 (675 nm)[a,b]
4	**2.37**	258 346 447(MLCT)	53100 33800 2078	415 750 (MLCT)	0.001	2.55 (413 nm)[a,c]
5	**2.38**	254 337 449 (MLCT)	76500 48000 4589	410 730 (MLCT)	0.070	1563 (650 nm)[a,b]
6	**2.39**	253 311 436(MLCT)	53300 45300 3097	367 384 720 (MLCT)	0.028	4.76 (440 nm)[a,c] 1098 (675 nm)[a,b]
7	**2.40**	252 306 432 (MLCT)	61200 45800 2630	362 380 750 (MLCT)	0.004	1697 (675 nm)[a,b]
8	**2.41**	227 275 461 (MLCT)	98500 71400 9160	750 (MLCT)	0.013	3.58 (393 nm)[a,c] 7.48 (494 nm)[a,c]
9	**2.42**	271 315 351	62000 61100 71500	395 414	4.2×10^{-4}	1.7 (416 nm)[a,c]
10	**2.43**	241 293 363	129700 63600 28500	444	3.4×10^{-3}	3.3 (446 nm)[a,c]
11	**2.6**	{383} (MLCT)[15]	–	{570}[15]	{0.015}[15]	{14300}[15]
12	**2.7**	228 279 383 (MLCT)	70700 41400 3620	560 (MLCT)	0.090	147000[a,b]
13	**2.48**	{380} (MLCT)[11f]	–	{540}[11f]	–	{819][11f]
14	**2.49**	227 289 389 (MLCT)	92200 75300 7340	574	0.070	248000[a,b]

Brackets reflect values reported in the literature. [a]Excited state lifetime at 77 K. [b]Excited state lifetime attributed to an MLCT transition. [c]Excited state lifetime attributed to a π–π* transition.

Heteroleptic copper(I) complexes display similar absorption spectra to that of the homoleptic copper(I) complexes with both complexes **2.7** and **2.49** exhibiting two intense peaks in the range 230–300 nm which are assigned to π–π^* transitions within the ligands (Figure 2.4.6).[12-15] However, the MLCT absorption maxima exhibit λ_{max} of 383 nm and 389 nm, respectively, which are significantly blue shifted in comparison to the majority of the homoleptic copper(I) complexes. This is consistent with data reported in the literature.[11c,d] This blue shift derives from the greater π-acceptor character of the diphosphine ligand compared to the phenanthroline derived ligands, resulting in a significantly different electronic environment about the metal centre.[1a] In both cases, despite λ_{max} being just outside the visible portion of the electromagnetic spectrum, the broad absorption profile extends into the visible portion and allows the complexes to be excited by visible (blue) light.

Emission spectra for the heteroleptic complexes **2.7** and **2.49** exhibit a single broad emission band with λ_{max} of 560 nm and 574 nm respectively (Figure 2.4.6). This is consistent with data reported in the literature.[11c,d] This is also significantly blue shifted in comparison to the homoleptic complexes and is a direct consequence of a larger energy gap between the ground state and the MLCT excited state. This large energy gap is advantageous for photoredox catalysts for several reasons. Firstly, it extends the excited state lifetime by lowering the transition probability between the MLCT excited state and the ground state, as described by the energy gap law.[39] Secondly, a higher energy for the excited state will reduce the energy gap between it and the oxidised copper(II) species, resulting in a more strongly reducing complex. Emission quantum yields of the heteroleptic copper(I) complexes are slightly increased in comparison to homoleptic copper(I) complexes. Remarkably, there is a spectacular increase of ~2 orders of magnitude in the excited state lifetime at 77 K. The energy gap law states that the larger the gap between the ground and excited state, the less efficient deactivation processes are.[38] This explains the much longer excited state lifetime for the heteroleptic complexes as the energy gap is much greater as evidenced by the blue shifted emission λ_{max}.

Comparison of the normalised absorbance and emission spectra is also useful to determine the onset of the emission band. This is defined as the intersection of the absorption and emission spectra.[11e] The onset of the emission band is used to determine the difference in energy between the ground and excited states. This can be used in conjunction with

electrochemical measurements to determine the redox potentials of the excited states of the complexes.

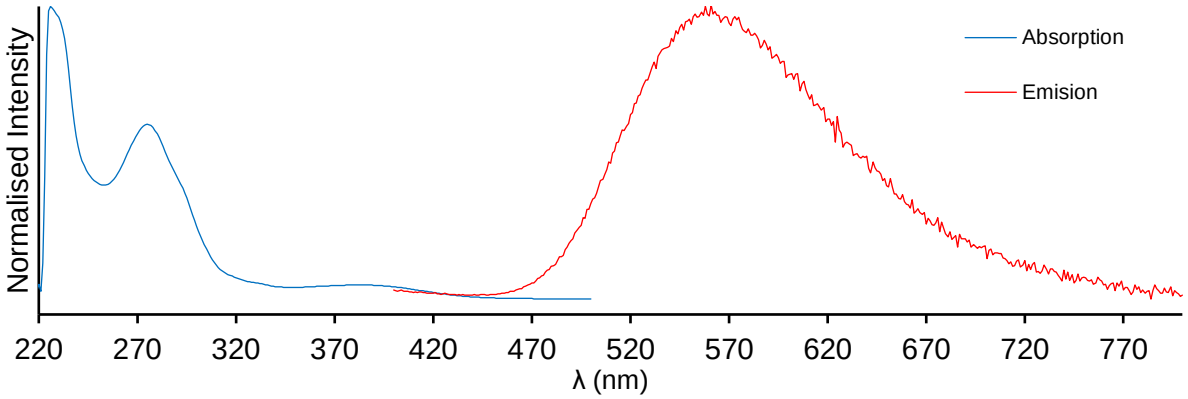

Figure 2.4.6: Normalised absorption and emission spectra of complex **2.7**.

2.4.4 *Electrochemical characterisation of copper(I) complexes*

The reduction and oxidation potentials of photoredox catalysts have a strong impact on their efficiency and the scope of synthetic or organic transformations they can catalyse.[3,11] Photoredox catalysts traditionally operate by mediating single electron transfer processes between organic substrates to facilitate chemical reactions. The redox potentials of both the organic acceptor/ donor and the photoredox catalyst will determine whether a single electron transfer event can occur.[26] Redox potentials for several common photoredox catalysts are presented in Table 2.4.4. Interestingly, homoleptic $[Cu(dap)_2]^+$ displays stronger reducing power than the prototypical $[Ru(bpy)_3]^{2+}$ and many iridium-based photoredox catalysts.

Unlike $[Ru(bpy)_3]^{2+}$, homoleptic bis(phenanthroline)copper(I) complexes are known to operate solely via an oxidative quenching cycle.[3] While this can be viewed as a limitation of this class of complex, it can also simplify mechanistic investigations as the reductive quenching cycle can be completely excluded. Conversely, heteroleptic copper(I) complexes are known to operate through both oxidative and reductive quenching cycles.[11] While the heteroleptic complexes showed higher oxidation potentials for the Cu^{I}/ Cu^{II} couple when examined using cyclic voltammetry, they maintained similar oxidation potentials for the Cu^{I*}/Cu^{II} couple to that of their homoleptic counterparts. This derives from the larger energy gap between the excited and ground states. Furthermore, reduction potentials for the Cu^{I*}/Cu^{0} couple were measured and several of these heteroleptic copper(I) complexes were

found to be more potent oxidants than most commonly used ruthenium- or iridium-based photoredox catalysts as is consistent with published results (Table 2.4.4).[11c,f] A summary of redox potentials measured for both homo- and heteroleptic complexes is provided in Table 2.4.5.

Table 2.4.4: Reported redox potentials of commonly utilised visible light photoredox catalysts.[a]

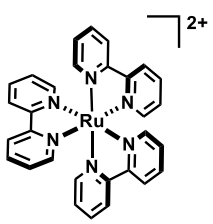

$[Ru(bpy)_3]^{2+}$

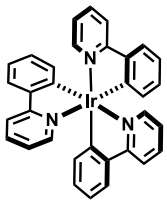

$[fac\text{-}Ir(ppy)_3]$

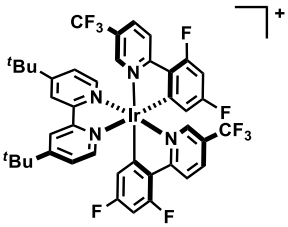

$[Ir\{dF(CF_3)ppy\}_2(dtbbpy)]^+$

Entry	Complex	$E_{1/2}$ (M^+/M^*)	$E_{1/2}$ (M^*/M^-)	$E_{1/2}$ (M^+/M)	$E_{1/2}$ (M/M^-)	reference
1	$[Ru(bpy)_3]^{2+}$	–0.81	+0.77	+1.29	–1.33	40
2	[*fac*-$Ir(ppy)_3$]	–1.73	+0.31	+0.77	–2.19	41
3	$[Ir\{dF(CF_3)ppy\}_2($ dtbbpy$)]^+$	–0.89	+1.21	+1.69	–1.37	42
4	$[Cu(dap)_2]^+$ (**2.1**)	–1.42	–	+0.63	–	–

[a]All potentials are given in volts versus the saturated calomel electrode (SCE). Measurements were performed in acetonitrile at room temperature.

The oxidation potential of the Cu^I/Cu^{II} couple was measured directly by cyclic voltammetry for both homo- and heteroleptic copper(I) complexes (Table 2.4.5). However, the reduction potential for the Cu^I/Cu^0 couple could only be measured for the heteroleptic complexes. As discussed in the previous section, the energy gap between the ground and excited state must be considered, and this was estimated from the onset of the MLCT emission band. This allowed the calculation of redox potentials from the photoexcited state to either the +2 or 0 oxidation states.

Table 2.4.5: Redox potentials of homo- and heteroleptic copper(I) complexes.[a]

entry	complex	$E_{1/2}$ (M^+/M^*)	$E_{1/2}$ (M^*/M^-)	$E_{1/2}$ (M^+/M)	$E_{1/2}$ (M/M^-)
1	**2.1**	–1.42	–	+0.63	–
2	**2.35**	–1.95	–	+0.69	–
3	**2.36**	–1.38	–	+0.66	–
4	**2.37**	–1.26	–	+0.68	–
5	**2.38**	–1.53	–	+0.51	–
6	**2.39**	–1.36	–	+0.78	–
7	**2.40**	–1.05	–	+0.89	–
8	**2.41**	{–1.54}[10b]	–	{+0.63}[10b]	–
9	**2.42**	–	–	+0.68	–
10	**2.43**	–	–	+0.79	–
11	**2.6**	–1.64	+1.01	+1.23	–1.75
12	**2.7**	–1.45	+0.99	+1.25	–1.71
13	**2.48**	{–1.02}[11f]	{+0.63}[11f]	{+1.25}[11f]	{–1.64}[11f]
14	**2.49**	{–1.34}[11c]	{+1.04}[11c]	{+1.34}[11c]	{–1.64}[11c]

[a]All potentials are given in volts versus the saturated calomel electrode (SCE). Measurements were performed in acetonitrile at room temperature. Brackets reflect values reported in the literature.

Within the homoleptic series, most complexes maintained oxidation potentials for the Cu^I/Cu^{II} couple similar to that of the parent complex **2.1** which was synthesised and studied, in house, as a control. However, there are several notable deviations. Both complexes **2.39** and **2.40** display higher potentials for the oxidation. Both complexes feature electron withdrawing groups which is the likely cause of such a deviation. At variance with this, while complex **2.38** which features two electron donating methoxy groups on each aryl ring,

showed a significantly lower potential for the oxidation, the closely related complex **2.37** maintained an oxidation potential very similar to the parent complex **2.1**. As such, no trend in the oxidation potential could be assigned to the electronic or steric nature of the ligands. This is further complicated when the Cu^{I*}/Cu^{II} couple is considered as substituent effects will also have an influence on the energy gap between the ground and excited states.

Another noteworthy result is the strong oxidation potential of complex **2.35**. While the oxidation potential of the Cu^{I}/Cu^{II} couple is similar to that of the parent complex, the reducing power of the complex when in its photoexcited state is significantly increased. Armaroli and co-workers first reported this complex in 2006 and they concluded that the bulky *tert*-butyl groups on the ligand have a significant effect on the ground state geometry of the complex which has a strong impact on electronic transition probabilities.[9] However, electrochemical data was not reported.

The heteroleptic copper(I) complexes displayed significantly different electrochemical properties. Both the Cu^{I}/Cu^{II} and Cu^{I}/Cu^{0} couples could be observed by cyclic voltammetry. In all cases, the former was significantly more positive than the homoleptic complexes meaning that the oxidation of the ground state copper(I) complex requires more energy. However, the large energy gap between the ground and excited states results in a reduction of the energy gap between the excited state and 2+ oxidation state. This results in oxidation potentials for the Cu^{I*}/Cu^{II} couple to be similar, and in some cases stronger, than that of the parent complex **2.1**. Furthermore, these complexes display considerable oxidising strength, with most being more strongly oxidising than $[Ru(bpy)_3]^{2+}$ and some iridium-based complexes, as is consistent with reported values.[10b,11c,f] This, along with their photophysical properties suggest that these complexes may be superior photoredox catalysts than the homoleptic bis(phenanthroline)copper(I) complexes which is consistent with reports published during this research.[11e-j]

2.5 Application of Copper(I) Complexes in Photoredox-Catalysed ATRA Reactions

2.5.1 Background

Atom-transfer radical addition (ATRA) reactions account for one of the most well developed classes of reactivity within photoredox catalysis.[43] These reactions typically proceed via outer sphere electron transfer between catalyst and substrates. A notable example of a copper photoredox-catalysed ATRA reaction was reported by Reiser and co-workers in 2015.[44] In this report, a photoredox-catalysed ATRA reaction facilitated by $[Cu(dap)_2]Cl$ provided notable divergent reactivity in comparison to $[Ru(bpy)_3]Cl_2$. Specifically, when olefin **2.53** and triflyl chloride (**2.54**) were subjected to the reaction conditions outlined in Scheme 2.5.1 using $[Ru(bpy)_3]Cl_2$ as photoredox catalyst, the sole product of the reaction was trifluoromethylchlorination product **2.56**. In contrast, when $[Ru(bpy)_3]Cl_2$ was substituted for $[Cu(dap)_2]Cl$ the major product of the reaction was trifluoromethylchlorosulfonylation product **2.55**. The authors suggested that the coordinatively unsaturated copper photoredox catalyst coordinates reactive intermediates derived from triflyl chloride (**2.54**) and is subsequently directly involved in key bond forming steps leading to the formation of trifluoromethylchlorosulfonylation product **2.55**. This inner sphere reactivity does not occur when utilising coordinatively saturated $[Ru(bpy)_3]Cl_2$ presumably because it is incapable of coordinating reactive intermediates. Consistent with this postulate, these researchers also observed that increasing steric bulk, both of the copper photoredox catalyst and olefinic substrate, disfavours the trifluoromethylchlorosulfonylation process leading to product **2.55** and favours the trifluoromethylchlorination process leading to product **2.56**.

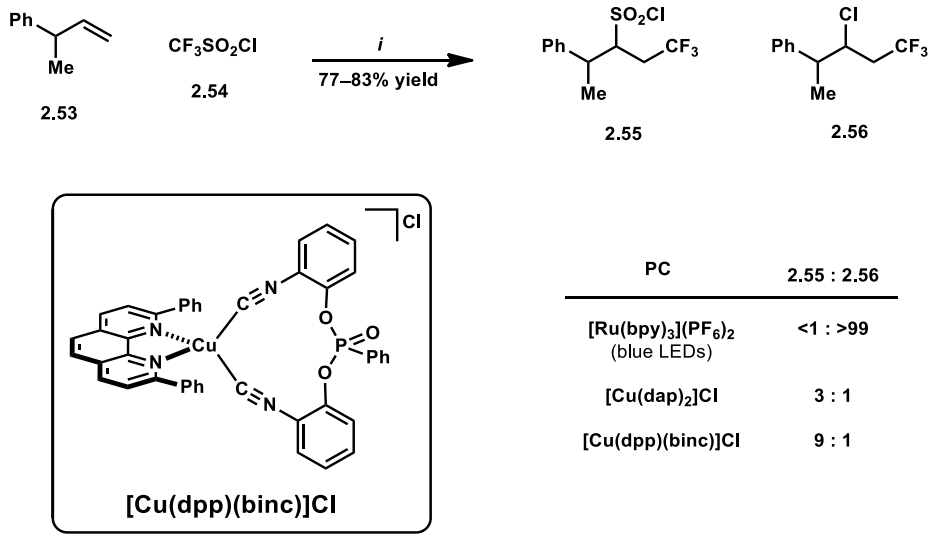

PC	2.55 : 2.56
$[Ru(bpy)_3](PF_6)_2$ (blue LEDs)	<1 : >99
$[Cu(dap)_2]Cl$	3 : 1
[Cu(dpp)(binc)]Cl	9 : 1

Scheme 2.5.1: Trifluoromethylation reactions with increased steric bulk in the substrate. Reagents and conditions: (*i*) 1% PC, 1 equiv **2.53**, 2 equiv **2.54**, 2 equiv K_2HPO_4, green LEDs, MeCN. PC = photocatalyst.

2.5.2 Indirect investigation of the structural features of copper(I) complexes

To investigate the relative influence of the general structural features of copper(I) complexes on the ATRA process described above, the photoredox-catalysed reaction of triflyl chloride (**2.54**) with 1-octene (**2.57**) was examined. The results are displayed in Table 2.5.1.

Table 2.5.1: Investigation of the relative influence of structural features of copper(I) complexes in an ATRA reaction involving inner sphere processes.

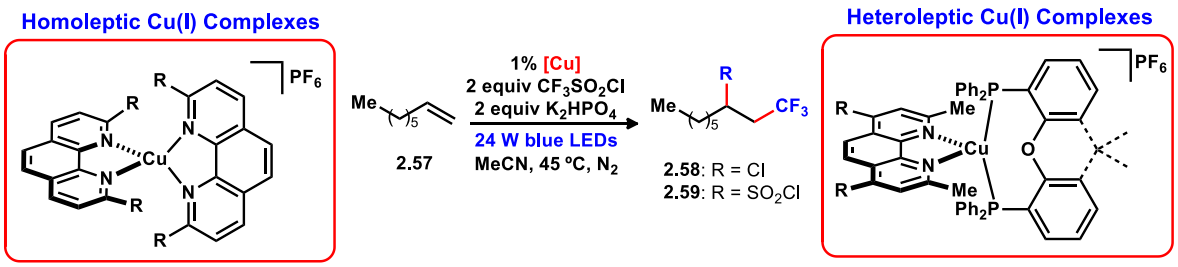

entry	[Cu]	2.58 yield (%)[a]	2.59 yield (%)[a]	entry	[Cu]	2.58 yield (%)[a]	2.59 yield (%)[a]
1	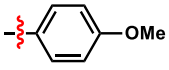 **2.1**	11	48	9	R = H P^P = xantphos **2.7**	6	76
2	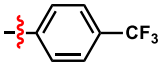 **2.40**	34	32	10	R = Ph P^P = xantphos **2.49**	7	68
3	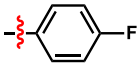 **2.39**	16	30	11	R = H P^P = DPEphos **2.6**	7	61
4	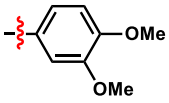 **2.37**	16	46	12	R = Ph P^P = DPEphos **2.48**	5	45
5	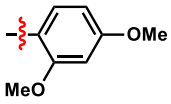 **2.38**	12	50				
6	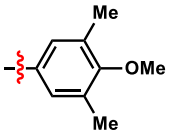 **2.36**	27	39				
7	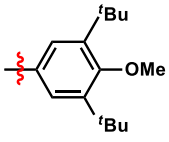 **2.35**	57	19				
8	 **2.41**	5	24				

[a] Yield determined by ^{19}F NMR spectroscopy with the aid of an internal standard (average of 2 experiments).

Each of the complexes that were screened promoted a reaction and delivered mixtures of products **2.58** and **2.59**, however most of these reactions did not proceed to complete conversion. $[Cu(dap)_2]Cl$ (**2.1**) delivered a ~5:1 ratio of products **2.59** and **2.58** (Table 2.5.1, entry 1). Intriguingly, the essentially isosteric complexes **2.40** and **2.39** delivered ~1:1 and ~2:1 ratios of chlorosulfonylation/ chlorination products, respectively (entries 2 & 3). Both these complexes feature *p*-electron withdrawing aryl substituents, thus, these data suggest that electronic factors may also play a significant role in controlling the outcome of the ATRA process. Complexes **2.37** and **2.38**, which feature *m*,*p*-$(OMe)_2C_6H_3$ and *o*,*p*-$(OMe)_2C_6H_3$ aryl substituents both delivered ~5:1 ratios of products **2.59** and **2.58** (entries 4 & 5). In contrast, complexes **2.36** and **2.35** which feature sterically bulky aryl substituents that potentially significantly hinder access to the metal centre delivered ~1.5:1 and a reversal of product distribution (~1:3 ratio) of products **2.59** and **2.58** (entries 6 & 7). This decreased selectivity for the chlorosulfonylation pathway when utilising more sterically hindered photoredox catalysts is in good agreement with observations made by Reiser and co-workers.[44] Furthermore, complex **2.41** and heteroleptic copper(I) complexes **2.6**-**2.7** & **2.48**-**2.49** , all of which feature decreased steric crowding about the metal centre compared to $[Cu(dap)_2]Cl$ (**2.1**) deliver increased ratios of the chlorosulfonylation/ chlorination products (~5:1 to ~13:1) (entries 8-12).

Next, 1-octene (**2.57**) was substituted for the more sterically hindered olefin **2.60** and subjected to otherwise identical reaction conditions (Table 2.5.2). When using this substrate (**2.60**), the product distribution was significantly biased to favour chlorination product **2.61** over the chlorosulfonylation product **2.62**. This is consistent with previous work reported by Reiser and co-workers.[44] Specifically, homoleptic copper(I) complexes **2.1**, **2.39**, and **2.36** furnished chlorination product **2.61** essentially exclusively, while complexes **2.40**, **2.37**, and **2.35** afforded ~1:7, ~1:3 and ~1:9 ratios of products **2.62**/ **2.61** respectively. Interestingly, copper complex **2.38** delivered a ~1.5:1 ratio of products **2.62**/ **2.61** which now favours the chlorosulfonylation product. The reasons behind this are unclear. Although complex **2.41** enabled the synthesis of compounds **2.62** and **2.61** in a ~1:1 ratio, heteroleptic complexes particularly favoured the chlorination pathway that leads to chloride **2.61**.

Table 2.5.2: Investigation of the relative influence of structural features of copper(I) complexes in an ATRA reaction involving inner sphere processes.

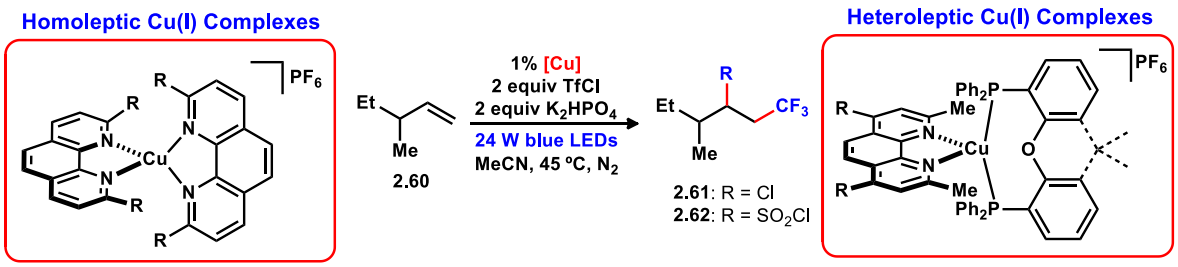

entry	[Cu]	2.61 yield (%)[a]	2.62 yield (%)[a]
1	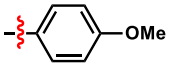 **2.1**	52	<2
2	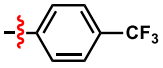 **2.40**	60	9
3	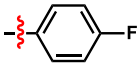 **2.39**	43	<2
4	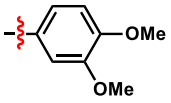 **2.37**	50	16
5	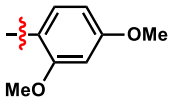 **2.38**	21	31
6	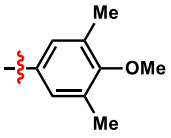 **2.36**	48	<2
7	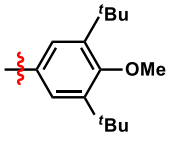 **2.35**	60	7
8	 **2.41**	21	26

entry	[Cu]	2.61 yield (%)[a]	2.62 yield (%)[a]
9	R = H P^P = xantphos **2.7**	43	19
10	R = Ph P^P = xantphos **2.49**	41	<2
11	R = H P^P = DPEphos **2.6**	39	8
12	R = Ph P^P = DPEphos **2.48**	26	<2

[a] Yield determined by ^{19}F NMR spectroscopy with the aid of an internal standard (average of 2 experiments).

2.6 Summary and Conclusions

A small library of both homo- and heteroleptic copper(I) complexes was prepared. A modular synthetic strategy afforded a range of 2,9-diaryl-1,10-phenanthrolines and, thus, allowed rapid access to a broad range of ligands and their related homoleptic copper(I) complexes. Previously reported heteroleptic copper(I) complexes could be synthesised in a single step from commercially available materials which reinforces the accessibility of these photoactive copper(I) complexes.

Extensive characterisation of the structural, photophysical and electrochemical properties of both homo- and heteroleptic classes of copper(I) complexes revealed some variations within each class and, importantly, more significant variation between classes. While the heteroleptic copper(I) complexes typically display somewhat increased emission quantum yields, the excited state lifetime of all heteroleptic copper(I) complexes is significantly increased. Furthermore, their ability to efficiently absorb visible light has been confirmed with heteroleptic copper(I) complexes displaying similar molar absorptivities to the related homoleptic copper(I) complexes and broad absorption profiles. Electrochemical characterisation shows that both homo- and heteroleptic copper(I) complexes are strong reductants. However, only the previously reported heteroleptic copper(I) complexes are strong oxidants too.

Homoleptic and heteroleptic phenanthroline-containing copper(I) complexes have been evaluated to determine their ability to promote ATRA processes that potentially involve inner sphere mechanistic pathways. These results are generally consistent with the expectation that increased steric hindrance around the metal centre will disfavour coordination of reactive intermediates leading to chlorosulfonylation products **2.59** and **2.62**. However, these results also reveal that electronic properties of the complexes may also play a significant role in determining the outcome of the reaction.

2.6 References

(1) For reviews on bis(phenanthroline)copper(I) complexes, see: (a) N. Armaroli, *Chem. Soc. Rev.* **2001**, *30*, 113–124; (b) N. Armaroli; G. Accorsi; F. Cardinali; A. Listorti, In *Photochemistry and Photophysics of Coordination Compounds: Copper*; V. Balzani; S. Campagna, Eds.; Springer: Berlin, Germany, **2007**; Topics in Current Chemistry *280*, pp 69–116; (c) A. Lavie-Cambot; M. Cantuel; Y. Leydet; G. Jonusauskas; D. M. Bassani; N. D. McClenaghan, *Coord. Chem. Rev.* **2008**, *252*, 2572–2584; (d) S. Paria; O. Reiser, *ChemCatChem* **2014**, *6*, 2477–2483. (e) C. B. Larsen; O. S. Wenger, *Chem. Eur. J.* **2018**, *24*, 2039–2058; (f) T. P. Nicholls; D. Leonori; A. C. Bissember, *Nat. Prod. Rep.* **2016**, *33*, 1248–1254; (g) A. Olding; T. P. Nicholls; A. C. Bissember, *Aust. J. Chem.* **2018**, *71*, 547–548.

(2) J.-M. Kern; J.-P. Sauvage, *J. Chem. Soc., Chem. Commun.* **1987**, 546–548.

(3) For examples of photoredox-catalysed processes utilising homoleptic bis(phenanthroline)copper(I) complexes see: (a) M. Pirtsch; S. Paria; T. Matsuno; H. Isobe; O. Reiser, *Chem. Eur. J.* **2012**, *18*, 7336–7340; (b) A. Baralle; L. Fensterbank; J.-P. Goddard; C. Ollivier, *Chem. Eur. J.* **2013**, *19*, 10809–10813; (c) S. Paria; M. Pirtsch; V. Kais; O. Reiser, *Synthesis* **2013**, *45*, 2689–2698; (d) X.-J. Tang; W. R. Dolbier, *Angew. Chem., Int. Ed*. **2015**, *54*, 4246–4249; (e) D. B. Bagal; G. Kachkovskyi; M. Knorn; T. Rawner; B. M. Bhanage; O. Reiser, *Angew. Chem., Int. Ed*. **2015**, *54*, 6999–7002; (f) G. Fumagalli; P. T. G. Rabet; S. Boyd; M. F. Greaney, *Angew. Chem., Int. Ed*. **2015**, *54*, 11481–11484; (g) Z. Zhang; X. Tang; C. S. Thomoson; W. R. Dolbier, *Org. Lett*. **2015**, *17*, 3528–3531; (h) S. K. Pagire; S. Paria; O. Reiser, *Org. Lett.* **2016**, *18*, 2106–2109; (i) T. Rawner; M. Knorn; E. Lutsker; A. Hossain; O. Reiser, *J. Org. Chem.* **2016**, *81*, 7139–7147; (j) P. T. G. Rabet; G. Fumagalli; S. Boyd, M. F. Greaney, *Org. Lett.* **2016**, *18*, 1646–1649; (k) T. Rawner; E. Lutsker; C. A. Kaiser; O. Reiser, *ACS Catal.* **2018**, *8*, 3950–3956; (l) M. M. Cetin; R. T. Hodson; C. R. Hart; D. B. Cordes; M. Findlater; D. J. Casadonte Jr; A. F. Cozzolino; M. F. Mayer, *Dalton Trans.* **2017**, *46*, 6553–6569; (m) W. Ma; D. Chen; Y. Ma; L. Wang; C. Zhao; W. Yang, *Polym. Chem.* **2016**, *7*, 4226–4236; (n) T. P. Nicholls; G. C. Constable; J. C. Robertson; M. G. Gardiner; A. C. Bissember, *ACS Catal.* **2016**, *6*, 451–457; (o) T. Rawner; M. Knorn; E. Lutsker; A. Hossain; O. Reiser, *J. Org. Chem.* **2016**,

81, 7139–7147; (p) T. Rawner; E. Lutsker; C. A. Kaiser; O. Reiser, *ACS Catal.* **2018**, *8*, 3950–3956; (q) A. Hossain; A. Vidyasagar; C. Eichinger; C. Lankes; J. Phan; J. Rehbein; O. Reiser, *Angew. Chem., Int. Ed.* **2018**, *57*, 8288–8292.

(4) C. T. Cunningham; K. L. H. Cunningham; J. F. Michalec; D. R. McMillan, *Inorg. Chem.* **1999**, *38*, 4388–4392.

(5) (a) N. Armaroli; V. Balzani; F. Barigelletti; L. De Cola; L. Flamigni; J.-P. Sauvage; C. Hemmert, *J. Am. Chem. Soc.* **1994**, *116*, 5211–5217; (b) C. Dietrich-Buchecker; B. Colasson; M. Fujita; A. Hori; N. Geum; S. Sakamoto; K. Yamaguchi; J.-P Sauvage, *J. Am. Chem. Soc.* **2003**, *125*, 5717–5725; (c) J. Frey; T. Kraus; V. Heitz; J.-P. Sauvage, *Chem. Commun.* **2005**, 5310–5312.

(6) (a) M. S. Lowry; S. Bernhard, *Chem. Eur. J.* **2006**, *12*, 7970–7977; (b) N. Armaroli; V. Balzani; J. P. Collin; P. Gaviña; J.-P. Sauvage; B. Ventura, *J. Am. Chem. Soc.* **1999,** *121*, 4397–4408; (c) N. Weber; C. Hamann; J. M. Kern; J.-P. Sauvage, *Inorg. Chem.* **2003**, *42*, 6780–6792.

(7) (a) N. Armaroli; C. Boudon; D. Felder; J. P. Gisselbrecht; M. Gross; G. Marconi; J. F. Nicoud; J. F. Nierengarten; V. Vicinelli, *Angew. Chem., Int. Ed.* **1999**, *38*, 3730–3733; (b) E. Gumienna-Kontecka; Y. Rio; C. Bourgogne; M. Elhabiri; R. Louis; A. M. Albrecht-Gary; J. F. Nierengarten, *Inorg. Chem.* **2004**, *43*, 3200–3209.

(8) B. A. Gandhi; O. Green; J. N. Burstyn, *Inorg. Chem.* **2007**, *46*, 3816–3825.

(9) V. Kalsani; M. Schmittel; A. Listorti; G. Accorsi; N. Armaroli, *Inorg. Chem.* **2006**, *45*, 2061–2067.

(10) (a) C. O. Dietrich-Buchecker; P. A. Marnot; J.-P. Sauvage; J. R. Kirchoff; D. R. McMillin, *J. Chem. Soc., Chem. Commun.* **1983**, 513–515; (b) D. R. McMillin; M. T. Buckner; B. T. Ahn, *Inorg. Chem.* **1977**, *16*, 943–945.

(11) For examples of photoredox-catalysed processes utilising heteroleptic phenanthroline containing copper(I)-based complexes see: (a) A. C. Hernandez-Perez; A. Vlassova; S. K. Collins, *Org. Lett*. **2012**, *12*, 988–991; (b) A. C. Hernandez-Perez; S. K. Collins, *Angew. Chem., Int. Ed*. **2013**, *52*, 12696–12700; (c) E. Mejía; S.-P. Luo; M. Karnahl; A. Friedrich; S. Tschierlei; A.-E. Surkus; H. Junge; S. Gladiali; S. Lochbrunner; M. Beller, *Chem. Eur. J.* **2013**, *19*, 15972–15978; (d) S.-P. Luo; E. Mejía; A. Friedrich; A. Pazidis; H. Junge; A.-E. Surkus; R. Jackstell; S. Denurra; S. Gladiali; S. Lochbrunner; M. Beller,

Angew. Chem., Int. Ed. **2013**, *52*, 419–423; (e) M. Knorn; T. Rawner; R. Czerwieniec; O. Reiser, *ACS Catal*. **2015**, *5*, 5186–5193; (f) B. Michelet; C. Deldaele; S. Kajouj; C. Moucheron; G. Evano, *Org. Lett.* **2017**, *19*, 3576–3579; (g) T. P. Nicholls; J. C. Robertson; M. G. Gardiner; A. C. Bissember, *Chem. Commun.* **2018**, *54*, 4589–4592; (h) W. Zhao; R. P. Wurz; J. P. Peters; G. C. Fu, *J. Am. Chem. Soc.* **2017**, *139*, 12153–12156; (i) M. Heberle; S. Tschierlei; N. Rockstroh; M. Ringenberg; W. Frey; H. Junge; M. Beller; S. Lochbrunner; M. Karnahl, *Chem. Eur. J.* **2017**, *23*, 312–319; (j) C. Minozzi; A. Caron; J.-C. Grenier-Petel; J. Santandrea; S. K. Collins, *Angew. Chem., Int. Ed.* **2018**, *57*, 5477–5481.

(12) R. A. Radar; D. R. McMillin; M. T. Buckner; T. G. Matthews; D. J. Casadonte; R. K. Lengel; S. B. Whittaker; L. M. Darmon; F. E. Lytle, *J. Am. Chem. Soc.* **1981**, *103*, 5906–5912.

(13) C. E. A. Palmer; D. R. McMillin, *Inorg. Chem.* **1987**, *26*, 3837–3840.

(14) A. Kaeser; M. Mohankumar; J. Mohanraj; F. Monti; M. Holler; J.-J. Cid; O. Moudam; I. Nierengarten; L. Karzamin-Brelot; C. Duhayon; B. Delavaux-Nicot; N. Armaroli; J.-F. Nierengarten, *Inorg. Chem.* **2013**, *52*, 12140–12151.

(15) D. G. Cuttell; S.-M. Kuang; P.E. Fanwick; D. R. McMillan; R. A. Walton, *J. Am. Chem. Soc.* **2002**, *124*, 6–7.

(16) (a) N. Gothard; M. W. Mara; J. Huang; J. M. Szarko; B. Rolczynski; J. V. Lockard; L. X. Chen, *J. Phys. Chem. A* **2012**, *116*, 1984–1992; (b) H. Guo; R. Zheng; H. Jiang, *Org. Prep. Proc. Int.* **2012**, *44*, 392–396; (c) J. Frey; T. Kraus; V. Heitz; J.-P. Sauvage, *Chem. Eur. J.* **2007**, *13*, 7584–7594

(17) A. C. Bissember; M. G. Banwell, *J. Org. Chem.* **2009**, *74*, 4893–4895.

(18) N. Miyaura; K. Yamada; A. Suzuki, *Tetrahedron Lett.* **1979**, *20*, 3437–3440.

(19) C. Gu; N. Huang; J. Gao; F. Xu; D. Jiang, *Angew. Chem., Int. Ed.* **2014**, *53*, 4850–4855.

(20) X.-G. Liu; W. Sun, *Eur. J. Inorg. Chem.* **2013**, *113*, 4732–4742.

(21) Y. Zhang; Z. Lu; A. Desai; W. D. Wulff, *Org. Lett.* **2008**, *10*, 5429–5432.

(22) T. Ishiyama; M. Murata; N. Miyaura, *J. Org. Chem.* **1995**, *60*, 7508–7510.

(23) M. Heberle; S. Tschierlei; N. Rockstroh; M. Ringenberg; W. Frey; H. Junge; M. Beller; S. Lochbrunner; M. Karnahl, *Chem. Eur. J.* **2017**, *23*, 312–319.

(24) C. W. Hamilton; D. S. Laitar; J. P. Sadighi, *Chem. Commun.* **2004**, 1628–1629.

(25) Y. Zhang; M. Schulz; M. Wächtler; M. Karnahl; B. Dietzek, *Coord. Chem. Rev.* **2018**, *356*, 127–146.

(26) C. K. Prier; D. A. Rankic; D. W. C. MacMillan, *Chem. Rev.* **2013**, *113*, 5322–5363.

(27) M. T. Miller; P. K. Gantzel; T. B. Karpishin, *Inorg. Chem.* **1998**, *37*, 2285–2290.

(28) J. E. Beves; B. A. Blight; C. J. Campbell; D. A. Leigh; R. T. McBurney, *Angew. Chem., Int. Ed.* **2011**, *50*, 9260–9327.

(29) (a) P. Coppens; I. I. Vorontsov; T. Graber; A. Y. Kovalevsky; Y.-S. Chen; G. Wu; M. Gembicky; I. V. Novazhilova, *J. Am. Chem. Soc.* **2004**, *126*, 5980–5981; (b) A. Y. Kovalavsky; M. Gembicky; I. V. Novozhilova; P. Coppens, *Inorg. Chem.* **2003**, *42*, 8794–8802; (c) M. T. Miller; P. K. Gantzel; T. B. Karpishin, *Inorg. Chem.* **1998**, *37*, 2285–2290.

(30) P. Yang; X.-J. Yang; B. Wu, *Eur. J. Inorg. Chem.* **2009**, 2951–2958

(31) P. C. Healy; L. M. Engelhardt; V. A. Patrick; A. H. White, *J. Chem. Soc., Dalton Trans.* **1985**, 2541–2545.

(32) M. Geoffroy; M. Wermeille; C. O. Buchecker; J.-P. Sauvage; G. Bernardinelli, *Inorg. Chim. Acta* **1990**, *167*, 157–164.

(33) J. R. Kirchhoff; R. E. Gamache Jr.; M. W. Blaskie; A. A. Del Paggio; R. K. Lengel; D. R. McMillin, *Inorg. Chem.* **1983**, *22*, 2380–2384.

(34) (a) V. Kalsani; H. Bodenstedt; D. Fenske; M. Schmittel, *Eur. J. Inorg. Chem.* **2005**, 1841–1849; (b) R. Colton; B. D. James; I. D. Potter; J. C. Traeger, *Inorg. Chem.* **1993**, *32*, 2626–2629.

(35) R. Giereth; W. Frey; H. Junge; S. Tschierlei; M. Karnahl, *Chem. Eur. J.* **2017**, *23*, 17432–17437.

(36) D. M. Arias-Rotondo; J. K. McCusker, *Chem. Soc. Rev.* **2016**, *45*, 5803–5820.

(37) (a) W. L. Parker; G. A. Crosby, *J. Phys. Chem.* **1989**, *93*, 5692–5696. (b) J. R. Kirchoff; R. E. Gamache; M. W. Blaskie; A. A. Del Pagio; R. K. Lenkel; D. R. McMillan, *Inorg. Chem.* **1983**, *22*, 2380–2384.

(38) A. S. Lee; Y. Y. Jo; S.-S. Choi; K.-Y. Baek; S. S. Hwang, *J. Nanosci. Nanotechnol.* **2017**, *17*, 5562–5565.

(39) R. Englman; J. Jortner, *Mol. Phys.* **1970**, *18*, 145–164.

(40) M. Haga; E. S. Dodsworth; G. Eryavec; P. Seymour; A. B. P. Lever, *Inorg. Chem.* **1985**, *24*, 1901–1906.

(41) L. Flamigni; A. Barbieri; C. Sabatini; B. Ventura; F. Barigelletti, In *Photochemistry and Photophysics of Coordination Compounds: Iridium;* V. Balzani, S. Campagna, Eds.; Springer: Berlin, Germany, **2007**; Photochemistry and Photophysics of Coordination Compounds II. Topics in Current Chemistry *281*, pp 143–203.

(42) M. S. Lowry; J. I. Goldsmith; J. D. Slinker; R. Rohl; R. A. Pascal; G. G. Malliaras; S. Bernhard, *Chem. Mater.* **2005**, *17*, 5712–5719.

(43) (a) M.-Y. Cao; X. Ren; Z. Lu, *Tetrahedron Lett.* **2015**, *56*, 3732–3742; (b) T. Koike; M. Akita, *Org. Chem. Front.* **2016**, *3*, 1345–1349.

(44) D. B. Bagal; G. Kachkovskyi; M. Knorn; T. Rawner; B. M. Bhanage; O. Reiser, *Angew. Chem., Int. Ed.* **2015**, *54*, 6999–7002.

Chapter Three

Extending the Synthetic Scope of Copper-Based Photoredox Catalysts

This chapter is divided into two parts and describes an investigation of several chemical transformations catalysed by copper-based photoredox catalysts. Part one describes an examination of the utility of the weak oxidising power of $[Cu(dap)_2]^+$ that led to the development of a Brønsted acid co-catalysed direct α-amino C–H functionalisation reaction. This transformation represents the first example of the oxidative functionalisation of a substrate mediated by the weak oxidative power of a copper(I) photoredox catalyst. These results suggest that the presence of TFA is essential to mediate the aerobic oxidation of the photoexcited state of $[Cu(dap)_2]^+$. Part two describes a range of chemical transformations that were screened to determine if the typically strong reducing power of copper(I) photoredox catalysts could also be exploited to further extend the synthetic scope of copper(I) photoredox catalysis.

3.1 Brønsted Acid Cocatalysis in Copper(I)-Catalysed α-Amino C–H Bond Functionalisation

3.1.1 Introduction

The direct α-amino C–H bond functionalisation of amines can be facilitated by traditional second and third row transition metal-based photoredox catalysts, such as $[Ru(bpy)_3]^{2+}$.[1] In 2015, at the beginning of this project, this had yet to be achieved using a copper-based photoredox catalyst. Homoleptic bis(phenanthroline)copper(I) complexes, such as $[Cu(dap)_2]^+$, are unable to operate through a reductive quenching cycle. As such, the oxidative quenching cycle must be exploited to achieve the oxidation of an amine. This requires a weakly oxidising copper(II) species to perform the oxidation of an amine. In this chapter, the use of $[Cu(dap)_2]Cl$ to effect annulation reactions of *N*,*N*-dialkylanilines and *N*-aryltetrahydroisoquinolines with electron deficient alkenes is described. This allowed the

rapid synthesis of a range of annulated tetrahydroquinolines and tetrahydroisoquinolines at room temperature (Scheme 3.1.1). This is the first example of the direct functionalisation of α-amino C−H bonds mediated by a copper-based photoredox catalyst. Furthermore, the unanticipated requirement of trifluoroacetic acid (TFA) in the reaction mixture was identified and investigated.

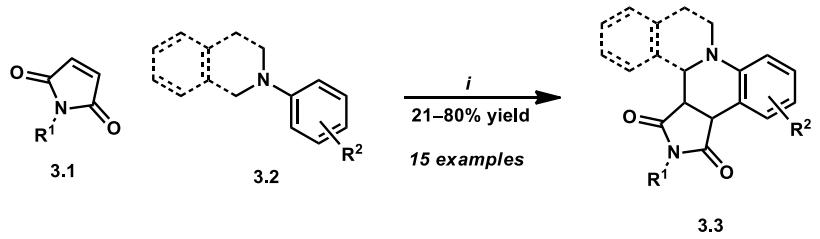

Scheme 3.1.1: Standard conditions for the synthesis of annulated tetrahydroquinolines and tetrahydroisoquinolines. Reagents and conditions: (*i*) 5% $[Cu(dap)_2]Cl$, 1 equiv **3.1**, 2 equiv **3.2**, 2 equiv TFA, green LEDs, DMF, r.t., air, 16 h.

In 2012, Bian and co-workers reported the synthesis of various annulated tetrahydroquinolines by the reaction of *N*,*N*-alkylanilines and a number of *N*-substituted maleimides in the presence of $[Ru(bpy)_3]^{2+}$ or iridium-based photoredox catalysts in low to high yields.[2,3] It was proposed that this reaction exploits the reductive quenching cycle of $[Ru(bpy)_3]^{2+}$ which is not viable for bis(phenanthroline)copper(I) photoredox catalysts.[2a,4] This process represents a powerful transformation in which two C−H bonds are cleaved, including an unactivated aryl C−H bond, two new C−C bonds are formed, and up to three contiguous stereocenters can be created in a single step.

An investigation into whether this transformation could also be effected by exploiting the oxidative quenching cycle of $[Cu(dap)_2]^+$ was performed. Indeed, it is well established that dioxygen can quench photoexcited states of bis(phenanthroline)copper(I) complexes via both energy and electron transfer processes.[5] As such, it was anticipated that upon irradiation with visible light at ambient temperature, in the presence of air, the ensuing photoexcited $[Cu^*(dap)_2]^+$ complex could undergo aerobic oxidation to provide $[Cu(dap)_2]^{2+}$ (Figure 3.1.1). Although this Cu(II) species is a weak oxidant ($E_{1/2}$ = +0.63 V vs. SCE) it was anticipated that its oxidative power may be sufficient to oxidise *N*,*N*-dimethylaniline to produce an α-amino

radical and regenerate $[Cu(dap)_2]^+$ to complete the catalytic cycle. The putative α-amino radical thus produced, could ultimately lead to annulated product **3.3**.

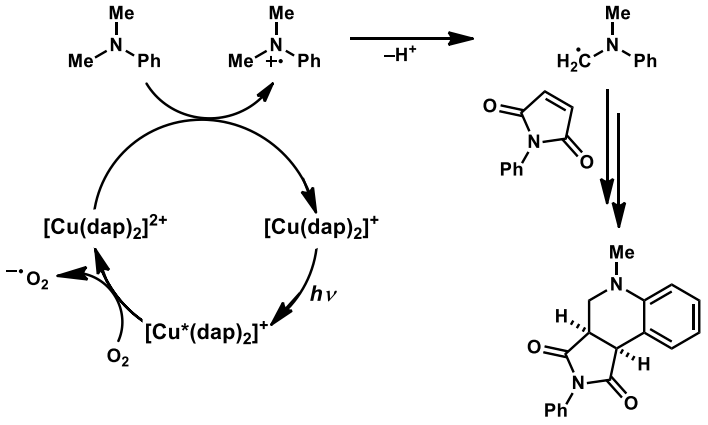

Figure 3.1.1: Outline of the anticipated oxidative quenching pathway for $[Cu(dap)_2]^+$ ultimately enabling α-amino C–H bond functionalisation.

3.1.2 Optimisation of reaction conditions

The optimisation of reaction conditions was partially performed by other group members.[6] These data are presented in Table 3.1.1. After examining a range of reaction parameters, it was ultimately determined that $[Cu(dap)_2]Cl$ enables the reaction of *N*-phenylmaleimide with *N*,*N*-dimethylaniline to directly provide tetrahydroquinoline **3.6** in good yield (Table 3.1.1, entry 1). Control experiments were performed under otherwise identical conditions, and it was found that the absence of $[Cu(dap)_2]Cl$, visible light, or both $[Cu(dap)_2]Cl$ and visible light, did not provide any significant product formation (entries 2–4). The presence of TFA is crucial, and in the absence of this Brønsted acid essentially no product is formed (entry 5). Interestingly, the presence of only 0.1 equiv of TFA leads to a 47% yield of product suggesting its cocatalytic role in the reaction (entry 6). The exact role of TFA in this reaction is particularly significant and was investigated further as part of this study (*vide infra*). If 1% $[Cu(dap)_2]Cl$ is employed, a considerable amount of product is still formed (entry 7). The substitution of $[Cu(dap)_2]Cl$ for 2,9-bis(4-methoxyphenyl)-1,10-phenanthroline (dap) delivered a 43% yield suggesting that the ligand itself is capable of catalysing this process (entry 8). It has been previously reported that dap is capable of mediating related processes including ATRA reactions under visible light irradiation.[7] Substituting $[Cu(dap)_2]Cl$ with $CuCl_2$, CuCl, or $Cu(OTf)_2$ or the use of MeCN as the solvent

causes the yield to decrease (entries 9–12). If 1.2 equiv of *N*,*N*-dimethylaniline is used or the reaction is irradiated with a 24 W CFL, then a lower yield is obtained (entries 13 and 14). This process is not sensitive to the presence of moisture (entry 15), and essentially no product is formed when air is excluded (entry 16).

Table 3.1.1: Copper-catalysed reaction of *N*-phenylmaleimide with *N*,*N*-dimethylaniline: Influence of reaction parameters.

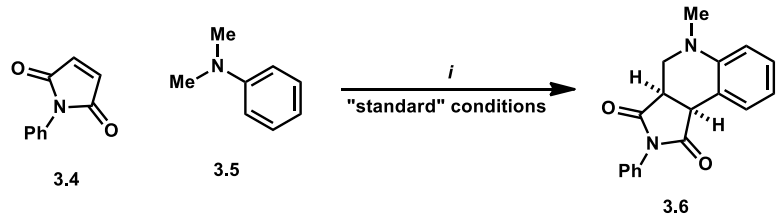

3.4 3.5 3.6

entry	variation from the "standard" conditions	yield (%)[a]
1	none	77
2	no $[Cu(dap)_2]Cl$	<2
3	no $h\nu$	<2
4	no $[Cu(dap)_2]Cl$ and no $h\nu$	<2
5	no TFA	<2
6	0.1 equiv TFA	47
7	1% $[Cu(dap)_2]Cl$	65
8	10% dap, instead of 5% $[Cu(dap)_2]Cl$	43
9	5% $CuCl_2$, instead of 5% $[Cu(dap)_2]Cl$	3
10	5% CuCl, instead of 5% $[Cu(dap)_2]Cl$	<2
11	5% $Cu(OTf)_2$, instead of 5% $[Cu(dap)_2]Cl$	4
12	MeCN, instead of DMF	48
13	1.2 equiv $PhNMe_2$	55
14	23 W CFL, instead of green LED	59
15	10 equiv H_2O	77
16	under N_2, instead of air	3

Procedure: (*i*) 5% $[Cu(dap)_2]Cl$, 1 equiv **3.4**, 2 equiv **3.5**, 2 equiv TFA, green LEDs, DMF, r.t., air, 16 h. [a]Determined via gas chromatography with the aid of a calibrated internal standard (average of two experiments).

3.1.3 Investigation into the scope of the reaction

Under the optimised reaction conditions it was observed that a number of maleimides react with various *N*,*N*-dimethylanilines to deliver a range of tetrahydroquinolines in low to good yields. In this way, several *N*-phenylmaleimide-derived heterocycles were prepared (Table 3.1.2, entries 1–4) and reactions with *N*-benzylmaleimide, (*R*)-(+)-*N*-(1-phenylethyl)maleimide, and *N*-pentafluorophenylmaleimide could also be effected (entries 5–7). Consistent with previous work employing $[Ru(bpy)_3]^{2+}$,[2a] reactions of *N*-arylpyrrolidines

proceeded with low conversion under the reaction conditions (entries 8 and 9). Unfortunately, reactions of *N*-phenylmaleimide with 4-(dimethylamino)benzonitrile, 3,4,5-trimethoxy-*N*,*N*-dimethylaniline, methyl 4-(dimethylamino)benzoate, 4-(dimethylamino)benzaldehyde, *N*,*N*-dimethylnaphthalen-1-amine, *N*,*N*-dimethylpyridin-2-amine, *N*-phenylpiperidine, or *N*-phenylmorpholine only provided trace amounts of the anticipated tetrahydroquinoline products under the standard conditions. Conversely, if the maleimide substrate is substituted for benzylidenemalononitrile which is also electron deficient, $[Cu(dap)_2]Cl$ is capable of mediating reactions of various *N*,*N*-dimethylanilines to provide functionalised tetrahydroquinoline products (entries 10−12).[2b] Many of these heterocycles are previously unreported compounds (**3.9**, **3.10**, **3.12**, **3.13** and **3.15**-**18**), and a number of these structures were secured via single crystal X-ray analysis (**3.8**, **3.11**, **3.12**, **3.14**, **3.17** & **3.18**) (Figure 3.1.2). In contrast to these results, related $CuCl_2$-catalysed reactions of *N*,*N*-dimethylanilines with benzylidenemalononitrile require elevated temperatures and an oxygen atmosphere.[8] The results presented here represent a more mild strategy to access related compounds.

Table 3.1.2: Copper-catalysed reactions of electron deficient olefins with *N*,*N*-dialkylanilines.

entry	product(s)		yield (%)[a]
1 2 3	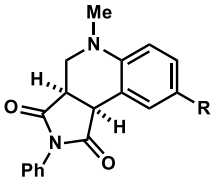	3.7, R = H: 3.8, R = Br: 3.9, R = *i*Pr:	70 42 65
4	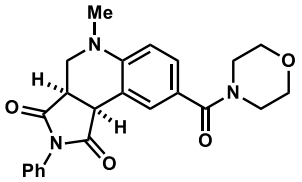	3.10	62
5 6	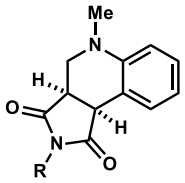	3.11, R = Bn: 3.12, R = C_6F_5:	35 47
7	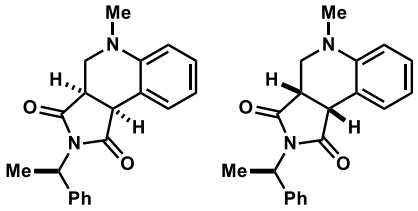	3.13	45[b]
8 9	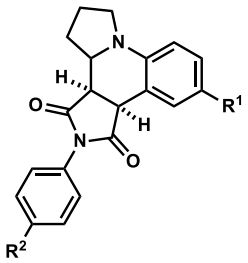	3.14, R^1, R^2 = H: 3.15, R^1 = CH_2CH_2OH R^2 = CH_2CH_2OAc:	46[b] 21[c,e]
10 11 12	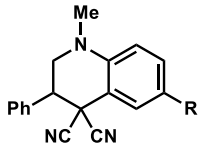	3.16, R = H: 3.17, R = Br: 3.18, R = *i*Pr:	42[d] 55[d] 80[d]

Procedure: 5% $[Cu(dap)_2]Cl$, 1 equiv olefin, 2 equiv *N*,*N*-dialkylaniline, 2 equiv TFA, green LED, DMF, r.t., air, 16 h. [a]Yield of purified product(s). [b]~1:1 mixture of diastereomers. [c]~2:1 mixture of syn:anti diastereomers. [d]Benzylidenemalononitrile used in place of maleimide substrate. [e]This product was prepared by G. E. Constable, another group member.[6]

In addition, $[Cu(dap)_2]Cl$ also facilitates analogous regio- and stereoselective reactions of *N*-aryltetrahydroisoquinolines with *N*-phenylmaleimide to provide unique and complex

heterocyclic scaffolds as single diastereoisomers (Table 3.1.3). This contrasts with the results of reactions with various *N*-arylpyrrolidines which provide diastereomeric mixtures (Table 3.1.2, entries 8 and 9). The *syn*- stereochemistry of the three ring junction hydrogens was confirmed by 2D NMR spectroscopy with correlations between these H atoms observed in a COSY experiment. These are the first examples of *N*-aryltetrahydroisoquinolines participating in direct annulation reactions with maleimides in this fashion under any conditions and these products are all previously unreported compounds. Moreover, this ring-annulated octahydroisoquinolino[2,1-*a*]pyrrolo[3,4-*c*]quinoline motif represents a new and unique heterocyclic framework. The structures of these three compounds were all further confirmed after standard spectroscopic techniques via single crystal X-ray analysis (Figure 3.1.2).

Table 3.1.3: Copper-catalysed reactions of *N*-phenylmaleimide with *N*-aryltetrahydroisoquinolines.

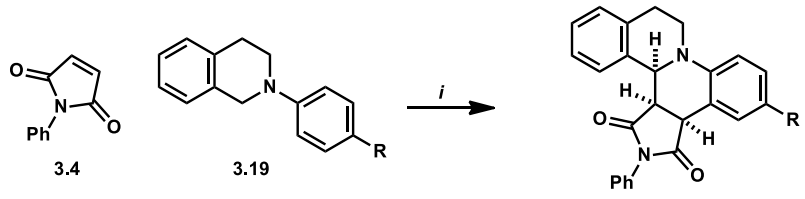

entry	product	R	yield (%)[a]
1	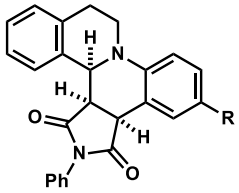	3.21, R = H	60
2		3.22, R = F	67
3		3.23, R = OMe	57

Procedure: 5% $[Cu(dap)_2]Cl$, 1 equiv **3.4**, 2 equiv **3.19**, 2 equiv TFA, green LED, DMF, r.t., air, 16 h. [a]Yield of purified product (syn diastereomer formed exclusively).

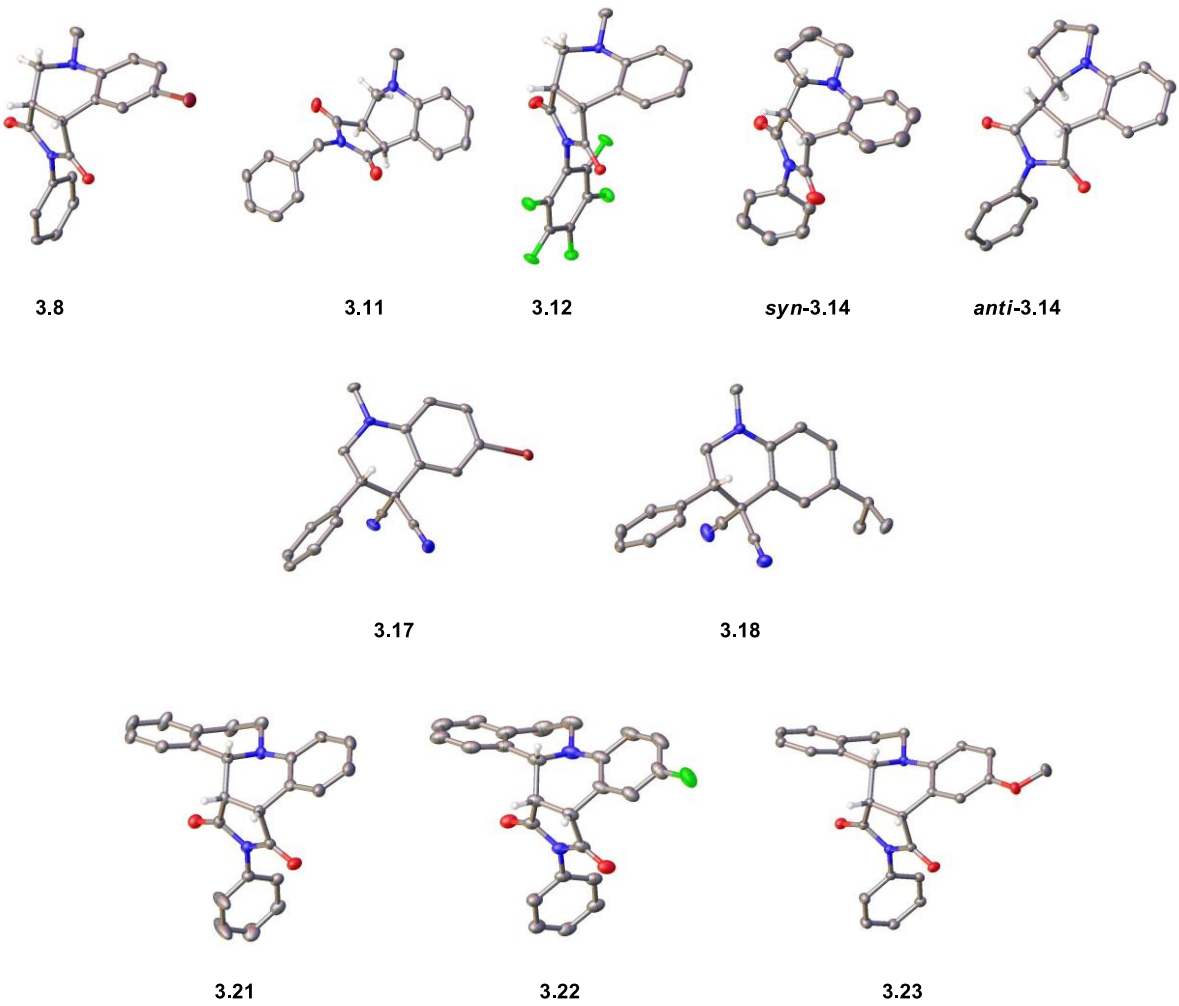

Figure 3.1.2: ORTEP representations of products **3.8**, **3.11**, **3.12**, *syn*- & *anti*-**3.14**, **3.17**, **3.18**, **3.21**, **3.22** and **3.23**. Thermal ellipsoids are drawn at the 50% probability level (second molecule in the asymmetric unit for **3.11** and disordered lattice solvent for **3.21** omitted for clarity.)

3.1.4 Investigation into the role of TFA

Brønsted acid-mediated processes represent a rather underexplored class of reactions in photoredox catalysis. However, the presence of Brønsted acids can have profound mechanistic implications that can even change the course of reactions.[9] The role of TFA in this copper(I)-mediated annulation reaction was further investigated by varying the TFA loading. The addition of only 0.1 equivalents of TFA enabled a 47% yield (Scheme 3.1.2). Increasing the amount of TFA up to 2.5 equivalents improved or essentially left the yields unchanged. When loadings up to 5 equivalents of TFA were used, a decrease in the yield of product was observed and with higher loadings of 15 and 30 equivalents, the reaction did not proceed efficiently with yields of 17% and 4% respectively. This is consistent with the formation of the

key α-amino radical requiring the presence of free amine (Figure 3.1.1). Presumably, high TFA loadings provide an environment in which *N*,*N*-dimethylaniline is essentially sequestered as its corresponding (unreactive) ammonium salt.

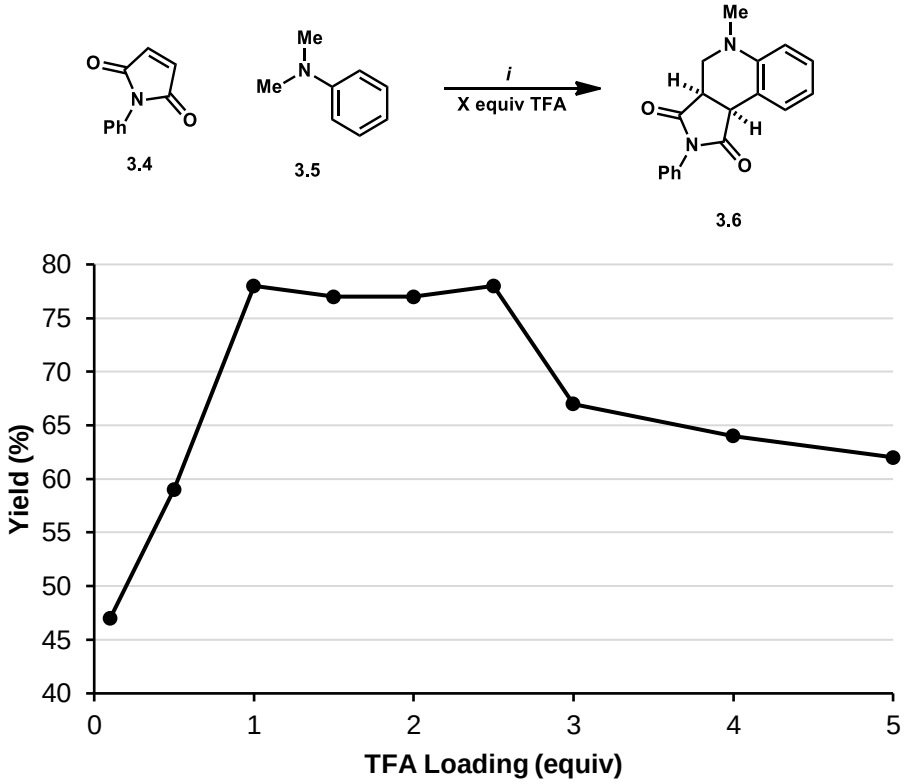

Scheme 3.1.2: Copper-catalysed reaction of *N*-phenylmaleimide with *N*,*N*-dimethylaniline: Effect of TFA loading. Reagents and conditions: (*i*) 5% $[Cu(dap)_2]Cl$, 1 equiv **3.4**, 2 equiv **3.5**, green LEDs, DMF, r.t., air, 16 h.

A ^{1}H NMR study was conducted, in which *N*,*N*-dimethylaniline was titrated with TFA. As the amount of TFA increased, the chemical shift of the methyl resonance also increased until the solution was saturated. At this point the chemical shift of the methyl resonance was no longer altered despite further addition of TFA. This saturation behaviour is consistent with protonation of the free amine to deliver the corresponding ammonium salt. Importantly, this suggests that in the presence of two equivalents of TFA, free *N*,*N*-dimethylaniline is still present. Thus, under the reaction conditions, the free amine is still available to reduce the Cu(II) complex.

A

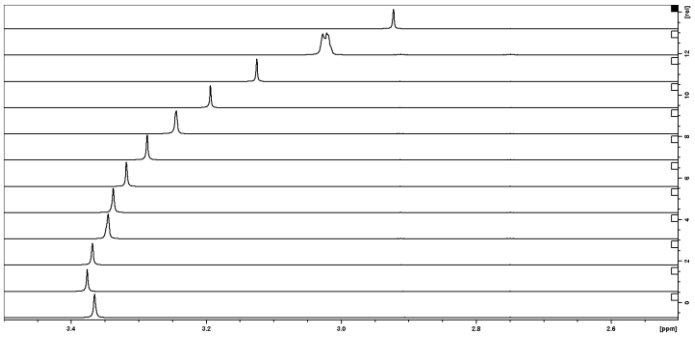

B

TFA (equiv)	Chemical Shift (ppm)
0.0	2.92
0.5	3.02
1.0	3.13
1.5	3.19
2.0	3.24
2.5	3.29
3.0	3.32
3.5	3.34
4.0	3.35
5.0	3.37
7.5	3.38
10.0	3.37

C

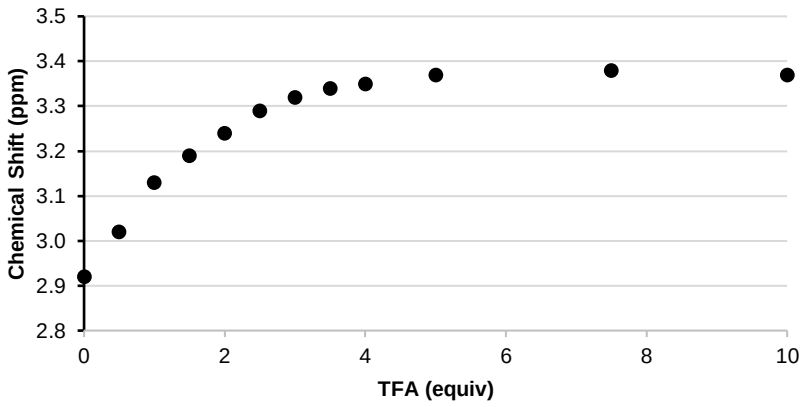

Scheme 3.1.3: ^{1}H NMR study: titration of *N*,*N*-dimethylaniline with TFA (A) ^{1}H NMR spectra, expansion: 3.5–2.5 ppm showing the methyl resonance of *N*,*N*-dimethylaniline at varying loadings of TFA. (B) Tabulated data. (C) Graphical illustration of saturation behavior of *N*,*N*-dimethylaniline at high loadings of TFA.

Next, the effect that the pK_a of the Brønsted acid additive had on the yield of the reaction was explored. When TFA (pK_a = −0.25 in H_2O) was substituted with acetic or formic acid modest yields were obtained (Table 3.1.4, entries 1–3).[10] However, the use of

dichloroacetic acid delivered the product in 58% yield (entry 4). Trichloroacetic acid delivered a modest yield (entry 5). It was found that when *p*-toluenesulfonic acid or triflic acid were employed very low yields were obtained (entries 6–7). Consequently, no clear trends associated with the pK_a could not be identified. When Lewis acids were employed very low yields were also obtained (entries 8–10). It was noted that a 43% yield could be obtained using the sacrificial oxidant diethyl 2-bromomalonate in place of TFA and essentially no reaction occurs employing diethyl malonate (entries 11 and 12). This observation is consistent with $[Cu^*(dap)_2]^+$ reducing diethyl 2-bromomalonate to provide $[Cu(dap)_2]^{2+}$, which can subsequently facilitate the oxidation of *N*,*N*-dimethylaniline and, ultimately, the formation of the tetrahydroquinoline product (Figure 3.1.1). However, in the presence of other bromides, such as either *p*-nitrobenzyl bromide or bromotrichloromethane essentially no product is formed (entries 13 and 14). In order to investigate the effects that salts may have on the ionic strength of the reaction mixture and the efficiency of the process, $NaBF_4$ and CF_3CCO_2Na were used as additives (entries 15 and 16).[11] However, in both cases, only low yields were obtained.

Table 3.1.4: Copper-catalysed reaction of *N*-phenylmaleimide with *N*,*N*-dimethylaniline: Influence of additives.

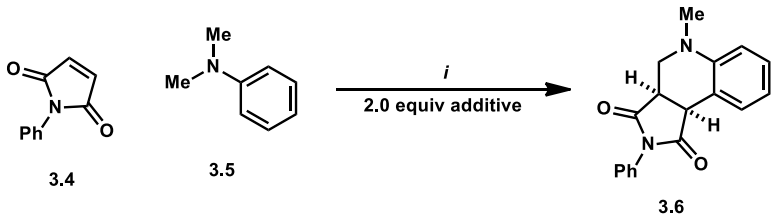

3.4 3.5 3.6

entry	additive	pK_a	yield (%)[a]
1	CF_3CO_2H	–0.25	77
2	CH_3CO_2H	4.76	13
3	HCO_2H	3.77	20
4	Cl_2CHCO_2H	1.29	58
5	Cl_3CO_2H	0.65	20
6	$TsOH·H_2O$	–1.3	7
7	TfOH	–14	<2
8	$AlCl_3$		<2
9	$EuCl_3$		<2
10	$Gd(OTf)_3$		8
11	$BrCH(CO_2CH_2CH_3)_2$		43
12	$CH_2(CO_2CH_2CH_3)_2$		3
13	*p*-$NO_2(C_6H_4)CH_2Br$		<2
14	$BrCCl_3$		3
15	$NaBF_4$		14
16	F_3CCO_2Na		16

Procedure: (*i*) 5% $[Cu(dap)_2]Cl$, 1 equiv **3.4**, 2 equiv **3.5**, 2 equiv additive, green LEDs, DMF, r.t., air, 16 h. Aqueous pK_a values are quoted. [a]Determined by gas chromatography with the aid of an internal standard (average of two experiments).

In 1989, Travin and co-workers investigated the autoxidation of bis(1,10-phenanthroline)copper(I) and observed this process to be extremely slow in dimethylformamide, acetonitrile, and nitromethane solutions (Figure 3.1.3).[12] Specifically, the authors noted that after 24 h only ~10% oxidation to the copper(II) complex occurred in an acetonitrile solution containing dissolved oxygen. Remarkably, it was illustrated that the addition of strong acids such as trichloroacetic, perchloric, or picric acid provides a spectacular rate enhancement which enables the complete oxidation of bis(1,10-phenanthroline)copper(I) within <3 ms ($k = 10^6$ Ms^{-1} in an acetonitrile solution). This study is the only published report that highlights and explicitly attempts to quantify the effect that strong Brønsted acids have on the autoxidation of bis(1,10-phenanthroline)copper(I) complexes.[13] In the transformation that has been developed, it is postulated that an essential role of TFA is to mediate the aerobic oxidation of a putative photoexcited [Cu(I)]* species.

This is crucial in facilitating the proposed (productive) quenching pathway for $[Cu(dap)_2]^+$ in this process (Figure 3.1.1).

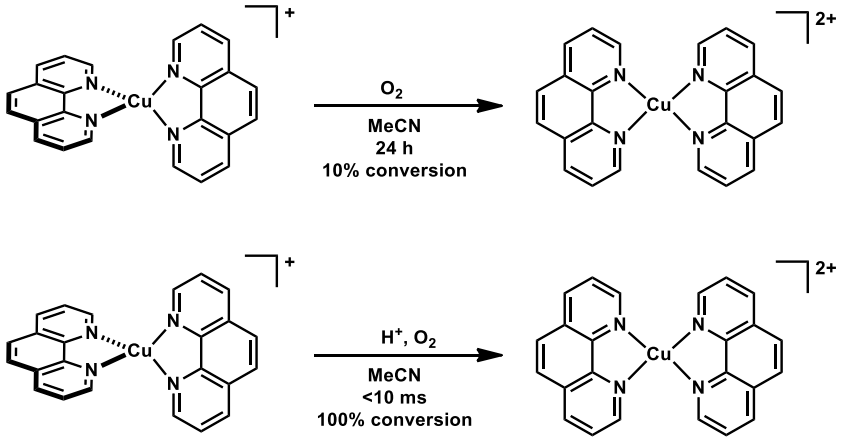

Figure 3.1.3: Enhancement of the rate of oxidation of [bis(1,10-phenanthroline)copper(I)]$^+$ in the presence of Brønsted acids observed by Travin and co-workers.[12]

Under the standard reaction conditions a 77% yield of annulated product **3.6** is obtained and with only a 10% loading of TFA a significant amount of product **3.6** is still produced (Table 3.1.5, entries 1 & 2). However, in the absence of TFA, no reaction is observed (entry 3). When TFA is replaced with the sacrificial oxidant diethyl 2-bromomalonate a significant amount of product is obtained (entry 4). These results are consistent with a TFA-mediated autoxidation of the photoexcited Cu(I)* species which also produces a superoxide anion. When the proposed on-cycle copper(II) species $[Cu(dap)_2]Cl_2$ is used in place of $[Cu(dap)_2]Cl$ the product is obtained in 76% yield demonstrating the chemical competence of this complex in the reaction (entry 5). Additionally, when this reaction was repeated using $[Cu(dap)_2]Cl_2$ in the absence of TFA, the product was still able to be formed in 36% yield (entry 6). These results are consistent with $[Cu(dap)_2]^{2+}$ oxidising *N*,*N*-dimethylaniline (**3.5**) to its corresponding α-amino radical, which can ultimately deliver the product **3.6**. Potentially, reactive oxygen species that are produced in downstream reaction steps may facilitate catalyst turnover or the direct oxidation of amine **3.5** (*vide infra*).[2a,14]

Table 3.1.5: Investigation of the chemical competence $[Cu(dap)_2]Cl_2$.

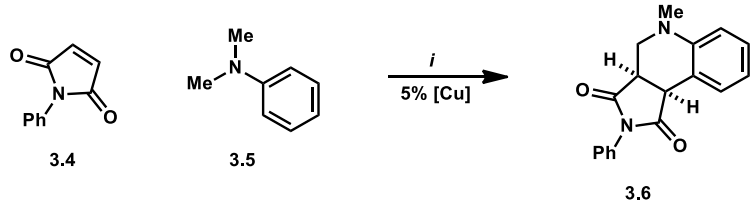

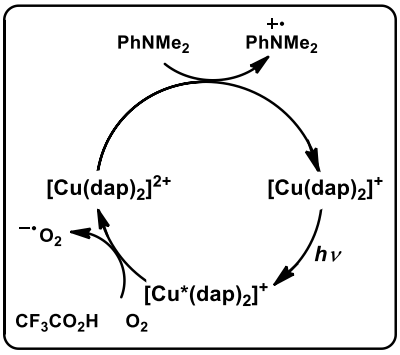

Entry	Catalyst	Variation	Yield (%)[a]
1	$[Cu(dap)_2]Cl$	2 equiv TFA	77
2	$[Cu(dap)_2]Cl$	10% TFA	47
3	$[Cu(dap)_2]Cl$	–	<2
4	$[Cu(dap)_2]Cl$	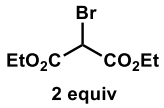 2 equiv	43
5	$[Cu(dap)_2]Cl_2$	2 equiv TFA	76
6	$[Cu(dap)_2]Cl_2$	–	37

Procedure: (*i*) 1 equiv **3.4**, 2 equiv **3.5**, green LED, DMF, r.t., air, 16 h. [a]Determined by gas chromatography with the aid of an internal standard (average of two experiments).

To provide more evidence for the above hypothesis, the autoxidation of $[Cu(dap)_2]Cl$ was monitored by ^1H NMR spectroscopy. The ^1H NMR spectrum of $[Cu(dap)_2]Cl$ is shown in Figure 3.1.4A and displays sharp resonances consistent with a diamagnetic Cu(I) species. After irradiation for 24 h with green LEDs in the absence of TFA this ^1H NMR spectrum was essentially left unchanged suggesting that minimal oxidation of the complex had occurred. Next, TFA (2 equivalents) was added to an irradiated solution of $[Cu(dap)_2]Cl$. The ^1H NMR spectrum was recorded immediately and it displayed only 2 of the 5 original resonances in the range 9.5–5.0 ppm, and these were severely broadened. This is consistent with complete oxidation to provide the paramagnetic Cu(II) species in the time that it took to perform the ensuing ^1H NMR experiment (Figure 3.1.4B).[a] Subsequently, after the addition of *N*,*N*-dimethylaniline (2 equivalents), the return of signals consistent with the presence of a diamagnetic, dap-coordinated copper(I) complex was observed in the ^1H NMR spectrum as

[a]The spectrum thus obtained (Figure 3.1.3B) was consistent with the ^1H NMR spectrum of an authentic sample of $[Cu(dap)_2]Cl_2$.

well as additional resonances consistent with *N*,*N*-dimethylaniline (Figure 3.1.4C).[b] These data, the reported slow aerobic oxidation of bis(phenanthroline)copper(I) complexes,[15] and the aforementioned results and observations, when taken together, are consistent with the TFA-mediated oxidative quenching of $[Cu^*(dap)_2]^+$ by dioxygen.

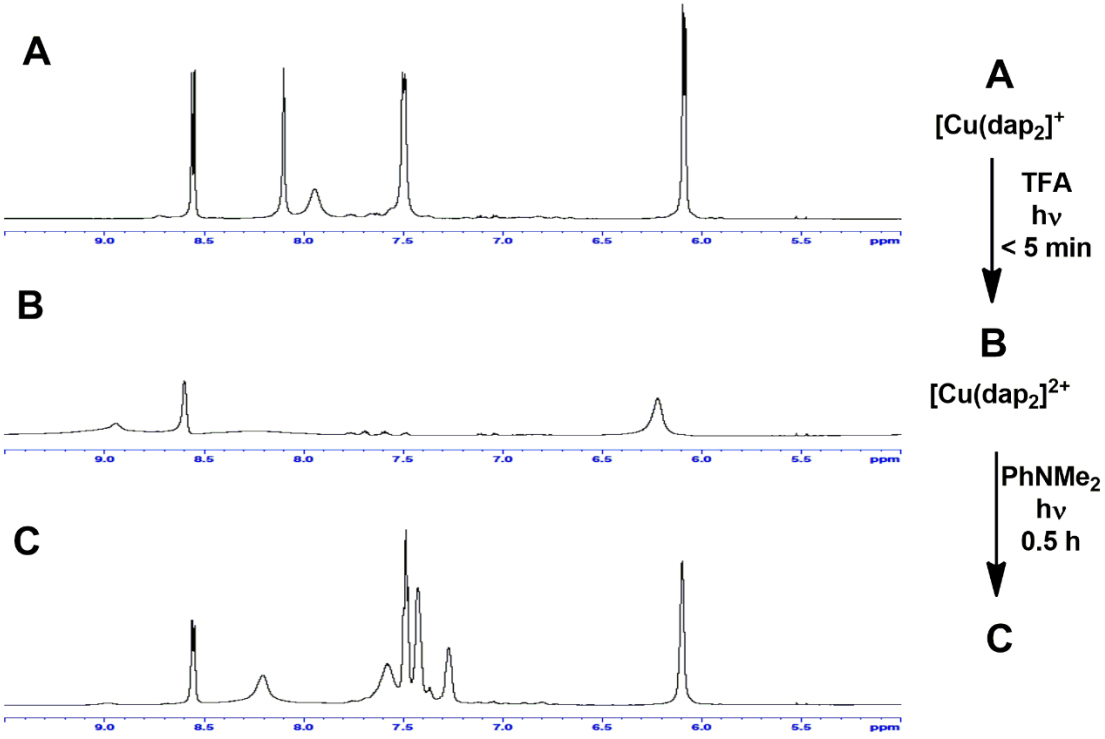

Figure 3.1.4: ^{1}H NMR investigation of the TFA-mediated oxidation of $[Cu(dap)_2]^+$, under irradiation with a green LED in air (scale 9.5–5.0 ppm; CD_3CN): (A) spectrum of $[Cu(dap)_2]Cl$; (B) spectrum obtained after the addition of 2 equiv of TFA to (A); (C) spectrum obtained after the subsequent addition of 2 equiv of *N*,*N*-dimethylaniline to (B).

These results suggest that TFA plays a crucial role in facilitating the autoxidation of a photoexcited copper(I) to copper(II) species in this process and a plausible mechanism for this annulation reaction is outlined in Figure 3.1.5.[2a] Thus, it is believed that, after photoexcitation, the TFA-mediated aerobic oxidation of $[Cu^*(dap)_2]^+$ provides $[Cu(dap)_2]^{2+}$ (Figure 3.1.5, step I). The ensuing species could oxidise *N*,*N*-dimethylaniline (step II) with concomitant regeneration of $[Cu(dap)_2]^+$. Both triethylamine and *N*,*N*-diisopropylethylamine

[b] The integration of aromatic resonances consistent with *N*,*N*-dimethylaniline match the resonance assigned to the dimethyl groups. Integration of signals assigned to the Cu(I)/Cu(II) complex do not match. This is likely due to signal broadening derived from the paramagnetic nature of the Cu(II) complex.

have been proposed to act as stoichiometric reductants enabling the regeneration of $[Cu(dap)_2]^+$ from $[Cu(dap)_2]^{2+}$ in other processes utilising $[Cu(dap)_2]Cl$.[1c,16] This mechanism for catalyst turnover is consistent with all of the experimental observations. Deprotonation of the resultant *N*,*N*-dimethylaniline radical cation would then lead to the formation of an α-amino radical (step III). This intermediate could then react with *N*-phenylmaleimide via a radical addition process (step IV). The ensuing radical species could engage in an intramolecular cyclisation (step V), and a subsequent aerobic oxidation (step VI) would then deliver the observed annulated tetrahydroquinoline product. This final oxidation (stepVI) may also produce peroxy radicals which can facilitate catalyst turnover or direct oxidation of *N*,*N*-dimethylaniline. As indicated in Figure 3.1.5, beyond mediating the oxidation of $[Cu^*(dap)_2]^+$, it is possible that TFA may also be involved in other aspects of this process.

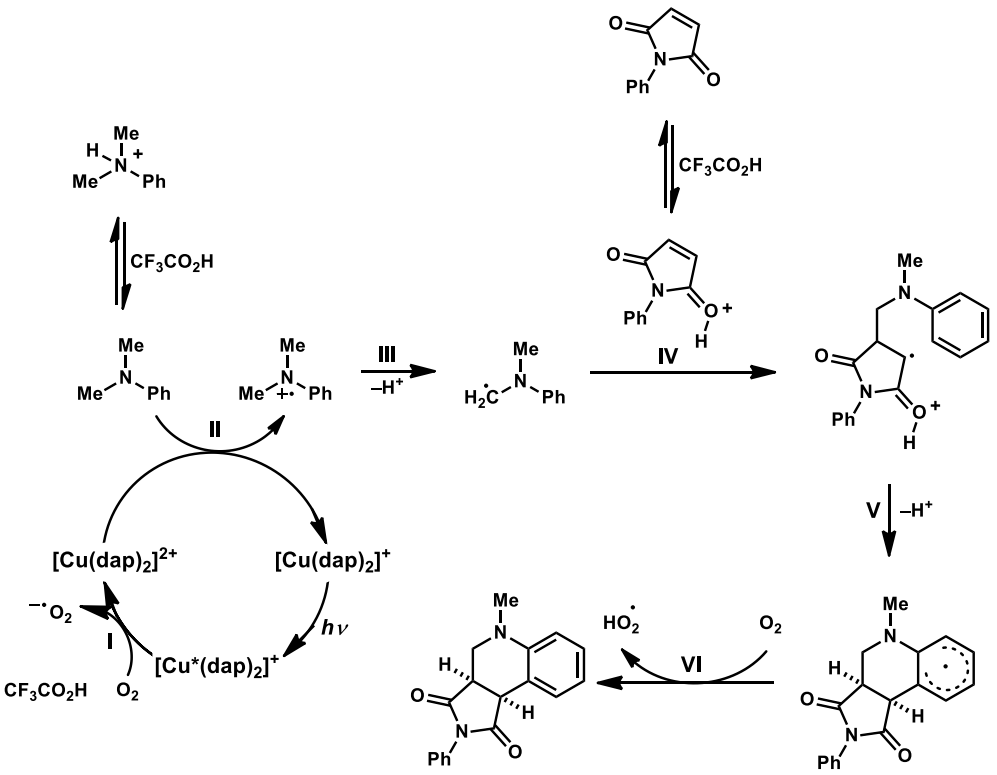

Figure 3.1.5: Outline of a possible mechanism for the $[Cu(dap)_2]Cl$-catalysed reaction of *N*-phenylmaleimide (**3.4**) with *N*,*N*-dimethylaniline (**3.5**).

It is anticipated that the results of this study may have important implications when considering the development of new processes featuring copper(I) photoredox catalysts and Brønsted acid-mediated radical reactions more generally.[17,18] Specifically, it is postulated that

this method for the oxidation of α-amino C−H bonds can be exploited to develop a variety of related processes. For example, it was subsequently established that the direct formation of a 12,13-dihydro-4b-*H*-isoquinolino[2,1-*a*]quinazolin-6(5*H*)-one scaffold from tetrahydroisoquinoline **3.24** can be effected in 56% yield employing unoptimised reaction conditions (Scheme 3.1.4). An X-ray crystal structure of annulated product **3.25** was obtained.

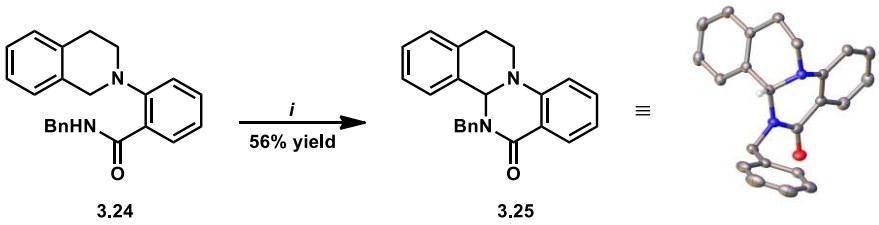

Scheme 3.1.4: [Cu(dap)$_2$]Cl-catalysed synthesis of an annulated heterocycle via an intramolecular cyclisation process. Reagents and conditions: (*i*) 2.5% [Cu(dap)$_2$]Cl, 1 equiv **3.24**, 1 equiv TFA, green LED, DMF, r.t., air, 16 h.

3.1.5 Summary and conclusions

In summary, the first example of the direct functionalisation of α-amino C−H bonds promoted by a copper-based photoredox catalyst has been developed. This is also the first example in which the weak oxidising capacity of $[Cu(dap)_2]^+$ has been utilised in photoredox catalysis. This chemistry enables the rapid synthesis of complex and important heterocyclic scaffolds including novel octahydroisoquinolino[2,1-*a*]pyrrolo[3,4-*c*]quinoline frameworks as single diastereoisomers. Most significantly, an unprecedented (and crucial) TFA-mediated aerobic oxidation of a putative photoexcited [Cu(I)]* species has been identified and exploited in order to facilitate a catalytic transformation. As such, it would appear that this process represents a somewhat rare example of a Brønsted acid-mediated radical reaction in organic synthesis.[17] It is anticipated that the outcomes of this research will contribute to expanding the scope and applications of visible-light-mediated copper(I) photoredox catalysis in organic synthesis in the future.

3.2 Exploiting the Strong Reducing Power of Copper(I) Complexes in Photoredox Catalysis

3.2.1 Overview

At the beginning of 2015, when this project began, bis(phenanthroline)copper(I) photoredox catalysts were known to catalyse only a very limited range of reaction types. Specifically, reductive couplings and ATRA reactions.[17,19] All of these transformations were proposed to have proceeded via the initial reduction of an organic substrate by the photoexcited copper(I) complex. The typically strong reducing power of photoexcited bis(phenanthroline)copper(I) complexes is likely the reason that such transformations were the first to be developed. As such, subsequent investigations focused on reductive transformations with a view to expanding the synthetic scope of copper photoredox catalysis.

The aim was to rapidly identify synthetically useful reactions that could be facilitated by a copper-based photoredox catalyst for subsequent development and optimisation. Accordingly, exhaustive investigations of each reaction type were not conducted, rather rapid screening of reaction conditions and substrates were performed in order to guide more extensive studies.

3.2.2 Reduction of alkyl halides

The seminal report by Sauvage and co-workers published in 1987 described the reductive coupling of *p*-nitrobenzylbromide (**3.26**) to deliver bis-(*p*-nitro)bibenzyl (**3.27**) under an inert atmosphere (Scheme 3.2.1A).[16a] This work was repeated with several photoredox catalysts for benchmarking purposes and to ensure that reported work could be repeated. The photocatalysts tested were $[Ir(ppy)_3]$, $[Cu(dap)_2]Cl$ and $[Cu(bcp)(XP)]PF_6$. After irradiation with white (Ir) or green (Cu) light the expected reductive coupling product was obtained for all photoredox catalysts, with full conversion of starting material as judged by ^1H NMR spectroscopy. Specifically, a shift of the methylene resonance from 4.51 ppm to 3.13 ppm was the most diagnostic resonance. $[Ir(ppy)_3]$ delivered a 38% yield, $[Cu(dap)_2]Cl$ afforded a 48% yield which is in good agreement with the yield reported by Sauvage. $[Cu(bcp)(XP)]PF_6$ provided a 64% yield of product **3.27**. This increased yield is potentially due to the extended excited state lifetime for $[Cu(bcp)(XP)]PF_6$ compared to $[Cu(dap)_2]Cl$.

Both [Cu(bcp)(XP)]PF_6 and [Ir(ppy)$_3$] feature greater reducing power compared to [Cu(dap)$_2$]Cl. Perhaps, the increased yield when using [Cu(bcp)(XP)]PF_6 is less likely to derive from a stronger reduction potential as [Ir(ppy)$_3$] delivered a decreased yield.

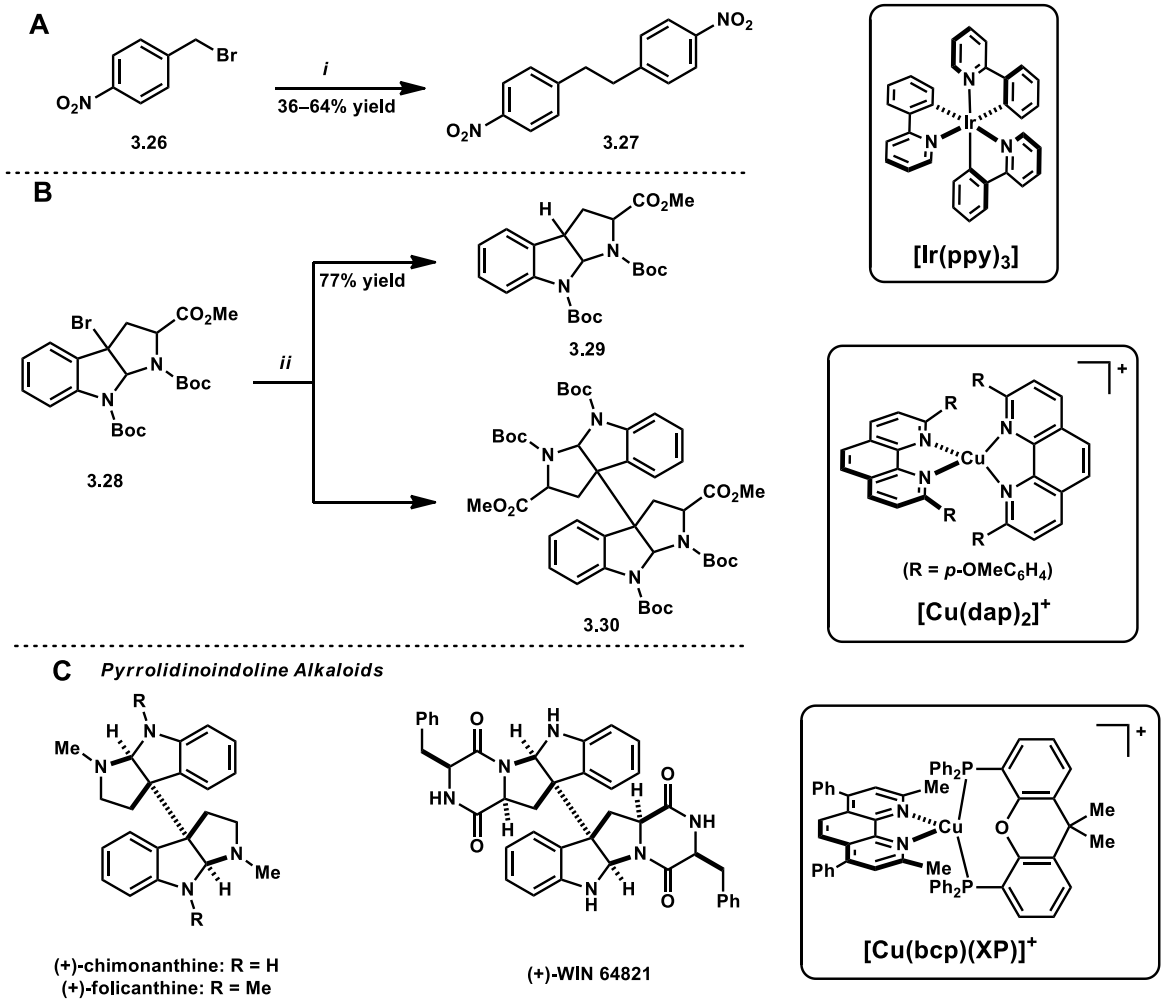

Scheme 3.2.1: (A) Benchmarking of reported copper photoredox-catalysed dimerisation; (B) Hydrodebromination and reductive dimerisation; (C) Examples of Pyrrolidinoindoline alkaloids. Reagents and conditions: (*i*) 1% [Ir(ppy)$_3$], [Cu(dap)$_2$]Cl or [Cu(bcp)(XP)]PF_6, 1.8 equiv NEt_3, hv, DMF; (*ii*) 2.5% [Ir(ppy)$_3$], [Cu(dap)$_2$]Cl or [Cu(bcp)(XP)]PF_6, 2 equiv NEt_3, blue LEDs, DMF. PC = photoredox catalyst

After reproducing this reported work, benzyl bromide **3.28** was reacted under similar conditions (Scheme 3.2.1B). Specifically, bromide **3.28** and the sacrificial reductant NEt_3, with a 2.5% loading of various photoredox catalysts, in DMF under blue LED irradiation. This substrate was selected for a number of reasons. First, structural similarities with known

pyrrolidinoindoline alkaloids present an opportunity to provide facile access to complex heterocycles, and dimerisation reactions of this substrate have been reported previously, however, not under photoredox catalysis (Scheme 3.2.1C).[20] In both cases, the halogen is located in a benzylic position. In the case of bromide **3.26**, homolysis at the benzylic position would result in production of a primary radical species. Conversely, homolysis at the analogous position of bromide **3.28** results in a typically more stable tertiary radical species.

Initially, this reaction was performed with only bromide **3.28**, photocatalyst and the sacrificial reductant triethylamine, to determine if the photocatalyst was able to effect the reduction of the substrate and deliver either the hydrodebromination product **3.29**, or potentially dimerisation product **3.30**. Indeed, when photocatalysts, $[Ru(bpy)_3](PF_6)_2$, $[Cu(dap)_2]Cl$ or $[Cu(bcp)(XP)]PF_6$ were utilised, the hydrodebromination product **3.29** was observed in all cases as determined by comparison of ^1H and ^{13}C NMR spectra to those reported in the literature.[20] A simple explanation that dimerisation did not occur is that the production of the new Csp^3–Csp^3 bond is highly sterically hindered which derives from the concave shape of the tricycle. More significantly, the photocatalytic reduction of bromide **3.28** would presumably lead to a tertiary alkyl radical species. Tertiary alkyl radicals are typically more stable than primary alkyl radicals. As such, dimerisation of the tertiary alkyl radical species may be hindered by this increased stability and H-atom abstraction becomes more feasible which leads to the observed hydrodebromination product **3.29**.

The observation of hydrodebromination product **3.29** suggests that the photoredox catalyst is capable of reducing bromide **3.28** to produce putative alkyl radical species. As such, methyl vinyl ketone, a Michael acceptor which is known to undergo radical addition processes was added to the reaction mixture under otherwise identical conditions and photoredox catalysts $[Ru(bpy)_3](PF_6)_2$, $[Cu(dap)_2]Cl$ and $[Cu(bcp)(XP)]PF_6$ were screened.[21] Unfortunately, the product of the reaction, in all cases, was the hydrodebromination product **3.29**. It is possible that the stability of the tertiary alkyl radical disfavours addition of methyl vinyl ketone. As such, a different approach aimed at functionalising this compound was performed. This involved a photoredox/ transition metal dual catalysis strategy. While this increases the complexity of the reaction significantly, this strategy fits well with the aim of rapidly screening reaction conditions.

There have been numerous reports of strategies featuring photoredox/ transition metal dual catalysis employed to effect C–C bond formation. However, there are no reports utilising a copper photoredox catalyst.[22] Given that these strategies have only been recently reported, mechanistic understanding of such transformations remains underdeveloped.[22] However, there are typically two main reaction modes through which these systems operate. On cycle transition metal intermediates can undergo photoredox-enabled oxidation/ reduction which then facilitates specific reaction steps, such as transmetallation or reductive elimination. In this way, energy barriers of transition states are lowered. An alternative strategy involves the photoredox-mediated production of radical intermediates that are subsequently coordinated by the transition metal catalyst. For example, Sanford and co-workers reported a photoredox/ transition metal dual catalysis system in which putative phenyl radicals **3.34** were produced by the reduction of phenyldiazonium **3.32** by photoredox catalyst $[Ru(bpy)_3]Cl_2$.[23] The resultant phenyl radical **3.34** was then coordinated by palladium complex **3.36** to ultimately deliver product **3.33** which incorporates a new C–C bond (Scheme 3.2.2).

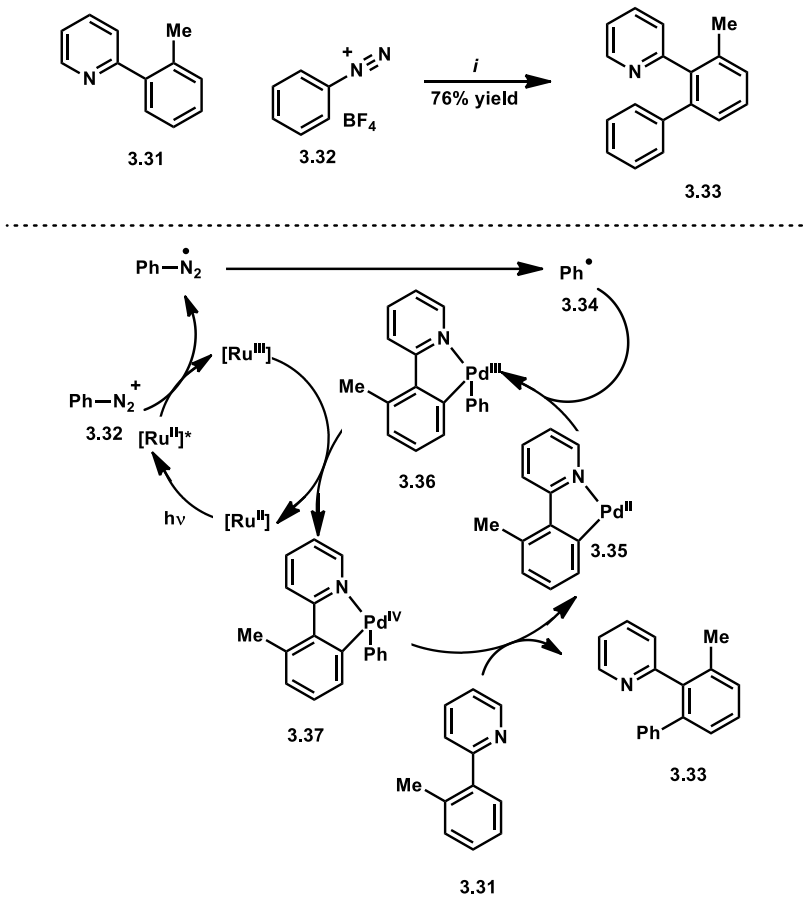

Scheme 3.2.2: Dual photoredox/ transition metal-catalysed reaction developed by Sanford and co-workers.[23] Reagents and conditions: (*i*) 2.5% $[Ru(bpy)_3]Cl_2 \cdot 6H_2O$, 10% $[Pd(OAc)_2]$, 1 equiv **3.31**, 4 equiv **3.32**, hv, MeOH, r.t.

A photoredox/ transition metal dual catalysis strategy was adopted to dimerise or functionalise bromide **3.28**. Initial attempts were made using $[Ru(bpy)_3](PF_6)_2$ as any complications relating to the lower coordinative stability of tetrahedral copper(I) complexes could be avoided. Previously, hydrodebromination product **3.29** was obtained when using a 2.5% loading of $[Ru(bpy)_3](PF_6)_2$ suggesting that an alkyl radical was produced, so this loading was maintained. Both nickel and palladium metal complexes were screened in this protocol with either 4,4'-di-*tert*-butyl-2,2'-bipyridine (dtbbpy) or triphenylphosphine ligands at varying loadings (10–30%). Initially, only $[Ru(bpy)_3](PF_6)_2$, transition metal catalyst system (either Ni or Pd source and the ligand), substrate **3.28** and sacrificial reductant NEt_3, were subjected to blue LED irradiation in either DMF or acetonitrile (Table 3.2.1, entries 1–5). However, in all cases, only hydrodebromination product **3.29** or starting material **3.28** were

observed. Better yields of hyrodebromination product **3.29** were observed when using $NiCl_2$•glyme and dtbbpy as the transition metal catalyst system and acetonitrile as the solvent. As such, both these variables were maintained for subsequent screening reactions unless otherwise noted.

Next, various electrophilic additives were screened including 2-bromobenzothiazole, allyl bromide and potassium phenyltrifluoroborate, however in all cases only the hydrodebromination product **3.29** and unreacted starting material **3.28** was observed (entries 6–8). Higher transition metal catalyst loadings were also screened but resulted in reduced yields of hydrodebromination product **3.29** (entries 9 & 10).

Finally, $[Ru(bpy)_3](PF_6)_2$ was substituted for copper photoredox catalysts $[Cu(dap)_2]Cl$, or $[Cu(bcp)(XP)]PF_6$ and these were screened in the presence of bromide **3.28** and triethylamine as sacrificial reductant, as well as $NiCl_2$•glyme and dtbbpy, to determine if the dimerisation product **3.30** could be produced under these conditions. Unfortunately, only hydrodebromination product **3.29** and starting material **3.28** were obtained. Given the absence of dimer **3.30** or any other functionalised product under all reaction conditions, further attempts were abandoned.

Table 3.2.1: Screening of various transition metal catalyst systems, electrophillic additives and reaction conditions in an attempt to produce dimer **3.30** or other functionalised compounds.

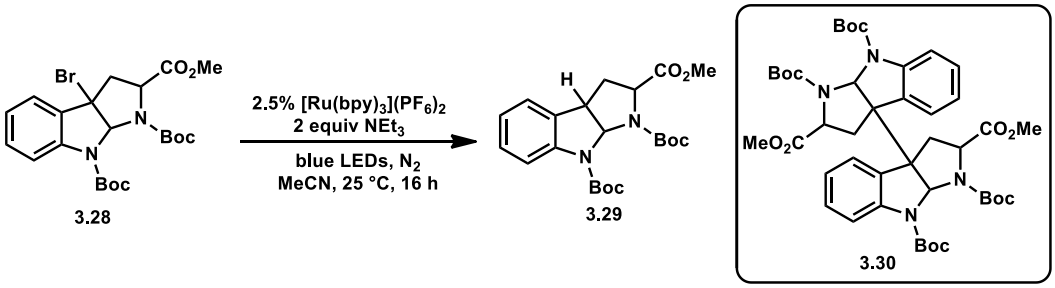

entry	catalyst system	variation from the above conditions	yield (%)[a]
1	**5% $NiCl_2$ 10% dtbbpy**	DMF instead of MeCN	65
2	**5% $NiCl_2$•glyme 10% dtbbpy**	DMF instead of MeCN	72
3	**5% $[Pd(PPh_3)_4]$**	DMF instead of MeCN	38
4	**5% $NiCl_2$•glyme 10% dtbbpy**	No change	77
5	**5% $[Pd(PPh_3)_4]$**	No change	40
6	**5% $NiCl_2$•glyme 10% dtbbpy**	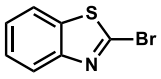 2 equiv	48
7	**5% $NiCl_2$•glyme 10% dtbbpy**	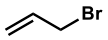 2 equiv	32
8	**5% $NiCl_2$•glyme 10% dtbbpy**	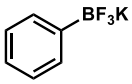 2 equiv	24
9	**10% $NiCl_2$•glyme 20% dtbbpy**	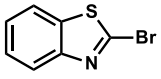 2 equiv	42
10	**15% $NiCl_2$•glyme 30% dtbbpy**	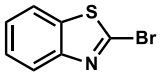 2 equiv	34
11	**5% $NiCl_2$•glyme 10% dtbbpy**	$[Cu(dap)_2]Cl$ instead of $[Ru(bpy)_3](PF_6)_2$	74
12	**5% $NiCl_2$•glyme 10% dtbbpy**	$[Cu(bcp)(XP)]PF_6$ instead of $[Ru(bpy)_3](PF_6)_2$	81

[a]Yield determined by ^1H NMR analysis with the aid of an internal standard (average of 2 experiments).

3.2.3 Hofmann–Löffler–Freytag reaction

The Hofmann–Löffler–Freytag (HLF) reaction is a remote functionalisation reaction that allows functionalisation at the δ-position of *N*-halogenated alkylamines, or cyclisation to produce pyrrolidines.[24] It is suggested that the reaction typically proceeds through a radical chain mechanism with homolytic cleavage of the N–X bond initiated by heat, irradiation with UV light or with radical initiators such as azodiisobutyronitrile (AIBN).[25] Then, 1,5-H atom abstraction produces a δ-alkyl radical which can be trapped by the halide anion to functionalise the δ-position. Subsequent nucleophilic attack by the amine lone pair at the δ-position delivers pyrrolidines via an S_N2 reaction (Scheme 3.2.3). An energetically favoured, 6-membered transition state promotes the 1,5-H atom abstraction.

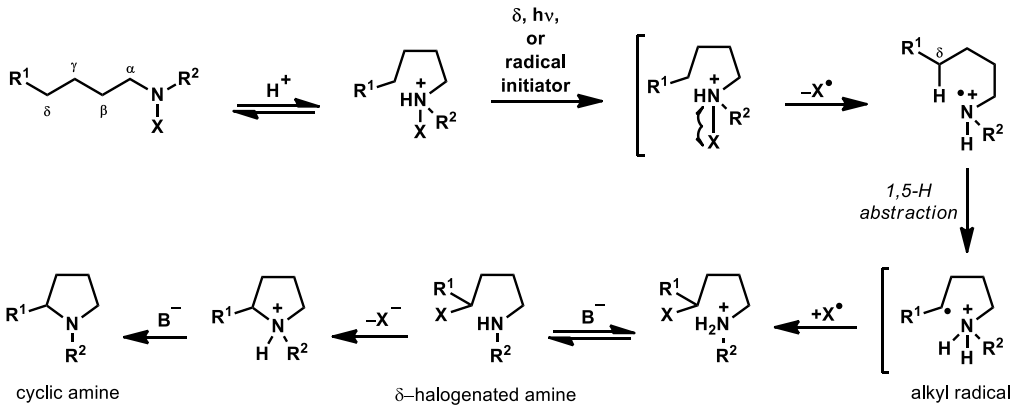

Scheme 3.2.3: Generally accepted mechanism of the HLF reaction.

It was anticipated that photoredox catalysis could be used to reduce the *N*-halogenated alkylamine to produce an *N*-centered radical cation that would undergo a HLF reaction. This has been reported previously but not with a copper-based photoredox catalyst.[26] Initial attempts employed *N*-tosyl-protected, *N*-chlorinated amine **3.38**, and irradiation from green LEDs in the presence of 5 mol% $[Cu(dmp)_2]Cl$. Base free conditions were used to avoid cyclisation of the expected δ-chlorinated amine **3.39** to avoid complications in purification or analysis. Control reactions were performed simultaneously. Specifically, experiments performed in the absence of catalyst, the absence of light, and in the

absence of catalyst and light. Unfortunately, in all cases only starting material was returned.[c] This is possibly due to the short excited state lifetime of $[Cu(dmp)_2]^+$ (90 ns) or the absence of a sacrificial reductant to facilitate catalyst turnover. As such, the reactions were repeated in the presence of 1.2 equivalents of K_2HPO_4. This base was chosen as it has been used previously in related copper-photocatalysed reactions.[27] Fortunately, a small amount (<10%) of the desired δ-chlorinated amine **3.39** was observed by ^{1}H NMR spectroscopy. Specifically, the appearance of a triplet resonance at 4.93 ppm assigned to the δ-CH proton suggests the presence of δ-chlorinated amine **3.39** and is consistent with reported spectra.[28] Interestingly, pyrrolidine **3.40** was not observed despite the presence of base (Scheme 3.2.4).

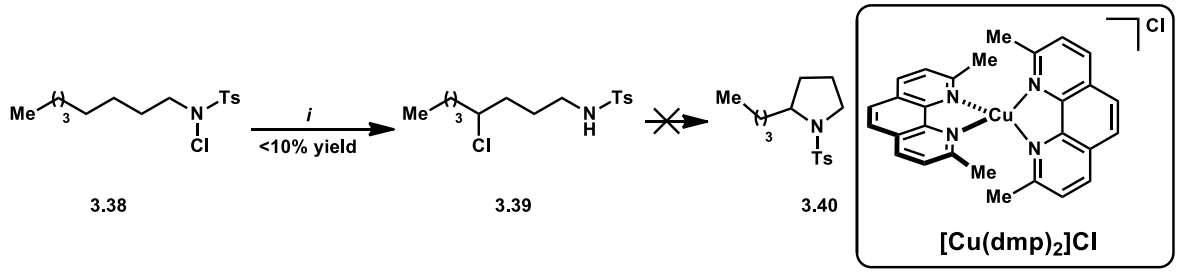

Scheme 3.2.4: Reduction of *N*-halogenated alkylamine **3.38** to produce δ-functionalised alkylamine **3.39**. Reagents and conditions: (*i*) 5% $[Cu(dmp)_2]Cl$, 1 equiv **3.38**, 1.2 equiv K_2HPO_4, green LEDs, r.t., DMF.

In an attempt to improve the yield of this reaction, different catalysts with longer photoexcited state lifetimes were screened under otherwise unchanged reaction conditions. The catalysts screened were $[Ru(bpy)_3](PF_6)_2$, $[Cu(dap)_2]Cl$, and $[Cu(bcp)(XP)]PF_6$. In all cases, improved yields of δ-chlorinated product **3.39** were observed, with all photoredox catalysts delivering complete consumption of starting material and yields of chloride **3.39** between 65–78%. (Scheme 3.2.5).

[c] As determined by TLC and ^{1}H NMR spectroscopy.

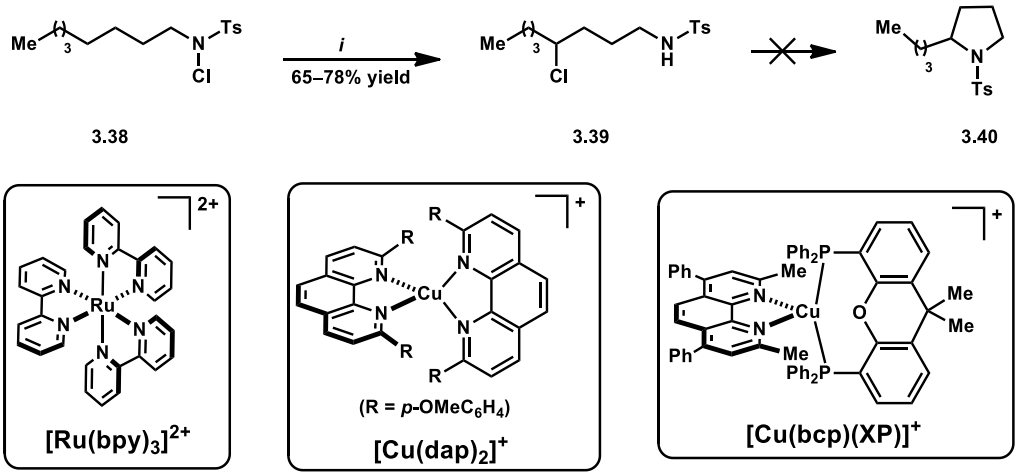

Scheme 3.2.5: Reduction of *N*-halogenated alkylamine **3.38** to produce δ-functionalised alkylamine **3.39**. Reagents and conditions: (*i*) 5% PC, 1 equiv **3.38**, 1.2 equiv K_2HPO_4, green LEDs, r.t., DMF. PC = photoredox catalyst.

These results suggest that a putative δ-alkyl radical was produced and subsequently trapped by chloride which is consistent with the typical mechanism of the HLF reaction.[25] Subsequent experiments were performed to determine if the δ-position could be functionalised with other nucleophiles. Although the development of a copper-photocatalysed transformation remained the ultimate goal, preliminary screening reactions were performed utilising $[Ru(bpy)_3](PF_6)_2$ to conserve supplies of $[Cu(dap)_2]Cl$ and to avoid complications derived from the coordinatively unsaturated nature of the copper(I) complexes.

Diazonium salt **3.41** was initially chosen to determine if the δ-position of amine **3.38** could be functionalised by nucleophiles other than chloride. This was examined under unchanged conditions to those described above but in the presence of 1 equivalent of diazonium salt **3.41** (Scheme 3.2.6A). Under these conditions only δ-chlorinated amine **3.39** was observed in 78% yield.[d] Interestingly, diazonium salt **3.41** was not observed in the crude reaction mixture, which was examined after all volatiles had been removed under reduced pressure. It is likely that diazonium salt **3.41** was reduced either by the action of $[Ru(bpy)_3](PF_6)_2$ or by visible light decomposition (*vide infra*) to deliver benzene and N_2 which is consistent with these observations. To determine if the reduction of diazonium **3.41** could

[d] As determined by TLC and ^1H NMR spectroscopy.

be achieved with a copper photoredox catalyst, $[Ru(bpy)_3](PF_6)_2$ was substituted for $[Cu(dap)_2]Cl$ and the reaction performed under otherwise identical conditions. Indeed, similar results were obtained (65% yield of **3.39**). However, these conditions still did not deliver δ-arylated product (Scheme 3.2.6A).

In an attempt to access δ-functionalised alkyl amines, a photoredox/ transition metal dual catalysis strategy was investigated. Palladium(0) sources, $[Pd(dba)_2]$ and $[Pd(PPh_3)_4]$ and nickel(0) source $[Ni(dppf)(P(OPh_3)_2]$ as well as $NiCl_2$•glyme were investigated with a range of nucleophiles including diazonium salt **3.41,** iodide **3.42**, potassium phenyltrifluoroborate (**3.43**), bis(pinacolato)diboron (**3.44**). In all cases, δ-functionalised product was not observed (Scheme 3.2.6B). Finally, the development of a trifluoromethylation protocol was attempted utilising $TMSCF_3$ (**3.45**) as nucleophile. This was attempted in the presence and absence of CsF which was expected to facilitate the cleavage of the Si–C bond. Unfortunately, only the δ-chloroamine **3.39** was observed by ^1H NMR spectroscopy. This was then attempted in the presence of 5 mol% $[Cu(MeCN)_4]PF_6$, in a similar fashion to the photoredox/ transition metal dual catalysis described above (Scheme 3.2.2). However, this also delivered δ-chloroamine **3.39** but the trifluoromethylated product was not observed (Scheme 3.2.6C). Given δ-chloroamine **3.39** was the only product identified throughout the above experiments, further attempts were abandoned. It is possible that the presence of chloride is hindering attempts to functionalise the δ-position of amine **3.38** by trapping the δ-alkyl radical intermediate before other nucleophiles or transition metal complexes can intercept this intermediate. If the chloride present in amine **3.38** could be replaced with a non-nucleophilic leaving group, this may facilitate a δ-functionalisation reaction.

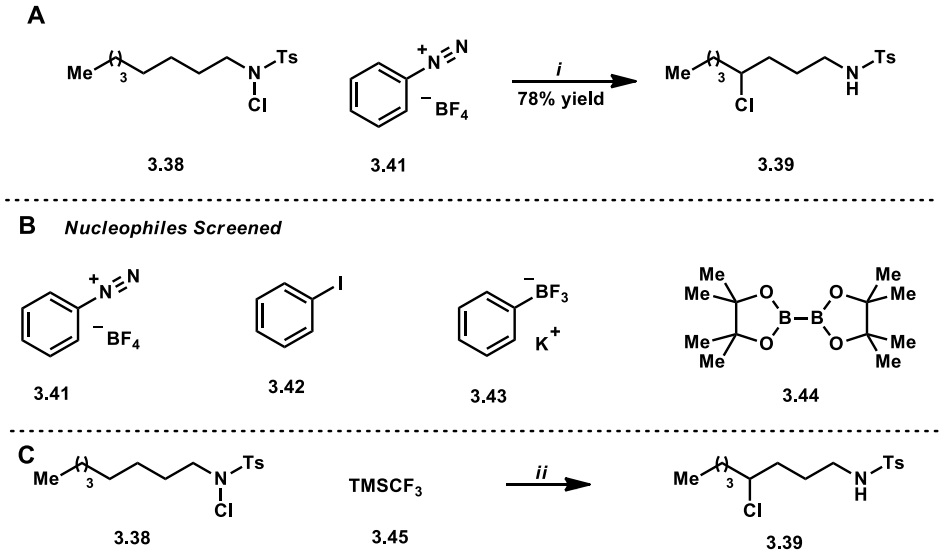

Scheme 3.2.6: (A) Attempted functionalisation of *N*-halogenated alkylamine **3.38** with diazonium salt **3.41**; (B) Various nucleophiles screened in the attempted functionalisation reaction; (C) Attempted trifluoromethylation reaction. Reagents and conditions: (*i*) 5% $[Ru(bpy)_3](PF_6)_2$, 1 equiv **3.38**, 1 equiv **3.41**, 1.2 equiv K_2HPO_4, Blue LEDs, r.t., DMF; (*ii*) 5% $[Ru(bpy)_3](PF_6)_2$, 5% $[Cu(MeCN)_4]PF_6$, 1 equiv **3.38**, 1 equiv **3.45**, 1.2 equiv K_2HPO_4, Blue LEDs, r.t., DMF.

3.2.4 Reduction of aryldiazonium Salts

One of the earliest examples of photoredox catalysis in organic synthesis involves the reduction of aryldiazonium salts. The Pschorr reaction is initially a copper-catalysed intramolecular coupling of an aryldiazonium salt with a substituted arene.[29] In 1984, Deronzier reported that this reaction could be catalysed by $[Ru(bpy)_3]^{2+}$ under visible light photoredox catalysis.[30] Reduction of aryldiazonium salts is very facile,[e] and if performed via SET, typically results in the production of an aryl radical with concomitant loss of N_2.[31] Given the strong reducing power of $[Cu(dap)_2]^+$, and results described in the previous section, it was anticipated that production of aryl radicals from aryldiazonium salts could be catalysed by $[Cu(dap)_2]^+$.

To test this hypothesis, diazonium **3.41** was subjected to blue light irradiation in the presence of photocatalysts $[Ru(bpy)_3](PF_6)_2$ and $[Cu(dap)_2]PF_6$ in acetonitrile under a nitrogen atmosphere. Interestingly, the product of the reaction was amide **3.46** in both cases. This is presumably formed by addition of acetonitrile to the putative phenyl radical and subsequent

[e] $E_{1/2}$ = –0.1 V vs. SCE for phenyldiazonium tetrafluoroborate.

trapping by residual water in the solvent or upon work up (Scheme 3.2.7). The reactions were repeated with both $[Ru(bpy)_3](PF_6)_2$ and $[Cu(dap)_2]PF_6$ and simultaneous control experiments to determine the necessity of photocatalyst and light. In addition, an experiment using $[Ru(bpy)_3](PF_6)_2$ under air with a small amount of water (3 drops) present was also performed. In all cases, the reactions were performed for only 2 hours to expedite the investigation of optimal reaction conditions. The results are summarised in Table 3.2.2.

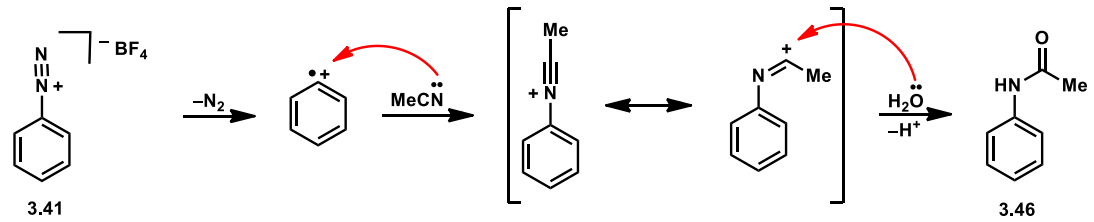

Scheme 3.2.7: Proposed mechanism for the production of amide **3.46**.

Table 3.2.2: Screening of reaction conditions to produce amide **3.46**.

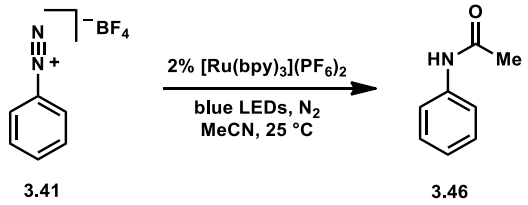

entry	Conditions	yield (%)[a]
1	No change	28
2	2% $[Cu(dap)_2]PF_6$ instead of $[Ru(bpy)_3](PF_6)_2$	42
3	No catalyst	39
4	air, 3 drops H_2O	10

[a]Yield determined by GC analysis with the aid of a calibrated internal standard (average of 2 experiments).

The reaction proceeded in 28% yield in the presence of $[Ru(bpy)_3](PF_6)_2$ but was more efficient using $[Cu(dap)_2]PF_6$ (42% yield) (Table 3.2.2, entries 1 & 2). Interestingly, the reaction proceeded in the absence of photocatalyst (entry 3). The reaction was impeded when using $[Ru(bpy)_3](PF_6)_2$ under air and in the presence of water (entry 4). These results suggest that a

photocatalyst is not necessary for an efficient reaction. Further, the presence of either air or water hinders the reaction but, given the incorporation of water in the product **3.46**, it is more likely that the atmosphere of air is responsible for the reduced yield. With these insights, the next set of screening reactions included the presence of 5 equivalents of water and white light irradiation under a range of conditions outlined in Table 3.2.3.

Table 3.2.3: Screening of reaction conditions to produce amide **3.46**.

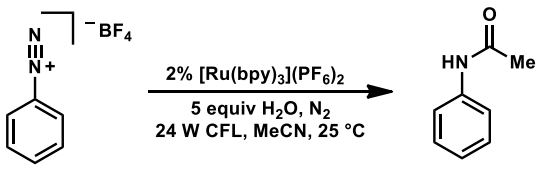

3.41 **3.46**

entry	Conditions	yield (%)[a]
1	No change	24
2	2% $[Cu(dap)_2]PF_6$ instead of $[Ru(bpy)_2](PF_6)_2$	24
3	No catalyst	25
4	No cataylst, air	24

[a]Yield determined by GC analysis with the aid of a calibrated internal standard (average of 2 experiments).

Under these conditions, the reaction was equally efficient in the presence or absence of either photocatalysts $[Ru(bpy)_3](PF_6)_2$ or $[Cu(dap)_2]PF_6$ (Table 3.2.3, entries 1–3). Interestingly, the presence of air did not seem to have an adverse effect on the reaction as was observed previously (Table 3.2.2, entry 4). Unfortunately, all yields were <30% after 2 hours. As such, the effect of the presence of water on the reaction outcome was examined as well as taking data points at varying time intervals. These data are presented in Table 3.2.4.

Table 3.2.4: Screening of reaction conditions and monitoring the formation of product **3.46** over time.

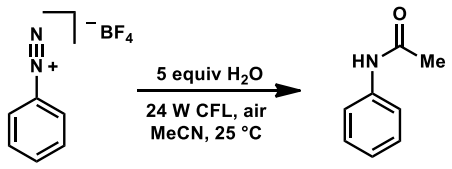

3.41 3.46

entry	Conditions	yield (%)[a] 2h	4h	6h	24h
1	No change	19	28	43	77
2	No added H_2O	13	24	35	44

[a]Yield determined by GC analysis with the aid of a calibrated internal standard (average of 2 experiments).

These experiments clearly demonstrate that the reaction is more efficient in the presence of 5 equivalents of water. However, the reaction does not proceed to completion even after 24 h. Finally, the reaction was performed under nitrogen with varying amounts of water and either with or without visible light irradiation. These results are summarised in Table 3.2.5.

Under these conditions, visible light irradiation consistently hindered the reaction (Table 3.2.5, entries 1–3). Reactions performed in the dark were more efficient and the presence of water was necessary for the reaction to proceed to completion more rapidly (entries 4–6). Reducing the amount of water to 5 equivalents afforded the most efficient reaction with quantitative yield after 48 hours (entry 5). It appears that the decomposition of diazonium **3.41** occurs efficiently in the presence of H_2O in acetonitrile even in the absence of light at 25 °C. Diazonium salts are inherently reactive species. The energetically favourable production of N_2 is likely the driving force for this decomposition under mild conditions.

Table 3.2.5: Screening of reaction conditions and monitoring the formation of product **3.46** over time.

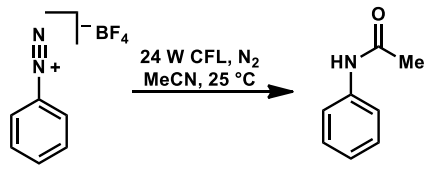

3.41 **3.46**

entry	Conditions	yield (%)[a]			
		2h	6h	24h	48h
1	10 equiv H_2O	17	32	61	74
2	5 equiv H_2O	18	45	57	65
3	No added H_2O	22	26	33	38
4	10 equiv H_2O, no $h\nu$	19	21	62	90
5	5 equiv H_2O, no $h\nu$	23	21	67	97
6	No H_2O, no $h\nu$	18	28	36	42

[a]Yield determined by GC analysis with the aid of a calibrated internal standard (average of 2 experiments).

In conclusion, an efficient reaction to produce amide **3.46** was developed with the optimal conditions being quite mild, however with a long reaction time (48 h). There are a number of reported procedures which feature acetonitrile incorporation to a range of diazonium salts,[32] however these feature either UV or microwave irradiation or elevated temperatures which may not be compatible with more complex molecules or some functional groups. The mild procedure reported here may provide an alternative approach for the amidation of complex molecules, however the scope of this reaction was not investigated.

3.2.5 Reduction of diphenylmethylbenzoates

In 2014, Reiser and co-workers reported the reduction of a series of diphenylmethylbenzoates catalysed by $[Ir(ppy)_2(dtbbpy)]PF_6$ under visible light photoredox catalysis.[33] The benzoates investigated featured different substitution patterns on the benzoate moiety which altered the reduction potential of the substrate (Scheme 3.2.8). When tested under the reported conditions, the reduction of benzoate **3.51** was found to be the most efficient and this was suggested to derive from its lower reduction potential. The reduction potential of the iridium photoredox catalyst used was reported as –1.51 V vs. SCE. Given the

similar reducing power of [Cu(dap)$_2$]Cl (–1.43 V vs. SCE), it was anticipated that this copper-based photoredox catalyst could provide comparable reactivity.

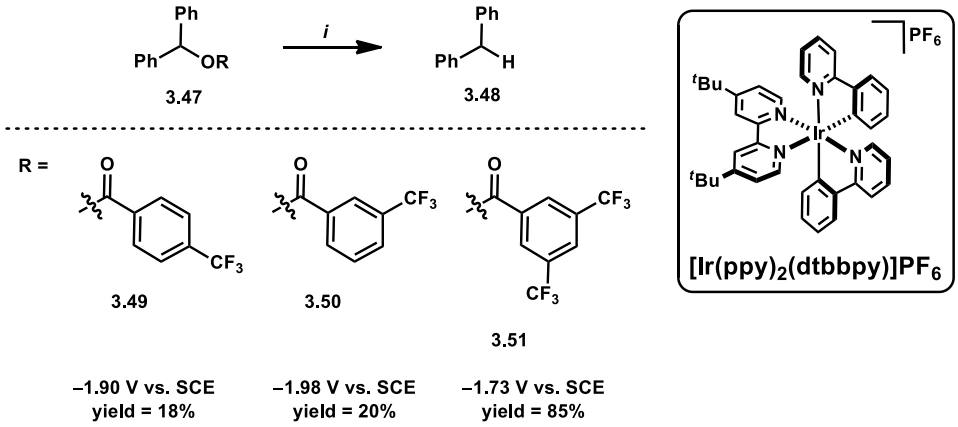

Scheme 3.2.8: Reduction of diphenylmethylbenzoates reported by Reiser.[32] Reagents and conditions: (*i*) 1 equiv **3.47**, 1% [Ir], 1.1 equiv Hantzsch ester, 2 equiv *i*Pr$_2$NEt, blue LEDs, MeCN/ H$_2$O (14:1), 40 °C, 16 h.

Initial testing of [Cu(dap)$_2$]Cl was conducted in parallel to [Ir(ppy)$_3$] under identical reaction conditions for benchmarking purposes.[f] The reaction conditions tested were identical to the optimal conditions reported by Reiser but with a higher catalyst loading, in the absence of water and with irradiation from a 24 W CFL (Scheme 3.2.9). This resulted in the observation of only trace amounts (<5%) of the reduction product **3.48** observed in both cases. This was determined by analysis of the ^{1}H NMR spectrum with the aid of an internal standard. Specifically the appearance of a singlet resonance at 3.92 ppm is consistent with the reduction product **3.48**.

[f]A control reaction with no catalyst present was also conducted. (No reduction product observed in this experiment).

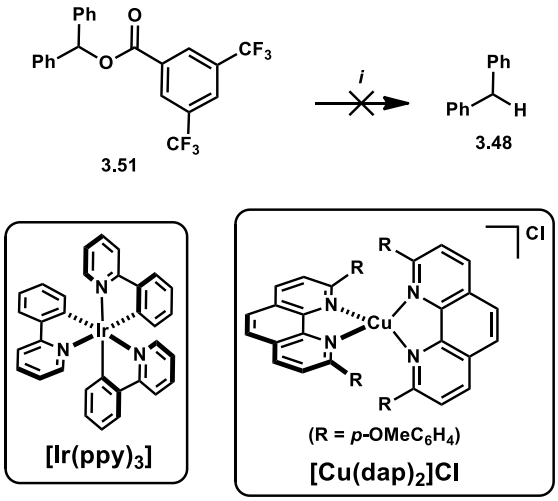

Scheme 3.2.9: Reduction of diphenylmethylbenzoates with [Ir] and [Cu] complexes. Reagents and conditions: (*i*) 1 equiv **3.51**, 2% [Ir] or [Cu], 2 equiv *i*Pr$_2$NEt, hv, MeCN, 40 °C, 16 h.

Reiser reported a rate enhancement when 100 equivalents of water were added to the system under otherwise unchanged conditions. As such, the above experiments were repeated in the presence of 100 equivalents of water. For the iridium-based photocatalyst this resulted in two products. Specifically, the reduction product **3.48** and the related dimer **3.52** were formed in quantitative yield (1:3 ratio).[g] Unfortunately, when the copper-based photocatalyst was used, only trace amounts of the reduction product **3.48** and diphenylmethanol (**3.53**) were observed (Scheme 3.2.10).

[g]The production of this dimer **3.52** was not reported by Reiser and co-workers.[33]

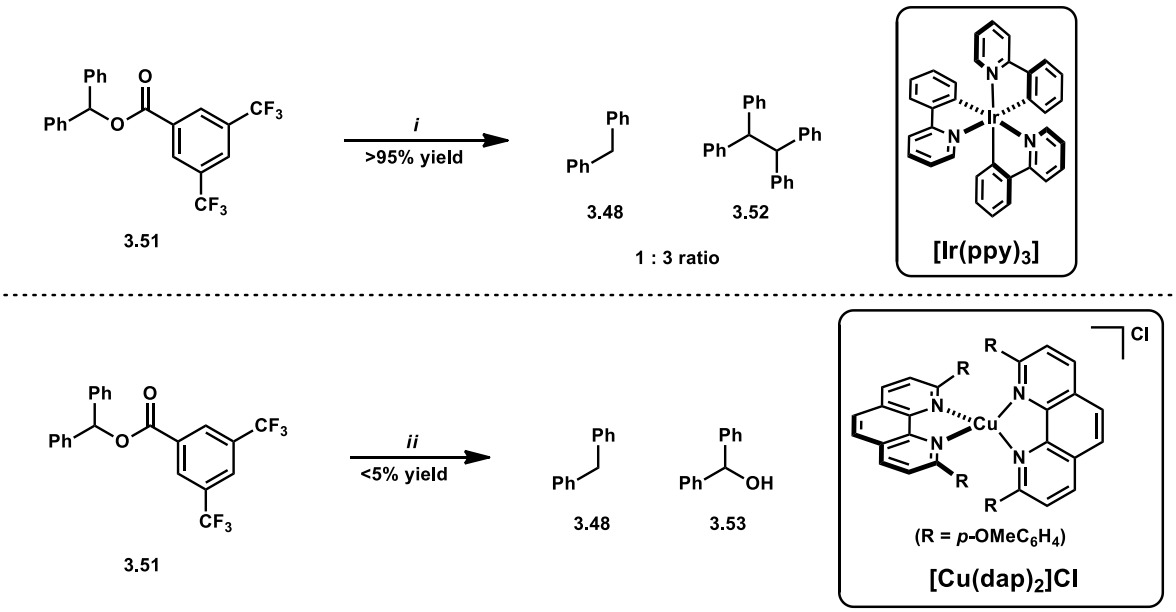

Scheme 3.2.10: Reduction of benzoate **3.51** by both iridium- and copper-based photoredox catalysts. Reagents and conditions: (*i*) 2% [Ir], 1 equiv **3.51**, 2 equiv *i*Pr$_2$NEt, 100 equiv H_2O, 24 W CFL, MeCN, 40 °C, 16 h; (*ii*) 2% [Cu], 1 equiv **3.51**, 2 equiv *i*Pr$_2$NEt, 100 equiv H_2O, 24 W CFL, MeCN, 40 °C, 16 h.

In an attempt to improve the yield of the reaction employing the copper-based photoredox catalyst, the reaction was repeated at an elevated temperature (80 °C). In this case, the iridium-based catalyst again delivered a quantitative yield of products **3.48** and **3.52**, however, now in a ratio of 1:7.3 (Scheme 3.2.11). The copper-based catalyst only produced the reduction product **3.48** and diphenylmethanol (**3.53**) in trace amounts. Given these results any further attempts to reduce diphenylmethylbenzoates were abandoned.

The poor reactivity of [Cu(dap)$_2$]Cl in comparison to [Ir(ppy)$_3$] in this instance can potentially be attributed to several factors. [Cu(dap)$_2$]$^+$ has a shorter excited state lifetime compared to [Ir(ppy)$_3$] and this may be compounded by the presence of water. The structural rearrangement that occurs upon photoexcitation for [Cu(dap)$_2$]$^+$ and the poor coordinative stability of the complex may result in efficient quenching of the photoexcited state by water or other Lewis basic species present in solution. If this occurs, then reduction of benzoate **3.51** cannot be achieved despite the strong reducing power of [Cu(dap)$_2$]Cl.

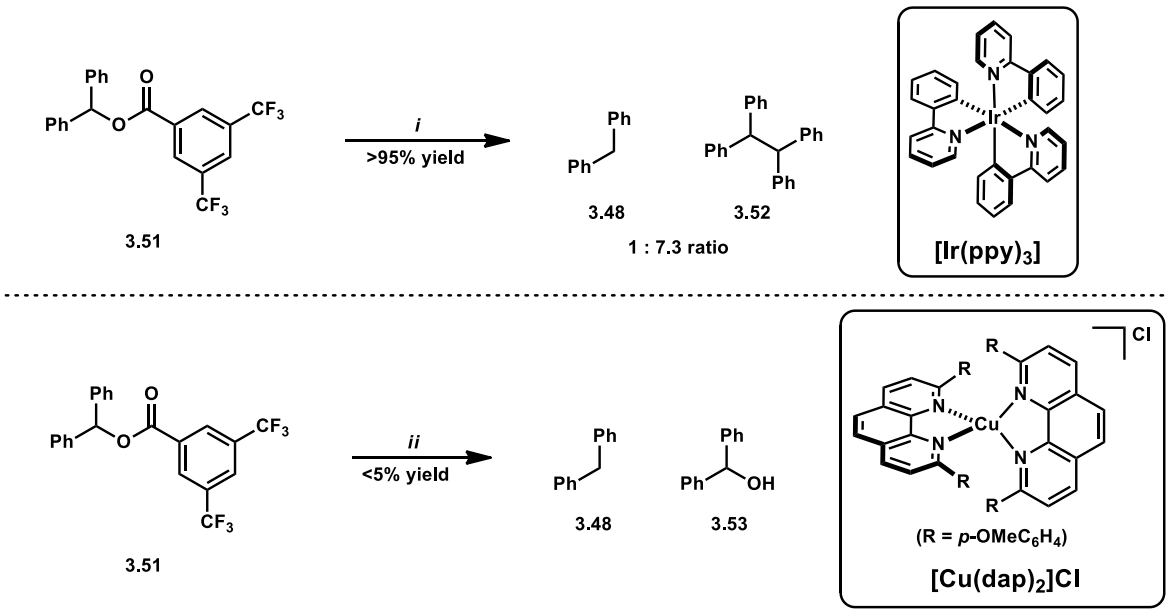

Scheme 3.2.11: Reduction of benzoate **3.51** by both iridium- and copper-based photoredox catalysts at elevated temperature. Reagents and conditions: (*i*) 2% [Ir], 1 equiv **3.51**, 2 equiv *i*Pr$_2$NEt, 100 equiv H_2O, 24 W CFL, MeCN, 80 °C, 16 h; (*ii*) 2% [Cu], 1 equiv **3.51**, 2 equiv *i*Pr$_2$NEt, 100 equiv H_2O, 24 W CFL, MeCN, 80 °C, 16 h.

3.2.6 Summary

The strong reducing power of $[Cu(dap)_2]^+$ and related copper-based photoredox catalysts has been shown to be sufficient to reduce a range of alkyl halides, *N*-halogenated alkylamines and diazonium salts. However, the development of synthetically useful dimerisation or functionalisation reactions proved to be challenging. The typically low coordinative stability of coordinatively unsaturated copper-based photoredox catalysts provides a possible explanation for such difficulties. An amidation reaction of a diazonium salt was identified which may provide a mild strategy for late stage amidation of related molecules which are sensitive to UV or microwave irradiation.

3.3 References

(1) (a) S. Maity; N. Zheng, *Synlett* **2012**, *23*, 1851−1856; (b) L. Shi; W. Xia, *Chem. Soc. Rev.* **2012**, *41*, 7687−7697; (c) C. K. Prier; D. A. Rankic; D. W. C. MacMillan, *Chem. Rev.* **2013**, *113*, 5322− 5363; (d) J. W. Beatty; C. R. J. Stephenson, *Acc. Chem. Res.* **2015**, *48*, 1474−1484.

(2) (a) X. Ju; D. Li; W. Li; W. Yu; F. Bian, *Adv. Synth. Catal.* **2012**, *354*, 3561−3567. For reactions of *N*,*N*-dimethylanilines with various benzylidenemalononitriles employing iridium-based photoredox catalysts see: (b) S. Zhu; A. Das; L. Bui; H. Zhou; D. P. Curran; M. Rueping, *J. Am. Chem. Soc.* **2013**, *135*, 1823−1829.

(3) For examples of other photochemical reactions of *N*,*N*-alkylanilines with *N*-substituted maleimides leading to annulated tetrahydroquinoline products, see: (a) M. A. Kirpichёnok; L. M. Mel'nikova; L. K. Denisov; I. I. Grandberg; N. P. Akimova, *Chem. Heterocycl. Compd.* **1989**, *25*, 23−29; (b) J. Tang; G. Grampp; Y. Liu; B.-X. Wang; F.-F. Tao; L.-J. Wang; X.-Z. Liang; H.-Q. Xiao; Y.-M. Shen, *J. Org. Chem.* **2015**, *80*, 2724−2732; (c) M. Baghbanzadeh; T. N. Glasnov; C. O. Kappel, *J. Flow Chem.* **2013**, *3*, 109−113. For examples of nonphotochemical reactions of *N*,*N*-alkylanilines with *N*-substituted maleimides leading to annulated tetrahydroquinoline products, see: (d) R. B. Roy; G. A. Swan, *Chem. Commun.* **1968**, 1446−1447; (e) M. Miura; S. Murata; K. Teramoto; M. Nomura, *Heterocycles* **1993**, *36*, 2147−2153; (f) M. Nishino; K. Hirano; T. Satoh; M. Miura, *J. Org. Chem.* **2011**, *76*, 6447−6451.

(4) S. Paria; O. Reiser, *ChemCatChem* **2014**, *6*, 2477−2483.

(5) (a) S. Goldstein; G. Czapski, *J. Am. Chem. Soc.* **1983**, *105*, 7276−7280; (b) S. Goldstein; G. Czapski, *Inorg. Chem.* **1985**, *24*, 1087−1092; (c) S. Goldstein; G. Czapski; R. van Eldik; H. Cohen; D. Meyerstein, *J. Phys. Chem.* **1991**, *95*, 1282−1285. For a study focusing on the quenching of photoexcited-state of $[Ru(bpy)_3]^{2+}$ by dioxygen see: (d) X. Zhang; M. A. J. Rodgers, *J. Phys. Chem.* **1995**, *99*, 12797−12803.

(6) T. P. Nicholls; G. E. Constable; J. C. Robertson; M. G. Gardiner; A. C. Bissember, *ACS Catalysis*, **2016**, *6*, 451–457.

(7) (a) M. Pirtsch; S. Paria; T. Matsuno; H. Isobe; O. Reiser, *Chem. Eur. J.* **2012**, *18*, 7336−7340; (b) D. B. Bagal; G. Kachkovskyi; M. Knorn; T. Rawner; B. M. Bhanage; O. Reiser, *Angew. Chem., Int. Ed.* **2015**, *54*, 6999−7002.

(8) M. Nishino; K. Hirano; T. Satoh; M. Miura, *J. Org. Chem.* **2011**, *76*, 6447−6451.

(9) (a) J. Du; L. R. Espelt; I. A. Guzei; T. P. Yoon, *Chem. Sci.* **2011**, *2*, 2115–2119; (b) L. R. Espelt; E. M. Wiensch; T. P. Yoon, *J. Org. Chem.* **2013**, *78*, 4107–4114.

(10) Aqueous pK_a values are quoted. For pK_a data see: (a) J. March, *Advanced Organic Chemistry*, 4th ed.; Wiley: New York, **1992**; (b) B. J. Berkowitz; E. Grunwald, *J. Am. Chem. Soc.* **1961**, *83*, 2956–2956; (c) H.-B. Zhang; L. Liu; Y.-L. Liu; Y.-J. Chen; J. Wang; D. Wang, *Synth. Commun.* **2007**, *37*, 173−181.

(11) X. Zhang; S. R. Yeh; S. Hong; M. Freccero; A. Albini; D. E. Falvey; P. S. Mariano, *J. Am. Chem. Soc.* **1994**, *116*, 4211−4220.

(12) N. G. Strizhakova; Y. A. Maletin; S. O. Travin, *Koordinats. Khim.* **1988**, *14*, 738−743.

(13) For studies exploring the oxidising properties of TFA, see: (a) L. Eberson; F. Radner. *Acta Chem. Scand.* **1991**, *45*, 1093−1095; (b) L. Eberson; F. Radner, *Acta Chem. Scand.* **1992**, *46*, 630−643. For research investigating the role of Brønsted acid catalysis in the oxidation of (non-copper-containing) transition-metal complexes featuring polypyridyl ligands see, for example: (c) J. S. Winterle; D. S. Kliger; G. S. Hammond, *J. Am. Chem. Soc.* **1976**, *98*, 3719−3721. (d) S. Fukuzumi; K. Ishikawa; K. Hironaka; T. Tanaka, *J. Chem. Soc., Perkin Trans. 2* **1987**, 751−760.

(14) B. H. Bielski, *J. Photochem. Photobiol.* **1978**, *28*, 645–649.

(15) Q. Qin; S. Yu, *Org. Lett.* **2015**, *17*, 1894–1897; (b) C. Q. O'Broin; P. Fernández; C. Martínez; K. Muñiz, *Org. Lett.* **2016**, *18*, 436–439; (c) J.-R. Chen; X.-Q. Hu; L.-Q. Lu; W.-J. Xiao, *Chem. Soc. Rev.* **2016**, *45*, 2044–2056; (d) P. Becker; T. Duhamel; C. J. Stein; M. Reiher; K. Muñiz, *Angew. Chem., Int. Ed.* **2017**, *56*, 8004–8008.

(16) (a) J.-M. Kern; J.-P. Sauvage, *J. Chem. Soc., Chem. Commun.* **1987**, 546–548; (b) A. Baralle; L. Festerbank; J.-P. Goddard; C. Ollivier, *Chem.–Eur. J.* **2013**, *19*, 10809–10813.

(17) For recent reports of Brønsted acid-mediated, photoredox catalyzed reactions, see: (a) J. Du; L. R. Espelt; I. A. Guzei; T. P. Yoon, *Chem. Sci.* **2011**, *2*, 2115−2119; (b) K. T. Tarantino; P. Liu; R. R. Knowles, *J. Am. Chem. Soc.* **2013**, *135*, 10022−10025; (c) R. Lono; H. G. Yayla; D. Y. Wang; M. F. Armstrong; R. R. Knowles, *J. Am. Chem. Soc.* **2013**, *135*,

17735−17738; (d) D. Uraguchi; N. Kinoshita; T. Kizu; T. Ooi, *J. Am. Chem. Soc.* **2015**, *137*, 13768−13771.

(18) For a review of Brønsted acid mediated radical processes, see: T. P. Nicholls; L. C. Henderson; A. C. Bissember, *Aust. J. Chem.* **2015**, *68*, 1791−1795.

(19) (b) M. Pirtsch; S. Paria; T. Matsuno; H. Isobe; O. Reiser, *Chem.–Eur. J.* **2012**, *18*, 7336–7340; (c) S. Paria; M. Pirtsch; V. Kais; O. Reiser, *Synthesis* **2013**, *45*, 2689–2698;

(20) M. Wada; T. Murata; H. Oikawa; H. Oguri, *Org. Biomol. Chem.* **2014**, *12*, 298–306.

(21) L. R. Espelt; E. M. Wiensch; T. P. Yoon, *J. Org. Chem.* **2013**, *78*, 4107–4114.

(22) K. L. Skubi; T. R. Blum; T. P. Yoon, *Chem. Rev.* **2016**, *116*, 10035–10074.

(23) D. Kalyani; K. B. McMurtrey; S. R. Neufeldt; M. S. Sanford, *J. Am. Chem. Soc.* **2011**, *133*, 18566–18569.

(24) G. Majetich; K. Wheless, *Tetrahedron* **1995**, *51*, 7095–7129.

(25) (a) E. J. Corey; W. R. Hertler, *J. Am. Chem. Soc*. **1960**, *82*, 1657–1668; (b) R. S. Neale; M. R. Walsh; N. L. Marcus, *J. Org. Chem.* **1965**, *30*, 3683–3688; (c) S. Hammerum, *Tetrahedron Lett.* **1981**, *22*, 157–160; (d) M. M. Green; B. A. Boyle; M. Vairamani; T. Mukhopadhyay; W. H. Saunders Jr.; P. Bowen; N. L. Allinger, *J. Am. Chem. Soc.* **1986**, *108*, 2381–2387.

(26) (a) Q. Qin; S. Yu, *Org. Lett.* **2015**, *17*, 1894–1897; (b) C. Q. O'Broin; P. Fernández; C. Martínez; K. Muñiz, *Org. Lett.* **2016**, *18*, 436–439; (c) J.-R. Chen; X.-Q. Hu; L.-Q. Lu; W.-J. Xiao, *Chem. Soc. Rev.* **2016**, *45*, 2044–2056; (d) P. Becker; T. Duhamel; C. J. Stein; M. Reiher; K. Muñiz, *Angew. Chem., Int. Ed.* **2017**, *56*, 8004–8008.

(27) D. B. Bagal; G. Kachkovskyi; M. Knorn; T. Rawner; B. M. Bhanage; O. Reiser, *Angew. Chem., Int. Ed.* **2015**, *54*, 6999–7002.

(28) Q. Qin; S. Yu, *Org. Lett.* **2015**, *17*, 1894–1897.

(29) F. W. Wassmundt; W. F. Kiesman, *J. Org. Chem.* **1995**, *60*, 196-201.

(30) H. Cano-Yelo; A. Deronzier, *J. Chem. Soc., Perkin Trans. 2* **1984**, 1093–1098.

(31) P. Allongue; M. Delamar; B. Desbat; O. Hitmi; J. Pinson; J.-M. Savéant, *J. Am. Chem. Soc.* **1997**, *119*, 201–207.

(32) (a) S. Milanesi; M. Fagnoni; A. Albini, *Chem. Commun.* **2003**, 216–217; (b) S. Milanesi; M. Fagnoni; A. Albini, *J. Org. Chem.* **2005**, *70*, 603–610; (c) R. Saev; M. D. Otero; B. Batanero; F. Barba, *J. Chem. Res.* **2008**, 492–494; (d) H. Wang; Q. Xu; S. Shen; S. Yu, *J.*

Org. Chem. **2017**, *82*, 770–775; (e) S. W. Youn; H. J. Yoo; E. M. Lee; S. Y. Lee, *Adv. Synth. Catal.* **2018**, *360*, 278–283.

(33) D. Rackl; V. Kais; P. Kreitmeier; O. Reiser, *Beilstein J. Org. Chem.* **2014**, *10*, 2157–2165.

Chapter Four

Investigating the Potential of Pulsed LED Irradiation in Synthesis

This chapter describes the initial discovery of an α-amino C–H/ C–F functionalisation reaction of perfluoroarenes with trialkylamines and the subsequent optimisation of this reaction. During the optimisation, the utility of pulsed LED irradiation was found to be crucial to facilitating a much more efficient process and increasing the rate of product formation. Ultimately, efficient photoinduced copper photoredox-catalysed α-amino C–H/ C–F functionalisation and hydrodefluorination reactions were developed under mild conditions by exploiting pulsed LED irradiation.

4.1 Introduction

In 2014, Weaver and co-workers reported the photocatalytic hydrodefluorination of fluorinated aromatics.[1] In this report, it was proposed that the iridium photoredox catalyst, [Ir(ppy)$_3$], initially reduced a perfluorinated substrate, such as hexafluorobenzene (**4.1**), to deliver a perfluororadical anion which fragments to give fluoride and a defluorinated neutral radical species. Subsequent H-atom abstraction from Hünig's base delivered hydrodefluorinated product **4.2** (Scheme 4.1.1). This report describes a powerful chemical transformation due to the relative inertness of C–F bonds in hexafluorobenzene (BDE = 145 kcal mol^{-1}).[2] The prevalence of fluorinated compounds in pharmaceutical, agrochemical and materials science potentially makes this, and related methodology, highly relevant to the development of valuable transformations.[3]

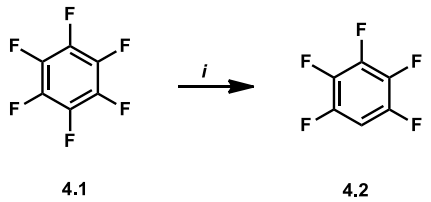

Scheme 4.1.1: Hydrodefluorination reaction developed by Weaver and co-workers. Reagents and conditions: (*i*) 0.5 mol% [Ir(ppy)$_3$], 1 equiv **4.1**, 3.3 equiv *i*Pr$_2$NEt, blue LEDs, 45 °C, MeCN, Argon, 24 h.

Several photocatalytic defluorination reactions have since been reported.[1,4] While there is one example utilising a pyrene-based photoredox catalyst,[4d] the remainder take advantage of the saturated coordination geometry and strong reduction potentials of iridium-based photoredox catalysts. Coordinative saturation was suggested to be necessary to prevent metal–fluorine bond formation that can lead to quenching of the photoexcited state or lead to catalyst decomposition.[1,4a,b,e] There have been no reports of a copper-based photoredox catalyst facilitating hydrodefluorination reactions. This is potentially due to coordinatively unsaturated copper(I) complexes displaying lower coordinative stability and their propensity to undergo pronounced structural rearrangements upon photoexcitation that exposes the metal centre to nucleophilic attack.[5] As such, the use of copper-based photoredox catalysts in these systems presents significant challenges.

The proposed mechanism for the iridium photoredox-catalysed HDF reaction is outlined in Scheme 4.1.2.[1] Initial reduction of perfluoroarene **4.1** by the photoexcited iridium complex leads to a radical anion. This radical anion undergoes fluoride extrusion to deliver a neutral radical species, which abstracts a H atom from Hünig's base to complete the transformation.

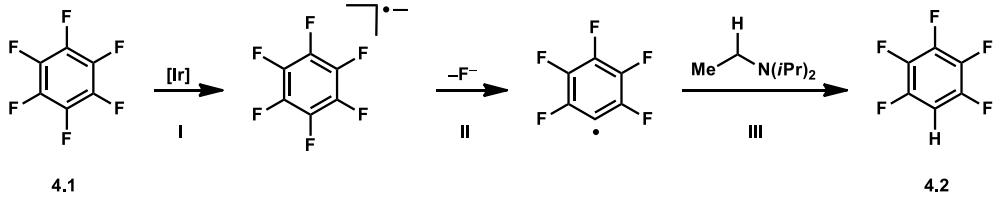

Scheme 4.1.2: Suggested mechanism of an Iridium photoredox-catalysed HDF reaction.

4.2 Development of a Dual α-Amino C–H/ C–F Functionalisation Reaction

4.2.1 Preliminary reaction optimisation

A study was undertaken to determine if copper-based photoredox catalysts could facilitate cleavage of relatively inert C–F bonds to ultimately deliver C–F functionalised products. Initially, reproduction of a hydrodefluorination (HDF) reaction reported by Weaver and co-workers was attempted using 1 mol% $[Ir(ppy)_3]$, $[Cu(dap)_2]Cl$ or $[Cu(bcp)(XP)]PF_6$ as photoredox catalysts and hexafluorobenzene (**4.1**) as reactant under otherwise identical reaction conditions to those reported by Weaver (Scheme 4.2.1A).[1] While $[Cu(dap)_2]Cl$ was found to be ineffective in this transformation, promising results were obtained using $[Ir(ppy)_3]$ and $[Cu(bcp)(XP)]PF_6$. After 24 hours, full conversion of starting material was observed in both cases, delivering the hydrodefluorination product pentafluorobenzene (**4.2**).[a] Intriguingly, when amide **4.3** was subjected to these reaction conditions using $[Cu(bcp)(XP)]PF_6$ as catalyst, an entirely different product was observed in which Hünig's base had added to the perfluorinated reactant **4.3** to deliver dual α-amino C–H/ C–F functionalisation product **4.4** in a 44% yield after 48 hours (Scheme 4.2.1B).[b] Interestingly, no hydrodefluorination product (**4.2**) was found in this case.

[a] As determined by ^{19}F NMR spectroscopy.

[b] As determined by ^{19}F NMR spectroscopy with the aid of an internal standard.

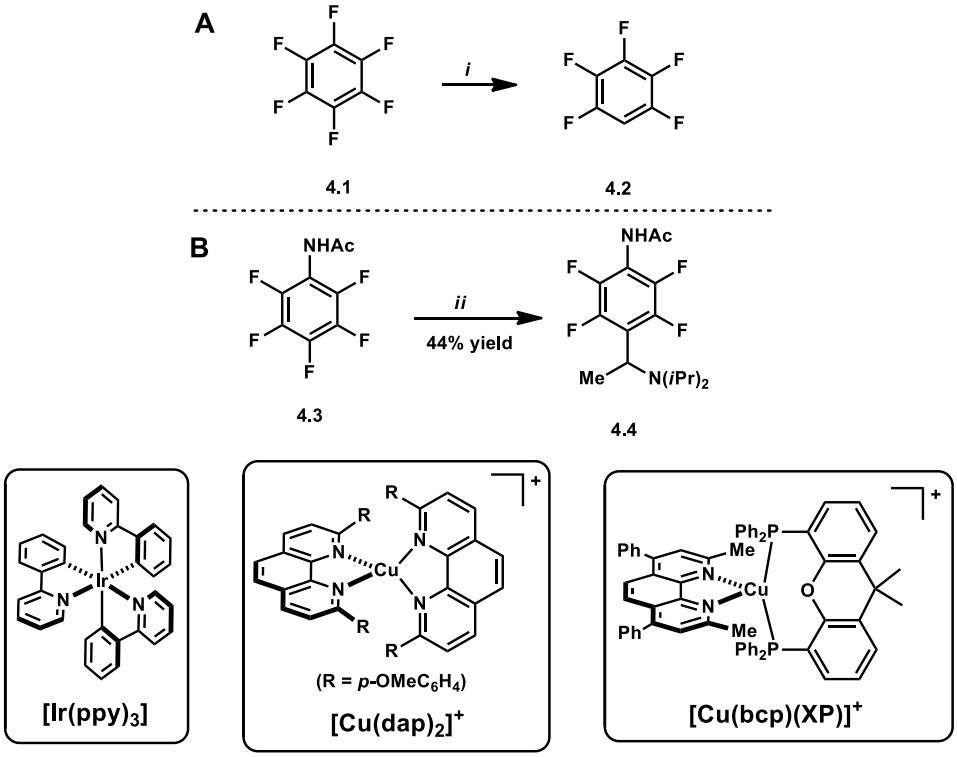

Scheme 4.2.1: Hydrodefluorination reaction and dual α-amino C–H/ C–F functionalisation reactions. Reagents and conditions: (*i*) 1 mol% PC, 1 equiv **4.1**, 3.3 equiv *i*Pr$_2$NEt, blue LEDs, 45 °C, MeCN, N_2, 24 h; (*ii*) 1 mol% [Cu(bcp)(XP)]PF_6, 1 equiv **4.3**, 3.3 equiv *i*Pr$_2$NEt, blue LED, 45 °C, MeCN, N_2, 48 h. PC = photoredox catalyst.

Given this interesting divergent reactivity when using a copper-based catalyst under very similar conditions to that reported by Weaver and co-workers,[1] the optimisation of this reaction was conducted. During the optimisation of this reaction, a closely related reaction was reported by Hashmi and co-workers. An iridium photoredox-catalysed dual α-amino C–H/C–F functionalisation of perfluorinated arenes with aryl amines was developed. In this case, a cationic iridium-based photoredox catalyst was utilised and both mono- and diarylation products could be accessed via this methodology (Scheme 4.2.2).[6]

To optimise the copper photoredox catalysed dual α-amino C–H/C–F functionalisation reaction, initially the amount of Hünig's base in the reaction mixture was screened. The results are presented in Table 4.2.1.

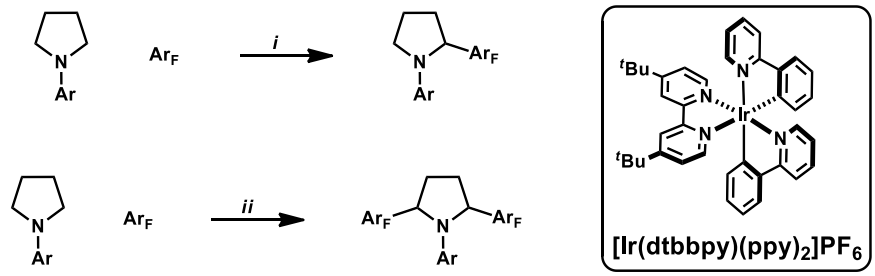

Scheme 4.2.2: Iridium photoredox-catalysed dual C–H/C–F functionalisation reaction of perfluoroarenes and aryl amines. Reagents and conditions: (*i*) 1% [Ir], 1 equiv aryl amine, 1.5 equiv Ar_F, 1.5 equiv NaOAc, acetone, blue LEDs, r.t..; (*ii*) 1% [Ir], 1 equiv aryl amine, 4 equiv Ar_F, 6 equiv $NaHCO_3$, H_2O, DMPU, blue LEDs, r.t., 48 h. Ar_F = perfluorinated aromatic compound.

Table 4.2.1: Screening the amount of Hünig's base in the reaction mixture in a dual α-amino C–H/ C–F functionalisation reaction.

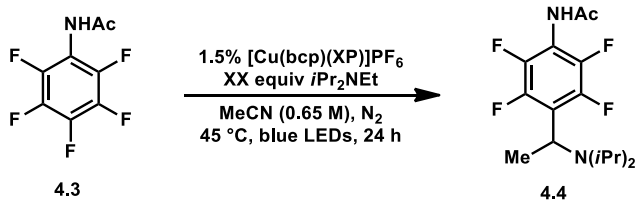

4.3 4.4

entry	*i*Pr$_2$NEt (equiv)	yield (%)[a]
1	1.2	28
2	1.5	39
3	2.0	43
4	2.5	35
5	3.0	18
6	3.5	17
7	4.0	17

[a] Yield determined by ^{19}F NMR spectroscopy with the aid of an internal standard (average of 2 experiments).

The results displayed in Table 4.2.1 show an increase in yield from 1.2 equivalents of Hünig's base up to 2.0 equivalents (Table 4.2.1, entries 1–3), at which point further increases in the amount of Hünig's base have a detrimental effect of the yield of the reaction (entries 4–7). The mass balance is accounted for by unreacted starting material given these reactions

only proceeded at low conversions. As such, a loading of 2.0 equivalents was selected as the optimal amount and this loading was maintained throughout subsequent optimisation experiments. Perhaps, lower loadings of Hünig's base do not provide a sufficiently high concentration of putative α-amino radicals in solution to interact with amide **4.3**. Next, the amount of solvent added to the reaction mixture was varied to determine the optimal concentration for the reaction. Concentrations of amide **4.3** between 0.078 M and 0.260 M were tested under otherwise identical reaction conditions. The results are presented in Table 4.2.2.

Table 4.2.2: Screening the concentration of the reaction mixture with respect to amide **4.3** in a dual α-amino C–H/ C–F functionalisation reaction.

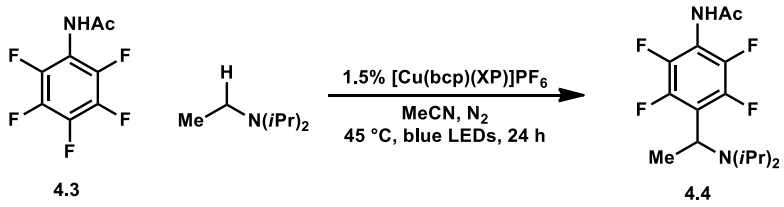

entry	concentration (M)	yield (%)[a]
1	0.0748	44
2	0.0975	48
3	0.117	52
4	0.130	54
5	0.195	54
6	0.260	52

[a] Yield determined by ^{19}F NMR spectroscopy with the aid of an internal standard (average of 2 experiments).

The results in Table 4.2.2 display an increase in yield when the concentration was increased from 0.078 M up to 0.130 M (Table 4.2.2, entries 1–4). An identical yield to that of entry 4 was obtained with a concentration of 0.195 M (entry 5) and a slightly less efficient reaction was observed with a concentration of 0.260 M (entry 6). As such, 0.130 M was selected as optimal and this concentration was maintained in subsequent optimisation experiments. While a concentration of 0.195 M gave an identical yield, this was not utilised in subsequent optimisation studies due to the impracticality of performing small scale

reactions at high concentrations which potentially leads to heterogenous mixtures. Potentially, higher concentrations could lead to aggregation of the catalyst which can lead to excited state quenching.[7] Furthermore, the effects of additives on the reaction also needed to be explored (*vide infra*). Next, a catalyst screen was performed. A range of 4 heteroleptic phenanthroline-containing copper-based complexes including [Cu(dmp)(XP)]PF_6, [Cu(bcp)(XP)]PF_6, [Cu(dmp)(DPEphos)]PF_6, and [Cu(bcp)(DPEphos)]PF_6 were screened as photoredox catalysts under otherwise identical reaction conditions. The results are presented in Table 4.2.3.

Table 4.2.3: Catalyst screen involving various heteroleptic copper-based complexes in a dual α-amino C–H/ C–F functionalisation reaction.

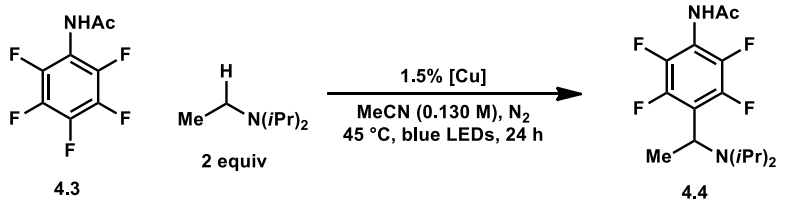

entry	catalyst	yield (%)[a]
1	[Cu(dmp)(XP)]PF_6	50
2	[Cu(bcp)(XP)]PF_6	55
3	[Cu(dmp)(DPEphos)]PF_6	48
4	[Cu(bcp)(DPEphos)]PF_6	31

[a] Yield determined by ^{19}F NMR spectroscopy with the aid of an internal standard (average of 2 experiments).

The complex [Cu(dmp)(XP)]PF_6 delivered a slightly reduced yield of insertion product **4.4** when compared with [Cu(bcp)(XP)]PF_6 (Table 4.2.3, entries 1 & 2). Both complexes featuring the DPEphos ligand also delivered reduced yields of insertion product **4.4** (entries 3 & 4). As such, the use of [Cu(bcp)(XP)]PF_6 was maintained for subsequent optimisation experiments. While yields when utilising [Cu(dmp)(XP)]PF_6 and [Cu(dmp)(DPEphos)]PF_6 remained similar to that of [Cu(bcp)(XP)]PF_6 there was a significant decrease in the yield when using [Cu(bcp)(DPEphos)]PF_6. This can be attributed to variation in the reducing power of the complexes. While the three complexes ([Cu(dmp)(XP)]PF_6, [Cu(bcp)(XP)]PF_6 and [Cu(dmp)(DPEphos)]PF_6) that delivered the highest yields all maintain

strong reducing power ($E_{1/2}$ = –1.34 to –1.64 V vs. SCE), [Cu(bcp)(DPEphos)]PF_6 has a lower reducing power in comparison ($E_{1/2}$ = –1.02 V vs. SCE). The lower reducing power may not be sufficient to efficiently reduce amide **4.3** ($E_{1/2}$ = –1.60 V vs. SCE)[8]. Next, the catalyst loading was investigated. The results are presented in Table 4.2.4.

Table 4.2.4: Screening the catalyst loading utilising [Cu(bcp)(XP)]PF_6 in a dual α-amino C–H/ C–F functionalisation reaction.

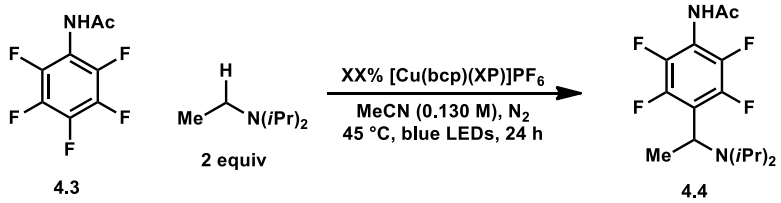

entry	catalyst loading (%)	yield (%)[a]
1	1.0	45
2	1.5	53
3	2.0	52
4	3.0	35
5	4.0	38
6	5.0	29
7	1.5 + 1.5 (after 12 h)	49

[a] Yield determined by ^{19}F NMR spectroscopy with the aid of an internal standard (average of 2 experiments).

A yield improvement was observed as the catalyst loading was increased from 1.0% to 1.5% (Table 4.2.4, entries 1 & 2). Increasing the loading to 2.0% delivered essentially the same yield as in the case of 1.5% (entry 3) and further increasing the catalyst loading above 2.0% delivered lower yields in all cases that were tested (entries 4–6). Another experiment was performed in which 1.5% of catalyst was present initially then a further 1.5% was added after 12 h. This resulted in essentially the same yield as in the case of 1.5% (entry 7). Given the possibility of catalyst decomposition with the use of coordinatively unsaturated copper complexes, it is possible that the loading of the catalyst in the reaction mixture decreases over time. As such, if there was substantial catalyst decomposition occurring, the sequential addition of catalyst may maintain a more constant loading over the entire reaction time. The

observation of a lower yield when utilising this technique when compared to the 1.5% catalyst loading suggests that catalyst decomposition may not be a major factor in the poor conversion observed. Next, the catalyst loading was screened at an elevated temperature (55 °C). The results are presented in Table 4.2.5.

Table 4.2.5: Screening the catalyst loading utilising [Cu(bcp)(XP)]PF_6 at 55 °C in a dual α-amino C–H/ C–F functionalisation reaction.

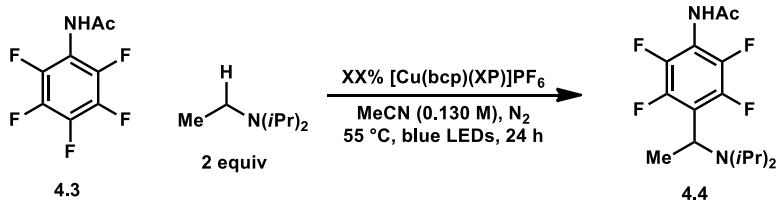

entry	catalyst loading (%)	yield (%)[a]
1	1.0	23
2	1.5	49
3	2.0	49
4	3.0	32
5	4.0	29
6	5.0	24

[a] Yield determined by ^{19}F NMR spectroscopy with the aid of an internal standard (average of 2 experiments).

Reaction at 55 °C, under otherwise identical conditions delivered the insertion product **4.4** in similar or reduced yields to those obtained at 45 °C in all cases (Table 4.2.5, entries 1–6). Typically, the excited state lifetime of photoactive compounds is decreased at higher temperatures because quenching processes become more efficient.[6b] This may explain the slightly reduced yield at elevated temperature.

At this stage, a number of other perfluorinated substrates were screened in place of amide **4.3** under the reaction conditions that had given the best result so far (Table 4.2.4, entry 2). These substrates included carbamate **4.5**, aniline **4.6** and sulfonamide **4.7**.[c] The results are presented in Table 4.2.6.

[c] The syntheses of carbamate **4.5** is described in subsection 4.3.1.

Table 4.2.6: Screening perfluorinated substrates **4.5**, **4.6** and **4.7** in a dual α-amino C–H/ C–F functionalisation reaction.

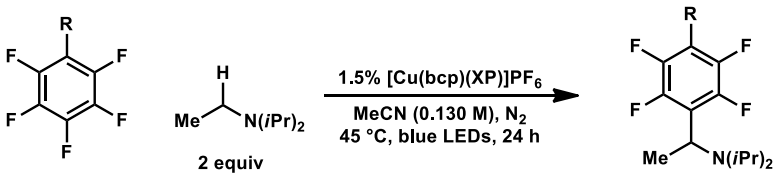

entry	R	yield (%)[a]
1	NHAc (**4.3**)	54
2	NHBoc (**4.5**)	19
3	NH_2 (**4.6**)	6
4	NHTs (**4.7**)	<2

[a] Yield determined by ^{19}F NMR spectroscopy with the aid of an internal standard (average of 2 experiments).

Amide **4.3** is included in this table for comparative purposes. While a 54% yield was obtained when utilising amide **4.3** as reactant (Table 4.2.6, entry 1), the closely related carbamate **4.5**, and aniline **4.6** delivered significantly reduced yields (entries 2 & 3) and no product was observed in the case of sulfonamide **4.7** (entry 4).

Because optimisation of the reaction conditions had, thus far, not resulted in a substantial increase in the yield of the reaction, a range of experiments were performed in which different additives were screened. For ease of exposition, only the results using amide **4.3** are specifically discussed, however, in many cases, identical experiments were performed using carbamate **4.5**, aniline **4.6** and sulfonamide **4.7** as reactants in place of amide **4.3**.

The first additive screened was imidazole. In a related photoredox-catalysed insertion reaction which features trialkylamines, Weaver and co-workers described an α-amino C–H functionalisation reaction in which coupling between a number of activated 2-chloroazoles and trialkylamines occurs. Importantly, the optimised conditions reported for this reaction involved the use of 2 equivalents of imidazole as an additive (Scheme 4.2.3).[9]

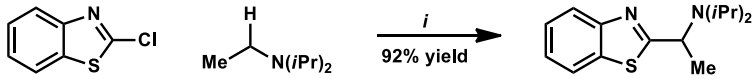

4.8 4.9

Scheme 4.2.3: α-Amino C–H functionalisation reaction developed by Weaver and co-workers. Reagents and conditions: (*i*) 0.75 mol% [Ir(ppy)$_3$], 1 equiv **4.8**, 1.2 equiv *i*Pr$_2$NEt, 2 equiv imidazole, blue LEDs, 45 °C, MeCN, Argon.

As such, the use of imidazole as an additive in the dual α-amino C–H/ C–F functionalisation developed here was screened under the partially optimised conditions (Table 4.2.4, entry 2). The amount of imidazole that had been reported to be optimal under Weaver's conditions was maintained (2 equivalents) and the amount of Hünig's base was varied. The results are presented in Table 4.2.7.

Table 4.2.7: Screening imidazole as an additive in a dual α-amino C–H/ C–F functionalisation reaction.

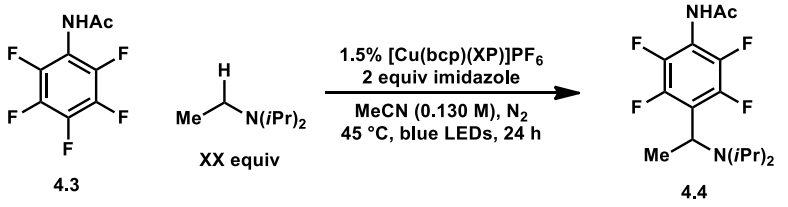

4.3 4.4

entry	*i*Pr$_2$NEt (equiv)	yield (%)[a]
1	2.0	7
2	1.5	5
3	1.2	<2

[a] Yield determined by ^{19}F NMR spectroscopy with the aid of an internal standard (average of 2 experiments).

In all cases, the addition of imidazole significantly reduced the yield of insertion product **4.4** and large amounts of starting material were returned with minimal amounts of unidentified decomposition products observed.[d] Given the coordinatively unsaturated nature of the copper-based catalyst and the structural rearrangement that occurs upon photoexcitation which exposes the metal centre to nucleophilic attack, it is possible that the

[d] As determined by TLC and ^{1}H & ^{19}F NMR spectroscopy.

Lewis basic imidazole can coordinate the catalyst metal centre resulting in quenching of the photoexcited state or decomposition. Next, a range of other additives were screened, including Cs_2CO_3, pyridine, K_2CO_3 and 1,8-diazabicyclo(5.4.0)undec-7-ene (DBU) with a loading of 2 equivalents. In each case, the reaction conditions were otherwise unchanged from those in Table 4.2.4, entry 2, except that the amount of Hünig's base was reduced to 1.2 equivalents. The results are presented in Table 4.2.8.

Table 4.2.8: Screening additives in a dual α-amino C–H/ C–F functionalisation reaction.

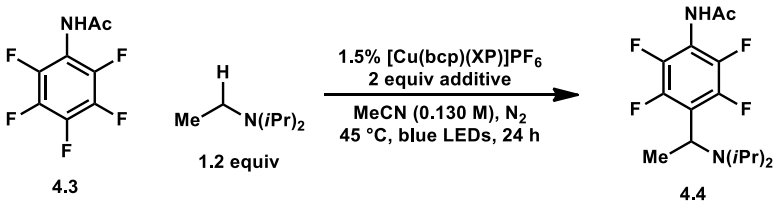

entry	additive	yield (%)[a]
1	none	32
2	Cs_2CO_3	<2
3	DBU	<2
4	K_2CO_3	45
5	pyridine	35

[a] Yield determined by ^{19}F NMR spectroscopy with the aid of an internal standard (average of 2 experiments).

The control reaction, performed in the absence of an additive delivered a 32% yield of insertion product **4.4** (Table 4.2.8, entry 1). This is consistent with a similar reaction performed previously when screening varying amounts of Hünig's base in the reaction (Table 4.2.1, entry 1). The use of 2 equivalents of Cs_2CO_3 or DBU resulted in a complex mixture of unidentifiable decomposition products with no starting material or product returned (entry 2 & 3).[e] Interestingly, the use of K_2CO_3 provided an increased 45% yield of product (entry 4) and the addition of pyridine left the yield essentially unchanged (entry 5). Given this promising result when using 2 equivalents of K_2CO_3, further optimisation using this additive was performed. A range of different variables were screened including an increased amount

[e] As determined by TLC and ^1H & ^{19}F NMR spectroscopy.

of Hünig's base, an increased catalyst loading, different concentrations and different solvents. The results are presented in Table 4.2.9.

Table 4.2.9: Screening a range of variables in a dual α-amino C–H/ C–F functionalisation reaction.

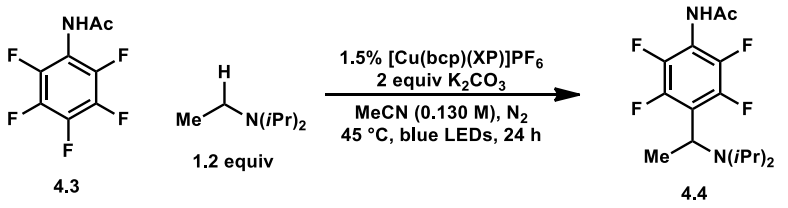

entry	variation from the above conditions	yield (%)[a]
1	none	44
2	2 equiv iPr$_2$NEt instead of 1.2 equiv	52
3	3.0% [Cu] instead of 1.5%	46
4	0.0325 M instead of 0.130 M	28
5	0.0650 M instead of 0.130 M	35
6	DMF instead of MeCN	40
7	CH_2Cl_2 instead of MeCN	26

[a] Yield determined by ^{19}F NMR spectroscopy with the aid of an internal standard (average of 2 experiments).

The control reaction with no variation in reaction conditions from Table 4.2.4, entry 2, delivered a similar outcome to previous results (Table 4.2.9, entry 1). Increasing the amount of Hünig's base to 2 equivalents from 1.2 equivalents delivered an increased 52% yield of product (entry 2). This yield was essentially unchanged from previous results under the same reaction conditions but in the absence of K_2CO_3 (Table 4.2.6, entry 1). Increasing the catalyst loading to 3.0% delivered a 46% yield (entry 3). Decreasing the concentration of the reaction mixture provided lower yields (entries 4 & 5) and the use of either DMF or CH_2Cl_2 instead of MeCN also delivered lower yields (entries 6 & 7). Despite the addition of K_2CO_3 resulting in an increased yield when only 1.2 equivalents of Hünig's base was used, this did not translate

to an increased yield when using 2 equivalents of Hünig's base. An essentially identical yield was obtained both in the presence or absence of K_2CO_3 when 2 equivalents of Hünig's base is used. As such, the use of K_2CO_3 was abandoned and another inorganic base, NaOAc was tested. Initial screening involved the use of 1.5 equivalents of NaOAc and varying the amount of both amide **4.3** and Hünig's base under otherwise unchanged reaction conditions from that which gave the highest yield so far (Table 4.2.6, entry 1). The results are presented in Table 4.2.10.

Table 4.2.10: Testing NaOAc as an additive in a dual α-amino C–H/ C–F functionalisation reaction.

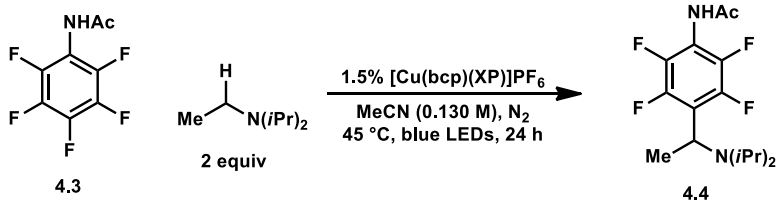

entry	variation from the above conditions	yield (%)[a]
1	none	54
2	1.5 equiv NaOAc	25
3	1.5 equiv NaOAc, 1.5 equiv **4.3**, 1 equiv iPr$_2$NEt	30

[a] Yield determined by ^{19}F NMR spectroscopy with the aid of an internal standard (average of 2 experiments).

The control reaction delivered a similar yield to that which had been obtained previously (Table 4.2.10, entry 1). The use of 1.5 equivalents of NaOAc as an additive significantly reduced the yield of insertion product **4.4** (25%, entry 2) and varying the amount of both amide **4.3** and Hünig's base also delivered a reduced 30% yield (entry 3). Given the lower yields when NaOAc was added to the reaction mixture further attempts using NaOAc or any other inorganic base were abandoned. Finally, a range of Lewis acids were screened as additives in the reaction mixture including $LiClO_4$, $Sc(OTf)_3$ and $Gd(OTf)_3$. All these Lewis acids were screened against amide **4.3** and $Gd(OTf)_3$ was also screened against carbamate **4.5**. The results are presented in Table 4.2.11.

Table 4.2.11: Testing Lewis acid additives in a dual α-amino C–H/ C–F functionalisation reaction.

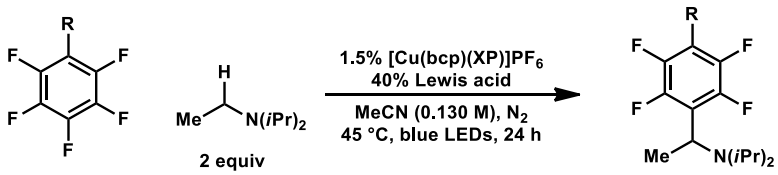

entry	Lewis acid	R = NHAc (4.3) yield (%)[a]	R = NHBoc (4.5) yield (%)[a]
1	$LiClO_4$	7	–
2	$Sc(OTf)_3$	12	–
3	$Gd(OTf)_3$	54	57
4	–	54	19

[a] Yield determined by ^{19}F NMR spectroscopy with the aid of an internal standard (average of 2 experiments).

While $LiClO_4$ and $Sc(OTf)_3$ were ineffective (Table 4.2.11, entries 1 & 2), the use of $Gd(OTf)_3$ as an additive delivered comparable results to the optimal conditions tested thus far (entry 3). Interestingly, when the reactant was switched to carbamate **4.5** a 57% yield was obtained (entry 3). This contrasts with the previous result when using carbamate **4.5** as reactant in the absence of $Gd(OTf)_3$ under otherwise identical reaction conditions, which delivered only a 19% yield (entry 4). It has previously been suggested that the Lewis acids are capable of lowering reduction potentials of 2′-hydroxychalcones.[10] This Lewis acid activation of 2′-hydroxychalcones allowed a related photoredox-catalysed [2 + 2]-cycloaddition reaction to proceed with increased efficiency. In the system reported here, it is possible that the Lewis acid, $Gd(OTf)_3$, plays a similar role in coordinating the amide or carbamate moieties present in reactants **4.3** and **4.5** which lowers their respective reduction potentials. Lewis acids may also be able to coordinate the nitrogen lone pair of tertiary amines which can also lower their reduction potentials.[11]

Despite extensive optimisation of many of the key variables for this dual α-amino C–H/ C–F functionalisation reaction only a modest 54% yield had been obtained with comparable conversion of starting material. As such, an alternative approach for the

optimisation of this reaction was necessary. One variable that had not yet been optimised was the nature of light that was used to irradiate the reaction mixture.

4.2.2 Identifying the potential of pulsed LED irradiation in synthesis

The nature and source of irradiation in visible-light-mediated photoredox catalysis is, perhaps, one of the most important variables that will determine the outcome of a reaction.[12] Despite this, there has been very limited optimisation around the source of irradiation beyond the use of wavelength specific LED irradiation or the use of light sources with increased intensity.[13] While intermittent illumination or pulsed irradiation strategies have been used to study mechanisms of photoredox-catalysed systems,[14] chemists are yet to harness the potential of pulsed irradiation in synthesis.

It has been reported that pulsed irradiation can provide greater photosynthetic activity and photochemical production in various plants.[15] Given that pulsed irradiation has been demonstrated to enhance complex processes in nature, such as phytochemical production, it is feasible that this effect could be translated to the synthesis of organic molecules in a laboratory. In order to test this hypothesis, the design and construction of an inexpensive (<$10) multiphase circuit that was driven by a DC power supply and connected to a photoreactor was necessary. This multiphase circuit allowed modulation of power, pulse frequency and duty cycle which facilitated an oscillating output.[f]

Initially, a pulse frequency of 100 kHz and a 25% duty cycle was chosen to test the effect of pulsed irradiation of the dual α-amino C–H/ C–F functionalisation reaction being developed. This pulse frequency was initially selected as it approximately matched the excited state lifetime of the catalyst ([Cu(bcp)(XP)]PF_6, τ = 6.4 μs).[16] The blue LED photoreactor operated at 18 W and delivered ~28 000 lux.[g] The results are presented in Table 4.2.12.

[f] The multiphase circuit was developed by J. C. Robertson, another group member.
[g] As measured at the centre of the photoreactor.

Table 4.2.12: Identifying the potential of pulsed LED irradiation in a dual α-amino C–H/ C–F functionalisation reaction.

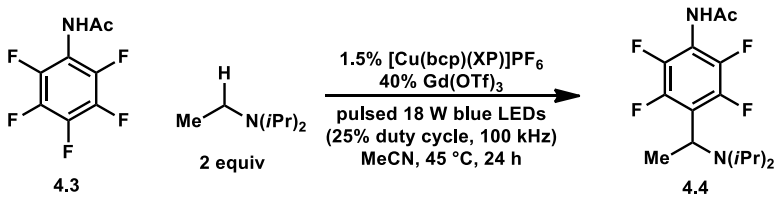

entry	variation from the above conditions	yield (%)[a]
1	none	89 (87)[b]
2	no $[Cu(bcp)(XP)]PF_6$	0
3	no hν	0
4	no $[Cu(bcp)(XP)]PF_6$, no hν	0
5	conventional irradiation (24 W blue LED)	54
6	10 kHz instead of 100 kHz	64
7	1 kHz instead of 100 kHz	58
8	No $Gd(OTf)_3$	83 (83)[b]
9	Air instead of N_2	38
10	1.5% $[Ru(bpy)_3](PF_6)_2$ instead of $[Cu(bcp)(XP)]PF_6$	<2
11	1.5% $[Ir(ppy)_3]$ instead of $[Cu(bcp)(XP)]PF_6$	17

[a] Yield determined by ^{19}F NMR spectroscopy with the aid of an internal standard (average of 2 experiments). [b]Isolated yield.

Pulsed LED irradiation was the key to developing an efficient process. By simply utilising the previously optimised conditions but now employing pulsed LED irradiation, it was found that insertion product **4.4** could be isolated in 87% yield (Table 4.2.12, entry 1). Importantly, the use of a 25% duty cycle results in irradiation occurring for only a quarter of the 24 h reaction time. Conversely, conventional irradiation results in irradiation occurring for 100% of the time. Control reactions were performed in the absence of catalyst, absence of light and the absence of both catalyst and light, all of which resulted in no product formation (entries 2–4). When the reaction mixture was subjected to conventional (continuous) blue LED irradiation with comparable lux (24 W, ~28 000 lux), the insertion product **4.4** was obtained in a considerably lower 54% yield with comparable conversion (entry 5). When this reaction was conducted for an extended reaction time the yield was not significantly

increased (61% yield after 65 h). When the pulse frequency was decreased by orders of magnitude the yield of insertion product **4.4** was significantly decreased and the reaction did not proceed to complete conversion (entries 6 & 7). This variation in yield when utilising different pulse frequencies suggests that the oscillating nature of the light is indeed responsible for a more efficient reaction. The absence of $Gd(OTf)_3$ did not affect the efficiency of the reaction significantly in the case of amide **4.3** (entry 8), however the yield when using other reactants was significantly affected by the presence of $Gd(OTf)_3$ (*vide infra)*. The yield of the reaction dropped significantly in the presence of air (entry 9). Interestingly, the use of $[Ru(bpy)_3](PF_6)_2$ resulted in no product formation while $[Ir(ppy)_3]$ delivered an inefficient reaction with low conversion of starting material (entries 10 & 11).

Next, time course experiments were performed for pulse frequencies of 100, 10 and 1 kHz (25% duty cycle in all cases) as well as conventional irradiation. The yield of the reaction was determined each hour over 10 h and another data point was obtained after 24 h. It should be noted that these experiments were performed in the absence of $Gd(OTf)_3$. The presence of $Gd(OTf)_3$, which was not completely soluble under the reaction conditions, created sampling issues which resulted in non-reproducible data. The results are presented in Figure 4.2.1.

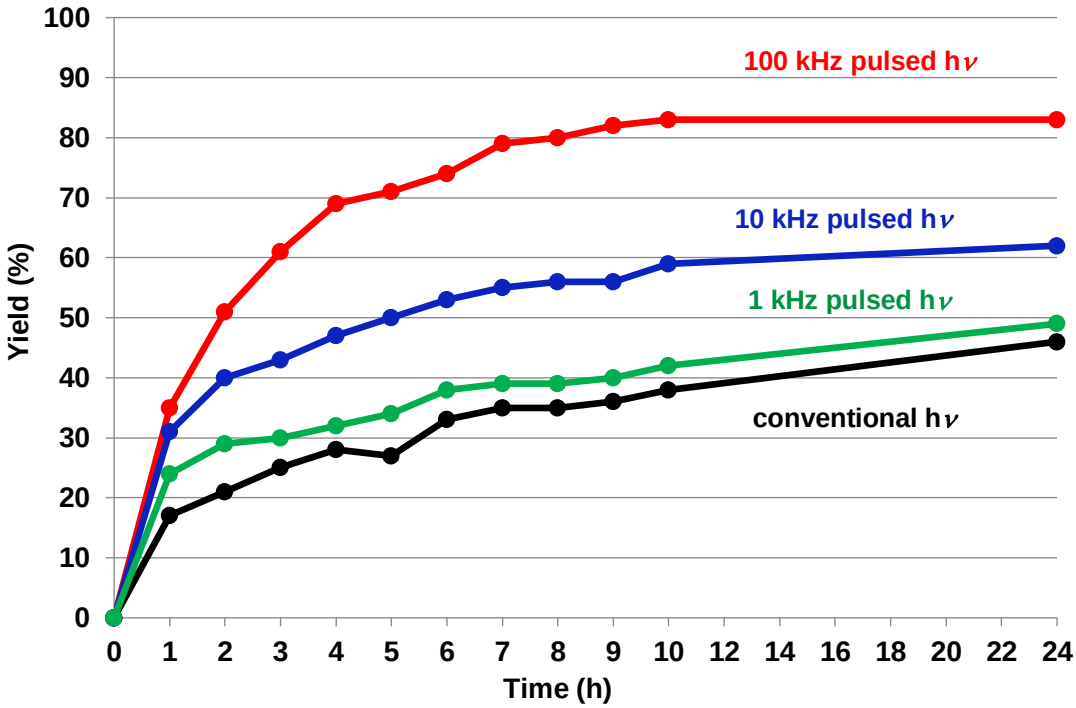

Figure 4.2.1: Monitoring the formation of insertion product **4.4** in visible light-mediated copper photoredox-catalysed dual α-amino C–H/ C–F functionalisation reactions employing: 100 kHz pulsed blue LED irradiation (red); 10 kHz pulsed blue LED irradiation (blue); 1 kHz pulsed blue LED irradiation (green) and conventional 24 W blue LED irradiation (black). Reagents and conditions: Table 4.2.12, entry 8, and the stated irradiation mode. Each data point represents the average of two experiments with yields determined by ^{19}F NMR spectroscopy with the aid of an internal standard.

The reaction performed utilising 100 kHz pulsed LED irradiation illustrates a marked improvement in reaction efficiency and yield with the reaction proceeding to full conversion after 10 h and no increase in yield observed after this time. Lowering the pulse frequency by orders of magnitude results in rate decreases and reduced yields. In both the 10 kHz and 1 kHz cases, the yield of the reaction continues to increase between the 10 h and 24 h data points and the reaction has not proceeded to complete conversion even after 24 h. Conventional irradiation results in the least efficient reaction and the lowest yield. This reaction also did not proceed to complete conversion after 24 h.

4.2.3 Investigation of the role of Gd(OTf)$_3$

The role of Gd(OTf)$_3$ in the dual α-amino C–H/ C–F functionalisation reaction may be more complicated than initially thought. An emission spectrum of [Cu(bcp)(XP)]PF$_6$ in diluted CH_2Cl_2 at 298 K with excitation at 330 nm is shown in Figure 4.2.2A and this displays a single emission maximum at 576 nm. However, when 40 mol% Gd(OTf)$_3$ was added to this

solution a second emission maximum at 448 nm is observed (Figure 4.2.2B). To identify this emission maximum a diluted CH_2Cl_2 solution containing 5 equivalents of $Gd(OTf)_3$ and 1 equivalent bathocuproine (bcp) was excited at 330 nm under identical conditions to those described above. A single emission maximum at 455 nm was observed which suggests the presence of a bcp-coordinated gadolinium complex (Figure 4.2.2C). Excited state lifetimes for each of these emission maxima were measured. The emission maximum in the range 448–455 nm exhibits essentially the same excited state lifetime in both solutions that it was detected (5.6 ns). The emission maximum at 576 nm is attributed to emission from the $[Cu(bcp)(XP)]PF_6$ The λ_{max} and excited state lifetime do not change in the presence of $Gd(OTf)_3$ suggesting that significant quantities of $[Cu(bcp)(XP)]PF_6$ remain intact under these conditions (40 mol% $Gd(OTf)_3$). These results indicate that ligand exchange between the gadolinium and copper metal centres is prevalent.

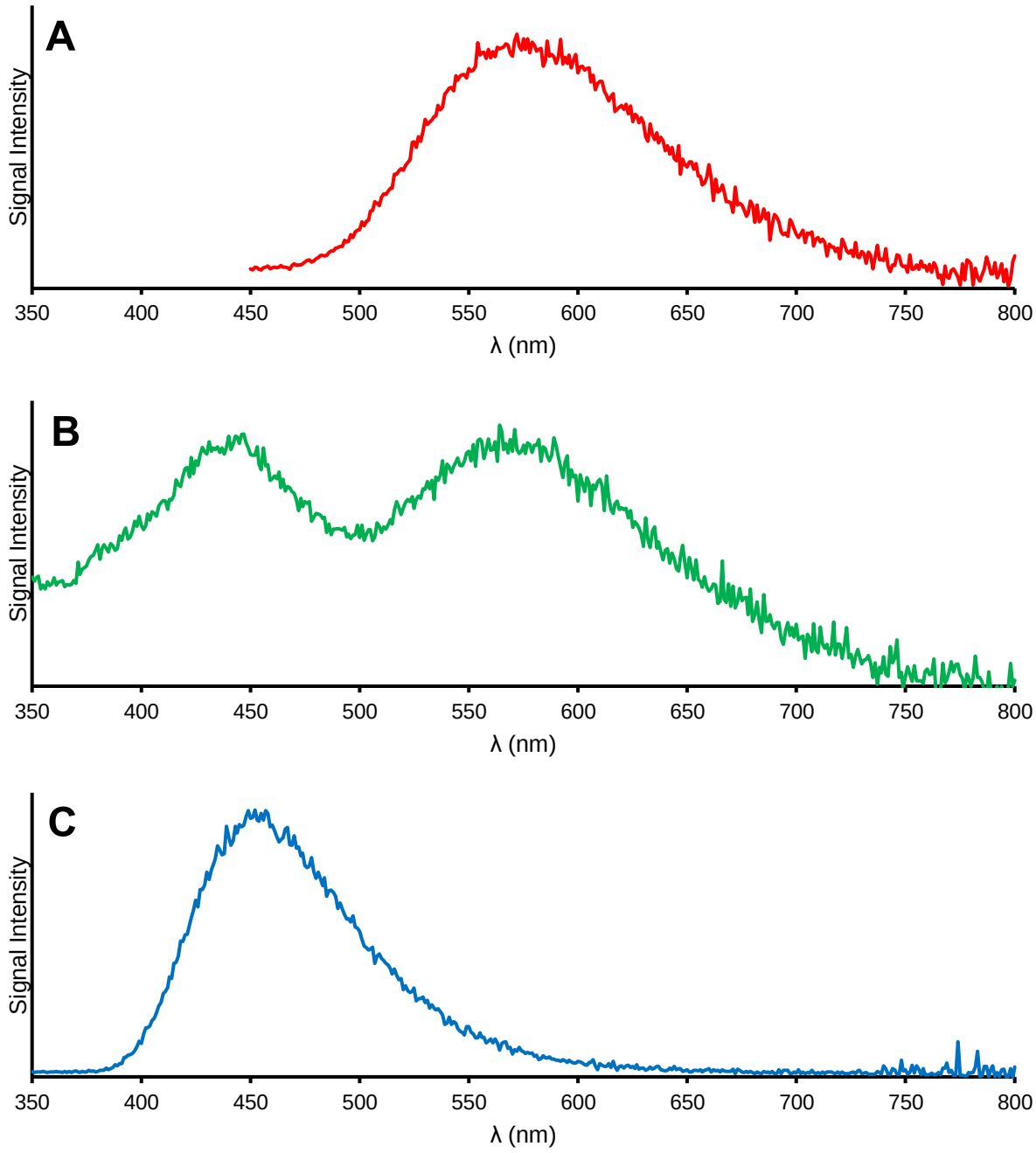

Figure 4.2.2: Emission spectra of CH_2Cl_2 solutions (10^{-5} M) containing $[Cu(bcp)(XP)]PF_6$ and $Gd(OTf)_3$ with excitation at 330 nm at 298 K. (A) Spectrum of $[Cu(bcp)(XP)]PF_6$; (B) Spectrum of 1 equiv $[Cu(bcp)(XP)]PF_6$ and 40 mol% $Gd(OTf)_3$; (C) Spectrum of 5 equiv $(Gd(OTf)_3$ and 1 equiv bcp.

To investigate the potential ligand exchange reaction further, a titration experiment was conducted in which increasing quantities of $Gd(OTf)_3$ were added to a solution containing one equivalent of $[Cu(bcp)(XP)]PF_6$ while maintaining constant concentration (10^{-5} M of the copper complex). The emission spectra of these solutions were recorded at 298 K with excitation at 330 nm and the quantum yield in the range 350–490 nm was calculated.

This wavelength range was chosen as it captures the majority of the emission from the bcp coordinated gadolinium complex while minimising contribution from the emission attributed to [Cu(bcp)(XP)]PF_6, however there is some overlap. The results are presented in Figure 4.2.3.

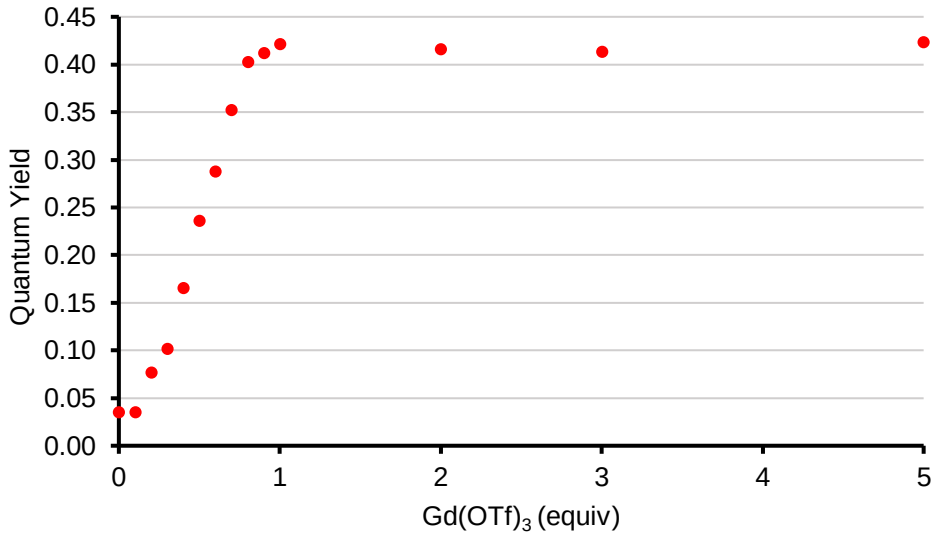

Figure 4.2.3: Monitoring the increase in quantum yield of a solution containing [Cu(bcp)(XP)]PF_6 and $Gd(OTf)_3$ as the amount of $Gd(OTf)_3$ is increased. The emission is attributed to a bcp coordinated gadolinium complex. Quantum yield was measured over the range 350–490 nm with excitation at 330 nm.

The quantum yield of the emission from the emission maximum attributed to the bcp-coordinated gadolinium complex increases significantly until 1 equivalent of $Gd(OTf)_3$ is present. Further addition of $Gd(OTf)_3$ does not affect the quantum yield. This saturation behaviour suggests that a complex with a 1:1 ratio of bcp ligand to gadolinium is formed.

In the copper photoredox-catalysed dual α-amino C–H/ C–F functionalisation reaction the increase in yield is highly dependent on the substrate. Several substrates deliver highly increased yields (such as C_6F_5NHBoc **4.5**, see Table 4.2.11) in the presence of 40 mol% $Gd(OTf)_3$ while amide **4.3** displays only a small increase in yield. This substrate dependence suggests that the $Gd(OTf)_3$ may serve primarily as a Lewis acid which facilitates more facile reduction of the substrates. However, the results presented in this section clearly demonstrate that the role of $Gd(OTf)_3$ may be more complicated.

4.3 Investigation of the Scope of the Reaction

4.3.1 Synthesis of starting materials

In order to investigate the scope of this α-amino C–H/ C–F functionalisation reaction several starting materials had to be synthesised. These included mono- and dicarbamates, primary and secondary amides, and O-heterocycles (Scheme 4.3.1). Also, a Weinreb amide and a range of esters were synthesised (Scheme 4.3.2). In all cases these starting materials were synthesised from readily available reagents and the reactions were not optimised.

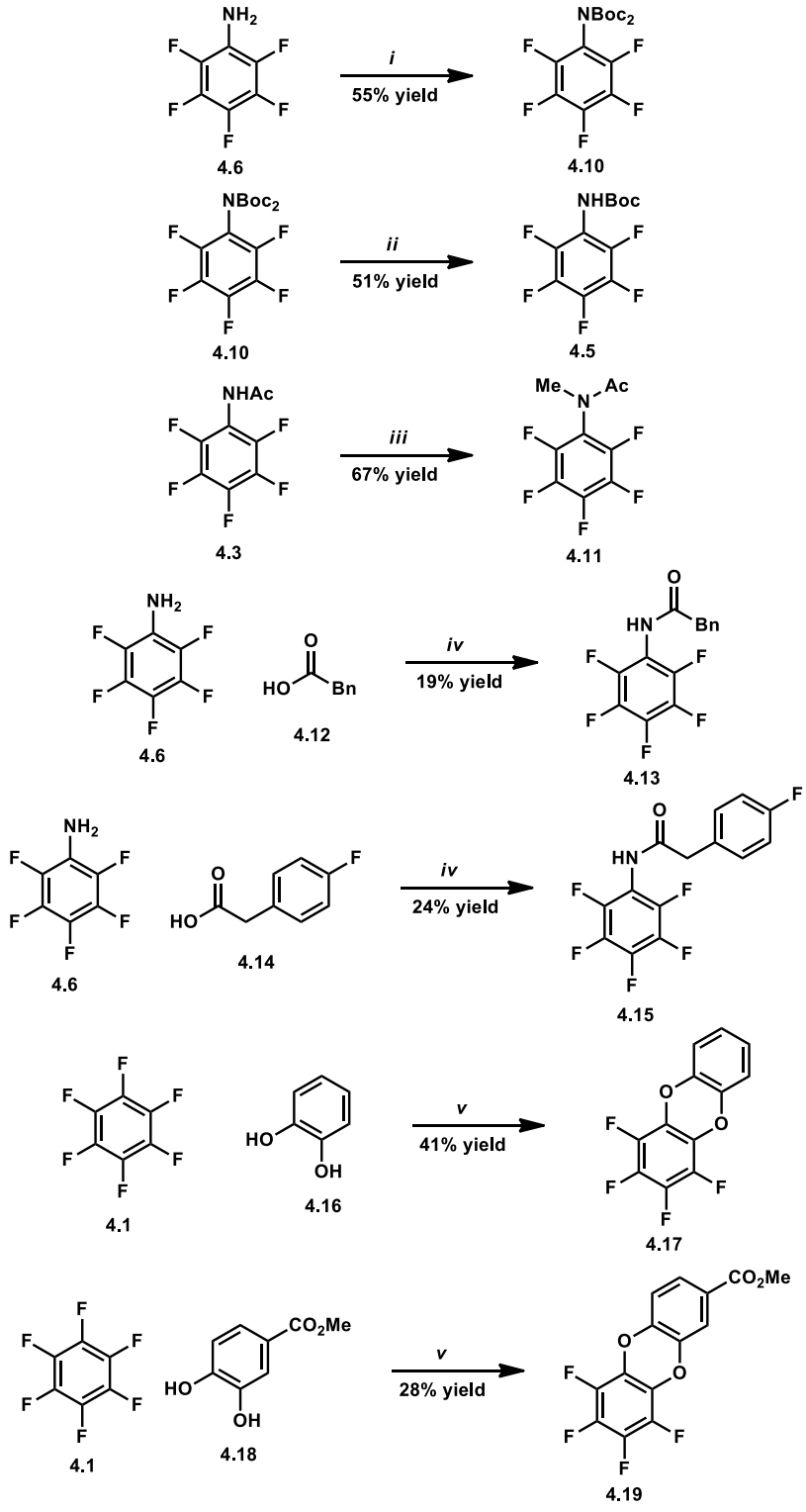

Scheme 4.3.1: Synthesis of starting materials for an α-amino C–H/ C–F functionalisation reaction. Reagents and conditions: (*i*) 1 equiv **4.6**, 1.2 equiv Boc_2O, 2% DMAP, 2 equiv Na_2CO_3, THF, N_2, 60 °C; (*ii*) 1 equiv **4.10**, 1 equiv TFA, N_2, 0 °C; (*iii*) 1 equiv **4.3**, 1.2 equiv NaH, 1.2 equiv MeI, DMF, N_2, 0–25 °C; (*iv*) 1 equiv **4.6**, 1.1 equiv **4.12** or **4.14**, 10% DMAP, 1.4 equiv EDCI, 2.5 equiv NEt_3, DMF, N_2, 0–25 °C; (*v*) 1 equiv **4.1**, 1 equiv **4.16** or **4.18**, 5 equiv K_2CO_3, MeCN, 80 °C.

Dicarbamate **4.10** was synthesised from aniline **4.6** using di-*tert*-butyl dicarbamate and *N*,*N*-dimethylaminopyridine (DMAP) as catalyst under typical conditions for the protection of an aniline in a 55% yield (Scheme 4.3.1). There was also a small amount (10%) of carbamate **4.5** produced under these reaction conditions. One of the Boc groups of dicarbamate **4.10** could be removed with TFA to deliver carbamate **4.5** in 51% yield. A methylation reaction of primary amide **4.3** using NaH and methyl iodide delivered secondary amide **4.11** in 67% yield. Carboxylic acids **4.12** or **4.14** were activated by 1-ethyl-3-(3-dimethylaminopropyl)carbodiimide (EDCI) and subsequently underwent a coupling reaction with aniline **4.6** with catalytic DMAP to deliver amides **4.13** and **4.15** in 19% and 24% yields respectively. The low yields in these instances are likely due to the pentafluorophenyl moiety present in aniline **4.6** inductively withdrawing electron density from the nitrogen atom resulting in less nucleophilic character. Nucleophilic aromatic substitution reactions were used to prepare *O*-heterocycles **4.17** and **4.19** from hexafluorobenzene (**4.1**) and diphenols **4.16** and **4.18** in 41% and 21% yields respectively.

Furthermore, a nucleophilic acyl substitution reaction was used to access Weinreb amide **4.22** (Scheme 4.3.2). This reaction proceeded in 19% yield starting from benzoyl chloride **4.20** and ammonium salt **4.21**. A Tishchenko reaction was used to dimerise aldehyde **4.23** with the use of the catalyst system [$RuCl_2$(*p*-cymene)$_2$] and triphenylphosphine. This delivered ester **4.24** in 21% yield.[17] EDCI coupling reactions were again performed to access esters **4.27**, **4.29** and **4.31** in 49%, 38% and 50% yields respectively. The yields in these cases were higher than the amide couplings reported in Scheme 4.3.1. In these instances, pentafluorobenzoic acid (**4.25**) was used as the electrophilic coupling partner and the inductive electron withdrawing effect of the pentafluorophenyl moiety now has a more favourable effect on the electrophilicity of this reactant.

With these starting materials in hand, a study investigating the scope of the pulsed LED irradiation-induced copper photoredox-catalysed process was undertaken.

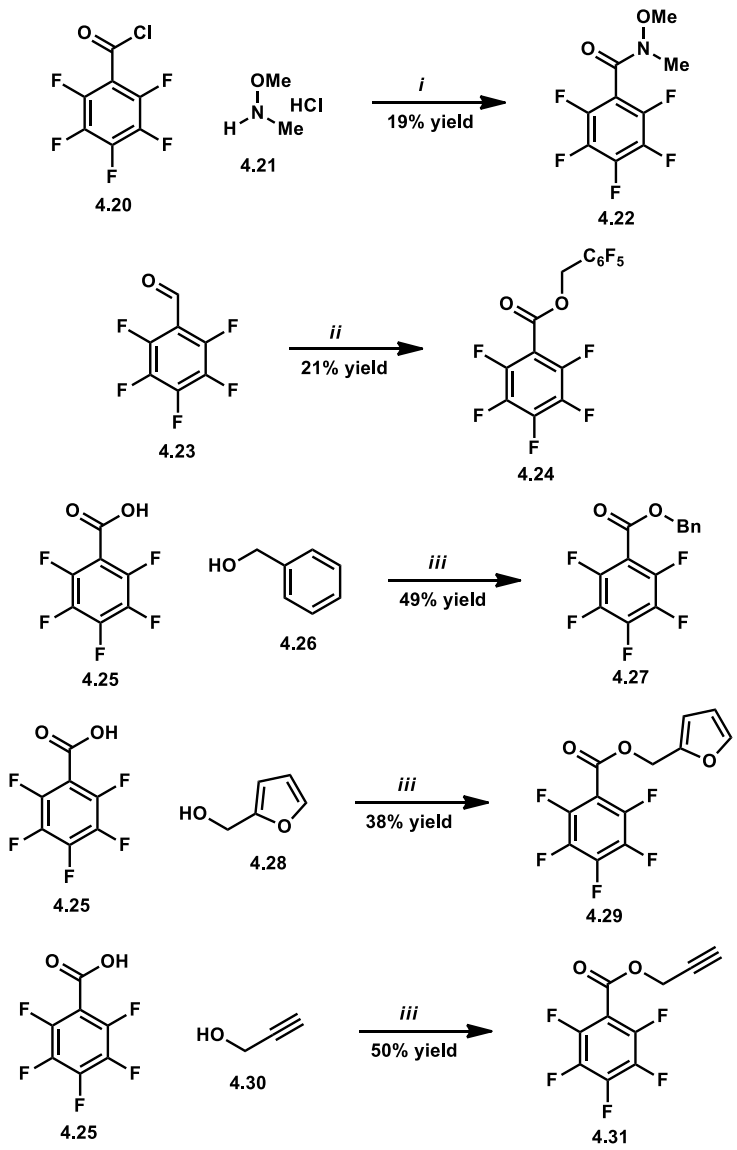

Scheme 4.3.2: Synthesis of starting materials for a hydrodefluorination (HDF) reaction. Reagents and conditions: (*i*) 1 equiv **4.20**, 1.2 equiv **4.21**, 3.5 equiv NEt_3, CH_2Cl_2, 25 °C; (*ii*) 1 equiv **4.23**, 2.5 % [$RuCl_2$(*p*-cymene)$_2$], 5% PPh_3, 30% HCOONa, dioxane, N_2, 80 °C; (*iii*) 1.1 equiv **4.25**, 1 equiv, **4.26**, **4.28** or **4.30**, 10% DMAP, 1.4 equiv EDCI, 2.5 equiv NEt_3, CH_2Cl_2, N_2, 0–25 °C.

4.3.2 Investigation of the scope of the dual α-amino C–H/ C–F functionalisation reaction

First, the scope of the reaction with respect to the tertiary amine reactant was investigated. A range of aliphatic amines,[h] as well as cyclic amines and diamines participated

[h] These amines were prepared by J. C. Robertson, another group member.

in the reaction (Figure 4.3.1). When utilising each of these amine reactants the *para*-substituted product was observed in all cases and this was the sole product for all monoamine reactants as well as *N*,*N*,*N*,*N*-tetramethylethylenediamine (TMEDA). However, when other diamine derivatives were used a small amount of *ortho*-substituted product was also observed. When utilising cyclic amines, reaction occurred at the cyclic α-amino position in all cases. This is potentially due to activation of this position derived from ring strain. Importantly, in the majority of cases, the use of 100 kHz pulsed LED irradiation led to increased product yields in contrast to conventional irradiation. *N*-aryl amine reactants, including *N*,*N*-dimethylaniline and *N*-phenylpyrrolidine, were also screened under the optimised reaction conditions. However these compounds did not participate in the reaction under these standard conditions. This contrasts with a related iridium photoredox-catalysed, dual α-amino C–H/ C–F functionalisation reaction developed by Hashmi and co-workers which enabled germane reactions with *N*-aryl amines.[6]

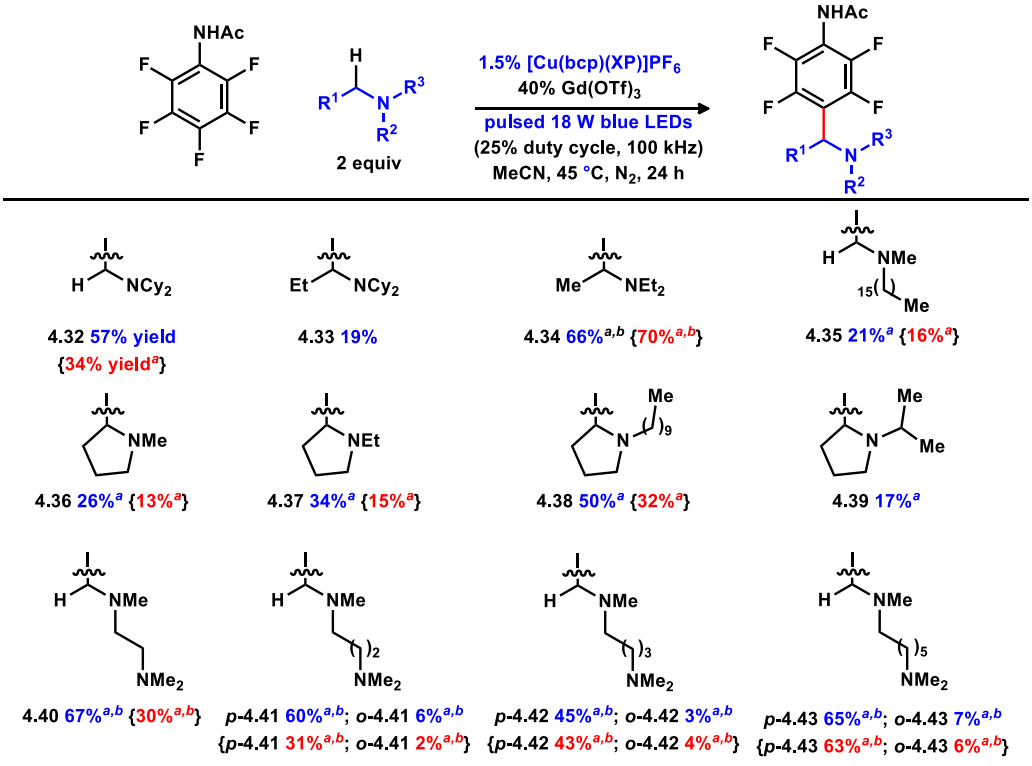

Figure 4.3.1: Copper photoredox-catalysed dual α-amino C–H/ C–F functionalisation induced by pulsed visible light irradiation: scope with respect to amine. [a] Determined by ^{19}F NMR spectroscopy with the aid of an internal standard (average of 2 experiments). [b] Reaction performed in the absence of $Gd(OTf)_3$. The yield of the reaction employing conventional 24 W LED irradiation is provided in brackets.

Next, the scope of the reaction with respect to the perfluorinated arene was investigated. A range of amides, a carbamate, and an aniline all participated in the reaction with Hünig's base. In addition, an aryl ether and *O*-heterocycles delivered respective insertion products (Figure 4.3.2).

Again, in all cases, the major product featured *para*-substitution while *ortho*-substitution was only observed in a limited number of cases as the minor product. In the majority of the reactions, pulsed irradiation provided higher product yields relative to conventional irradiation.

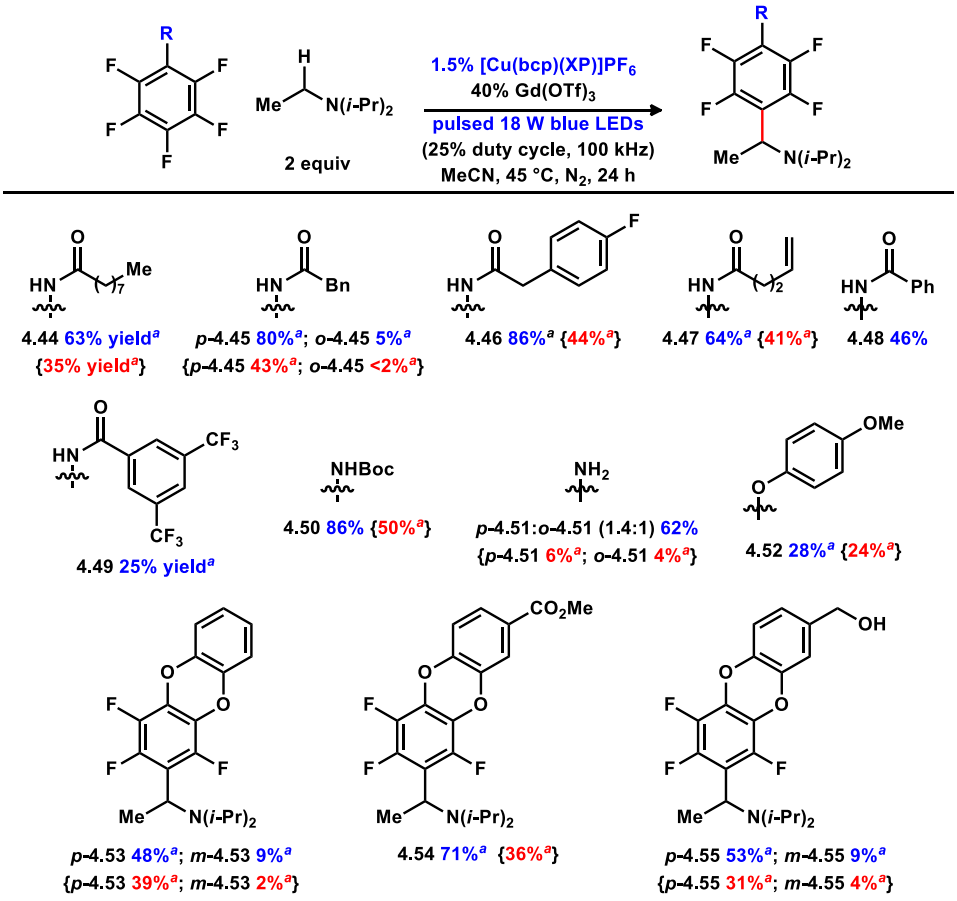

Figure 4.3.2: Copper photoredox-catalysed dual α-amino C–H/ C–F functionalisation induced by pulsed visible light irradiation: scope with respect to perfluorinated arene. [a] Determined by ^{19}F NMR spectroscopy with the aid of an internal standard (average of 2 experiments). [b] Reaction performed in the absence of $Gd(OTf)_3$. The yield of the reaction employing conventional 24 W LED irradiation is provided in brackets.

In contrast to these results, several reactants delivered hydrodefluorination (HDF) products **4.56**–**4.67** (Figure 4.3.3). The majority of these reactants feature less electron

donating substituents at the *para*-position. These results are more consistent with reported hydrodefluorination processes observed when iridium- or pyrene-based photoredox catalysts were utilised in the presence of Hünig's base.[1,4]

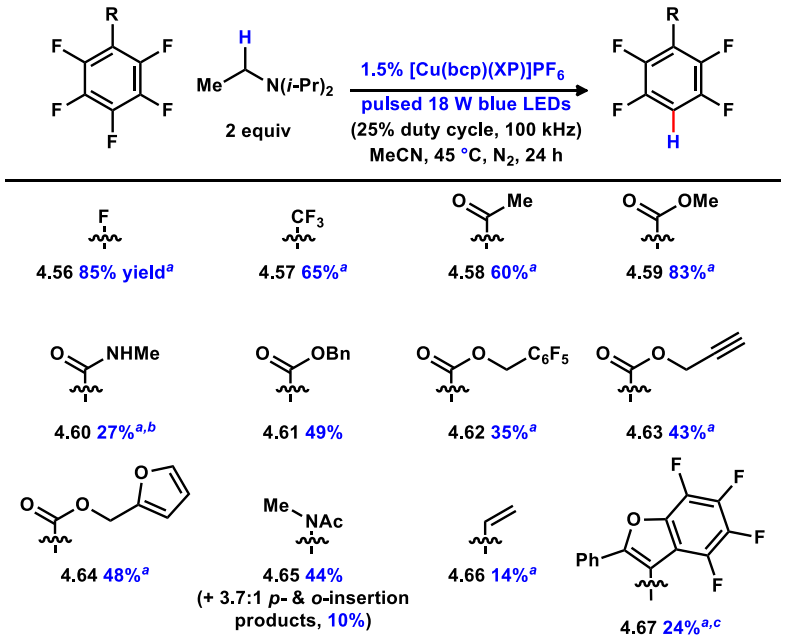

Figure 4.3.3: Copper photoredox-catalysed hydrodefluorination reactions of perfluorinated arenes. [a] Determined by ^{19}F NMR spectroscopy with the aid of an internal standard (average of 2 experiments). [b] The substrate for this reaction was a Weinreb amide (pentafluoro-*N*-methoxy-*N*-methylbenzamide). [c] Reaction performed in 2 : 1 MeCN/ DMF.

It should be noted that the reactant used in the reaction that produced amide **4.60** was Weinreb amide **4.22**. The N–O bond has been cleaved under the reaction conditions resulting in the reduction of the amide nitrogen as well as performing a HDF reaction. In the reaction that produced heterocycle **4.67** the starting material was insoluble in MeCN so a 2 : 1 mixture of MeCN/ DMF was used in this case. Interestingly, HDF products **4.62** and **4.67** were the only products observed in the respective reactions despite the presence of a second perfluorinated arene ring.

4.3.3 Synthesis of a novel perfluorinated analogue of pyrrolidine alkaloids

Pyrrolidine alkaloids (–)-codonopsinine and (+)-radicamine B represent natural products which exhibit interesting biological activity (Scheme 4.3.3A).[18] (–)-Codonopsinine has displayed antibiotic and hypotensive activity,[19] and (+)-radicamine B is known for its

diuretic, and haemostat activity.[20] As such, the development of efficient synthetic procedures to access these compounds and related analogues is of high value. The new copper photoredox-catalysed α-amino C–H/ C–F functionalisation reaction reported here provides potential access to novel fluorinated analogues of biologically active pyrrolidine alkaloids including (–)-codonopsinine and (+)-radicamine B. A reaction was performed in which carbamate **4.5** and *N*-methylpyrrolidine (**4.68**) were subjected to the reaction conditions. This delivered pyrrolidine **4.69** in an unoptimised 31% yield (Scheme 4.3.3B). Pyrrolidine **4.69** could provide access to novel fluorinated analogues of pyrrolidine alkaloids. Indeed, it may be possible to deprotect and diazotise pyrrolidine **4.69**, before performing a simple functionalisation reaction such as hydrolysis or methanolysis.[21]

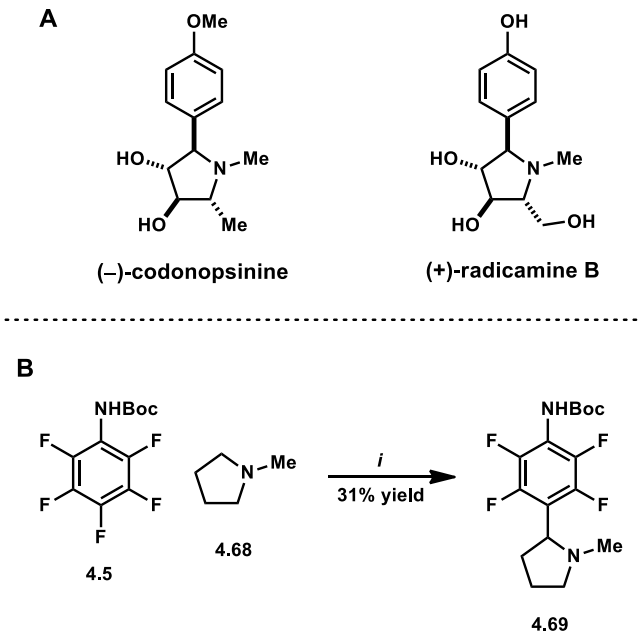

Scheme 4.3.3: (A) Pyrrolidine alkaloids that display biological activity; (B) Synthesis of a potential precursor to fluorinated analogues of pyrrolidine alkaloids. Reagents and conditions: (*i*) Table 4.2.12, entry 1.

4.4 Mechanistic Investigation

4.4.1 Mechanistic experiments

Several experiments were conducted to probe the reaction mechanism in more detail. Substituting $[Cu(bcp)(XP)]PF_6$ for $[Cu(MeCN)_4]PF_6$, bathocuproine (bcp) and xantphos (XP)

resulted in a lower yield of insertion product **4.4** and incomplete conversion (Scheme 4.4.1A). This suggests that [Cu(bcp)(XP)]PF_6 is responsible for catalysing the reaction rather than other copper species derived from this complex. When the reaction was performed in the presence of the radical scavenger 2,2,6,6-tetramethylpiperidinooxy (TEMPO) (50 mol%) a very low yield (8%) of insertion product **4.4** was observed as well as low conversion (Scheme 4.4.1B). Higher loadings of TEMPO (1 or 2 equiv) completely inhibited the reaction. These data are consistent with the reaction proceeding through a single electron pathway. It is likely that TEMPO reacts rapidly with any radical species formed under the reaction conditions which inhibits the productive pathway to insertion product **4.4**. When bromide **4.70** was subjected to the optimised reaction conditions, hydrodebromination product **4.71** was formed exclusively in 54% yield (Scheme 4.4.1C). This is consistent with the faster fragmentation of bromide from radical anions leading to aryl radicals, in comparison to the analogous fragmentation of fluorides.[22] Potentially, this result may also explain the observation of hydrodefluorination products when utilising reactants with electron withdrawing groups (Figure 4.3.3). A more electron deficient arene ring could promote a faster fragmentation of fluoride which ultimately leads to the observed hydrodefluorination products.

In addition, electrochemical characterisation of amide **4.3** ($E_{1/2}$ = –1.60 V vs. SCE)[8] and [Cu(bcp)(XP)]PF_6 ($E_{1/2}$ = –1.64 V vs. SCE)[16] suggests that an electron transfer process may take place in this reaction. A tentative mechanistic pathway is outlined in Scheme 4.4.1D. The copper photoredox catalyst may be capable of reducing amide **4.3** to deliver a radical anion. The catalyst may also be able to oxidise Hünig's base which leads to the α-amino radical. These two persistent radical species may then combine, in some fashion, with the loss of fluoride, to deliver the insertion product **4.4**.[23]

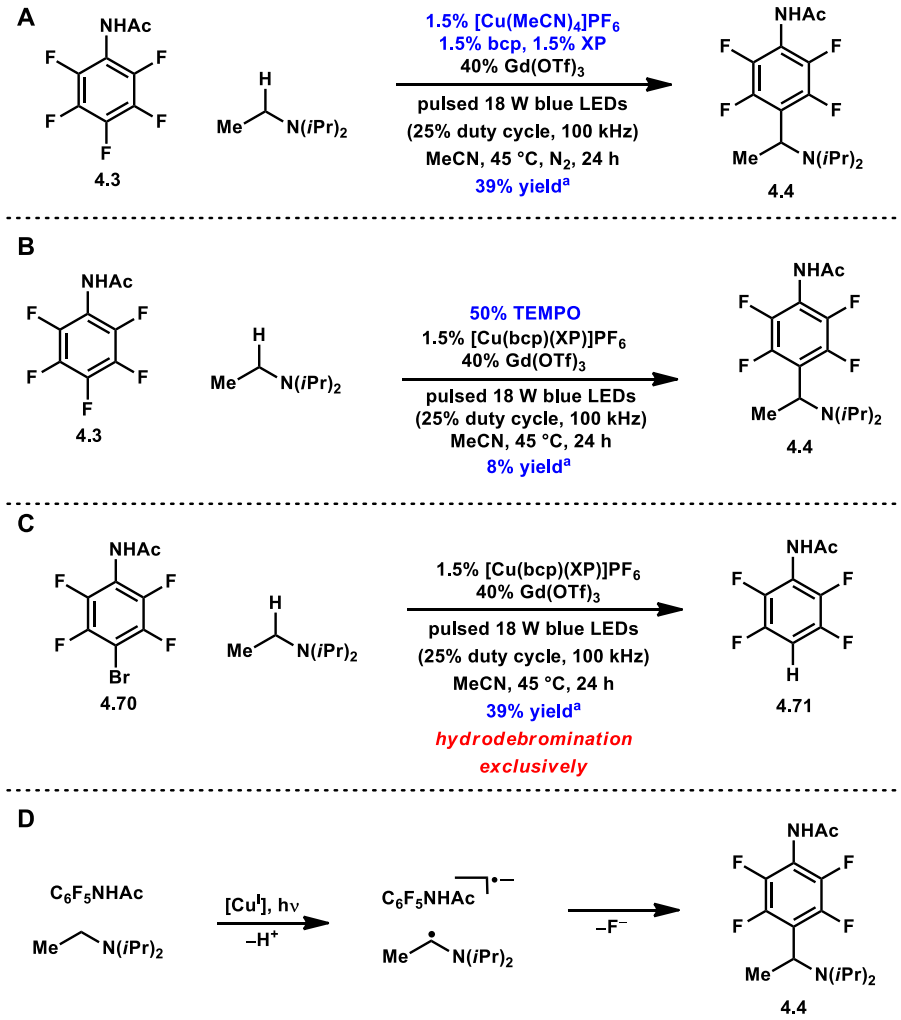

Scheme 4.4.1: (A) Results employing $[Cu(MeCN)_4]PF_6$, xantphos (XP) and bathocuproine (bcp); (B) Results employing 2,2,6,6-tetramethylpiperidinooxy (TEMPO); (C) Copper photoredox-catalysed hydrodebromination of bromide **4.70**; (D) Tentative mechanistic hypothesis. [a] Determined by ^{19}F NMR spectroscopy with the aid of an internal standard (average of 2 experiments).

The exact role of pulsed LED irradiation that enables a much more efficient reaction and increased yields is still under investigation and there is not sufficient data to allow a definitive explanation. However, the greatest efficiency and yield were obtained when utilising 100 kHz pulsed irradiation. This frequency approximately matches the excited state lifetime of the copper catalyst (6.4 μs). Potentially, an intense burst of irradiation can excite the catalyst before switching off. This allows time for the catalyst to decay to the ground state before another pulse of light excites it again. Alternatively, in this time, the catalyst may interact with substrates which begins the productive pathway to the product and also results

in quenching of the excited state before another pulse of light. This may allow the catalyst to spend more time in its active excited state in comparison to conventional irradiation.

A related copper-based photoredox catalyst, [Cu(bcp)(DPEphos)]PF_6, has been used in a range of transformations by Evano and co-workers.[24] Catalyst decomposition was reported over extended reaction times under similar conditions to that reported here. It is possible that the use of pulsed irradiation limits catalyst decomposition by avoiding two-photon absorption. If the catalyst were in a high energy photoexcited state and then absorbed another photon it is possible that this further input of energy may result in catalyst decomposition. Two-photon absorption events may be avoided by the use of pulsed irradiation as this allows time for the catalyst to decay to the ground state before another burst of irradiation. The quantum yield of two photon absorption events is typically very low, however, this may become significant over extended reaction times.[25] It should also be noted that positive effects when using pulsed irradiation were observed at early time points in the dual α-amino C–H/ C–F functionalisation reaction.

Potentially, radical chain processes may be prevalent in the dual α-amino C–H/ C–F functionalisation reaction. Many recent reports of photoredox-catalysed transformations suggest that formation of the final product proceeds via a closed catalytic cycle (Figure 4.4.1).[1,4,6] Conversely, radical chain mechanisms have been posited to operate in tandem with a closed catalytic cycle in related photoredox-catalysed transformations.[26] This is consistent with many other reactions involving radical intermediates.[27] If a radical chain mechanism is operative in the dual α-amino C–H/ C–F functionalisation reaction, it is possible that the pulsed irradiation strategy offers an advantage over conventional irradiation by allowing the chain propagation cycle to proceed unhindered by complications derived from a competing closed catalytic cycle which may be less efficient under pulsed irradiation conditions. The quantum yield for the key transformation has not been determined during this project. This will be the subject of future work. A high quantum yield for the reaction ($\phi \gg 1$) is a significant indicator of prevalent radical chain processes.[26] 'Light/ dark' experiments, in which the yield of the reaction is quantified over intermittent light and dark periods have also been used previously to identify radical chain processes.[28]

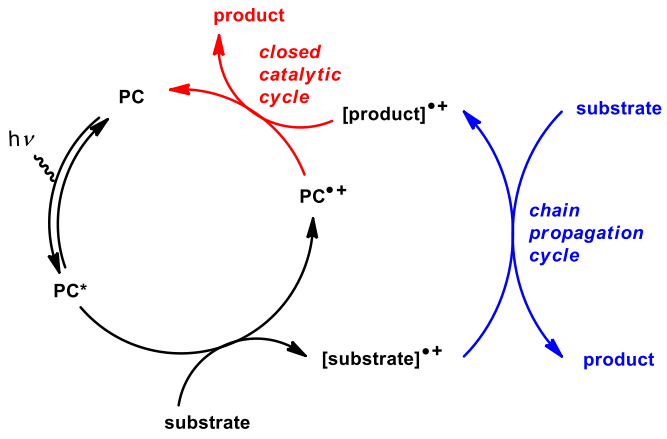

Figure 4.4.1: Generalised mechanism for oxidative photoredox-catalysed reactions.[26]

4.4.2 Divergent reactivity

An interesting aspect of this chemistry is the observation of divergent reaction outcomes depending on the specific catalyst used. Weaver and co-workers reported the hydrodefluorination of amide **4.3** under very similar reaction conditions but using an iridium photoredox catalyst [Ir(ppy)$_3$] (Scheme 4.4.2A). In contrast, when using a copper photoredox catalyst, as is reported here, insertion product **4.4** is obtained (Scheme 4.4.2B). It is possible that the cationic nature of the copper photoredox catalyst has a stabilising effect on the perfluororadical anion which extends the lifetime of this radical species and allows the dual α-amino C–H/ C–F functionalisation reaction to occur rather than hydrodefluorination which occurs when using the neutral *fac*-[Ir(ppy)$_3$] catalyst. This is supported by similar observations made by Hashmi and co-workers. A related photoredox-catalysed reaction was reported in which a cationic iridium-based catalyst was used. Using very similar conditions and substrates, a dual α-amino C–H/ C–F functionalisation was observed rather than a HDF reaction.[6] This catalyst-controlled divergent reactivity could be exploited to facilitate the production of libraries of related fluorinated compounds that would potentially be valuable to the pharmaceutical and agrochemical industries.

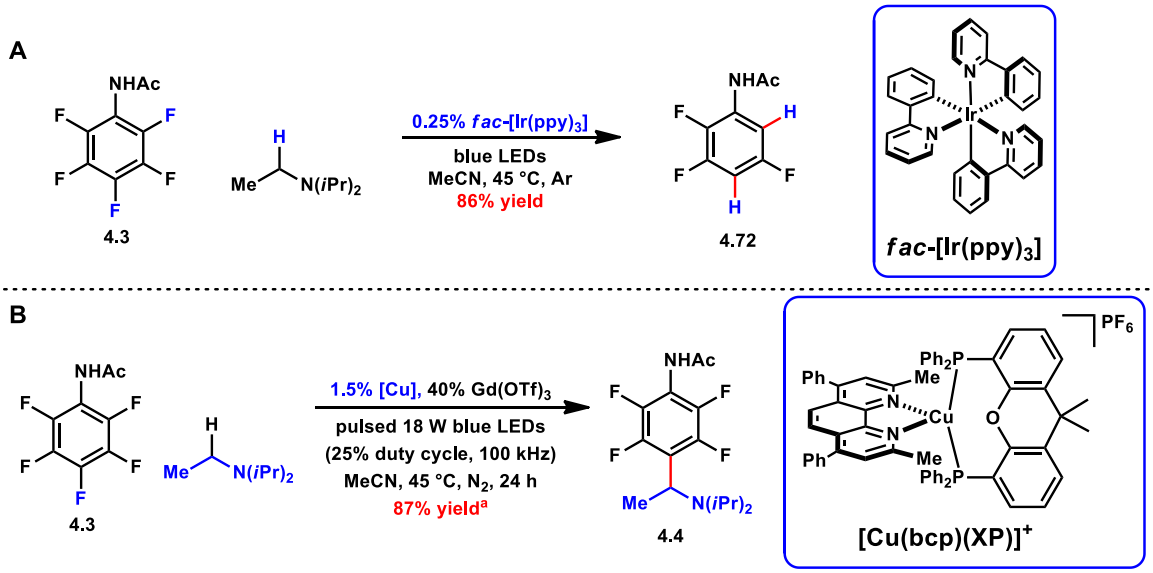

Scheme 4.4.2: (A) Hydrodefluorination reaction observed by Weaver and co-workers when using *fac*-[Ir(ppy)$_3$] as photoredox catalyst; (B) Dual α-amino C–H/ C–F functionalisation reaction observed when using [Cu(bcp)(XP)]PF$_6$ as photoredox catalyst.

4.5 Alkylation Reaction

An unusual alkylation product **4.73** was obtained when substituting triethylamine for Hünig's base in the presence of Gd(OTf)$_3$, under otherwise unchanged reaction conditions (Table 4.5.1).

Table 4.5.1: Investigation of an unusual alkylation reaction.

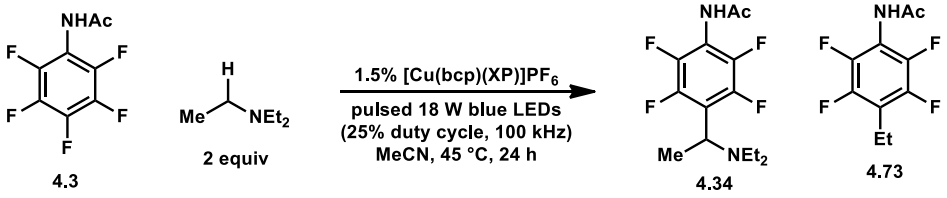

entry	additive	yield[a]:	4.34 (%)	4.73 (%)
1	none		66	0
2	40% Gd(OTf)$_3$		15	15

[a]Yield determined by ^{19}F NMR spectroscopy with the aid of an internal standard (average of 2 experiments).

Under the standard reaction conditions, but in the absence of $Gd(OTf)_3$, the expected insertion product **4.34** was the exclusive product of the reaction in 66% yield (Table 4.5.1, entry 1). However, when adding 40% $Gd(OTf)_3$ under otherwise unchanged reaction conditions, a 1 : 1 ratio of insertion product **4.34** and alkylation product **4.73** was observed in a reduced overall yield (30%) (entry 2). Next, insertion product **4.34** was isolated and subjected to the reaction conditions {with $Gd(OTf)_3$}. This experiment returned insertion product **4.34** quantitatively suggesting that insertion product **4.34** is not a precursor to alkylation product **4.73**. However, there remains the possibility that insertion product **4.34** leads to alkylation product **4.73** but the catalyst is not turned over under these conditions. As such, an experiment in which one equivalent of hexafluorobenzene (**4.1**) was added to the reaction mixture under otherwise identical conditions to (entry 2). This reaction quantitatively returned unreacted insertion product **4.34**, and alkylation product **4.73** was not observed. Importantly, pentafluorobenzene (**4.2**) was observed in 46% yield suggesting that catalyst turnover occured.

Tripropylamine and tributylamine were also subjected to the reaction conditions to preliminarily test the generality of the reaction. The results are presented in Scheme 4.5.1.

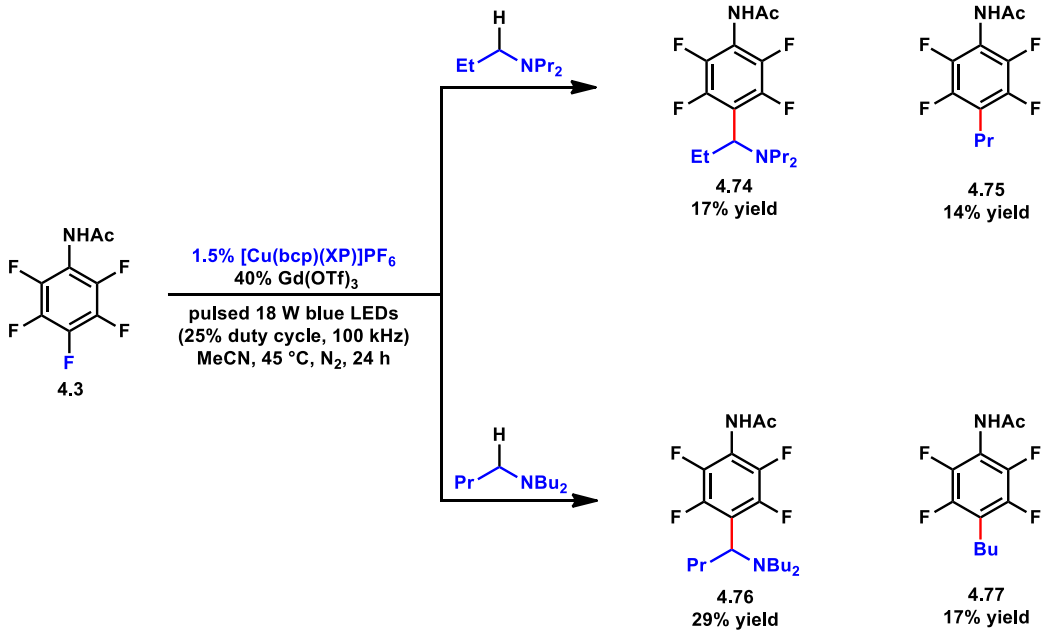

Scheme 4.5.1: Preliminary investigation of the scope of an alkylation reaction.

Both tripropylamine and tributylamine participated in the reaction and delivered mixtures of the insertion and alkylation products. In the case of tripropylamine, the yield and ratio of the products remained similar to that when utilising triethylamine (51%, ~1 : 1). In contrast, when utilising tributylamine, the overall yield is increased (46%) and insertion product **4.76** is favoured, delivering a product ratio of ~3 : 2 (**4.76** : **4.77**).

This unusual alkylation reaction warrants further investigation primarily with respect to elucidating the mechanism by which this reaction occurs. The potential to develop an efficient alkylation reaction to deliver a library of fluorinated alkyl analogues may also be valuable to the pharmaceutical and agrochemical industries.

4.6 Summary and Outlook

A pulsed LED irradiation strategy was exploited to develop a novel α-amino C–H/ C–F functionalisation reaction. The use of pulsed irradiation was crucial to developing a more efficient process. The results of this proof of concept study highlight the generally untapped potential of pulsed LED irradiation in photoredox catalysis and organic synthesis more generally. Potentially, if the pulsed irradiation strategy reported here is coupled with catalyst development, the applications of copper-based photoredox catalysis may be able to be extended significantly. One area that may particularly benefit from this pulsed irradiation strategy is the development of an alkylation reaction for which preliminary results were discussed. Subsequent studies will focus on investigating the exact role of the pulsed irradiation effect which delivers an enhanced reaction rate and efficiency in addition to exploring the wider applications of this strategy in photoredox catalysis and organic synthesis more generally.

4.7 References

(1) S. M. Senaweera; A. Singh; J. D. Weaver, *J. Am. Chem. Soc.* **2014**, *136*, 3002–3005.

(2) A. Arora; J. D. Weaver, *Acc. Chem. Res.* **2016**, *49*, 2273–2283.

(3) T. Ahrens; J. Kohlmann; M. Ahrens; T. Braun, *Chem. Rev.* **2015**, *115*, 931–972.

(4) (a) A. Singh; J. J. Kubik; J. D. Weaver, *Chem. Sci.* **2015**, *6*, 7206–7212; (b) S. Senaweera; J. D. Weaver, *J. Am. Chem. Soc.* **2016**, *138*, 2520–2523; (c) A. Singh; C. J. Fennell; J. D.

Weaver, *Chem. Sci.* **2016**, *7*, 6796–6802; (d) J. Lu; N. S. Khetrapal; J. A. Johnson; X. C. Zeng; J. Zhang, *J. Am. Chem. Soc.* **2016**, *138*, 15805–15808; (e) M. B. Khaled; R. K. El Mokadem; J. D. Weaver III, *J. Am. Chem. Soc.* **2017**, *139*, 13092–13101.

(5) (a) N. Armaroli, *Chem. Soc. Rev.* **2001**, *30*, 113–124; (b) N. Armaroli; G. Accorsi; F. Cardinali; A. Listorti, In *Photochemistry and Photophysics of Coordination Compounds: Copper*; V. Balzani; S. Campagna, Eds.; Springer: Berlin, Germany, **2007**; Topics in Current Chemistry *280*, pp 69–116.

(6) J. Xie; M. Rudolph; F. Rominger; A. S. K. Hashmi, *Angew. Chem., Int. Ed.* **2017**, *56*, 7266–7270.

(7) R. Kumar; S. N. Ugale; A. M. Kale; R. S. Bhosale; R. Narayan, *ChemistrySelect* **2018**, *3*, 9393–9401.

(8) S. S. Laev; L. Y. Gurskaya; G. A. Selivanova; I. V. Beregovaya; L. N. Shchegoleva; N. V. Vasil'eva; M. M. Shakirov; V. D. Shteingarts, *Eur. J. Org. Chem.* **2007**, 306–316.

(9) A. Singh; A. Arora; J. D. Weaver, *Org. Lett.* **2013**, *15*, 5390–5393.

(10) T. R. Blum; Z. D. Miller; D. M. Bates; I. A. Guzei; T. P. Yoon, *Science* **2016**, *354*, 1391–1395.

(11) M. K. Jackl; L. Legnani; B. Morandi; J. W. Bode, *Org. Lett.* **2017**, *19*, 4696–4699.

(12) C. K. Prier; D. A. Rankic; D. W. C. MacMillan, *Chem. Rev.* **2013**, *113*, 5322–5363.

(13) (a) S. Protti; M. Fagnoni, *Photochem. Photobiol. Sci.* **2009**, *8*, 1499–1516; (b)T. P. Yoon; M. A. Ischay; J. Du, *Nature Chem.* **2010**, *2*, 527–532; (c) D. M. Schultz; T. P. Yoon, *Science* **2014**, *343*, 1239176.

(14) (a) F. Briers; D. L. Chapman; E. Walters, *J. Chem. Soc.* **1926**, *129*, 562–569; (b) W. I. Bengough; S. A. McIntosh; R. A. M. Thomson, *Nature* **1959**, *184*, 266–267; (c) K. U. Ingold, *Pure Appl. Chem.* **1997**, *69*, 241–243; (d) C. D. McTiernan; S. P. Pitre; J. C. Scaiano, *ACS Catal.* **2014**, *4*, 4034–4039; (e) S. P. Pitre; C. D. McTiernan; W. Vine; R. DiPucchio; M. Grenier; J. C. Scaiano, *Sci. Rep.* **2015**, *10*, 16397.

(15) (a) D. J. Tennessen; R. J. Bula; T. D. Sharkey, *Photosynth. Res.* **1995**, *44*, 261–269; (b) K. Yoneda; Y. Mori, *PCT Appl.*, EP1374665A1, **2004**; (c) E. Olvera-Gonzalez; D. Alaniz-Lumbreras; R. Ivanov-Tsonchev; J. Villa-Hernańdez; C. Olvera-Olvera; E. Gonzaĺez-Ramírez; M. Araiza-Esquivel; V. Torres-Argüelles; V. Castaño, *Comput. Electron. Agric.* **2013**, *92*, 48–53.

(16) E. Mejia; S.-P. Luo; M. Karnahl; A. Friedrich; S. Tschierlei; A.-E. Surkus; H. Junge; S. Gladiali; S. Lochbrunner; M. Beller, *Chem. Eur. J.* **2013**, *19*, 15972–15978.

(17) M.-O. Simon; S. Darses, *Adv. Synth. Catal.* **2010**, *352*, 305–308.

(18) M. Lingamurthy; Y. Jagadeesh; K. Ramakrishna; B. V. Rao, *J. Org. Chem.* **2016**, *81*, 1367–1377.

(19) (a) S. F. Matkhalikova; V. M. Malikov; S. Y. Yunusov, *Khim. Prir. Soedin* **1969**, *5*, 30–32; (b) S. F. Matkhalikova; V. M. Malikov; S. Y. Yunusov, *Khim. Prir. Soedin* **1969**, *5*, 606–607; (c) M. T. Khanov; M. B. Sultanov; M. R. Egorova, *Farmakol. Alkaloidov Serdech. Glikoyidov.* **1971**, 210–212.

(20) (a) P. Compain; O. R. Martin, *Bioorg. Med. Chem.* **2001**, *9*, 3077–3092; (b) N. Asano, *Glycobiology* **2003**, *13*, 93R–104R.

(21) Z. Wu; R. Glaser, *J. Am. Chem. Soc.* **2004**, *126*, 10632–10639.

(22) J. F. Bunnett, *Acc. Chem. Res.* **1978**, *11*, 413–420.

(23) B. A. DeHaven; J. T. Tokarski III; A. A. Korous; F. Mentink-Vigier; T. M. Makris; A. M. Brugh; M. D. E. Forbes; J. van Tol; C. R. Bowers; L. S. Shimizu, *Chem. Eur. J.* **2017**, *23*, 8315–8319.

(24) B. Michelet; C. Deldaele; S. Kajouj; C. Moucheron; G. Evano, *Org. Lett.* **2017**, *19*, 3576–3579.

(25) P. Gautam; Y. Wang; G. Zhang; H. Sun; J. M. W. Cahn, *Chem. Mater.* **2018**, *Just Accepted Manuscript*, DOI: 10.1021/acs.chemmater.8b02723.

(26) M. A. Cismesia; T. P. Yoon, *Chem. Sci.* **2015**, *6*, 5426–5434.

(27) (a) D. P. Curran, *Synthesis* **1988**, 417–439; (b) D. P. Curran, *Synthesis*, **1988**, 489–513.

(28) A. Call; C. Casadevall; F. Acuña-Parés; A. Casitas; J. Lloret-Fillol, *Chem. Sci.* **2017**, *8*, 4739–4749.

Chapter Five

Summary and Outlook

5.1 Summary

This research project has focused on the development of copper-based photoredox catalysis with two key themes:

1. To prepare a range of new homoleptic phenanthroline-based copper(I) complexes to study their structural, photophysical and electrochemical properties to inform the use of these complexes in synthesis;
2. To exploit the intrinsic properties of these complexes to create novel photoredox-catalysed reactions.

A range of both known and previously unreported homoleptic bis(2,9-diaryl-1,10-phenanthroline)copper(I) complexes as well as known heteroleptic phenanthroline-containing copper(I) complexes were synthesised. These complexes were spectroscopically characterised and the solid state structures of seven of these complexes were determined by X-ray analysis. The quantification of the distortion away from an ideal coordination geometry suggests that the 2,9-diaryl substituents play a significant role in the overall structure of the homoleptic complexes. While heteroleptic complexes display significantly reduced distortion. The photophysical and electrochemical properties of these complexes were also investigated. In this way, complex **2.35** was identified as one of the most reducing phenanthroline-based copper(I) complexes that has been reported ($E_{1/2}{}^{I*/II} = -1.95$ V vs. SCE). Nearly all of the homoleptic and heteroleptic complexes that have been prepared display ^{3}MLCT behaviour upon photoexcitation which allows access to long lived photoexcited states. In several cases, emission quantum yields and molar absorptivities are increased in comparison to the prototypical copper-based photoredox catalyst $[Cu(dap)_2]^+$. As such, these complexes may find useful applications in photoredox catalysis.

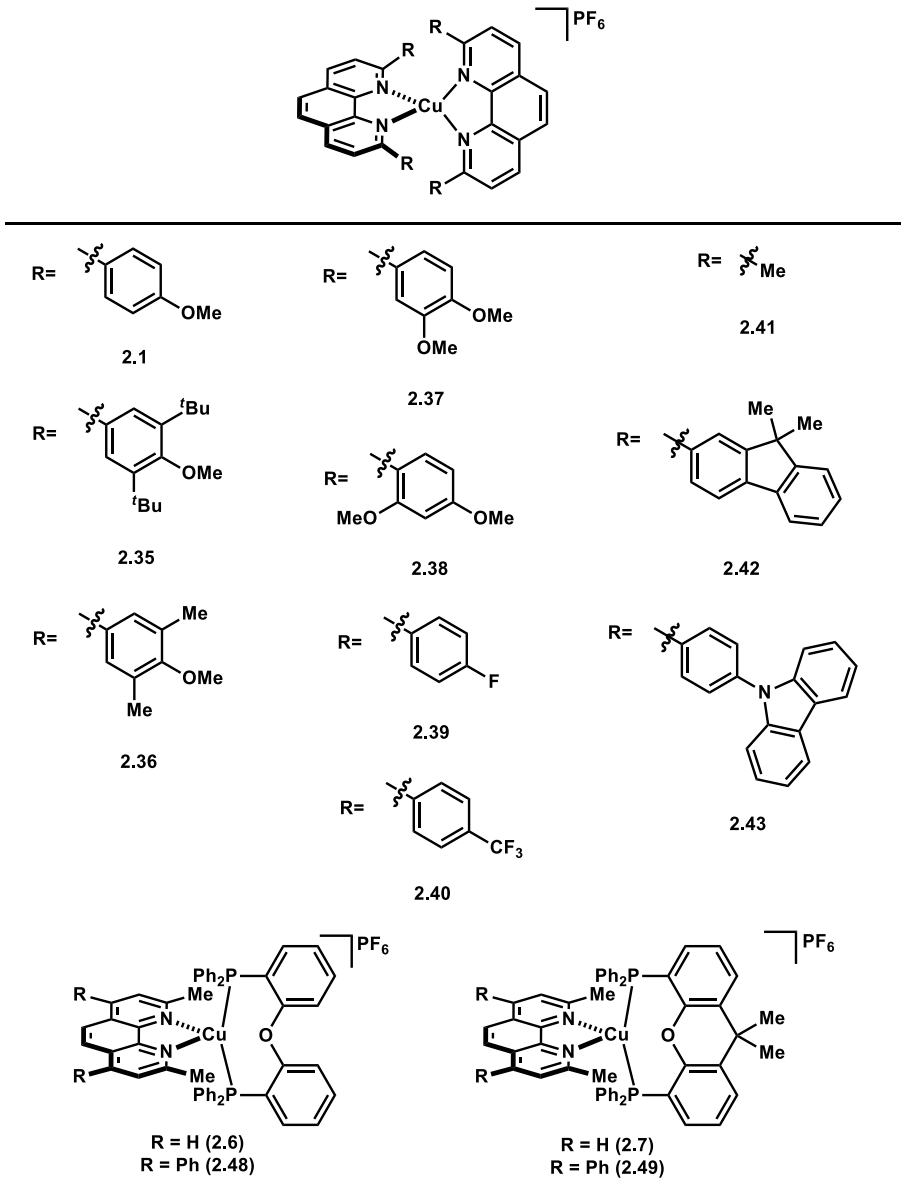

Figure 5.1.1: Range of homoleptic and heteroleptic phenanthroline-containing copper(I) complexes synthesised in this study.

The synthesised homoleptic and heteroleptic copper(I) complexes were evaluated in order to determine their capacity to promote ATRA processes. Specifically, ATRA reactions which were proposed to operate through mechanisms featuring inner-sphere processes. The outcomes of these photoredox-catalysed reactions were generally consistent with the varying steric bulk of the copper complex employed. However, these results reveal that electronic factors may also play a significant role in controlling the viability of the putative inner sphere pathway in this chemistry.

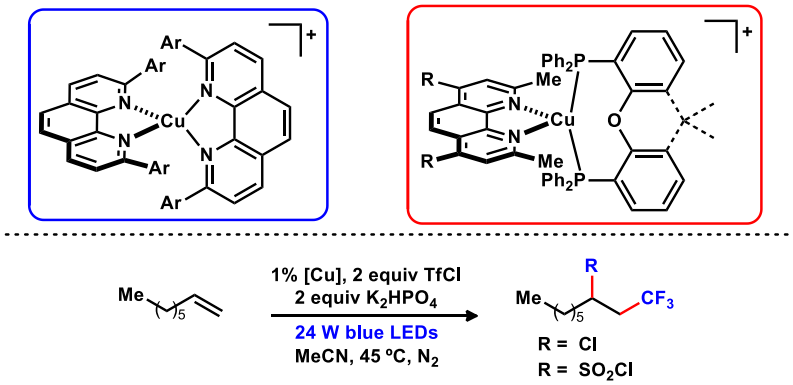

Scheme 5.1.1: Evaluating the capacity of copper(I) complexes to promote ATRA processes which feature interesting inner sphere processes.

The weak oxidising power of [Cu(dap)$_2$]Cl has been exploited to effect the direct functionalisation of α-amino C–H bonds. This chemistry enabled the rapid synthesis of complex and important heterocyclic scaffolds including novel octahydroisoquinolino[2,1-*a*]pyrrolo[3,4-*c*]-quinoline frameworks as single diastereomers. Most importantly, an unprecedented and crucial TFA-mediated aerobic oxidation of a putative photoexcited copper(I) species was identified and was shown to be necessary to facilitate catalyst turnover. As such, it would appear that this process represents a rare example of a Brønsted acid-mediated radical reaction in organic synthesis.

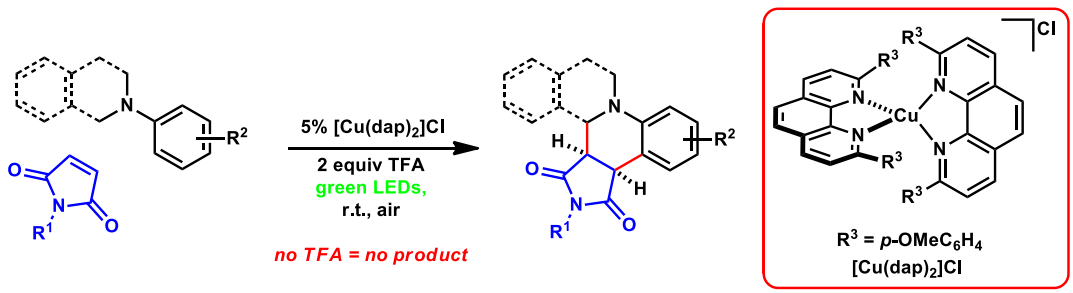

Scheme 5.1.2: Exploiting the weak oxidising power of [Cu(dap)$_2$]Cl to effect the direct functionalisation of α-amino C–H bonds in Povarov reactions.

Pulsed LED irradiation was exploited to develop a novel copper photoredox-catalysed dual α-amino C–H/ C–F functionalisation reaction. This pulsed irradiation strategy

was crucial for establishing a more efficient process. The results of this study highlight the generally untapped potential of pulsed LED irradiation in organic synthesis for the first time. The reaction was found to have broad scope which enabled the production of a library of perfluorinated aromatic compounds. Interesting divergent reactivity was observed when comparing a cationic copper-based photoredox catalyst with a neutral iridium-based photoredox catalyst. Also, preliminary results of a mechanistically interesting alkylation reaction were presented.

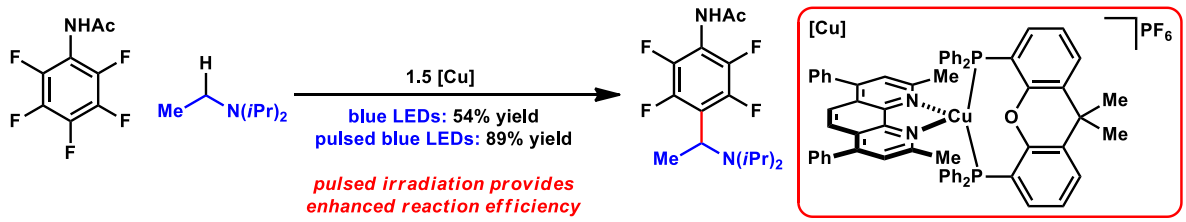

Scheme 5.1.3: Investigating the potential of pulsed LED irradiation in photoredox catalysis. A dual α-amino C–H/ C–F functionalisation reaction was developed which provides access to a range of perfluorinated aromatic compounds.

5.2 Outlook

The work presented in this research project has contributed to extending the scope of phenanthroline-containing copper(I) complexes in photoredox catalysis. This work has primarily focused on the development of homoleptic bis(2,9-diaryl-1,10-phenanthroline)copper(I) complexes. While this project was underway, the utility of heteroleptic phenanthroline-containing copper(I) complexes in photoredox catalysis was further demonstrated by other research groups. Further development of this class of copper-based photoredox-catalysts may facilitate the expansion of the scope and applications of visible light copper(I) photoredox catalysis in organic synthesis in the future.

The identification of the potential of pulsed LED irradiation represents a conceptual advance in the field of visible-light-mediated transformations. However, the specific mechanism by which this process operates is not yet understood. Further investigations focused on determining the specific reasons behind the increased reaction rates and increased yields, as well as its generality, are required.

Chapter Six

Experimental

6.1 General

6.1.1 Materials and methods

Anhydrous CH_2Cl_2 was distilled over CaH_2, under N_2, and stored over molecular sieves, under N_2, prior to use. Anhydrous toluene, acetonitrile, hexane, diethyl ether and tetrahydrofuran were purchased from Chem-Supply and passed through columns on an Innovative Technologies Solvent Purification system. Unless otherwise noted, all reagents were purchased from Sigma-Aldrich, Combi-Blocks, AK Scientific or Oakwood Chemical and used as received. Boronic acids were purchased from Boron Molecular and used as received. *i*Pr$_2$NEt and *N*,*N*-dimethylaniline were distilled prior to use. Unless otherwise noted, all other starting materials were either purchased from commercial sources and used as received or prepared according to reported procedures.

NMR experiments were performed either on a Bruker Avance III NMR spectrometer operating at 400 MHz (^{1}H), 100 MHz (^{13}C), 376 MHz (^{19}F) or 161 MHz (^{31}P) or on a Bruker Avance III NMR spectrometer operating at 600 MHz (^{1}H), 150 MHz (^{13}C), or 576 MHz (^{19}F). The deuterated solvent used was $CDCl_3$, CD_3CN, D_2O, CD_3OD or DMSO-d_6. Spectra were calibrated by assignment of the residual solvent peak. Coupling constants (*J*) were recorded in Hz.

Infrared spectrometry was performed on a Shimadzu FTIR 8400s spectrometer, with samples analysed either as thin films on NaCl plates or using an ATR attachment.

ESIMS analyses were conducted on a Thermo-Scientific LTQ-Orbitrap mass spectrometer. EIMS analyses were performed using a Kratos Analytical Concept ISQ hybrid magnetic sector quadrupole tandem or Shimadzu GCMS-QP2010 mass spectrometers.

TLC was performed using Merck silica gel 60-F_{254} plates. Developed TLC plates were visualised by UV absorbance (254 nm) or through application of heat to a plate stained with cerium molybdate {$Ce(NH_4)_2(NO_3)_6$, $(NH_4)_6Mo_7O_{24}{\cdot}4H_2O$, H_2SO_4, H_2O}. Flash column chromatography was performed with flash grade silica gel (60 μm) and the indicated eluent in accordance with standard techniques.[1]

6.1.2 Pulsed LED photoreactor experimental set up

Our in-house constructed circuit featured a series of integrated circuits (IC) (making up the timing circuit) and voltage regulating components that were used to pulse the blue LED photoreactor:

A Goodwill Instrument Co. GPD-5030 dual tracking power supply was used to provide 12 V DC to a voltage regulator (L7805CP), which reduced this output to 5 V DC (Figures 6.1.1 & 6.1.2). This enabled the power supply to drive both the integrated circuits (ICs) and the LED photoreactor. The timing circuit was created by taking the 5 V output of the regulator and connecting the 555-timer chip (NE555N) in an astable configuration and feedback from the resistors and capacitor (between the voltage regulator output and common ground) causes a voltage instability in the 555-timer chip that allows it to oscillate between on and off.

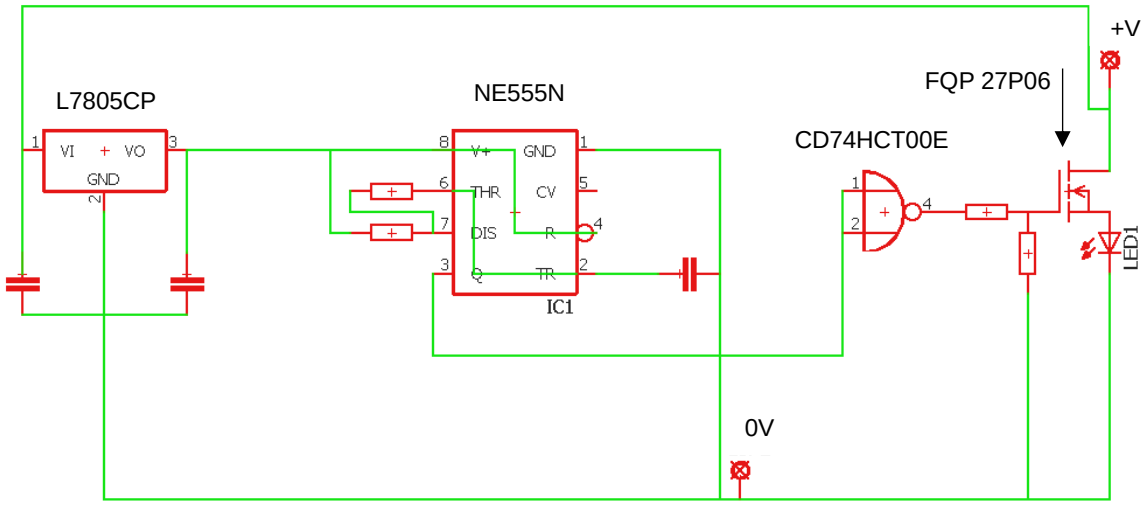

Figure 6.1.1: Schematic representation of the circuit used to pulse the LED photoreactor.

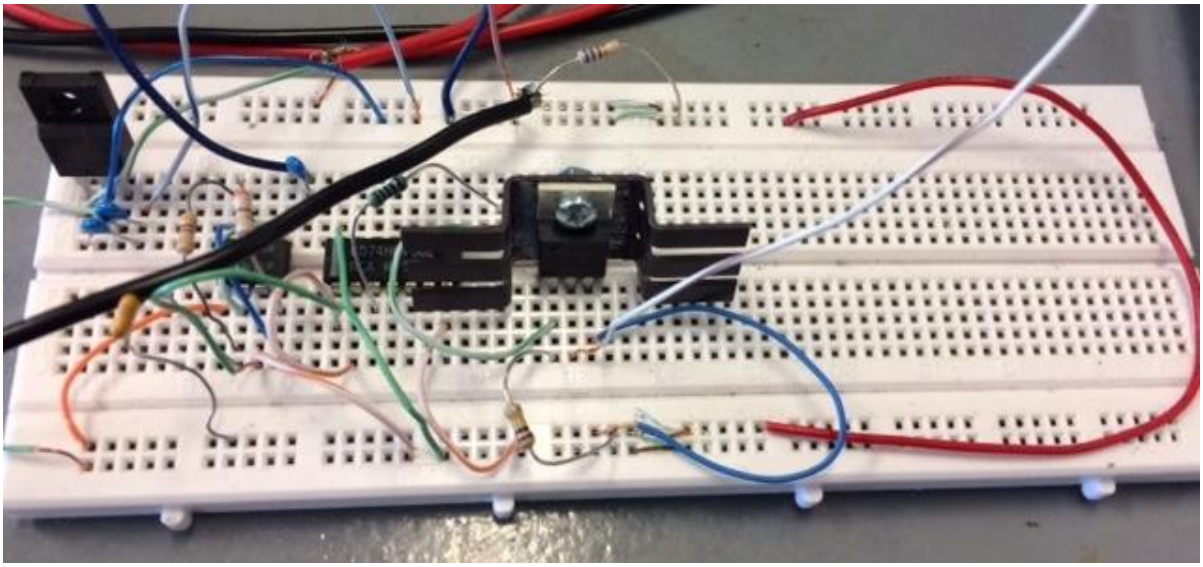

Figure 6.1.2: Photograph of the circuit constructed and employed to pulse the LED photoreactor.

The combination of the resistor and capacitor values in the circuit caused an oscillation of approximately 100 kHz with a 75% duty cycle. However, because LEDs operating at these currents with 75% duty cycle would overheat, the output of the 555-timer chip was inverted by a quad NOR flip-flop IC (CD74HCT00E). The NOR flip-flop gate inputs were connected in parallel, meaning that they were either both low or both high. The NOR flip-flop gate inverts the input, so when the input is high, the output was low and vice versa. This created an output that was a square wave voltage operating at 100 kHz and a 25% duty cycle, which was then fed into the base of a MOSFET transistor (FQP27P06). This allowed current to flow from the collector to the emitter, this activation completed the circuit and turned the LEDs back on. The transistor was needed as it allowed the controlled timing and pulsing obtained by the timing circuit and enabled the 12 V power supply to drive the LEDs. As a result the LEDs operated at 100 kHz and a 25% duty cycle.

The custom photoreactor was constructed using 2 m of blue or green LEDs strips (120 LEDs) purchased from Banggood.com (Figure 6.1.3). Under our above-mentioned pulsed LED conditions this photoreactor operates at 18 W (12 V, 1.5 A) providing 454 nm (blue), ~28,000 lux (measured at the centre of the photoreactor using a Trotec BF05 Luxmeter) irradiation. A photograph of the complete experimental set-up is provided (Figure 6.1.4). Under conventional (continuous) operation this photoreactor operates at 24 W (12 V, 2 A)

providing 453 nm (blue), or 515 nm (green), ~28,000 lux (measured at the center of the photoreactor using a Trotec BF05 Luxmeter).

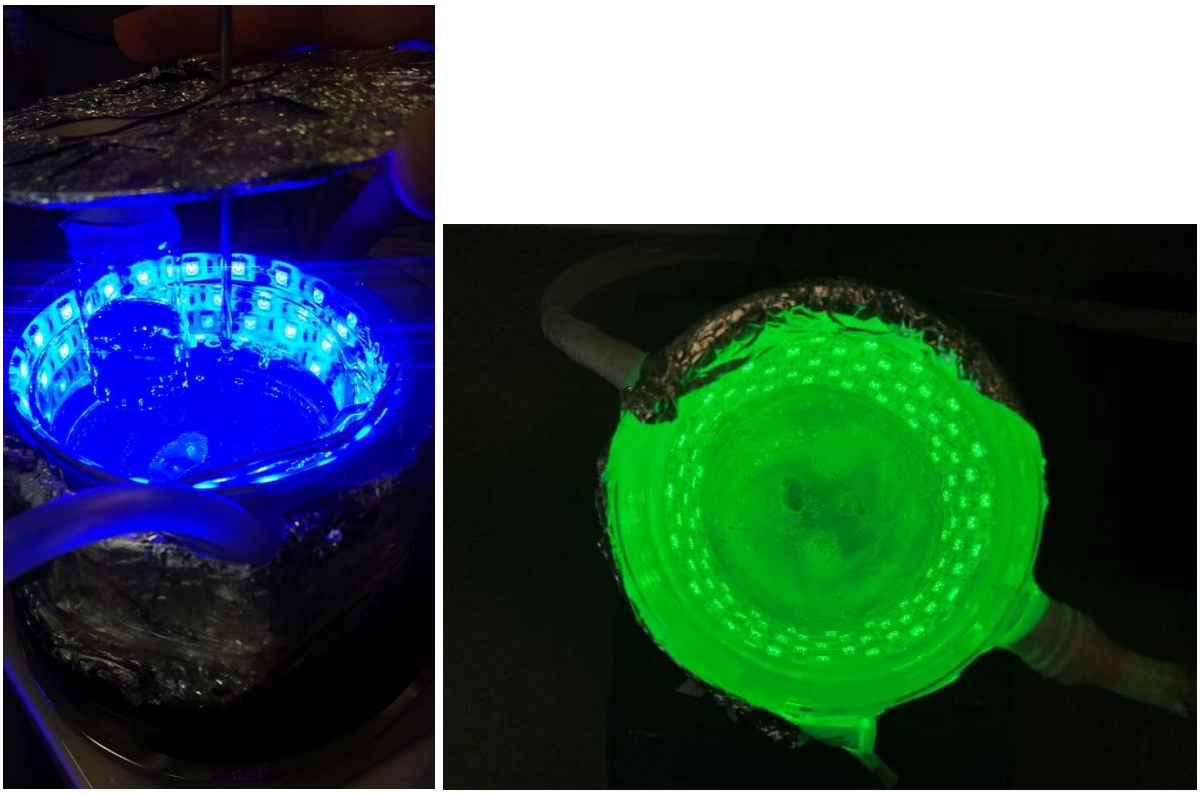

Figure 6.1.3: Photograph of blue and green LED photoreactors.

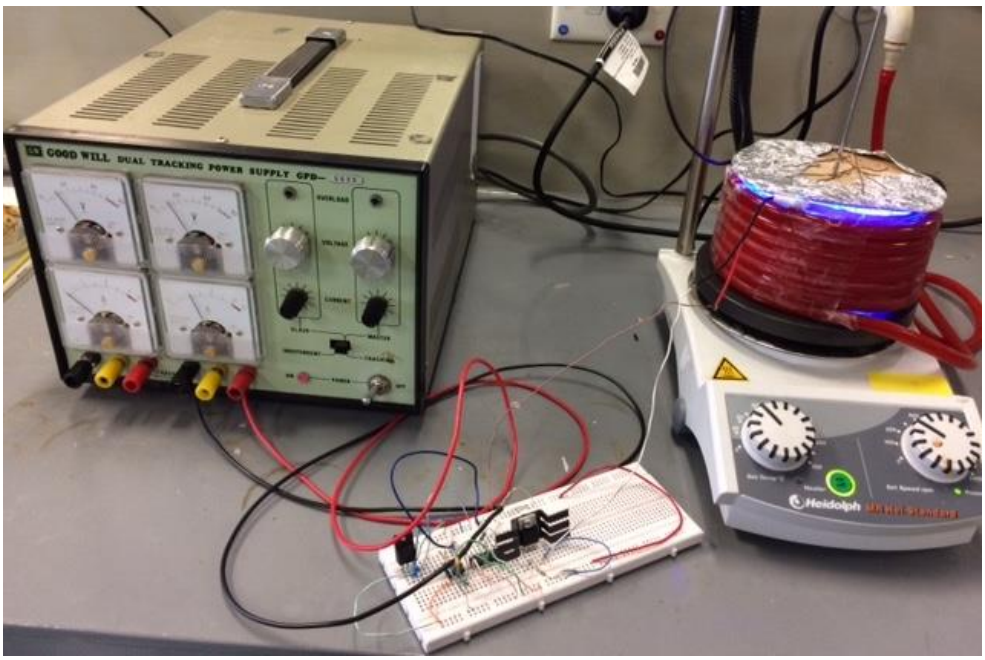

Figure 6.1.4: Photograph of pulsed LED photoreactor experimental set up.

6.1.3 Crystallography

X-ray data were collected at 100 K on crystals mounted on a Hampton Scientific cryoloop on a Bruker AXS D8 Quest diffractometer using Cu-Kα radiation (λ = 1.54178 Å) or on the MX1 or MX2 beamlines of the Australian Synchrotron. The structures were solved by direct methods with SHELXT,[2] refined using full matrix least squares routines against F^2 with SHELXL-97 and visualised with OLEX2.[3] All non-hydrogen atoms were refined anisotropically. All hydrogen atoms were placed in calculated positions and refined using a riding model with fixed C–H distances of 0.95 Å (sp^2CH), 0.99 Å (CH_2), 0.98 Å (CH_3). The thermal parameters of all hydrogen atoms were estimated as U_{iso}(H) = 1.2U_{eq}(C), except for CH_3 where U_{iso}(H) = 1.5U_{eq}(C). A summary of crystallographic data is provided below.

2.1: $C_{52}H_{40}CuF_6N_4O_4P$, M = 993.39, triclinic, a = 13.7555(4), b = 14.1948(4), c = 14.2099(6) Å, α = 100.0947(18), β = 118.9449(11), γ = 106.6158(14)°, U = 2157.70(14) Å^3, T = 100 K, space group P–1 (no. 2), Z = 2, 70597 reflections measured, 7587 unique (R_{int} = 0.0434), 6528 > 4σ(F), R = 0.0368 (observed), wR_2 = 0.0969 (all data).

2.6: $C_{51}H_{42}Cl_2CuF_6N_2OP_3$, M = 1040.21, triclinic, a = 10.9820(3), b = 12.2497(3), c = 18.7891(4) Å, α = 105.4750(10), β = 94.8130(10), γ = 106.1570(10)°, U = 2305.37(10) Å^3, T = 100 K, space group P1 (no. 1), Z = 2, 78463 reflections measured, 15895 unique, (R_{int} = 0.0378), 15025 > 4σ(F), R = 0.0312 (observed), wR_2 = 0.0768 (all data).

2.7: $C_{53}H_{44}CuF_6N_2OP_3$, M = 995.35, triclinic, a = 11.5656(3), b = 14.0327(3), c = 15.0921(4) Å, α = 88.9570(9), β = 67.4769(8), γ = 87.7534(9)°, U = 2260.82(10) Å^3, T = 100 K, space group P–1 (no. 2), Z = 2, 27540 reflections measured, 7268 unique, (R_{int} = 0.0284), 6537 > 4σ(F), R = 0.0277 (observed), wR_2 = 0.0663 (all data).

2.34: $C_{138}H_{174}Cu_3F_{18}N_{12}O_6P_3$, M = 2722.41, monoclinic, a = 18.437(4), b = 36.048(7), c = 21.692(4) Å, β = 95.06(3)°, U = 14361(5) Å^3, T = 100 K, space group $P2_1/n$ (no. 14), Z = 4, 257728 reflections measured, 42839 unique, (R_{int} = 0.0820), 26283 > 4σ(F), R = 0.1271 (observed), wR_2 = 0.3989 (all data).

2.35: $C_{184}H_{244}Cu_2F_{12}N_{10}O_{11}P_2$, M = 3188.90, monoclinic, a = 43.219(10), b = 15.561(4), c = 26.670(11) Å, β = 102.720(9)°, U = 17496(6) Å^3, T = 100 K, space group $P2/c$ (no. 13), Z = 4, 156936 reflections measured, 46557 unique (R_{int} = 0.0548), 27444 > 4σ(F), R = 0.0721 (observed), wR_2 = 0.2416 (all data).

2.40: $C_{52}H_{31}CuF_{18}N_5P$, M = 1186.35, monoclinic, a = 13.3534(7), b = 25.1829(12), c = 13.9516(7) Å, β = 116.8790(10)°, U = 4811.5(4) Å^3, T = 100 K, space group $C2/c$ (no. 15), Z = 4, 11427 reflections measured, 2291 unique (R_{int} = 0.0330), 2018 > 4σ(F), R = 0.0368 (observed), wR_2 = 0.0838 (all data).

2.42: $C_{86}H_{67}CuF_6N_5P$, M = 1378.95, monoclinic, a = 24.792(3), b = 18.900(2), c = 15.4325(13) Å, β = 108.117(8)°, U = 6872.7(13) Å^3, T = 100 K, space group $C2/c$ (no. 15), Z = 4, 21703 reflections measured, 6032 unique (R_{int} = 0.0632), 4932 > 4σ(F), R = 0.0529 (observed), wR_2 = 0.1432 (all data).

2.49: $C_{69}H_{62}CuF_6N_2O_2P_3$, M = 1221.65, triclinic, a = 10.9098(2), b = 13.2865(3), c = 24.5525(5) Å, α = 97.7860(10), β = 95.8720(10), γ = 98.0770(10)°, U = 3464.36(12) Å^3, T = 100 K, space group P–1 (no. 2), Z = 2, 115256 reflections measured, 12161 unique, (R_{int} = 0.0369), 10869 > 4σ(F), R = 0.0405 (observed), wR_2 = 0.1078 (all data).

3.8: $C_{18}H_{15}BrN_2O_2$, M = 371.23, monoclinic, a = 10.2210(9), b = 6.2580(10), c = 24.249(2) Å, β = 97.5310(10)°, U = 1537.7(3) Å^3, T = 100 K, space group $P2_1/n$ (no. 14), Z = 4, 16640 reflections measured, 4287 unique (R_{int} = 0.0430), 3919 > 4σ(F), R = 0.0437 (observed), wR_2 = 0.1172 (all data).

3.11: $C_{19}H_{18}N_2O_2$, M = 306.35, monoclinic, a = 9.882(2), b = 36.918(5), c = 8.620(4) Å, β = 99.990(11)°, U = 3097.1(16) Å^3, T = 100 K, space group $P2_1/c$ (no. 14), Z = 8, 29134 reflections measured, 7375 unique (R_{int} = 0.0682), 5659 > 4σ(F), R = 0.0744 (observed), wR_2 = 0.1474 (all data).

3.12: $C_{18}H_{11}F_5N_2O_2$, M = 382.29, monoclinic, a = 11.3420(14), b = 6.5280(11), c = 21.294(2) Å, β = 95.503(2)°, U = 1569.4(4) Å^3, T = 100 K, space group $P2_1/c$ (no. 14), Z = 4, 14095 reflections measured, 3609 unique (R_{int} = 0.0394), 3244 > 4σ(F), R = 0.0441 (observed), wR_2 = 0.1152 (all data).

3.14a: $C_{20}H_{18}N_2O_2$, M = 318.36, monoclinic, a = 11.0350(8), b = 6.9000(5), c = 11.373(2) Å, β = 115.012(4)°, U = 784.75(18) Å^3, T = 100 K, space group $P2_1$ (no. 4), Z = 2, 15435 reflections measured, 4274 unique (R_{int} = 0.0675), 3590 > 4σ(F), R = 0.0776 (observed), wR_2 = 0.2324 (all data).

3.14b: $C_{20}H_{18}N_2O_2$, M = 318.36, monoclinic, a = 5.238(2), b = 12.589(2), c = 11.597(3) Å, β = 91.334(15)°, U = 764.5(4) Å^3, T = 100 K, space group Pc (no. 7), Z = 2, 14663 reflections

measured, 4370 unique (R_{int} = 0.0429), 4261 > 4σ(F), R = 0.0378 (observed), wR_2 = 0.1021 (all data).

3.17: $C_{18}H_{14}BrN_3$, M = 352.23, monoclinic, a = 8.6369(3), b = 26.7510(8), c = 6.9978(2) Å, β = 106.7900(10)°, U = 1547.89(8) Å^3, T = 100 K, space group $P2_1/c$ (no. 14), Z = 4, 20006 reflections measured, 2738 unique (R_{int} = 0.0329), 2674 > 4σ(F), R = 0.0223 (observed), wR_2 = 0.0536 (all data).

3.18: $C_{21}H_{21}N_3$, M = 315.41, triclinic, a = 7.784(5), b = 10.507(3), c = 11.117(3) Å, α = 106.154(5), β = 96.466(8), γ = 97.82(2)°, U = 854.3(6) Å^3, T = 100 K, space group P–1 (no. 2), Z = 2, 7913 reflections measured, 3653 unique (R_{int} = 0.0353), 3039 > 4σ(F), R = 0.0458 (observed), wR_2 = 0.1180 (all data).

3.21: $C_{25}H_{20}N_2O_2$•0.568(CH_2Cl_2), M = 428.65, monoclinic, a = 12.2626(3), b = 7.2788(2), c = 12.3394(3) Å, β = 104.510(2)°, U = 1066.25(5) Å^3, T = 100 K, space group $P2_1$ (no. 4), Z = 2, 15091 reflections measured, 3680 unique (R_{int} = 0.0580), 3252 > 4σ(F), R = 0.0383 (observed), wR_2 = 0.0882 (all data).

3.22: $C_{25}H_{19}FN_2O_2$, M = 398.42, monoclinic, a = 12.2430(11), b = 7.2460(15), c = 21.8670(19) Å, β = 105.022(2)°, U = 1873.6(5) Å^3, T = 100 K, space group $P2_1/n$ (no. 14), Z = 4, 20089 reflections measured, 5175 unique (R_{int} = 0.0719), 4101 > 4σ(F), R = 0.0624 (observed), wR_2 = 0.1650 (all data).

3.23: $C_{26}H_{22}N_2O_3$, M = 410.45, monoclinic, a = 12.3520(14), b = 7.3610(17), c = 22.1220(10) Å, β = 98.421(8)°, U = 1989.7(5) Å^3, T = 100 K, space group $P2_1/n$ (no. 14), Z = 4, 21818 reflections measured, 5774 unique (R_{int} = 0.0644), 4794 > 4σ(F), R = 0.0518 (observed), wR_2 = 0.1414 (all data).

3.25: $C_{23}H_{20}N_2O$, M = 340.41, monoclinic, a = 12.8640(10), b = 9.8120(10), c = 13.6520(9) Å, β = 92.938(2)°, U = 1720.9(2) Å^3, T = 100 K, space group $P2_1/n$ (no. 14), Z = 4, 32776 reflections measured, 4808 unique (R_{int} = 0.0570), 4374 > 4σ(F), R = 0.0514 (observed), wR_2 = 0.1359 (all data).

6.1.4 Photophysical measurements

Absorption spectra were recorded at room temperature on a Perkin Elmer Lambda 35 UV/Vis spectrometer in Professor Max Massi's laboratory at Curtin University. Uncorrected steady-state emission and excitation spectra were recorded using an Edinburgh FLSP980-stm

spectrometer equipped with a 450 W xenon arc lamp, double excitation and emission monochromators and a Peltier-cooled Hamamatsu R928P photomultiplier (185–850 nm). Emission and excitation spectra were corrected for source intensity (lamp and grating) and emission spectral response (detector and grating) by a calibration curve supplied with the instrument. Overall quantum yields in solution were determined by the optically dilute method,[4] at the excitation wavelength obtained from the absorption spectra on a wavelength scale [nm] and compared to the reference emitter by using the following equation:

$$\Phi_s = \Phi_r \left[\frac{I_s}{I_r}\right]\left[\frac{A_r}{A_s}\right]\left[\frac{n_s^2}{n_r^2}\right]$$

where I is the integrated intensity of the luminescence, A is the absorbance at the excitation wavelength, n is the refractive index of the solvent, and Φ is the quantum yield. The subscripts r and s refer to the reference and the sample, respectively. Absorption and emission spectra were measured in 10^{-5} M CH_2Cl_2 solutions under the same experimental conditions as the standard; air-equilibrated water solution of $[Ru(bpy)_3]Cl_2$, where bpy is 2,2′-bipyridine, (Φ_r = 2.8%)[5] Experimental uncertainties are estimated to be ±10% for quantum yields. Excited state decays (τ) were determined using the time-correlated single photon counting (TCSPC) technique and recorded on the same Edinburgh FLSP980-stm spectrometer using a microsecond flashlamp or a pulsed picosecond LED (EPLED 360, FWHM < 800 ps) as the excitation source, with repetition rates between 1 kHz and 1 MHz, and the above-mentioned R928P PMT as the detector. The goodness of fit was assessed by minimising the reduced χ^2 function and by visual inspection of the weighted residuals. Experimental uncertainties are estimated to be ±10%. To record the luminescence spectra and measure excited state decays at 77 K, the samples were placed in quartz tubes (2 mm diameter) and inserted in a special quartz Dewar filled with liquid nitrogen. All the solvents used in the preparation of the solutions for the photophysical investigations were of spectrometric grade.

6.1.5 Electrochemical measurements

Cyclic voltammetry was performed at room temperature using a Metrohm Autolab PGSTAT101 and data acquired with Metrohm Autolab, Nova 2.0 software. Experiments were performed in dry, degassed acetonitrile (0.25 mM for homoleptic copper(I) complexes, 1.0 mM for heteroleptic copper(I) complexes), NBu_4PF_6 (0.1 M) electrolyte, with a CH

Instruments glassy carbon working electrode, Pt wire counter electrode, and Ag wire quasi-reference electrode. Ferrocene was added as an internal standard (Fc^+/Fc at 0 V) to reference experiments.

6.2 General Procedures

6.2.1 General procedure 1

Ligands **2.23**–**2.27**, **2.29**–**2.30** and **2.32**–**2.33** were synthesised by modifying conditions previously reported by Sauvage and co-workers.[6] These reactions were unoptimised. A solution of Na_2CO_3 (18 equiv) in H_2O was added to a magnetically stirred solution of 2,9-dichloro-1,10-phenanthroline (**2.11**) (1 equiv) and the organoborane (4 equiv) in toluene maintained at ambient temperature under N_2. $[Pd(PPh_3)_4]$ (10%) was added and the ensuing mixture was heated at 95 °C. After 16 h, the mixture was cooled to ambient temperature, the phases separated, and the aqueous phase was extracted with CH_2Cl_2 (2 x 20 mL). The combined organic extracts were then dried (Na_2SO_4), filtered, and concentrated under reduced pressure. The ensuing residue was subjected to flash column chromatography on silica gel.

6.2.2 General procedure 2

Ligands **2.28** and **2.31** were synthesised by modifying conditions previously reported by Stille and co-workers.[7] These reactions were unoptimised. $[Pd(PPh_3)_4]$ (5%) was added to a magnetically stirred solution of the organostannane (4 equiv) and 2,9-dichloro-1,10-phenanthroline (**2.11**) (1 equiv) in toluene maintained at ambient temperature under N_2. The ensuing mixture was heated to 110 °C. After 20 h, the mixture was cooled to ambient temperature and concentrated under reduced pressure. The ensuing residue was subjected to flash column chromatography on silica gel.

6.2.3 General procedure 3

Compounds **2.1** and **2.35**–**2.43** were synthesised by modifying conditions previously reported by Reiser.[8] $[Cu(MeCN)_4]PF_6$ (1 equiv) and the phenanthroline ligand (2 equiv) were dissolved in CH_2Cl_2. The ensuing magnetically stirred dark purple solution was maintained

at ambient temperature under N_2. After 2 h, hexanes was added and the precipitated complex was collected by filtration.

6.2.4 General procedure 4

Compounds **2.6–2.7** and **2.48–2.49** were synthesised according to this procedure. $[Cu(MeCN)_4]PF_6$ (1 equiv) and the diphosphine ligand (1 equiv) were combined and dissolved in CH_2Cl_2 (100 mL), under an atmosphere of nitrogen and magneticcally stirred at ambient temperature. After 2 h, a CH_2Cl_2 solution (25 mL) containing the phenanthroline ligand (1 equiv) was added dropwise. Stirring was continued for an additional 1 h before the solution was concentrated under reduced pressure to give a pale yellow solid. Recrystallisation afforded the respective complexes.

6.2.5 General procedure 5

Compounds **3.6–3.23** were synthesised according to this procedure (0.35 mmol scale). $[Cu(dap)_2]Cl$ (15.5 mg, 17.5 μmol) was added to a solution of the olefin (0.35 mmol), the tertiary amine (0.70 mmol), and TFA (54 μL, 0.70 mmol) in DMF (6 mL) in a 20 mL vial (containing a magnetic stir bar) in air. The vial was then capped and irradiated with green LEDs (515 nm). The reaction mixture was stirred at ambient temperature for 24 h, then poured into a separatory funnel and toluene (20 mL) and brine (15 mL) were added. The separated aqueous phase was extracted with toluene (2 x 20 mL). The combined organic phases were dried ($MgSO_4$), filtered and concentrated under reduced pressure and the ensuing residue was subjected to flash chromatography on silica gel.

6.2.6 General procedure 6

Compounds **4.4** and **4.32–4.55** were prepared according to this procedure. In a nitrogen-filled glovebox, $[Cu(bcp)(XP)]PF_6$ (8.6 mg, 7.5 μmol) was added to a 20 mL screw top vial (PTFE tape lined thread) containing the perfluorinated substrate (500 μmol), tertiary amine (1.00 mmol), $Gd(OTf)_3$ (121 mg, 200 μmol), MeCN (3.85 mL), and a magnetic stir bar. The vial was then capped, the joint was wrapped with PARAFILM®, and removed from the glovebox and placed in a water bath (suspended with copper wire) maintained at 45 °C that was contained within a 18 W blue LED photoreactor (switched off) and magnetically stirred. The vial was

then irradiated (25% duty cycle at 100 kHz). After 24 h, the reaction mixture was analysed by ^{19}F NMR spectroscopy (after the addition of 1-bromo-4-fluorobenzene as an internal standard) or concentrated under reduced pressure and the ensuing residue was subjected to flash column chromatography on silica gel.

6.2.7 General procedure 7

Compounds **4.56–4.67** were prepared according to this procedure. In a nitrogen-filled glovebox, [Cu(bcp)(XP)]PF_6 (8.6 mg, 7.5 μmol) was added to a 20 mL screw-top vial (PTFE tape-lined thread) containing the perfluorinated substrate (500 μmol), *i*Pr_2NEt (**4a**) (129 mg, 1.00 mmol), MeCN (7.70 mL), and a magnetic stir bar. The vial was then capped, the joint was wrapped with PARAFILM®, and removed from the glovebox and placed in a water bath (suspended with copper wire) maintained at 45 °C that was contained within a 18 W blue LED photoreactor (switched off) and magnetically stirred. The vial was then irradiated (25% duty cycle at 100 kHz). After 24 h, the reaction mixture was analysed by ^{19}F NMR spectroscopy (after the addition of 1-bromo-4-fluorobenzene as an internal standard) or concentrated under reduced pressure and the ensuing residue was subjected to flash column chromatography on silica gel. Previously reported compounds **4.56–4.60** and **4.66–4.67** were not isolated. In these cases, reaction mixtures were analysed by ^{19}F NMR and EIMS.

6.3 Preparation of Compounds

9-(4-bromophenyl)-9*H*-carbazole

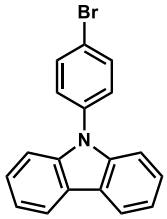

This compound was prepared according to a modified protocol described by Wang and co-workers.[9] Copper(I) iodide (0.570 mg, 3.00 mmol) was added to a DMPU solution (10 mL) containing carbazole (5.00 g, 30 mmol), 1,4-dibromobenzene (7.10 g, 30 mmol), potassium carbonate (8.30 g, 60 mmol) and 18-crown-6 (0.265 mg, 1.00 mmol) under an atmosphere of nitrogen. The resulting reaction mixture was heated to 180 °C. After 11 h, the mixture was cooled to ambient temperature. A 2 M solution of HCl was slowly added and the resulting

grey precipitate was collected by vacuum filtration and washed successively with NH_4OH (10 mL of a concentrated aqueous solution) and water (10 mL). The product was subjected to flash chromatography on silica gel (0–5% EtOAC/hexane) and then recrystallised from hot hexane to afford the previously reported compound as colourless blocks (2.10 g, 22% yield).[9]

^{1}H NMR (400 MHz, $CDCl_3$) δ 8.21 (d, *J* = 7.8 Hz, 2H), 7.78 (d, *J* = 8.6 Hz, 2H), 7.52–7.42 (complex m, 6H), 7.37 (t, *J* = 7.3 Hz, 2H) ppm.

^{13}C NMR (100 MHz, $CDCl_3$) δ 140.7, 136.9, 133.2, 128.8, 126.2, 123.6, 121.0, 120.5, 120.4, 109.7 ppm.

IR (NaCl) 1597, 1586, 1497, 1479, 1452, 1364, 1337, 1316, 1231, 1011, 827, 750, 725 cm^{-1}.

EIMS *m*/*z* 321 [M^+], 241, 121.

Bis(2,9-di(4-methoxyphenyl)-1,10-phenanthroline)copper(I) hexafluorophosphate (**2.1**)

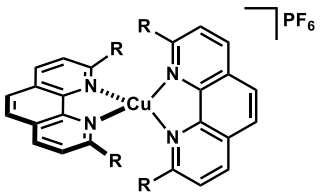

R = *p*-$OMeC_6H_4$

This compound was prepared according to General Procedure 3. Reaction with 2,9-di(4-methoxymethyl)phenyl-1,10-phenanthroline (296 mg, 0.754 mmol). Precipitation with hexanes afforded the previously reported complex as a dark red solid (348 mg, 93% yield).[6]

^{1}H NMR (400 MHz, $CDCl_3$) δ 8.57 (d, *J* = 8.1 Hz, 4H), 8.08 (s, 4H), 7.87 (d, *J* = 8.1 Hz, 4H), 7.41 (d, *J* = 8.6 Hz, 8H), 6.05 (d, *J* = 8.3 Hz, 8H), 3.49 (s, 12H) ppm.

^{13}C NMR (100 MHz, $CDCl_3$) δ 160.2, 156.4, 143.5, 137.4, 131.2, 129.2, 128.0, 126.3, 124.5, 112.6, 55.4 ppm.

IR (neat) 1604, 1582, 1489, 1251, 1162, 1024, 833, 729 cm^{-1}.

ESIMS *m*/*z* 847 [M^+], 423.

(2,9-Dimethyl-1,10-phenanthroline)(bis((2-diphenylphosphino)phenyl)) ether)copper(I) hexafluorophosphate (**2.6**)

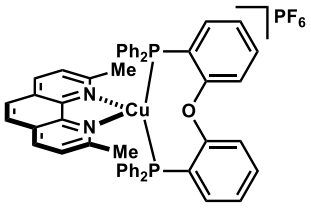

This compound was prepared according to General Procedure 4. Reaction with bis((2-diphenylphosphino)phenyl)) ether (500 mg, 0.928 mmol) and 2,9-dimethyl-1,10-phenanthroline. Recrystallisation by slow diffusion of diethyl ether into a saturated CH_2Cl_2 solution afforded the previously reported compound as pale yellow blocks (638 mg, 72% yield).[10]

^{1}H NMR (600 MHz, $CDCl_3$) δ 8.37 (d, *J* = 8.2 Hz, 2H), 7.86 (s, 2H), 7.60 (d, *J* = 8.2 Hz, 2H), 7.36 (td, *J* = 7.8, 1.7 Hz, 2H), 7.26 M, 2H), 7.21 (m, 6H), 7.05 (t, *J* = 7.4 Hz, 8H), 6.97 (m, 10H), 2.46 (6H) ppm.

^{13}C NMR (150 MHz, $CDCl_3$) δ 159.0, 158.4 (t, *J* = 5.8 Hz), 143.0, 138.0, 133.8, 132.8 (t, *J* = 7.9 Hz), 132.2, 131.7 (t, *J* = 16.6 Hz), 129.9, 128.5 (t, = 4.5 Hz), 127.7, 126.1, 125.6, 125.4 (t, *J* = 13.5 Hz), 125.3, 120.1, 27.1 ppm.

^{31}P NMR (161 MHz, $CDCl_3$) δ –144.2 (quin, *J* = 710 Hz) ppm.

(2,9-Dimethyl-1,10-phenanthroline)(4,5-Bis(diphenylphosphino)-9,9-dimethylxanthene)copper(I) hexafluorophosphate (**2.7**)

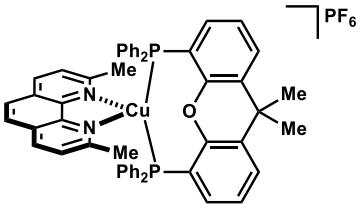

This compound was prepared according to General Procedure 4. Reaction with 4,5-bis(diphenylphosphino)-9,9-dimethylxanthene (300 mg, 0.518 mmol) and 2,9-dimethyl-1,10-phenanthroline (108 mg, 0.518 mmol). Recrystallisation by slow diffusion of diethyl ether into a saturated acetonitrile solution afforded the previously reported compound as pale yellow needles (402 mg, 78% yield).[11]

^{1}H NMR (600 MHz, $CDCl_3$) δ 8.34 (d, *J* = 8.2 Hz, 2H), 7.84 (s, 2H), 7.66 (d, *J* = 7.7 Hz, 2H), 7.55 (d, *J* = 8.1 Hz, 2H), 7.26–7.23 (m, 4H), 7.21(t, *J* = 7.7 Hz, 2H), 7.05–7.01 (complex m, 16H), 6.93–6.88 (m, 2H), 2.27 (s, 6H), 1.77 (s, 6H) ppm.

^{13}C NMR (150 MHz, $CDCl_3$) δ 158.5, 155.1 (t, *J* = 6.6 Hz), 142.9, 138.0, 133.9, 133.0 (t, *J* = 7.7 Hz), 131.4 (7, *J* = 16.1 Hz), 130.4, 130.0, 128.7 (t, *J* = 4.4 Hz), 127.8, 127.5, 126.1, 125.4, 125.3, 121.6 (t, *J* = 12.7 Hz), 36.2, 28.5, 27.2 ppm.

HRESIMS [M^+] Found 849.2212. $CuC_{53}H_{44}N_2OP_2$ requires 849.2219.

2,9-Dichloro-1,10-phenanthroline (**2.11**)

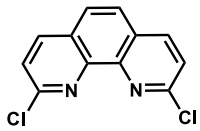

This compound was prepared according to a modified protocol described by Jiang and co-workers.[12] Phosphoryl chloride (2.64 g, 17.2 mmol) was added to a suspension of diazepino[1,2,3,4-*lmn*][1,10]phenanthroline-2,9-dione (435 mg, 1.72 mmol) and phosphorous pentachloride (718 mg, 3.45 mmol) in toluene (5 mL) and then placed under an atmosphere of nitrogen and the resulting reaction mixture was heated at 110 ˚C. After 16 h, the mixture was cooled to 0 ˚C and water (5 mL) slowly added. NH_4OH (concentrated aqueous solution) was slowly added until pH > 10. The phases were separated and the aqueous layer was extracted with CH_2Cl_2 (3 x 20 mL). The combined organic phases were dried (Na_2SO_4), filtered and concentrated under reduced pressure. The resulting residue was recrystallised by slow cooling of a hot methanol solution to yield the previously reported compound as pale yellow blocks (274 mg, 64% yield).[12]

^{1}H NMR (400 MHz, $CDCl_3$) δ 8.23 (d, *J* = 8.5 Hz, 2H), 7.85 (s, 2H), 7.67 (d, *J* = 8.3 Hz, 2H) ppm.

^{13}C NMR (100 MHz, $CDCl_3$) δ 152.1, 145.1, 138.9, 127.9, 126.4, 125.1 ppm.

IR (NaCl) 1597, 1580, 1553, 1479, 1348, 1138, 1119, 895, 851, 729 cm^{-1}.

EIMS *m*/*z* 248 [M^+], 213.

5*H*-[1,4]Diazepino[1,2,3,4-*lmn*][1,10]phenanthrolinediium diiodide (2.12)

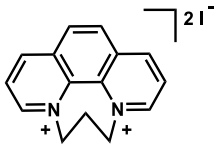

This compound was prepared according to a modified protocol described by Jiang and co-workers.[12] 1,3-Diiodopropane (20.49 g, 69.3 mmol) was added to a solution of 1,10-phenanthroline (5.00 g, 27.7 mmol) in toluene (50 mL). The resulting reaction mixture was then heated at reflux. After 24 h, the mixture was cooled to ambient temperature. Hexane (50 mL) was added to precipitate a yellow powder which was collected by filtration, washed with hexane (2 x 20 mL) and dried under reduced pressure to yield the previously reported compound (12.47 g, 95%).[12]

^{1}H NMR (400 MHz, D_2O) δ 9.70 (d, J = 5.8 Hz, 1H), 9.47 (dd, J_1 = 8.5 Hz, J_2 = 1.0 Hz, 1H), 8.62 (s, 1H), 8.58 (dd, J_1 = 8.5 Hz, J_2 = 6.0 Hz, 1H), 5.19 (t, J = 6.9 Hz, 2H), 3.46 (q, J = 7.0 Hz, 1 H) ppm.

^{13}C NMR (100 MHz, D_2O) δ 151.0, 147.4, 134.3, 130.4, 127.5, 60.6, 30.9 ppm.

IR (neat) 1591, 1546, 1453, 1370, 1341, 1216, 1148, 1002, 926, 858, 783, 694 cm^{-1}.

5*H*-[1,4]Diazepino[1,2,3,4-*lmn*][1,10]phenanthroline-2,9-dione (2.13)

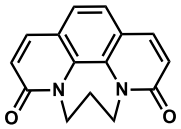

This compound was prepared according to a modified protocol described by Jiang and co-workers.[12] A *tert*-butanol solution (150 mL) containing 5*H*-[1,4]diazepino[1,2,3,4-*lmn*][1,10]phenanthrolinediium dichloride (12.47 g, 26.2 mmol) was sonicated at room temperature for 0.5 h before KO^{t}Bu (11.76 g, 104.8 mmol) was added. The resulting reaction mixture was heated at 40 °C. After 24 h, the mixture was cooled to ambient temperature and solvent was removed under reduced pressure. The resulting residue was dissolved in H_2O (150 mL) and extracted with CH_2Cl_2 (4 x 60 mL). The organic fractions were combined and dried (Na_2SO_4), filtered and solvent removed under reduced pressure. The ensuing residue was dissolved in CH_2Cl_2 and passed through a silica plug (5:95 MeOH/CH_2Cl_2). Solvent was

removed under reduced pressure to afford the previously reported compound (4.97 g, 75% yield) as a brown powder.[12]

^{1}H NMR (400 MHz, $CDCl_3$) δ 7.70 (d, *J* = 9.5 Hz, 1H), 7.34 (s, 1H), 6.77 (d, *J* = 9.5 Hz, 1H), 4.29 (t, *J* = 6.3 Hz, 2H), 2.43 (q, *J* = 6.5 Hz, 1H) ppm.

^{13}C NMR (100 MHz, $CDCl_3$) δ 162.8, 138.9, 132.3, 123.3, 123.0, 122.9, 45.8, 25.8 ppm.

IR (neat) 1638, 1589, 1495, 1440, 1152, 855, 837, 734, 686 cm^{-1}.

EIMS *m*/*z* 252 [M^+], 237, 223, 208, 197.

9-(4-(Tributylstannyl)phenyl)-9*H*-carbazole (2.15)

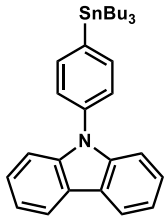

This compound was prepared according to a modified protocol described by Sun and co-workers.[13] *n*-Butyllithium (1.46 mL, 1.6 M in hexane, 2.33 mmol) was added dropwise to a THF solution (5 mL) containing 9-(4-bromophenyl)-9*H*-carbazole (500 mg, 1.55 mmol) at –78 °C under an atmosphere of N_2. The resulting mixture was stirred at –78 °C for 1 h then tributyltinchloride (505 mg, 1.55 mmol) was added dropwise. The resulting reaction mixture was then allowed to warm to room temperature over 4 h. Solvent was removed under reduced pressure and the resulting pale yellow residue was redissolved in CH_2Cl_2 (10 mL) and passed through a celite plug and solvent removed under reduced pressure. The ensuing residue was subjected to flash chromatography on silica gel using hexane as eluent to afford the previously reported compound (610 mg, 74% yield) as a colourless oil.[14]

^{1}H NMR (400 MHz, $CDCl_3$) δ 8.17 (d, *J* = 7.8 Hz, 2H), 7.77–7.65 (m, 2H), 7.54 (d, *J* = 7.9 Hz, 2H), 7.50 (complex m, 4H), 7.31 (t, *J* = 7.2 Hz, 2H), 1.70–1.60 (m, 6H), 1.21–1.14 (m, 6H), 0.97–0.94 (m, 9H) ppm.

^{13}C NMR (100 MHz, $CDCl_3$) δ 141.8, 141.0, 137.9, 137.6, 126.5, 126.0, 123.5, 120.4, 120.0, 110.0, 29.3, 27.6, 13.8, 9.9 ppm.

IR (NaCl) 1694, 1653, 1586, 1559, 1501, 1452, 1231, 748, 725 cm^{-1}.

Tributyl(4-fluorophenyl)stannane (**2.17**)

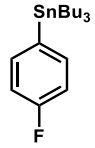

This compound was prepared according to a modified protocol described by Sun and co-workers.[13] *n*-Butyllithium (4.22 mL, 1.6 M in hexane, 6.76 mmol) was added dropwise to a THF solution (15 mL) containing 1-fluoro-4-iodobenzene (1.0 g, 4.51 mmol) at –78 °C under an atmosphere of N_2. The resulting solution was stirred at –78 °C for 1 h then tributyltinchloride (1.47 g, 4.51 mmol) was added dropwise. The resulting reaction mixture was then allowed to warm to room temperature over 4 h. Solvent was removed under reduced pressure and the resulting pale yellow residue was redissolved in hexane (10 mL) and passed through a celite plug and solvent removed under reduced pressure. The ensuing residue was subjected to flash chromatography on silica gel using hexane as eluent to afford the previously reported compound (809 mg, 35% yield) as a colourless oil.[15]

^{1}H NMR (400 MHz, $CDCl_3$) δ 7.43 (t, *J* = 7.2 Hz, 2H), 7.06 (t, *J* = 8.8 Hz, 2H), 1.60–1.50 (m, 6H), 1.35, (sextet, *J* = 7.3 Hz, 6H), 1.07 (t, *J* = 8.1 Hz, 6H), 0.91 (t, *J* = 7.2 Hz, 9H) ppm.

^{13}C NMR (100 MHz, $CDCl_3$) δ 138.0, 137.9, 115.3, 115.1, 29.2, 27.5, 13.8, 9.8 ppm.

IR (NaCl) 1653, 1582, 1491, 1229, 1163, 813, 505 cm^{-1}.

4-Bromo-2,6-di-*tert*-butyl-1-methoxybenzene (**2.19**)

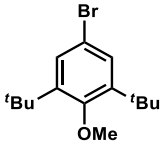

This compound was prepared according to a modified protocol described by Zhang and co-workers.[16] To a DMSO solution (10 mL) containing sodium hydride (202 mg, 8.41 mmol) (60% suspension in mineral oil) at 0 °C, stirred vigorously to avoid freezing DMSO, was added 4-bromo-2,6-di-*tert*-butylphenol (1.00 g, 3.51 mmol) slowly in portions. The reaction mixture was warmed to ambient temperature then iodomethane (1.99 g, 14.0 mmol) was added dropwise. The resulting reaction mixture was stirred at ambient temperature for 16 h then water (5 mL) and hexane (5 mL) were added. The layers were separated and the aqueous layer was extracted with hexane (3 x 10 mL) and the combined organic fractions were then

washed with water (4 x 5 mL), dried ($MgSO_4$), filtered and concentrated under reduced pressure to afford the previously reported compound (3.57 mmol, 100% yield) as a pale yellow oil.[16]

^{1}H NMR (400 MHz, $CDCl_3$) δ 7.35 (s, 2H), 3.70 (s, 3H), 1.43 (s, 18H) ppm.

^{13}C NMR (100 MHz, $CDCl_3$) δ 162.5, 143.0, 133.3, 83.5, 64.2, 35.7, 32.1, 24.9 ppm.

4-Methoxy-3,5-di-*tert*-butylphenylboronic acid pinacol ester (**2.20**)

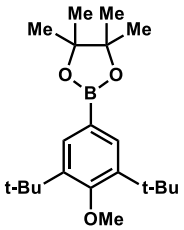

4-Bromo-2,6-di-*tert*-butyl-1-methoxybenzene (1.0 g, 3.34 mmol), bispinacolatodiboron (849 mg, 3.34 mmol), potassium acetate (394 mg, 4.01 mmol) and $[Pd(PCy_3)_2Cl_2]$ (49 mg, 0.0668 mmol) were taken up in DMF (10 mL) under an atmosphere of nitrogen. The resulting reaction mixture was heated at 150 °C with magnetic stirring. After 16 h, the mixture was cooled and diluted with H_2O (5 mL) and toluene (15 mL). The phases were separated, and the aqueous layer was extracted with toluene (2 x 15 mL). The combined organic fractions were dried ($MgSO_4$), filtered and concentrated under reduced pressure. The resulting residue was subjected to flash chromatography on silica gel (0–5% ethyl acetate/hexane) to afford the previously reported compound (909 mg, 79% yield) as a colourless solid.[17]

^{1}H NMR (400 MHz, $CDCl_3$) δ 7.73 (s, 2H), 3.03 (s, 3H), 1.47 (s, 18H) 1.35 (s, 12H) ppm.

^{13}C NMR (100 MHz, $CDCl_3$) δ 158.9, 146.2, 129.7, 116.5, 64.5, 36.1, 32.0 ppm.

2,9-Di(4-methoxyphenyl)-1,10-phenanthroline (**2.23**)

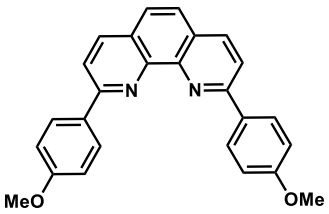

This compound was prepared according to General Procedure 1. Reaction with 4-methoxyphenylboronic acid (195 mg, 1.28 mmol). Subjected to flash column chromatography

on silica gel (0–5% MeOH/CH_2Cl_2) to provide the previously reported compound as a colourless amorphous solid (182 mg, 48% yield).[6]

^{1}H NMR (400 MHz, $CDCl_3$) δ 8.46 (d, *J* = 8.7 Hz, 4H), 8.31 (d, *J* = 8.3 Hz, 2H), 8.12 (d, *J* = 8.3 Hz, 2H), 7.78 (s, 2H), 7.14 (d, *J* = 8.7 Hz, 4H), 3.95 (s, 2H) ppm.

^{13}C NMR (100 MHz, $CDCl_3$): δ 161.19, 156.5, 145.7, 137.2, 132.0, 129.2, 127.7, 125.8, 119.7, 114.4, 55.6 ppm.

IR (NaCl) 1603, 1587, 1574, 1487, 1252, 1028, 835, 799, 729 cm^{-1}.

EIMS: *m*/*z* 392 [M^+] , 377, 192.

2,9-Di(4-methoxy-3,5-di-*tert*-butylphenyl)-1,10-phenanthroline (**2.24**)

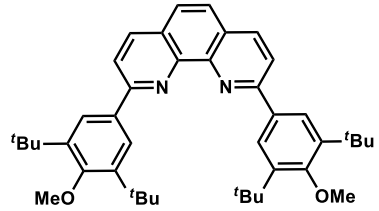

This compound was prepared according to General Procedure 1. Reaction with 4-methoxy-3,5-di-*tert*-butylphenylboronic acid pinacol ester (556 mg, 1.61 mmol). Subjected to flash column chromatography on silica gel (EtOAc/hexanes 0–30%) to provide the previously reported compound as a colourless amorphous solid (84 mg, 34% yield).[18]

^{1}H NMR (400 MHz, $CDCl_3$) δ 8.29 (d, *J* = 8.2 Hz, 2H), 8.13 (s, 4H), 8.03 (d, *J* = 8.6 Hz, 2H), 7.79 (s, 2H), 3.78 (s, 6H), 1.58 (s, 36H) ppm.

2,9-Di(4-methoxy-3,5-dimethylphenyl)-1,10-phenanthroline (**2.25**)

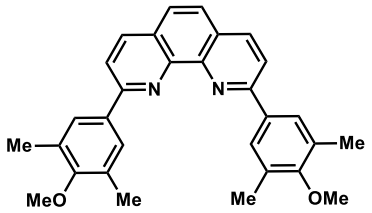

This compound was prepared according to General Procedure 1. Reaction with 4-methoxy-3,5-dimethylphenylboronic acid (410 mg, 3.21 mmol). Subjected to flash column chromatography (1% NEt_3/CH_2Cl_2) to provide the previously unreported compound as a colourless amorphous solid (99 mg, 38% yield).

^{1}H NMR (400 MHz, $CDCl_3$) δ 8.28 (d, *J* = 8.6 Hz, 2H), 8.22 (s, 4H), 8.12 (d, *J* = 8.12, 2H), 7.76 (s, 2H), 3.83 (s, 6H), 2.48 (s, 12H) ppm.

^{13}C NMR (100 MHz, $CDCl_3$) δ 158.7, 156.3, 145.8, 136.9, 134.6, 131.1, 128.3, 127.7, 125.8, 119.6, 59.9, 16.5 ppm.

IR (NaCl) 1479, 1321, 1229, 1190, 1165, 1074, 1013, 841, 634 cm^{-1}.

EIMS *m*/*z* 448 [M^+], 433, 418, 403, 388.

2,9-Di(3,4-dimethoxyphenyl)-1,10-phenanthroline (**2.26**).

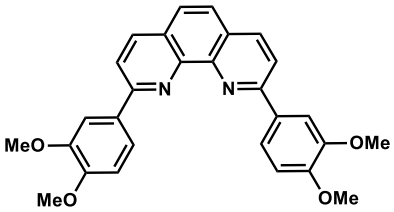

This compound was prepared according to General Procedure 1. Reaction with 3,4-dimethoxyphenylboronic acid (293 mg, 1.61 mmol). Subjected to flash column chromatography (20–50% EtOAc/hexanes, then 1% MeOH/CH_2Cl_2) to provide the previously unreported compound as a colourless amorphous solid (100 mg, 55% yield).

^{1}H NMR (400 MHz, $CDCl_3$) δ 8.27–8.23 (complex m, 4H), 8.07 (d, *J* = 8.4 Hz, 2H), 7.94 (d, *J* = 8.4 Hz, 2H), 7.74 (s, 2H), 7.01 (d, *J* = 8.4 Hz, 2H), 4.13 (s, 6H), 3.99 (s, 6H) ppm.

^{13}C NMR (100 MHz, $CDCl_3$) δ 156.3, 150.8, 149.5, 145.9, 136.9, 132.7, 127.7, 125.7, 120.6, 119.5, 111.5, 111.2, 56.4, 56.1 ppm.

IR (NaCl) 1593, 1520, 1489, 1456, 1414, 1273, 1221, 1173, 1157, 1138, 1024, 851, 795, 768, 735, cm^{-1}.

EIMS *m*/*z* 452 [M^+], 437, 421, 405, 377.

2,9-Di(2,4-dimethoxyphenyl)-1,10-phenanthroline (**2.27**)

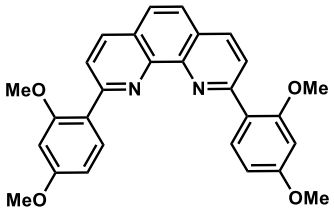

This compound was prepared according to General Procedure 1. Reaction with 2,4-dimethoxyphenylboronic acid (585 mg, 3.21 mmol). Subjected to flash column

chromatography (30–50% EtOAc/hexanes) to provide the previously unreported compound as a colourless amorphous solid (113 mg, 31% yield).

^{1}H NMR (400 MHz, $CDCl_3$) δ 8.41 (d, *J* = 8.5 Hz, 2H), 8.26 (d, *J* = 8.4 Hz, 2H), 8.20 (d, *J* = 8.4 Hz, 2H), 7.74 (s, 2H), 7.76 (dd, *J* = 8.5, 2.3 Hz 2H), 6.62 (d, *J* = 2.3 Hz 2H), 3.914 (s, 6H), 3.911 (s, 6H) ppm.

^{13}C NMR (100 MHz, $CDCl_3$) δ 161.8, 158.9, 155.8, 146.0, 135.4, 133.4, 127.1, 125.6, 124.4, 122.6, 105.6, 99.0, 55.8, 55.5 ppm.

ESIMS *m*/*z* 453 ($M + H^+$).

2,9-Di(4-fluorophenyl)-1,10-phenanthroline (**2.28**)

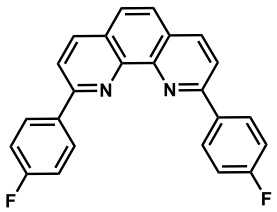

This compound was prepared according to General Procedure 2. Reaction with tributyl(4-fluorophenyl)stannane (1.64 g, 3.21 mmol). Subjected to flash chromatography on silica gel (0–20% EtOAc/hexanes) to afford the previously unreported compound (29 mg, 10% yield) as a colourless amorphous solid.

^{1}H NMR (400 MHz, $CDCl_3$) δ 8.46 (dd, *J* = 8.8, 5.5 Hz, 4H), 8.33 (d, *J* = 8.4 Hz, 2H), 8.11 (d, *J* = 8.4 Hz, 2H), 7.81 (s, 2H), 7.30 (m, 4H) ppm.

^{13}C NMR (150 MHz, $CDCl_3$) δ 164.8, 163.1, 155.8, 146.0, 137.1, 129.5 (d, *J* = 8.4 Hz), 127.7, 126.0, 119.8, 115.8 (d, *J* = 21.7 Hz) ppm.

^{19}F NMR (565 MHz, $CDCl_3$) δ –112.3 (s, 2F) ppm.

IR (NaCl) 1487, 1221, 1157, 932, 907, 838, 722 cm^{-1}.

ESIMS *m*/*z* 369 ($M + H^+$).

2,9-Di(4-(trifluoromethyl)phenyl)-1,10-phenanthroline (**2.29**)

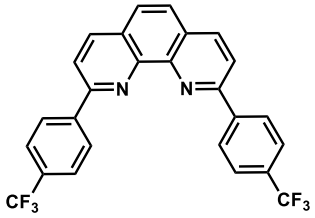

This compound was prepared according to General Procedure 1. Reaction with 4-(trifluoromethyl)phenylboronic acid (610 mg, 3.21 mmol). Subjected to flash column chromatography on silica gel (0–20% EtOAc/hexanes) to provide the previously unreported compound as a colourless amorphous solid (182 mg, 48% yield).

^{1}H NMR (400 MHz, $CDCl_3$) δ 8.57 (d, *J* = 8.5 Hz, 4H), 8.39 (d, *J* = 8.5 Hz, 2H), 8.20 (d, *J* = 8.5 Hz, 2H), 7.90–7.86 (complex m, 6H) ppm.

^{13}C NMR (100 MHz, $CDCl_3$) δ 155.6, 146.3, 142.8, 137.5, 131.3 (q, *J* = 32.4 Hz), 128.6, 128.1, 126.7, 126.0 (q, *J* = 3.8 Hz), 124.4 (q, *J* = 272 Hz), 120.5 ppm.

IR (NaCl) 1327, 1163, 1113, 1087, 1013, 847, 797, 733, 694 cm^{-1}.

EIMS *m*/*z* 468 [M^+], 399.

2,9-Bis(9,9-dimethyl-9*H*-fluoren-2-yl)-1,10-phenanthroline (**2.30**)

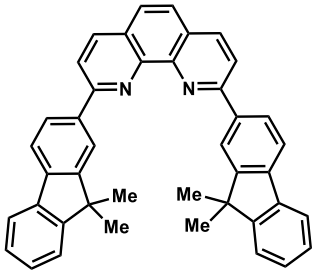

This compound was prepared according to General Procedure 1. Reaction with (9,9-dimethyl-9*H*-fluoren-2-yl)boronic acid (500 mg, 2.10 mmol). Subjected to flash column chromatography on silica gel (0–10% EtOAc/hexanes) to afford the previously unreported compound (52 mg, 17% yield) as a pale yellow amorphous solid.

^{1}H NMR (400 MHz, $CDCl_3$) δ 8.71 (d, *J* = 1.2 Hz, 2H), 8.43 (dd, *J* = 7.9, 1.6 Hz, 2H), 8.35 (d, *J* = 8.4 Hz, 2H), 8.24 (d, *J* = 8.4 Hz, 2H), 7.95 (d, *J* = 8.0 Hz, 2H), 7.88–7.85 (m 2H), 7.82 (s, 2H), 7.57–7.54 (m, 2H), 7.46–7.39 (complex m, 4H), 1.72 (s, 12H) ppm.

^{13}C NMR (100 MHz, $CDCl_3$) δ 157.3, 154.6, 154.4, 146.1, 140.8, 138.9, 138.8, 137.1, 128.0, 127.8, 127.2, 127.1, 126.1, 122.8, 122.2, 120.6, 120.5, 120.4, 47.3, 27.5 ppm.

IR (NaCl) 1684, 1653, 1584, 1559, 1504, 1447, 1364, 1283, 1225, 1211, 1099, 854, 833, 820, 781, 760, 739 cm^{-1}.

ESIMS *m*/*z* 565 ($M + H^+$).

2,9-Bis(4-(9*H*-carbazol-9-yl)phenyl)-1,10-phenanthroline (**2.31**)

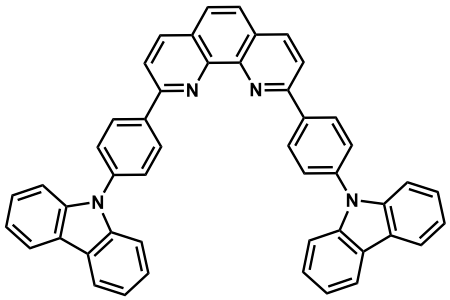

This compound was prepared according to General Procedure 2. Reaction with 9-(4-(tributylstannyl)phenyl)-9*H*-carbazole (610 mg, 1.15 mmol). Subjected to flash column chromatography on silica gel (hexane then CH_2Cl_2) to afford the previously unreported compound (101 mg, 53% yield) as a pale yellow amorphous solid.

^1H NMR (400 MHz, $CDCl_3$) δ 8.72 (d, *J* = 8.4 Hz, 4H), 8.45 (d, *J* = 8.4 Hz, 2H), 8.29 (d, *J* = 8.4 Hz, 2H), 8.18 (d, *J* = 7.8 Hz, 4H), 7.91 (s, 2H), 7.84 (d, *J* = 8.4 Hz, 4H), 7.57 (d, *J* = 8.2 Hz, 4H), 7.47 (t, *J* = 7.6 Hz, 4H), 7.33 (t, *J* = 7.4 Hz, 4H) ppm.

^{13}C NMR (100 MHz, $CDCl_3$) δ 156.3, 146.5, 140.9, 139.0, 138.8, 137.4, 129.4, 128.3, 127.5, 126.4, 126.2, 123.7, 120.5, 120.3, 120.2, 110.1 ppm.

IR (NaCl) 1684, 1653, 1559, 1489, 1451, 1362, 750, 723 cm^{-1}.

ESIMS *m*/*z* 663 ($M + H^+$).

2,9-di(furan-3-yl)-1,10-phenanthroline (**2.32**)

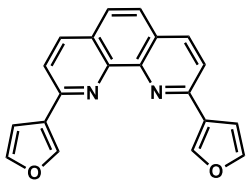

This compound was prepared according to General Procedure 1. Reaction with 3-furanylboronic acid (360 mg, 3.21 mmol). Subjected to flash column chromatography on silica gel (20–60% EtOAc/hexanes) followed by recrystallisation from hot toluene to afford the previously unreported compound (141 mg, 56% yield) as colourless needles.

^{1}H NMR (400 MHz, $CDCl_3$) δ 8.34 (s, 2H), 8.16 (d, *J* = 8.4 Hz, 2H), 7.77 (d, *J* = 8.4 Hz, 2H), 7.67 (s, 2H), 7.59 (t, *J* = 1.7 Hz, 2H), 7.30 (dd, *J* = 1.7, 0.6 Hz, 2H) ppm.

IR (NaCl) 1344, 1294, 1277, 1171, 1117, 1069, 847 cm^{-1}.

EIMS *m*/*z* 604 [M^+], 564, 535, 282.

2,9-Bis(2,4-bis(trifluoromethyl)phenyl)-1,10-phenanthroline (**2.33**)

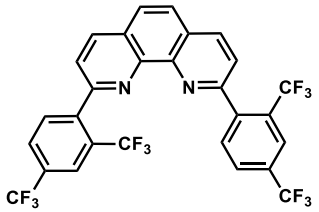

This compound was prepared according to General Procedure 1. Reaction with 2,4-bis(trifluoromethyl)phenylboronic acid (828 mg, 3.21 mmol). Subjected to flash column chromatography on silica gel (0–30% EtOAc/hexanes) to afford the previously unreported compound (141 mg, 56% yield) as a colourless amorphous solid.

^{1}H NMR (400 MHz, $CDCl_3$) δ 8.42 (d, *J* = 8.3 Hz, 2H), 8.08 (s, 2H), 8.04-7.93 (complex m, 6H), 7.90 (d, *J* = 8.1 Hz, 2H) ppm.

^{13}C NMR (100 MHz, $CDCl_3$) δ 151.7, 145.7, 143.9, 142.4, 136.7, 127.8, 127.7, 125.7, 120.1, 109.4 ppm.

ESIMS *m*/*z* 312 [M^+], 284, 255.

Bis(2,9-di(4-methoxy-3,5-di-*tert*-butylphenyl)-1,10-phenanthroline)copper(I) hexafluorophosphate (**2.35**)

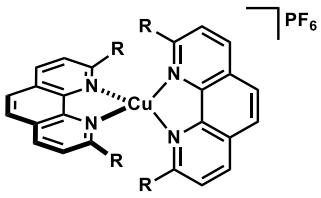

R = *p*-OMe-*m*,*m*-^{t}Bu$_2$C$_6$H$_2$

This compound was prepared according to General Procedure 3, however, this reaction required 7 days to proceed to completion. Reaction with 2,9-di(4-methoxy-3,5-di-*tert*-butylphenyl)-1,10-phenanthroline (115 mg, 0.186 mmol). Precipitation with hexanes afforded the previously reported complex as a dark red solid (105 mg, 78% yield).[19]

^{1}H NMR (600 MHz, $CDCl_3$) δ 8.43 (d, *J* = 8.4 Hz, 4H), 8.04 (s, 4H), 7.85 (d, *J* = 8.3 Hz, 4H), 7.49 (s, 8H), 3.23 (s, 12H), 0.93 (s, 72H) ppm.

^{13}C NMR (150 MHz, $CDCl_3$) δ 161.6, 157.2, 143.8, 143.7, 136.4, 133.2, 128.5, 126.7, 125.84, 125.78, 64.6, 35.5, 31.3 ppm.

HRESIMS [M^+] Found 1295.7327. $C_{84}H_{104}CuN_4O_4$ requires 1295.7348.

Bis(2,9-di(4-methoxy-3,5-dimethylphenyl)-1,10-phenanthroline)copper(I) hexafluorophosphate (**2.36**)

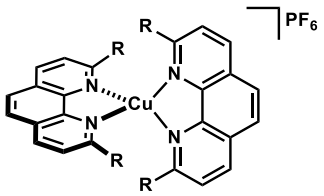

R = *p*-OMe-*m*,*m*-$(Me)_2C_6H_2$

This compound was prepared according to General Procedure 3. Reaction with 2,9-di(4-methoxy-3,5-dimethylphenyl)-1,10-phenanthroline (99 mg, 0.219 mmol). Precipitation with hexanes afforded the previously unreported complex as a dark red solid (89 mg, 73% yield).

^{1}H NMR (400 MHz, DMSO-d_6) δ 8.75 (d, *J* = 8.2 Hz, 4H), 8.28 (s, 4H), 8.06 (d, *J* = 8.2 Hz, 4H), 7.21 (s, 8H), 3.28 (s, 12H), 1.40 (s, 24H) ppm.

^{13}C NMR (100 MHz, DMSO-d_6) δ 157.0, 155.6, 142.7, 137.4, 133.8, 128.9, 128.7, 127.8, 126.4, 124.4, 58.9, 14.9 ppm.

HRESIMS [M^+] Found 959.3583. $C_{60}H_{56}CuN_4O_4$ requires 959.3592.

Bis(2,9-di(3,4-dimethoxyphenyl)-1,10-phenanthroline)copper(I) hexafluorophosphate (**2.37**)

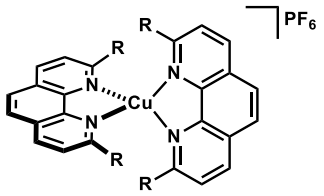

R = *m*,*p*-$(OMe)_2C_6H_3$

This compound was prepared according to General Procedure 3. Reaction with 2,9-di(3,4-dimethoxyphenyl)-1,10-phenanthroline (100 mg, 0.222 mmol. Precipitation with hexanes afforded the previously unreported complex as a dark red solid (117 mg, 95% yield).

^{1}H NMR (400 MHz, DMSO-d_6) δ 8.70 (d, J = 8.0 Hz, 4H), 8.20-8.05 (complex m, 8H), 7.12 (d, J = 7.5 Hz, 4H), 6.96 (s, 4H), 6.03 (d, J = 7.9 Hz, 4H), 3.46 (s, 12H), 3.23 (s, 12H) ppm.

^{13}C NMR (150 MHz, DMSO-d_6) δ 155.7, 149.2, 147.4, 142.9, 137.2, 131.0, 127.5, 125.8, 124.5, 120.2, 110.6, 109.8, 55.1, 54.5 ppm.

ESIMS m/z 967 [M + H$^+$].

HRESIMS [M$^+$] Found 967.2738. $C_{56}H_{48}CuN_4O_8$ requires 967.2763.

Bis(2,9-di(2,4-dimethoxyphenyl)-1,10-phenanthroline)copper(I) hexafluorophosphate (2.38)

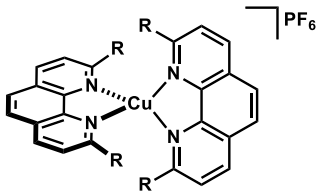

R = *o*,*p*-(OMe)$_2$C$_6$H$_3$

This compound was prepared according to General Procedure 3. Reaction with 2,9-di(2,4-dimethoxyphenyl)-1,10-phenanthroline (113 mg, 0.250 mmol). Precipitation with hexanes afforded the previously unreported complex as a dark red solid (133 mg, 95% yield).

^{1}H NMR (400 MHz, DMSO-d_6) δ 8.61 (d, J = 8.3 Hz, 4H), 8.09 (s, 4H), 7.91 (d, J = 8.3 Hz, 4H), 7.08 (d, J = 8.4 Hz, 4H), 5.99 (d, J = 2.2 Hz, 4H), 5.40 (dd, J = 8.4, 2.2 Hz, 4H), 3.46 (s, 12H), 3.44 (s, 12H) ppm.

^{13}C NMR (150 MHz, DMSO-d_6) δ 160.6, 156.7, 154.0, 142.7, 135.7, 129.8, 127.2, 127.0, 125.9, 120.4, 103.1, 96.8, 55.0, 54.7 ppm.

HRESIMS [M + H$^+$] Found 967.2763. $C_{56}H_{48}CuN_4O_8$ requires 967.2768.

Bis(2,9-di(4-fluorophenyl)-1,10-phenanthroline)copper(I) hexafluorophosphate (**2.39**)

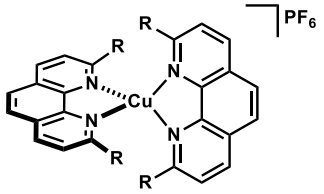

R = *p*-FC_6H_4

This compound was prepared according to General Procedure 3. Reaction with 2,9-di(4-fluorophenyl)-1,10-phenanthroline (26 mg, 0.071 mmol). Precipitation with hexanes afforded the previously unreported complex as a dark red solid (32 mg, 97% yield).

^{1}H NMR (400 MHz, CD_3CN) δ 8.65 (d, *J* = 8.4 Hz, 4H), 8.15 (s, 4H), 7.98 (d, *J* = 8.3 Hz, 4H), 7.51 (m, 8H), 6.34 (t, *J* = 8.7 Hz, 8H) ppm.

^{13}C NMR (150 MHz, DMSO-d_6) δ 161.7, 155.5, 143.2, 138.4, 138.4, 135.5 (d, *J* = 2.6 Hz), 130.3 (d, *J* = 8.6 Hz), 128.6, 126.9, 125.2, 114.4 (d, *J* = 21.8 Hz) ppm.

HRESIMS [M^+] Found 799.1522. $C_{48}H_{28}CuN_4F_4$ requires 799.1541.

Bis(2,9-di(4-(trifluoromethyl)phenyl)-1,10-phenanthroline)copper(I) hexafluorophosphate (**2.40**)

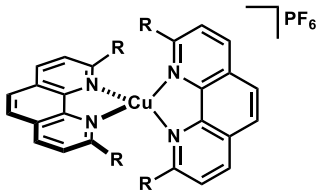

R = *p*-$CF_3C_6H_4$

This compound was prepared according to General Procedure 3. Reaction with 2,9-di(4-trifluoromethyl)phenyl-1,10-phenanthroline (182 mg, 0.389 mmol). Precipitation with hexanes afforded the previously unreported complex as a dark red solid (218 mg, 97% yield).

^{1}H NMR (400 MHz, DMSO-d_6) δ 8.86 (d, *J* = 8.3 Hz, 4H), 8.27 (s, 4H), 8.18 (d, *J* = 8.3 Hz, 4H), 7.66 (d, *J* = 8.0 Hz, 8H), 6.92 (d, *J* = 8.1 Hz, 8H) ppm.

^{13}C NMR (150 MHz, DMSO-d_6) δ 154.5, 142.6, 142.0, 138.3, 128.6, 128.5, 126.8, 124.7, 123.88, 123.86, 123.4 (q, *J* = 273.3 Hz) ppm.

ESIMS *m*/*z* 999 [M + H^+].

HRESIMS [M +H^+] Found 999.1390. $C_{52}H_{28}CuN_4F_{12}$ requires 999.1413.

Bis(2,9-dimethyl-1,10-phenanthroline)copper(I) hexafluorophosphate (**2.41**)

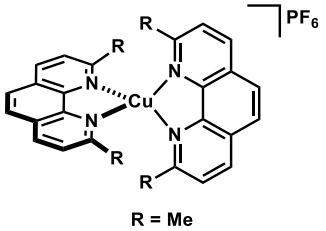

This compound was prepared according to General Procedure 3. Reaction with 2,9-dimethyl-1,10-phenanthroline (500 mg, 2.40 mmol). Precipitation with hexanes afforded the previously reported complex as a dark red solid (727 mg, 97% yield).[20]

^{1}H NMR (400 MHz, $CDCl_3$) δ 8.56 (d, *J* = 7.4 Hz, 2H), 8.07 (s, 2H), 7.81 (d, *J* = 7.4 Hz, 2H), 2.43 (s, 6H) ppm.

^{13}C NMR (100 MHz, $CDCl_3$) δ 157.8, 143.2, 137.6, 127.8, 126.3, 125.8, 26.0 ppm.

IR (NaCl) 1587, 1559, 1506, 1497, 1429, 1360, 1150, 868, 731, 552 cm^{-1}.

ESIMS *m*/*z* 479 [M + H^+], 209.

Bis(2,9-bis(9,9-dimethyl-9*H*-fluoren-2-yl)-1,10-phenanthroline)copper(I) hexafluorophosphate (**2.42**)

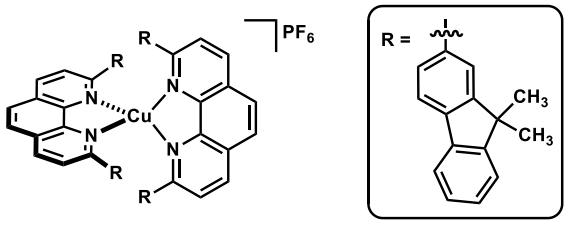

This compound was prepared according to General Procedure 3. Reaction with 2,9-bis(9,9-dimethyl-9*H*-fluoren-2-yl)-1,10-phenanthroline (52 mg, 0.0869 mmol). Precipitation with hexanes afforded the previously unreported complex as a dark red solid (49 mg, 95% yield).

^{1}H NMR (400 MHz, DMSO-d_6) δ 8.55 (d, *J* = 8.4 Hz, 4H), 8.07 (d, *J* = 8.4 Hz, 4H), 7.96 (s, 4H), 7.89 (s, 4H), 7.57–7.53 (m, 4H), 7.45(d, *J* = 7.9 Hz, 4H), 7.43–7.38 (m, 4H), 7.35–7.27 (complex m, 8H), 6.92 (d, *J* = 7.8 Hz, 4H), 0.93 (s, 24H) ppm.

^{13}C NMR (150 MHz, DMSO-d_6) δ 156.2, 153.3, 152.4, 143.3, 139.3, 137.6, 137.3, 137.2, 128.1, 127.9, 127.2, 127.1, 126.1, 125.3, 122.6, 121.7, 120.3, 118.7, 46.1, 26.1 ppm.

ESIMS *m*/*z* 1191 [M + H^+].

HRESIMS [M + H^+] Found 1191.4412. $C_{84}H_{64}CuN_4$ requires 1191.4422.

Bis(2,9-bis(4-(9*H*-carbazol-9-yl)phenyl)-1,10-phenanthroline)copper(I) hexafluorophosphate (**2.43**)

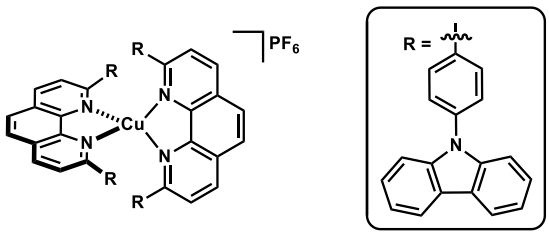

This compound was prepared according to General Procedure 3. Reaction with 2,9-bis(4-(9*H*-carbazol-9-yl)phenyl)-1,10-phenanthroline (100 mg, 0.150 mmol). Precipitation with hexanes afforded the previously unreported complex as a dark red solid (222 mg, 97% yield).

^{1}H NMR (400 MHz, DMSO-d_6) δ 8.89 (d, J = 8.3 Hz, 4H), 8.36 (d, J = 8.2 Hz, 4H), 8.27–8.19 (complex m, 12 H), 8.01 (d, J = 8.0 Hz, 8H), 7.51 (t, J = 7.5 Hz, 8H), 7.33 (t, J = 7.3 Hz, 8H), 7.04 (d, J = 7.9 Hz, 8H), 6.85 (d, J = 8.0 Hz, 8H) ppm.

^{13}C NMR (150 MHz, DMSO-d_6) δ 155.5, 142.8, 139.3, 138.3, 137.4, 137.2, 129.7, 128.3, 126.7, 126.2, 125.5, 125.0, 122.8, 120.6, 120.4, 109.4 ppm.

ESIMS m/z 1388 [M + H$^+$].

HRESIMS [M + H$^+$] Found 1388.4244. $C_{84}H_{64}CuN_4$ requires 1388.4270.

(2,9-Dimethyl-1,10-phenanthroline)(4,5-Bis(diphenylphosphino)-9,9-dimethylxanthene)copper(I) hexafluorophosphate (**2.48**)

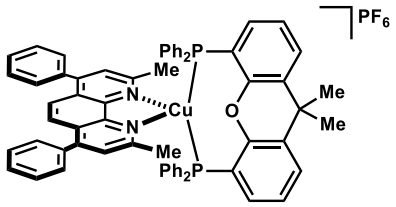

This compound was prepared according to General Procedure 4. Reaction with 4,5-bis(diphenylphosphino)-9,9-dimethylxanthene (300 mg, 0.518 mmol) and 2,9-dimethyl-1,10-phenanthroline (108 mg, 0.518 mmol). Recrystallisation by slow diffusion of diethyl ether into a saturated acetonitrile solution afforded the previously reported complex as orange blocks (482 mg, 81% yield).[11]

^{1}H NMR (600 MHz, $CDCl_3$) δ 7.80 (s, 2H), 7.69 (d, J = 7.8 Hz, 2H), 7.61–7.53 (complex m, 6H), 7.49 (d, J = 7.5 Hz, 4H), 7.47 (s, 2H), 7.32–7.27 (complex m, 4H), 7.24 (t, J = 7.8 Hz, 2H), 7.14–7.06 (complex m, 16H), 6.99 (m, 2H), 2.35 (s, 6H), 1.78 (s, 6H).

^{13}C NMR (150 MHz, $CDCl_3$) δ 158.0, 155.2 (t, *J* = 6.6 Hz), 150.3, 143.8, 136.5, 133.9, 133.1 (t, *J* = 7.7 Hz), 131.6 (t, *J* = 16.4 Hz), 130.5, 130.1, 129.6, 129.5, 129.2, 128.8 (t, *J* = 4.5 Hz), 127.7, 125.8, 125.6, 125.5, 123.7, 121.6 (t, *J* = 12.7 Hz), 36.3, 28.7, 27.5.

HRESIMS [M + H^+] Found 1001.2834. $CuC_{65}H_{52}N_2OP_2$ requires 1001.2845.

(2,9-Dimethyl-4,7-diphenyl-1,10-phenanthroline)(bis((2-diphenylphosphino)phenyl)) ether)copper(I) hexafluorophosphate (**2.49**)

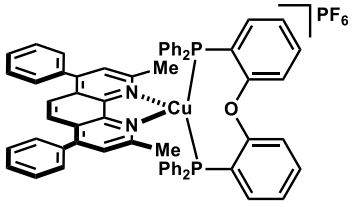

This compound was prepared according to General Procedure 4. Reaction with bis((2-diphenylphosphino)phenyl)) ether (500 mg, 0.928 mmol) and 2,9-dimethyl-4,7-diphenyl-1,10-phenanthroline (335 mg, 0.928 mmol). Recrystallisation by slow diffusion of diethyl ether into a saturated CH_2Cl_2 solution afforded the previously unreported complex as pale yellow blocks (750 mg, 73% yield).[21]

^{1}H NMR (400 MHz, $CDCl_3$) δ 7.85 (s, 2H), 7.59 (q, *J* = 7.9 Hz, 8H), 7.52 (m, 6H), 7.39 (t, *J* = 7.5 Hz, 2H), 7.24 (t, *J* = 7.0 Hz, 6H), 7.12 – 6.98 (complex m, 18H), 2.54 (s, 6H) ppm.

^{13}C NMR (150 MHz, $CDCl_3$) δ 158.5 (t, *J* = 6.3 Hz), 158.4, 150.3, 143.9, 136.4, 133.8, 132.9 (t, *J* = 7.7 Hz), 130.1, 129.9, 129.4 (t, *J* = 9.1 Hz), 129.2, 129.0, 128.7 (t, *J* = 4.4 Hz), 128.6 (t, *J* = 4.6 Hz), 128.2, 125.7, 125.3, 123.7, 120.2, 27.4 ppm.

^{31}P NMR (161 MHz, $CDCl_3$) δ -144.3 (quin, *J* = 712 Hz) ppm.

3-Chloro-1,1,1-trifluorononane (**2.58**)

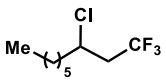

In a nitrogen-filled glovebox, CF_3SO_2Cl (102 mg, 600μmol) was added to a 4 mL screw top vial (PTFE tape-lined thread) containing 1-octene (33.9 mg, 300 μmol), K_2HPO_4 (105 mg, 600 μmol) and $[Cu(dap)_2]PF_6$ (3.0 mg, 3.0 μmol), MeCN (300 μL) and a magnetic stir bar. The vial was then capped, the joint was wrapped with PARAFILM®, and removed from the glovebox and placed in a water bath (suspended with copper wire) maintained at 45 °C that was contained within a 24 W blue LED photoreactor and magnetically stirred. The vial was then

irradiated. After 24 h, the reaction mixture was quenched by passing through a silica plug (contained within a Pasteur pipette; Et_2O elution) and concentrated under reduced pressure. The resulting residue was subjected to flash column chromatography (silica gel, 0–15% EtOAc/hexane elution) to afford the previously reported compound as a colourless oil (29.5 mg, 45% yield).[22]

^{1}H NMR (600 MHz, $CDCl_3$) δ 4.15 (m, 1H), 3.05 (m, 2H), 2.57 (m, 2H), 2.10 (m, 2H), 1.32 (m, 6H), 0.89 (t, J = 7.0 Hz, 3H) ppm.

^{19}F NMR (576 MHz, $CDCl_3$) δ –66.1 (t, J = 10 Hz, 3F) ppm.

^{13}C NMR (150 MHz, $CDCl_3$) δ 123.1, 69.9, 36.8 (q, J = 31 Hz), 31.3, 30.4, 28.8, 25.9, 22.5, 14.0 ppm.

3-Chloro-1,1,1-trifluorononane (**2.59**)

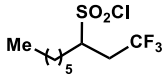

In a nitrogen-filled glovebox, CF_3SO_2Cl (102 mg, 600μmol) was added to a 4 mL screw top vial (PTFE tape-lined thread) containing 1-octene (33.9 mg, 300 μmol), K_2HPO_4 (105 mg, 600 μmol) and $[Cu(dap)_2]PF_6$ (3.0 mg, 3.0 μmol), MeCN (300 μL) and a magnetic stir bar. The vial was then capped, the joint was wrapped with PARAFILM®, and removed from the glovebox and placed in a water bath (suspended with copper wire) maintained at 45 °C that was contained within a 24 W blue LED photoreactor and magnetically stirred. The vial was then irradiated. After 24 h, the reaction mixture was quenched by passing through a silica plug (contained within a Pasteur pipette; Et_2O elution) and concentrated under reduced pressure. The resulting residue was subjected to flash column chromatography (silica gel, 0–15% EtOAc/hexane elution) to afford the previously reported compound as a colourless oil (6 mg, 7% yield).[22]

^{1}H NMR (600 MHz, $CDCl_3$) δ 3.75 (m, 1H), 3.03 (m, 2H), 2.49 (m, 2H), 1.93 (m, 2H), 1.31 (m, 6H), 0.89 (t, J = 7.0 Hz, 3H) ppm.

^{19}F NMR (576 MHz, $CDCl_3$) δ –66.0 (t, J = 11 Hz, 3F) ppm.

^{13}C NMR (150 MHz, $CDCl_3$) δ 124.1, 70.1, 59.1 (q, J = 31 Hz), 31.5, 30.2, 30.0, 29.3, 22.7, 14.1 ppm.

3-Chloro-1,1,1-trifluoro-4-methylhexane (**2.61**)

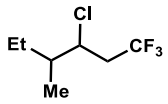

In a nitrogen-filled glovebox, CF_3SO_2Cl (102 mg, 600μmol) was added to a 4 mL screw top vial (PTFE tape-lined thread) containing 3-methylpent-1-ene (25.5 mg, 300 μmol), K_2HPO_4 (105 mg, 600 μmol) and $[Cu(dmp)_2]PF_6$ (3.0 mg, 3.0 μmol), MeCN (300 μL) and a magnetic stir bar. The vial was then capped, the joint was wrapped with PARAFILM®, and removed from the glovebox and placed in a water bath (suspended with copper wire) maintained at 45 °C that was contained within a 24 W blue LED photoreactor and magnetically stirred. The vial was then irradiated. After 24 h, the reaction mixture was quenched by passing through a silica plug (contained within a Pasteur pipette; Et_2O elution) and concentrated under reduced pressure. The resulting residue was subjected to flash column chromatography (silica gel, 0–15% EtOAc/hexane elution) to afford the previously unreported compound as a colourless oil (9 mg, 16% yield).

^1H NMR (600 MHz, $CDCl_3$) δ 4.13 (m, 1H), 2.05 (m, 2H), 1.94 (m, 1H), 1.54 (quin, *J* = 4.3 Hz, 2H), 0.93 (s, 3H), 0.89 (s, 3H) ppm.

^{19}F NMR (576 MHz, $CDCl_3$) δ –66.2 (t, *J* = 10 Hz, 3F) ppm.

^{13}C NMR (150 MHz, $CDCl_3$) δ 123.6, 65.2, 40.3 (q, *J* = 26 Hz), 40.0, 25.9, 19.3, 10.6 ppm.

HRESIMS [M + H^+] Found 185.0585. $C_7H_{12}ClF_3$ requires 185.0580.

1,1,1-Trifluoro-4-methylhexane-3-sulfonyl chloride (**2.62**)

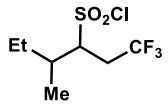

In a nitrogen-filled glovebox, CF_3SO_2Cl (102 mg, 600μmol) was added to a 4 mL screw top vial (PTFE tape-lined thread) containing 3-methylpent-1-ene (25.5 mg, 300 μmol), K_2HPO_4 (105 mg, 600 μmol) and $[Cu(dmp)_2]PF_6$ (3.0 mg, 3.0 μmol), MeCN (300 μL) and a magnetic stir bar. The vial was then capped, the joint was wrapped with PARAFILM®, and removed from the glovebox and placed in a water bath (suspended with copper wire) maintained at 45 °C that was contained within a 24 W blue LED photoreactor and magnetically stirred. The vial was then irradiated. After 24 h, the reaction mixture was quenched by passing through a silica plug (contained within a Pasteur pipette; Et_2O elution) and concentrated under

reduced pressure. The resulting residue was subjected to flash column chromatography (silica gel, 0–15% EtOAc/hexane elution) to afford the previously unreported compound as a colourless oil (13 mg, 21% yield).

^{1}H NMR (600 MHz, $CDCl_3$) δ 3.72 (m, 1H), 2.48 (m, 2H), 1.63 (m, 1H), 1.48 (m, 2H), 0.98 (t, *J* = 7.2 Hz, 3H), 0.90 (s, *J* = 7.3 Hz, 3H) ppm.

^{19}F NMR (576 MHz, $CDCl_3$) δ –66.4 (t, *J* = 14 Hz, 3F) ppm.

^{13}C NMR (150 MHz, $CDCl_3$) δ 125.8, 63.1, 39.8 (q, *J* = 31 Hz), 35.6, 27.8, 16.4, 11.8 ppm.

HRESIMS [M + H^+] Found 252.0192. $C_7H_{12}ClF_3O_2S$ requires 252.0199.

(3a*R*,9b*S*)-5-Methyl-2-phenyl-3a,4,5,9b-tetrahydro-1*H*-pyrrolo[3,4-*c*]quinoline-1,3(2*H*)dione (**3.7**)

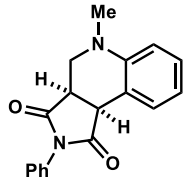

This compound was prepared according to General Procedure 5. Reaction between *N*,*N*-dimethylaniline and *N*-phenylmaleimide. The product was subjected to flash chromatography on silica gel (5–15% EtOAc/hexane elution; 0.5% NEt_3 was present in the eluent) and then recrystallised to provide the previously reported compound as a colourless solid (72 mg, 70% yield).[23]

^{1}H NMR (400 MHz, $CDCl_3$) δ 7.56 (d, *J* = 7.9 Hz, 1H), 7.45 (t, *J* = 7.9 Hz, 2H), 7.38 (t, *J* = 7.4 Hz, 1H), 7.31–7.25 (complex m, 3H), 6.94 (t, *J*= 7.9 Hz, 1H), 6.78 (d, *J* = 7.9 Hz, 1H), 4.17 (d, *J* = 9.7 Hz, 1H), 3.63 (dd, *J* = 11.5, 2.6 Hz, 1H), 3.54 (dt, *J* = 9.3, 3.0 Hz, 1H), 3.14 (dd, *J* = 11.5, 4.4 Hz, 1H), 2.87 (s, 3H) ppm.

^{13}C NMR (150 MHz, $CDCl_3$) δ 177.7, 175.8, 148.5, 132.1, 130.4, 129.1, 128.8, 128.6, 126.4, 119.8, 118.7, 112.7, 50.7, 43.6, 42.2, 39.6 ppm.

(3a*R*,9b*S*)-8-Bromo-5-methyl-2-phenyl-3a,4,5,9b-tetrahydro-1*H*-pyrrolo[3,4-*c*]quinoline1,3(2*H*)-dione (**3.8**)

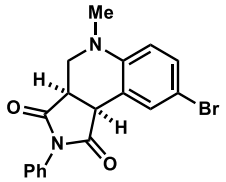

This compound was prepared according to General Procedure 5. Reaction between 4-bromo-*N*,*N*-dimethylaniline and *N*-phenylmaleimide. The product was subjected to flash chromatography on silica gel (5–15% EtOAc/hexane elution; 0.5% NEt_3 was present in the eluent) and then recrystallised to provide the previously reported compound as a colourless solid (55 mg, 42% yield).[23]

^{1}H NMR (400 MHz, $CDCl_3$) δ 7.66 (d, *J* = 2.1 Hz, 1H), 7.49–7.26 (complex m, 6H), 6.63 (d, *J* = 8.8 Hz, 1H), 4.11 (d, *J* = 9.6 Hz, 1H), 3.62 (dd, *J* = 11.7, 2.6 Hz, 1H) 3.54 (dt, *J* = 9.1, 2.6 Hz, 1H), 3.12 (dd, *J* = 11.6, 4.4 Hz, 1H), 2.84 (s, 3H) ppm.

^{13}C NMR (100 MHz, $CDCl_3$) δ 177.3, 175.2, 147.6, 132.9, 132.0, 131.6, 129.2, 128.8, 126.4, 120.5, 114.4, 111.9, 50.5, 43.4, 41.9, 39.6 ppm.

(3a*R*,9b*S*)-8-Isopropyl-5-methyl-2-phenyl-3a,4,5,9b-tetrahydro-1*H*-pyrrolo[3,4*c*]quinoline-1,3(2*H*)-dione (**3.9**)

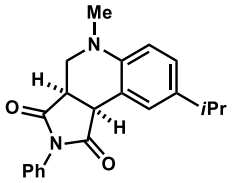

This compound was prepared according to General Procedure 5. Reaction between 4-isopropyl-*N*,*N*-dimethylaniline and *N*-phenylmaleimide. The product was subjected to flash chromatography on silica gel (5–15% EtOAc/hexane elution; 0.5% NEt_3 was present in the eluent) and then recrystallised to provide the previously unreported compound as a colourless solid (76 mg, 65% yield).

^{1}H NMR (400 MHz, $CDCl_3$) δ 7.50–7.28 (complex m, 6H), 7.15 (dd, *J* = 8.6, 2.0 Hz, 1H), 6.74 (d, *J* = 8.4 Hz, 1H), 4.16 (d, *J* = 9.4 Hz, 1H), 3.61 (dd, *J* = 11.8, 2.4 Hz, 1H), 3.53 (m, 1H), 3.11 (dd, *J* = 11.0, 4.3 Hz, 1H), 2.93 (q, *J* = 7.2 Hz, 1H), 2.85 (s, 3H), 1.30 (d, *J* = 7.0 Hz, 6H) ppm.

^{13}C NMR (100 MHz, $CDCl_3$) δ 177.8, 175.9, 146.5, 140.2, 134.2, 132.1, 129.0, 128.52, 128.49, 126.5, 126.4, 118.5, 112.6, 50.8, 43.5, 42.2, 39.6, 33.2, 24.3, 24.1 ppm.

IR (NaCl) 2958, 2867, 1780, 1709, 1511, 1499, 1456, 1386, 1370, 1318, 1194, 1175, 1155, 1001, 910, 816, 732, 690 cm^{-1}.

EIMS *m*/*z* 334 [M^+], 316, 301.

HREIMS [M^+] Found 334.1679. $C_{21}H_{22}N_2O_2$ requires 334.1681.

(3a*R*,9b*S*)-5-Methyl-8-(morpholine-4-carbonyl)-2-phenyl-3a,4,5,9b-tetrahydro-1*H*-pyrrolo[3,4-*c*]quinoline-1,3(2*H*)-dione (**3.10**)

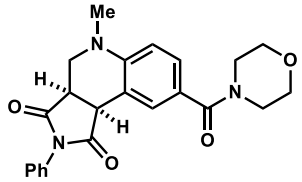

This compound was prepared according to General Procedure 5. Reaction between (4-(dimethylamino)phenyl)(morpholino)methanone and *N*-phenylmaleimide (performed on a 0.22 mmol scale). The product was subjected to flash chromatography on silica gel (5–50% EtOAc/hexane then 5% MeOH/ CH_2Cl_2 elution; 0.5% NEt_3 was present in the eluent) and then recrystallised to provide the previously unreported compound as a colourless solid (55 mg, 62% yield).

^{1}H NMR (400 MHz, $CDCl_3$) δ 7.61 (d, *J* = 1.7 Hz, 1H), 7.49–7.36 (complex m, 4H), 7.30–7.25 (complex m, 2H), 6.78 (d, *J* = 8.5 Hz, 1H), 4.18 (d, *J* = 9.7 Hz, 1H), 3.77–3.56 (complex m, 10H), 3.21 (dd, *J* = 11.8, 4.5 Hz, 1H), 2.91 (s, 3H) ppm.

^{13}C NMR (100 MHz, $CDCl_3$) δ 177.3, 175.5, 170.4, 149.8, 132.0, 130.0, 129.3, 129.0, 128.8, 126.4, 125.7, 117.9, 112.6, 67.1, 50.3, 43.2, 41.9, 39.5 ppm.

IR (NaCl) 2964, 2922, 2855, 1780, 1713, 1709, 1674, 1622, 1499, 1456, 1429, 1387, 1373, 1322, 1278, 1259, 1186, 1114, 1027, 850, 762, 733, 693, 626 cm^{-1}.

EIMS *m*/*z* 405 [M^+], 387, 319, 301, 247, 162, 121.

HREIMS [M^+] Found 405.1686. $C_{23}H_{23}N_3O_4$ requires 405.1689.

(3a*R*,9b*S*)-2-Benzyl-5-methyl-3a,4,5,9b-tetrahydro-1*H*-pyrrolo[3,4-*c*]quinoline-1,3(2*H*)dione (**3.11**)

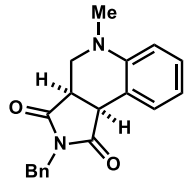

This compound was prepared according to General Procedure 5. Reaction between *N*,*N*-dimethylaniline and *N*-benzylmaleimide. The product was subjected to flash chromatography on silica gel (5–15% EtOAc/hexane elution; 0.5% NEt_3 was present in the eluent) and then recrystallised to provide the previously reported compound as a colourless solid (38 mg, 35% yield).[24]

^{1}H NMR (400 MHz, $CDCl_3$) δ 7.50 (d, *J* = 7.7 Hz, 1H), 7.34–7.22 (complex m, 6H), 6.93 (t, *J* = 7.7 Hz, 1H), 6.75 (d, *J* = 8.0 Hz, 1H), 4.67 (q, *J* = 14.2 Hz, 2H), 4.01 (d, *J* = 9.4 Hz, 1H), 3.52 (dd, *J* = 11.4, 2.7 Hz, 1H), 3.38 (dq, *J* = 9.2, 2.9 Hz, 1H), 3.08 (dd, *J* = 11.4, 4.5 Hz, 1H), 2.83 (s, 3H) ppm.

^{13}C NMR (150 MHz, $CDCl_3$) δ 178.4, 176.4, 148.3, 135.7, 130.3, 128.72, 128.69, 128.4, 127.9, 120.0, 119.0, 112.7, 50.8, 43.6, 42.9, 42.1, 39.5 ppm.

(3a*R*,9b*S*)-5-Methyl-2-(perfluorophenyl)-3a,4,5,9b-tetrahydro-1*H*-pyrrolo[3,4-*c*]quinoline-1,3(2*H*)-dione (**3.12**)

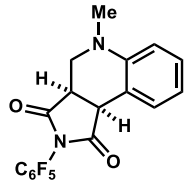

This compound was prepared according to General Procedure 5. Reaction between *N*,*N*-dimethylaniline and *N*-1-(perfluorophenyl)-1*H*-pyrrole-2,5-dione. The product was subjected to flash chromatography on silica gel (0–10% EtOAc/hexane elution; 0.5% NEt_3 was present in the eluent) to provide the previously unreported compound as a colourless solid (63 mg, 47% yield).

^{1}H NMR (400 MHz, $CDCl_3$) δ 7.50 (d, *J* = 7.5 Hz, 1H), 7.28 (t, *J* = 7.4 Hz, 1H), 6.95 (t, *J* = 7.4 Hz, 1H), 6.80 (d, *J* = 8.2 Hz, 1H), 4.29 (d, *J* = 9.41 Hz, 1H), 3.68 (m, 1H), 3.58 (dd, *J* = 11.6, 3.0 Hz, 1H), 3.17 (dd, *J* = 11.6, 4.5 Hz, 1H), 2.89 (s, 3H) ppm.

^{13}C NMR (100 MHz, $CDCl_3$) δ 175.6, 173.8, 148.6, 143.5 (d, J = 257 Hz), 142.2 (d, J = 257 Hz), 138.0 (d, J = 252 Hz), 130.3, 129.2, 120.0, 117.9, 112.9, 107.4, 51.0, 44.4, 42.8, 39.5 ppm.

^{19}F NMR (565 MHz, $CDCl_3$) δ –141.9 (dt, *J* = 22.3, 5.8 Hz, 1F), –142.9 (dt, *J* = 22.3, 6.0 Hz ,1F), –151.1 (t, *J* = 21.2 Hz, 1F), –160.9 (tt, *J* = 21.7, 6.0 Hz, 2F).

IR (NaCl) 1732, 1601, 1524, 1499, 1360, 1300, 1173, 1138, 988, 810, 758 cm^{-1}.

EIMS *m*/*z* 382 [M$^+$].

HREIMS [M$^+$] Found 382.0740. $C_{18}H_{11}F_5N_2O_2$ requires 382.0741.

5-Methyl-2-((*R*)-1-phenylethyl)-3a,4,5,9b-tetrahydro-1*H*-pyrrolo[3,4-*c*]quinoline-1,3(2*H*)-dione (**3.13**)

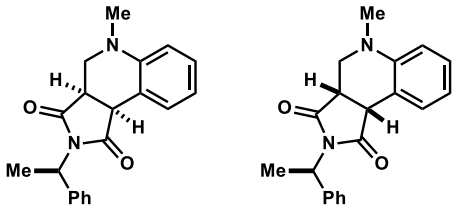

These compounds were prepared according to General Procedure 5. Reaction between *N*,*N*-dimethylaniline and (*R*)-(+)-*N*-(1-phenylethyl)maleimide. The product was subjected to flash chromatography on silica gel (5–15% EtOAc/hexane elution; 0.5% NEt_3 was present in the eluent) to provide the previously unreported compound as a colourless oil and as a 1:1 mixture of diastereoisomers (as judged by ^{1}H NMR analysis of the crude reaction mixture) (50 mg, 45% yield).

^{1}H NMR (400 MHz, $CDCl_3$) δ 7.49–7.20 (complex m, 7H), 6.91 (q, *J* = 7.8 Hz, 1H), 6.74 (dd, *J* = 8.3, 1.5 Hz, 1H), 5.42 (sextet, *J* = 7.2 Hz, 1H), 3.94 (t, *J* = 9.8 Hz, 1H), 3.46 (td *J* = 9.8, 2.8 Hz, 1H), 3.32 (m, 1H), 3.06 (quintet, *J* = 5.8 Hz, 1H), 2.82 (d, *J* = 13.7 Hz, 3H), 1.78 (dd, *J* = 16.8, 7.3 Hz, 3H) ppm.

^{13}C NMR (100 MHz, $CDCl_3$) δ 178.6, 178.5, 176.7, 176.5, 162.5, 148.5, 139.5, 130.33, 130.31, 129.7, 128.62, 128.60, 128.44, 128.40, 127.6, 127.2, 127.1, 126.5, 122.5, 119.8, 119.7, 119.3, 119.0, 112.6, 112.5, 51.1, 51.0, 50.63, 50.58, 43.37, 43.34, 42.04, 41.96, 39.5, 39.4, 29.8, 16.82, 16.77 ppm.

IR (NaCl) 2924, 1774, 1703, 1695, 1601, 1498, 1451, 1394, 1360, 1316, 1222, 1193, 910, 754, 731, 698 cm^{-1}.

EIMS *m*/*z* 320 [M$^+$], 302, 287, 215, 144.

HREIMS [M$^+$] Found 320.1528. $C_{20}H_{20}N_2O_2$ requires 320.1525.

(3a*R*,3b*R*,11b*S*)-2-Phenyl-3a,3b,4,5,6,11b-hexahydro-1*H*-dipyrrolo[1,2-*a*:3',4'-*c*]quinoline-1,3(2*H*)-dione (**3.14a**) &
(3a*R*,3b*S*,11b*S*)-2-Phenyl-3a,3b,4,5,6,11b-hexahydro-1*H*-dipyrrolo[1,2-a:3',4'-*c*]quinoline-1,3(2*H*)-dione (**3.14b**)

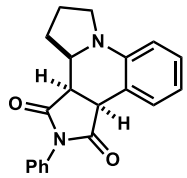

3.14a

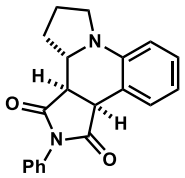

3.14b

These compounds were prepared according to General Procedure 5. Reaction between *N*-phenylpyrrolidine and *N*-phenylmaleimide. The product was subjected to flash chromatography on silica gel (5–15% EtOAc/hexane elution; 0.5% NEt_3 was present in the eluent) and then recrystallised to provide the previously reported compounds as a colourless solid as a 1:1 mixture of diastereoisomers (as judged by ^{1}H NMR analysis of the crude reaction mixture) (40 mg, 36% yield). These diastereoisomers were partially separable by chromatography under the conditions stated above.[25]

3.14a: ^{1}H NMR (400 MHz, $CDCl_3$) δ 7.56 (d, *J* = 7.7 Hz, 1H), 7.46–7.40 (complex m, 2H), 7.36 (m, 1H), 7.27–7.20 (complex m, 3H), 6.89 (t, *J* = 7.6 Hz, 1H), 6.66 (d, *J* = 8.0 Hz, 1H), 4.24 (d, *J* = 9.1 Hz, 1H), 3.67 (dd, *J* = 9.1, 3.8 Hz, 1H), 3.51 (sextet, *J* = 3.6 Hz, 1H), 3.31 (sextet, *J* = 3.9 Hz, 1H), 3.03–2.92 (complex m, 2H), 2.20–2.07 (complex m, 2H), 2.03–1.94 (m, 1H) ppm.

^{13}C NMR (150 MHz, $CDCl_3$) δ 176.2, 175.7, 147.9, 132.1, 130.0, 129.1, 128.7, 128.5, 126.6, 119.2, 118.3, 112.8, 59.1, 48.0, 46.0, 44.5, 26.4, 23.5 ppm.

3.14b: ^{1}H NMR (400 MHz, $CDCl_3$) δ 7.79 (d, *J*= 7.7 Hz, 1H), 7.53–7.47 (complex m, 2H), 7.41 (m, 1H), 7.34–7.30 (complex m, 2H), 7.27 (m, 1H), 6.91 (td, *J* = 7.5, 1.1 Hz, 1H), 6.70 (dd, *J* = 8.1, 0.7 Hz, 1H), 4.14 (d, *J* = 8.1 Hz, 1H), 3.55 (m, 1H), 3.20 (m, 1H), 3.13 (m 1H), 2.96 (m, 1H), 2.48 (m, 1H), 2.19 (m, 1H), 2.14–1.98 (complex m, 2H) ppm.

^{13}C NMR (100 MHz, $CDCl_3$) δ 175.9, 175.6, 144.7, 132.0, 130.8, 129.3, 128.8, 128.7, 126.6, 118.5, 116.1, 112.9, 58.6, 47.3, 46.0, 41.6, 31.4, 22.6 ppm.

1-Methyl-3-phenyl-2,3-dihydroquinoline-4,4(1*H*)-dicarbonitrile (**3.16**)

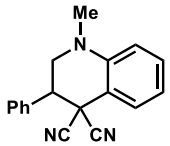

This compound was prepared according to General Procedure 5. Reaction between benzylidenemalonitrile and *N*,*N*-dimethylaniline. The product was subjected to flash chromatography on silica gel (5–20% EtOAc/hexane elution; 0.5% NEt_3 was present in the eluent) and then recrystallised to provide the previously unreported compound as a colourless solid (40 mg, 42% yield).

^{1}H NMR (600 MHz, $CDCl_3$) δ 7.55 (dd, *J* = 7.7, 1.3 Hz, 1H), 7.51–7.46 (complex m, 5H), 7.37 (t, *J* = 7.9 Hz, 1H), 6.85 (t, *J* = 7.5 Hz, 1H), 6.77 (d, *J* = 8.4 Hz, 1H), 3.99 (t, *J* = 11.4 Hz, 1H), 3.63 (dd, *J* = 11.4, 3.8 Hz, 1H), 3.55 (dd, *J* = 12.4, 3.9 Hz, 1H), 3.06 (s, 3H) ppm.

^{13}C NMR (150 MHz, $CDCl_3$) δ 144.1, 134.9, 131.9, 129.5, 129.3, 128.9, 128.6, 117.8, 115.3, 114.2, 112.9, 112.7, 51.5, 45.7, 42.6, 38.9 ppm.

IR (NaCl) 2361, 1607, 1508, 14564, 1433, 1356, 1337, 1308, 1223, 1121, 1001, 748, 700 cm^{-1}.

EIMS *m*/*z* 273 [M^+], 230, 182.

HREIMS [M^+] Found 273.1258. $C_{18}H_{15}N_3$ requires 273.1266.

6-Bromo-1-methyl-3-phenyl-2,3-dihydroquinoline-4,4(1*H*)-dicarbonitrile (**3.17**)

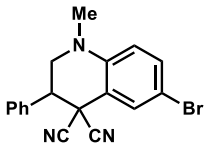

This compound was prepared according to General Procedure 5. Reaction between benzylidenemalonitrile and 4-bromo-*N*,*N*-dimethylaniline. The product was subjected to flash chromatography on silica gel (5–15% EtOAc/hexane elution; 0.5% NEt_3 was present in the eluent) and then recrystallised to provide the previously unreported compound as a colourless solid (68 mg, 55% yield).

^{1}H NMR (400 MHz, $CDCl_3$) δ 7.65 (d, *J* = 2.2 Hz, 1H), 7.48 (s, 5H), 7.44 (dd, *J* = 9.0, 2.1 Hz, 1H), 6.64 (d, *J* = 8.9 Hz, 1H), 3.99 (m, 1H), 3.57 (m, 2H), 3.04 (s, 3H) ppm.

^{13}C NMR (100 MHz, $CDCl_3$) δ 143.1, 134.7, 134.3, 131.2, 129.7, 129.4, 128.5, 114.7, 114.4, 114.2, 113.7, 108.9, 51.3, 45.5, 42.1, 38.9 ppm.

IR (NaCl) 2360, 2342, 1600, 1507, 1454, 1406, 1358, 1335, 1294, 1252, 1221, 1119, 951, 910, 804, 732, 700 cm^{-1}.

EIMS *m*/*z* 351 [M^+], 308, 229, 201, 181.

HREIMS [M^+] Found 351.0372. $C_{18}H_{14}BrN_3$ requires 351.0371.

6-Isopropyl-1-methyl-3-phenyl-2,3-dihydroquinoline-4,4(1*H*)-dicarbonitrile (**3.18**)

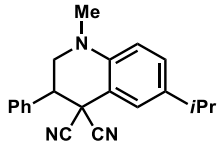

This compound was prepared according to General Procedure 5. Reaction between benzylidenemalonitrile and 4-isopropyl-*N*,*N*-dimethylaniline. The product was subjected to flash chromatography on silica gel (5–10% EtOAc/hexane elution; 0.5% NEt_3 was present in the eluent) to provide the previously unreported compound as a colourless solid (88 mg, 80% yield).

^{1}H NMR (400 MHz, $CDCl_3$) δ 7.54–7.46 (complex m, 5H), 7.40 (d, *J* = 1.6 Hz, 1H), 7.25 (dd, *J* = 8.6, 1.8 Hz, 1H), 6.74 (d, *J* = 8.6 Hz, 1H), 3.95 (t, *J* = 11.9 Hz, 1H), 3.64 (dd, *J* = 11.4, 3.7 Hz, 1H), 3.51 (dd, *J* = 12.3, 3.7 Hz, 1H), 3.03 (s, 3H), 2.90 (heptet, *J* = 6.9 Hz, 1H), 1.28 (d, *J* = 6.9 Hz, 6H) ppm.

^{13}C NMR (150 MHz, $CDCl_3$) δ 142.4, 138.7, 135.1, 129.8, 129.5, 129.3, 128.6, 126.8, 115.5, 114.4, 113.0, 112.7, 51.6, 46.0, 42.7, 39.0, 33.2, 24.16, 24.14 ppm.

IR (NaCl) 2961, 1618, 1520, 1501, 1456, 1356, 1335, 1290, 1119, 814, 770, 735, 702 cm^{-1}.

EIMS *m*/*z* 315 [M^+], 300, 272, 257, 128.

HREIMS [M^+] Found 315.1733. $C_{21}H_{21}N_3$ requires 315.1735.

(11b*S*,11c*R*,14a*S*)-13-Phenyl-6,7,13,14a-tetrahydroisoquinolino[2,1-*a*]-pyrrolo[3,4-*c*]quinoline-12,14(11b*H*,11c*H*)-dione (**3.21**)

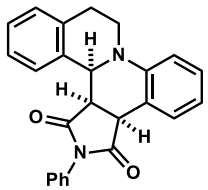

This compound was prepared according to General Procedure 5. Reaction between *N*-phenyl-1,2,3,4-tetrahydroisoquinoline and *N*-phenylmaleimide. The product was subjected to flash

chromatography on silica gel (5–25% EtOAc/hexane elution; 0.5% NEt_3 was present in the eluent) and then recrystallised to provide the previously unreported compound as a colourless solid and as a single diastereoisomer (80 mg, 60% yield).

^{1}H NMR (400 MHz, $CDCl_3$) δ 7.61 (d, *J* = 7.6 Hz, 1H), 7.41–7.19 (complex m, 10H), 7.03 (t, *J* = 7.6 Hz, 1H), 6.93 (d, *J* = 8.0 Hz, 1H), 4.49 (d, *J* = 3.1 Hz, 1H), 4.35 (d, *J* = 9.6 Hz, 1H), 4.01 (dd, *J* = 9.8, 3.4 Hz, 1H), 3.78 (dq, *J* = 10.6, 2.2 Hz, 1H), 3.13 (td, *J* = 13.5, 4.4 Hz, 1H), 3.00 (td, *J* = 11.4, 2.4 Hz, 1H), 2.88 (d, *J* = 15.0 Hz, 1H) ppm.

^{13}C NMR (100 MHz, $CDCl_3$) δ 175.4, 175.1, 149.8, 135.4, 133.8, 132.0, 130.5, 128.9, 128.6, 128.5, 128.3, 126.6, 126.4, 126.3, 126.0, 120.58, 120.55, 112.7, 59.4, 51.1, 44.7, 42.8, 29.5 ppm.

IR (NaCl) 17143, 1600, 1495, 1456, 1379, 1198, 1179, 910, 754, 726, 691, 623 cm^{-1}.

EIMS *m*/*z* 380 [M^+], 246, 232, 119, 87.

HREIMS [M^+] Found 380.1532. $C_{25}H_{20}N_2O_2$ requires 380.1525.

(11b*S*,11c*R*,14a*S*)-2-Fluoro-13-phenyl-6,7,13,14a-tetrahydroisoquinolino[2,1-*a*]pyrrolo[3,4-*c*]quinoline-12,14(11b*H*,11c*H*)-dione (**3.22**)

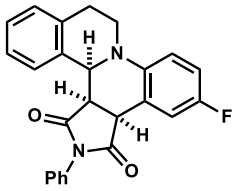

This compound was prepared according to General Procedure 5. Reaction between 2-(4-fluorophenyl)-1,2,3,4-tetrahydroisoquinoline and *N*-phenylmaleimide. The product was subjected to flash chromatography on silica gel (5–15% EtOAc/hexane elution; 0.5% NEt_3 was present in the eluent) and then recrystallised to provide the previously unreported compound as a colourless solid and as a single diastereoisomer (93 mg, 67% yield).

^{1}H NMR (400 MHz, $CDCl_3$) δ 7.41–7.17 (complex m, 10H), 7.00 (td, *J* = 8.4, 2.8 Hz, 1H), 6.85 (m, 1H), 4.46 (s, 1H), 4.32 (d, *J* = 9.4 Hz, 1H), 4.01 (dd, *J* = 9.4, 2.8 Hz, 1H), 3.70 (dq, *J* = 10.6, 2.2 Hz, 1H), 3.10 (td, *J* = 13.4, Hz, 1H), 2.97 (td, *J* = 11.4, 2.0 Hz, 1H), 2.87 (d, *J* = 15.0 Hz, 1H) ppm.

^{13}C NMR (150 MHz, $CDCl_3$) δ 174.9, 174.8, 158.0, 156.5, 146.4 (d, J = 1.6 Hz), 135.3, 133.6, 131.9, 129.0, 128.6 (d, J = 13.2 Hz), 126.8, 126.6, 126.4, 126.1, 122.1 (d, J = 7.8 Hz), 117.3 (d, J = 23.1 Hz), 115.1 (d, J = 22.0 Hz), 113.7 (d, J = 7.8 Hz), 59.9, 50.9, 44.8, 43.2, 29.6 ppm.

IR (neat) 1695, 1494, 1486, 1373, 1186, 986, 941, 913, 882, 855, 811, 765, 738, 692, 622 cm^{-1}.

EIMS *m*/*z* 398 [M^+], 264, 250, 235.

HREIMS [M+] Found 398.1443. $C_{25}H_{19}FN_2O_2$ requires 398.1431.

(11b*S*,11c*R*,14a*S*)-2-Methoxy-13-phenyl-6,7,13,14a-tetrahydroisoquinolino[2,1-*a*]pyrrolo[3,4-*c*]quinoline-12,14(11b*H*,11c*H*)-dione (**3.23**)

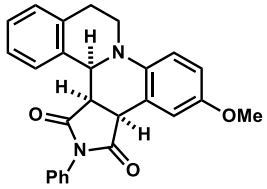

This compound was prepared according to General Procedure 5. Reaction between 2-(4-methoxyphenyl)-1,2,3,4-tetrahydroisoquinoline and *N*-phenylmaleimide. The product was subjected to flash chromatography on silica gel (5–15% EtOAc/hexane elution; 0.5% NEt_3 was present in the eluent) and then recrystallised to provide the previously unreported compound as a colourless solid and as a single diastereoisomer (82 mg, 57% yield).

^{1}H NMR (400 MHz, $CDCl_3$) δ 7.40–7.17 (complex m, 10H), 6.89–6.83 (complex m, 2H), 4.44 (d, *J* = 3.1 Hz, 1H), 4.33 (d, *J* = 9.6 Hz, 1H), 4.01 (dd, *J* = 9.4, 3.4 Hz, 1H), 3.85 (s, 3H), 3.69 (dq, *J* = 10.4, 2.2 Hz, 1H), 3.09 (td, *J* = 13.4, 4.6 Hz, 1H), 2.94 (td, *J* = 10.8, 2.6, 1H), 2.86 (d, *J* = 15.2 Hz, 1H) ppm.

^{13}C NMR (100 MHz, $CDCl_3$) δ 175.2, 175.1, 154.0, 135.4, 133.9, 132.0, 129.0, 128.6, 128.4, 126.7, 126.44, 126.40, 126.1, 121.7, 116.0, 114.3, 113.8, 60.0, 55.9, 50.8, 45.0, 43.3, 29.6 ppm.

IR (NaCl) 1713, 1498, 1456, 1379, 1253, 1243, 1192, 10347, 757, 736, 691 cm^{-1}.

EIMS *m*/*z* 410 [M+], 392, 262, 119.

HREIMS [M+] Found 410.1634. $C_{26}H_{22}FN_2O_3$ requires 410.1630.

5-Benzyl-12,13-dihydro-4b*H*-isoquinolino[2,1-*a*]quinazolin-6(5*H*)-one (**3.25**)

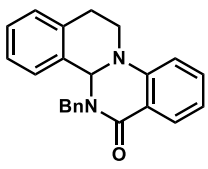

$[Cu(dap)_2]Cl$ (15.5 mg, 17.5 μmol) was added to a solution of *N*-benzyl-2-(3,4-dihydroisoquinolin-2(1*H*)-yl)benzamide (240 mg, 0.70 mmol), TFA (80 mg, 0.70 mmol) in DMF (6 mL) in a 20 mL vial (containing a magnetic stir bar) in air. The vial was then capped and irradiated with a green LED (515 nm). The reaction mixture was stirred at ambient

temperature for 120 h, then poured into a separatory funnel, toluene (20 mL), and brine (15 mL) were added and the phases separated. The separated aqueous phase was further extracted with toluene (2 x 20 mL). The combined organic phases were then washed with brine (2 x 10 mL), dried ($MgSO_4$), filtered, and concentrated under reduced pressure. The ensuing residue was subjected to flash chromatography on silica gel (3–10% EtOAc/ (1:1 CH_2Cl_2/hexane) elution; 1 % NEt_3 was present in the eluent) and then recrystallised to provide the previously reported compound as a colourless solid (132 mg, 56% yield).[26]

^{1}H NMR (400 MHz, $CDCl_3$) δ 7.99 (dd, *J* = 7.7 Hz, *J* = 1.2 Hz, 1H), 7.36–7.25 (complex m, 7H), 7.21–7.15 (complex m, 2H), 7.03 (m, 1H), 6.90–6.84 (complex m, 2H), 5.75 (m, 1H), 5.68 (s, 1H), 4.39 (d, *J* = 15.3 Hz, 1H), 3.99 (dd, *J* = 13.7 Hz, *J* = 5.4 Hz, 1H), 3.49 (m, 1H), 3.10 (m, 1H), 2.70 (dd, *J* = 17.0 Hz, *J* = 3.8 Hz, 1H) ppm.

^{13}C NMR (100 MHz, $CDCl_3$) δ 163.5, 147.5, 137.3, 135.2, 134.8, 133.4, 129.5, 129.3, 128.7, 128.3, 127.7, 127.5, 126.2, 126.0, 119.4, 118.5, 113.7, 71.7, 49.6, 44.6, 24.6 ppm.

IR (neat) 1651, 1605, 1454, 1385, 1304, 1263, 752 cm^{-1}.

Bis(2,9-di(4-methoxyphenyl)-1,10-phenanthroline)copper(II) dichloride

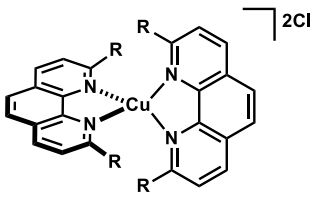

2,9-Di(4-methoxyphenyl)-1,10-phenanthroline (114 mg, 0.289 mmol) was added to a solution of $CuCl_2 \bullet 2H_2O$ (25 mg, 0.145 mmol) in THF (10 mL) and magnetically stirred for 0.5 h. Precipitation with hexanes afforded the previously unreported complex as a dark purple solid (129 mg, 97% yield).

^{1}H NMR (400 MHz, CD_3CN) δ 8.59 (bs, 8H), 6.18 (bs, 8H), 5.05 (bs, 24H) ppm; 3 signals observed, paramagnetic.

HRESIMS [M^+] Found 847.2323. $C_{54}H_{40}N_4O_4Cu$ requires 847.2340.

1,8-Di-*tert*-butyl 2-methyl 3,3a-dihydropyrrolo[2,3-*b*]indole-1,2,8(2*H*,8a*H*)-tricarboxylate (**3.29**)

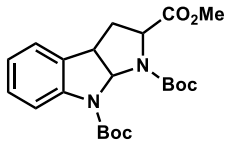

1,8-Di-*tert*-butyl 2-methyl 3a-bromo-3,3a-dihydropyrrolo[2,3-*b*]indole-1,2,8(2*H*,8a*H*)-tricarboxylate (51 mg, 0.103 mmol) was combined with [Cu(bcp)(XP)]PF_6 (3.0 mg, 2.6 μmol), nickel(II) chloride (2.7 mg, 21 μmol), 4,4'-di-tert-butyl-2,2'-bipyridine (8.3 mg, 31μmol) and triethylamine (29 μL, 0.203 mmol) under an atmosphere of nitrogen then DMF (1 mL) was added. The resulting reaction mixture was irradiated with blue LEDs at 25 °C with magnetic stirring. After 16 h, solvent was removed under reduced pressure and the ensuing residue was passed through a silica pad (3 cm height contained within a sintered glass funnel, 10% EtOAc/hexane elution) to afford the previously reported compound as a colourless solid (34 mg, 77% yield).[27]

^{1}H NMR (400 MHz, $CDCl_3$) δ 7.37 (m, 1H), 7.25 (t, *J* = 7.7 Hz, 1H), 7.18 (d, *J* = 7.6 Hz, 1H), 7.07 (t, *J* = 7.5 Hz, 1H), 6.39 (d, *J* = 6.0 Hz, 1H), 4.02-3.94 (m, 1H), 3.75 (s, 3H), 2.56 (m, 1H), 2.31 (m, 1H), 1.43 (s, 18H) ppm.

***N*-(5-Chlorohexadecyl)-4-methylbenzenesulfonamide** (**3.39**)

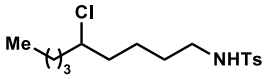

N-Chloro-*N*-hexadecyl-4-methylbenzenesulfonamide (86 mg, 0.200 mmol) was combined with sodium hydrogen phosphate (34 mg, 0.240 mmol) and $[Cu(dap)_2]Cl$ (1.8 mg, 2.00 μmol) under an atmosphere of nitrogen before acetonitrile (3 mL) was added. The resulting reaction mixture was irradiated with green LEDs at 25 °C. After 16 h, solvent was removed under reduced pressure. The ensuing residue was subjected to flash column chromatography (silica gel, 0–10% EtOAc/hexane elution) to provide the previously reported compound as a colourless oil (31 mg, 36% yield).[28]

^{1}H NMR (400 MHz, $CDCl_3$) δ 7.77 (d, *J* = 8.5 Hz, 2H), 7.32 (d, *J* = 7.8 Hz, 2H), 4.69 (t, *J* = 6.0 Hz, 1H), 2.94 (q, *J* = 6.8 Hz, 2H), 2.44 (s, 3H), 1.84-1.58 (m, 2H), 1.46 (t, *J* = 7.1 Hz, 2H), 1.27 (s, 8H), 0.90 (t, *J* = 7.1 Hz, 3H) ppm.

Phenyldiazonium tetrafluoroborate (**3.41**)

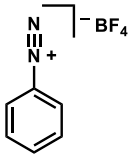

A solution containing $NaNO_2$ (700 mg, 10.0 mmol) in H_2O (1.5 mL) was added to a solution containing HBF_4 (3.5 mL of a 50% aqueous solution) and aniline (931 mg, 10.0 mmol) in H_2O (4 mL) maintained at 0 °C and magnetically stirred. After 1 h, the ensuing precipitate was collected by filtration and washed with H_2O (2 x 5 mL). The ensuing solid was redissolved in acetone (10 mL) and precipitated with Et_2O (~30 mL), collected by filtration and washed with Et_2O (2 x 3 mL) to afford the previously reported compound a colourless solid (863 mg, 45 % yield).[29]

^{1}H NMR (400 MHz, DMSO-d_6) δ 8.67 (dd, *J* = 8.8, 1.2 Hz, 2H), 8.26 (dd, 7.7, 2.2 Hz, 1H), 7.98 (dd, *J* = 8.7, 7.7 Hz, 2H) ppm.

***N*-Phenylacetamide** (**3.46**)

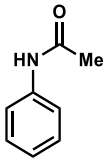

Benzenediazonium tetrafluoroborate (100 mg, 0.521 mmol) was combined with H_2O (47 mg, 2.61 mmol) in acetonitrile (1 mL) under an atmosphere of nitrogen and magnetically stirred in the dark. After 48 h, all volatiles were removed under reduced pressure and the ensuing residue was subjected to flash chromatography (silica gel, 0–10% EtOAc/ hexane elution; 1% NEt_3 was present in the eluent) to provide the previously reported compound (68 mg, 97% yield) as a colourless solid.[30]

^{1}H NMR (400 MHz, $CDCl_3$) δ 7.75 (bs, 1H), 7.48 (d, *J* = 8.0 Hz, 2H), 7.28 (t, *J* = 7.8 Hz, 7.08 (t, *J* = 7.9 Hz, 1H), 2.22 (s, 3H) ppm.

_N_-(Perfluorophenyl)acetamide (4.3)

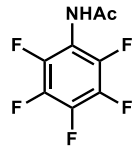

Acetic anhydride (1394 mg, 13.66 mg) was added to a solution of 2,3,4,5,6–pentafluoroaniline (2000 mg, 10.92 mmol) in toluene (30 mL) under an atmosphere of nitrogen then concentrated sulfuric acid (107 mg, 1.09 mmol) was added. The resulting reaction mixture was heated at 80 °C. After 16 h, the mixture was cooled to ambient temperature and hexane (50 mL) was added. The resulting precipitate was collected by filtration and recrystallised from hot toluene to afford the previously reported compound (1630 mg, 66% yield) as colourless needles.[31]

^{1}H NMR (600 MHz, $CDCl_3$) δ 6.92 (bs, 1H), 2.27, (s, 3H) ppm.

^{19}F NMR (564 MHz, $CDCl_3$) δ –144.8 (d, *J* = 17.8 Hz, 2F), –156.3 (t, *J* = 20.5 Hz, 1F), –162.2 (t, *J* = 19.0 Hz, 2F) ppm.

_N_-(4-(1-(Diisopropylamino)ethyl)-2,3,5,6-tetrafluorophenyl)acetamide (4.4)

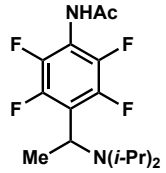

This compound was prepared according to General Procedure 6. Reaction between *N*-(pentafluorophenyl)acetamide (500 μmol) and *i*Pr$_2$NEt. The ensuing residue obtained from the reaction mixture was subjected to flash column chromatography (silica gel, 0–30% EtOAc/hexane elution; 1% NEt_3 was also present in the eluent) and then was recrystallised to provide the previously unreported compound as a colourless solid (145 mg, 87% yield).

^{1}H NMR (600 MHz, $CDCl_3$) δ 7.04 (bs, 1H), 4.66 (q, *J* = 7.3 Hz, 1H), 3.37 (sept, *J* = 6.7 Hz, 2H), 2.24 (s, 3H), 1.51 (d, *J* = 7.2 Hz, 3H), 1.12 (d, *J* = 6.6 Hz, 6H), 0.94 (d, *J* = 6.8 Hz, 6H) ppm.

^{19}F NMR (564 MHz, $CDCl_3$) δ –142.2 (s, 2F), –146.6 (s, 2F) ppm.

^{13}C NMR (150 MHz, $CDCl_3$) δ 168.3, 144.8 (d, *J* = 242 Hz), 142.3 (d, *J* = 249 Hz), 124.5, 113.7, 46.0, 45.7, 22.7, 22.4, 19.7 ppm.

IR (neat) 2965, 1673, 1529, 1501, 1275, 1215, 1148, 1083, 1005, 985, 940, 726 cm^{-1}.

HRESIMS Found $[M + H]^+$, 335.1738. $C_{16}H_{23}F_4N_2O$ requires 335.1741.

***Tert*-butyl (pentafluorophenyl)carbamate (4.5)**

TFA (260 μL, 3.39 mmol) was added to a CH_2Cl_2 solution (10 mL) containing di(*tert*-butyl) (pentafluorophenyl)dicarbamate (1.30 g, 3.39 mmol) maintained at 0 °C under N_2 and magnetically stirred. After 3 h, the solution was concentrated under reduced pressure. The resulting residue was subjected to flash column chromatography (silica gel, 0–10% EtOAc/hexane elution; 1% NEt_3 was present in the eluent) to provide the previously unreported compound (490 mg, 51% yield) as a colourless solid.

^{1}H NMR (400 MHz, $CDCl_3$) δ 5.98 (bs, 1H), 1.53 (s, 9H) ppm.

^{19}F NMR (376 MHz, $CDCl_3$) δ –146.3 (d, J = 16 Hz, 2F), –157.8 (t, J = 21 Hz, 1F), –162.8 (m, 2F) ppm.

^{13}C NMR (150 MHz, $CDCl_3$) δ 152.2, 142.9 (d, J = 254 Hz), 149.7 (d, J = 256 Hz), 137.8 (d, J = 252 Hz), 112.7, 82.4, 28.0 ppm.

IR (NaCl) 3318, 1710, 1525, 1487, 1451, 1326, 1278, 1251, 1162, 1012, 974 cm^{-1}.

EIMS (*m*/*z*, relative intensity) 183 {[M–Boc]$^+$, 6}, 41 (30), 57 (100).

4-Methyl-*N*-(perfluorophenyl)benzenesulfonamide (4.7)

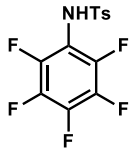

4-(Dimethylamino)pyridine (320 mg, 2.62 mmol) was added to a solution of *p*-toluenesulfonyl chloride (1000 mg, 5.25 mmol) in pyridine (30 mL). This solution was stirred at ambient temperature for 15 min then 2,3,4,5,6-pentafluoroaniline (1150 mg, 6.29 mmol) was added. The resulting reaction mixture was heated at 80 °C. After 24 h, the mixture was cooled and solvent removed under reduced pressure. The resulting residue was subjected to flash chromatography on silica gel (0–30% EtOAc/hexane elution) to afford the previously reported compound (215 mg, 10% yield) as a colourless solid.[32]

^{1}H NMR (400 MHz, $CDCl_3$) δ, 7.74 (d, J = 8.3 Hz, 2H), 7.34 (d, J = 8.2 Hz, 2H), 6.32 (bs, 1H), 2.48 (s, 3H) ppm.

^{19}F NMR (376 MHz, $CDCl_3$) δ –145.0 (d, *J* = 16.3 Hz, 2F), –154.0 (t, *J* = 21.5 Hz, 1F), –161.2 (m, 2F) ppm.

Di(t*ert*-butyl) (pentafluorophenyl)dicarbamate (**4.10**)

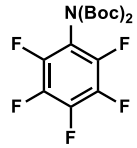

4-(Dimethylamino)pyridine (13.3 mg, 0.109 mmol) was added to a magnetically stirred mixture of pentafluoroaniline (1.00 g, 5.46 mmol), Boc_2O (1431 mg, 6.55 mmol) and Na_2CO_3 (1158 mg, 10.92 mmol) in THF (10 mL) maintained at ambient temperature under N_2. The ensuing mixture was then heated at 60 °C. After 16 h, the mixture was cooled to ambient temperature and H_2O (5 mL) and EtOAc (20 mL) were added and the phases were separated. The aqueous phase was then extracted with EtOAc (2 x 20 mL) and the combined organic fractions were dried (Na_2SO_4), filtered, and concentrated under reduced pressure. The ensuing residue was then subjected to chromatography (silica plug, contained in a sintered glass funnel: ~3 cm height, 5 cm diameter; CH_2Cl_2 elution) to provide the previously unreported compound (1.15 g, 55% yield) as a colourless solid.

^{1}H NMR (400 MHz, $CDCl_3$) δ 1.45 (s, 18H) ppm.

^{19}F NMR (376 MHz, $CDCl_3$) δ –145.9 (d, *J* = 17 Hz, 2F), –154.7 (t, *J* = 21 Hz, 1F), –163.0 (t, *J* = 19 Hz, 2F) ppm.

^{13}C NMR (150 MHz, $CDCl_3$) δ 149.2, 143.6 (d, *J* = 251 Hz), 141.1 (d, *J* = 256 Hz), 137.5 (d, *J* = 252 Hz), 115.0 (td, *J* = 15, 5 Hz), 84.6, 27.7 ppm.

IR (NaCl) 1810, 1777, 1734, 1519, 1372, 1271, 12448, 1149, 1119, 1099, 1066, 994, 852 cm^{-1}.

EIMS (*m*/*z*, relative intensity) 227 {[M–(Boc, ^{t}Bu)]$^+$, 7}, 57 (100).

***N*-Methyl-*N*-(pentafluorophenyl)acetamide** (**4.11**)

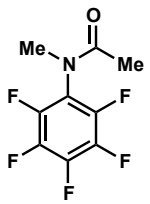

NaH (149 mg of 60% dispersion in mineral oil, 3.73 mmol) was added to a solution of *N*-(pentafluorophenyl)acetamide (500 mg, 2.22 mmol) in DMF (8 mL) maintained at 0 °C under

N_2 and magnetically stirred. After 0.5 h, iodomethane (166 μL, 2.66 mmol) was added dropwise and the ensuing mixture was warmed to ambient temperature. After 16 h, EtOAc/hexane (20 mL of 1:1 v/v solution) and H_2O (10 mL) were added and the phases separated. The aqueous phase was then further extracted with EtOAc/hexane (2 x 20 mL of 1:1 v/v solution) and the combined organic fractions were dried (Na_2SO_4), filtered, and concentrated under reduced pressure. The ensuing residue was subjected to flash column chromatography (silica gel, 20% EtOAc/hexane elution) to provide the previously unreported compound (358 mg, 67% yield) as a colourless oil.

^{1}H NMR (400 MHz, $CDCl_3$) δ 3.36 (s, 0.7H), 3.23 (s, 2.3H), 2.33 (s, 0.7H), 1.94 (s, 2.3H) ppm; 4 signals observed (rotamers present).

^{19}F NMR (376 MHz, $CDCl_3$) δ –145.16 (d, J = 15.8 Hz, 0.4F), –145.72 (d, J = 15.8 Hz, 1.6F), –153.0 (t, J = 21.3 Hz, 0.8F), –155.4 (t, J = 21.3 Hz, 0.2F), –160.3 (m, 1.6 F), –162.2 (m, 0.4F) ppm; 6 signals observed (rotamers present).

^{13}C NMR (150 MHz, $CDCl_3$) δ 170.6, 170.1, 144.1 (d, J = 250 Hz), 141.4 (d, J = 255 Hz), 140.9 (d, J = 255 Hz), 138.0 (d, J = 257 Hz), 119.0 (td, J = 15Hz, 6 Hz), 117.9 (td, J = 15 Hz, 6 Hz), 38.4, 35.8, 21.4, 21.1 ppm; 12 signals observed (rotamers present).

IR (NaCl) 1685, 1522, 1510, 1374, 1342, 1323, 991 cm^{-1}.

HRESIMS $[M + H]^+$ Found, 240.0442. $C_9H_6F_5NO$ requires 240.0442.

_N_-(Perfluorophenyl)-2-phenylacetamide (4.13)

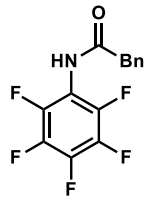

(4-Dimethylamino)pyridine (67 mg, 0.546 mmol), pentafluoroaniline (1000 mg, 5.46 mmol), and 2-phenylacetic acid (818 mg, 6.01 mmol) were combined under an atmosphere of nitrogen then CH_2Cl_2 (20 mL) was added and the ensuing mixture wasmagnetically stirred for 15 m. Then benzotriazol-1-yl-oxytripyrrolidinophosphonium hexafluorophosphate (PyBOP) (3980 mg, 7.65 mg) and NEt_3 (1382 mg, 13.7 mmol) were added sequentially and the resulting reaction mixture was magnetically stirred at 25 °C. After 16 h, the reaction mixture was diluted with H_2O (5 mL) and EtOAc/hexane (20 mL of a 1:1 v/v solution). The phases

were separated and the aqueous layer was further extracted with EtOAc/hexane (2 x 20 mL of a 1:1 v/v solution). The combined organic phase was then washed with $KHSO_4$ (20 mL of a saturated aqueous solution), $NaHCO_3$ (20 mL of a saturated aqueous solution), and H_2O (20 mL), successively. The organic phase was then dried (Na_2SO_4), filtered, and concentrated under reduced pressure. The ensuing residue was then subjected to flash column chromatography (silica gel, 0–30% EtOAc/hexane elution; 1% NEt_3 was present in the eluent) to provide the previously reported compound (320 mg, 19% yield) as a colourless solid.[33]

^{1}H NMR (400 MHz, $CDCl_3$) δ 7.47–7.42 (m, 2H), 7.40–7.36 (m, 3H), 6.69 (bs, 1H), 3.84 (s, 2H) ppm.

^{19}F NMR (376 MHz, $CDCl_3$) δ –144.81 (d, J = 16 Hz, 2F), –156.2 (t, J = 21 Hz, 1F), –162.3 (t, J = 20 Hz, 2F) ppm.

^{13}C NMR (150 MHz, $CDCl_3$) δ 169.4, 143.1 (d, J = 252 Hz), 140.2 (d, J = 252 Hz), 137.8 (d, J = 256 Hz), 133.7, 129.48, 129.44, 128.0, 111.6 (t, J = 13 Hz), 43.5 ppm.

2-(4-Fluorophenyl)-*N*-(pentafluorophenyl)acetamide (**4.15**)

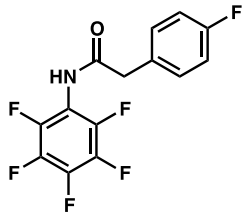

4-(Dimethylamino)pyridine (67 mg, 546 μmol) was added to a magnetically stirred solution of pentafluoroaniline (1.00 g, 5.46 mmol) and 2-(4-fluorophenyl)acetic acid (926 mg, 6.01 mmol) in DMF (20 mL) maintained at 0 °C under N_2. After 5 m, EDCI (1.47 g, 7.65 mmol) and NEt_3 (1.90 mL, 13.7 mmol) were added and the ensuing mixture was slowly warmed to 25 °C. After 16 h, the reaction mixture was diluted with H_2O (5 mL) and EtOAc/hexane (20 mL of a 1:1 v/v solution). The phases were separated and the aqueous layer was further extracted with EtOAc/hexane (2 x 20 mL of a 1:1 v/v solution). The combined organic phase was then washed with $KHSO_4$ (20 mL of a saturated aqueous solution), $NaHCO_3$ (20 mL of a saturated aqueous solution), and H_2O (20 mL), successively. The organic phase was then dried (Na_2SO_4), filtered, and concentrated under reduced pressure. The ensuing residue was then subjected to flash column chromatography (silica gel, 0–30% EtOAc/hexane elution; 1% NEt_3

was present in the eluent) to provide the previously unreported compound (400 mg, 24% yield) as a colourless solid.

^{1}H NMR (400 MHz, $CDCl_3$) δ 7.35 (dd, J = 8.0, 5.5 Hz, 2H), 7.13 (t, J = 8.8 Hz, 2H), 6.64 (bs, 1H), 3.81 (s, 2H) ppm.

^{19}F NMR (376 MHz, $CDCl_3$) δ –113.9 (s, 1F), –144.8 (d, J = 16 Hz, 2F), –155.9 (t, J = 21 Hz, 1F), –162.1 (t, J = 19 Hz, 2F) ppm.

^{13}C NMR (150 MHz, $CDCl_3$) δ 169.1, 163.3, 161.6, 143.0 (d, J = 143 Hz), 137.8 (d, J = 253 Hz), 131.1 (d, J = 8 Hz), 129.3 (d, J = 3 Hz), 116.3 (d, J = 22 Hz), 111.5 (t, J = 19 Hz), 42.5 ppm.

IR (NaCl) 3153, 2989, 2982, 1671, 1511, 1496, 1227, 1016, 1002, 963, 838 cm^{-1}.

EIMS (m/z, relative intensity) 319 (M^+, 1), 136 (55), 109 (100).

1,2,3,4-Tetrafluorodibenzo[*b*,*e*][1,4]dioxine (**4.17**)

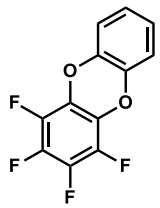

Hexafluorobenzene (1.10 g, 6.00 mmol) and K_2CO_3 (4.15 g, 30.0 mmol) were combined under an atmosphere of nitrogen then MeCN (20 mL) was added. 1,2-Dihydroxybenzene (920 mg, 6.00 mmol) was added to the ensuing magnetically stirred mixture which was then heated at reflux. After 16 h, the reaction mixture was cooled and NaCl (30 mL of a saturated aqueous solution) and EtOAc (30 mL) were added and phases separated. The aqueous phase was then further extracted with EtOAc (3 x 20 mL) and organic fractions were combined, dried ($MgSO_4$), filtered, and concentrated under reduced pressure. The ensuing solid was then recrystallised from EtOAc and triturated (Et_2O) to provide the previously reported compound (621 mg, 41% yield) as a colourless solid.[34]

^{1}H NMR (400 MHz, $CDCl_3$) δ 7.06–6.96 (m, 2H), 6.87 (d, J = 21 Hz, 2H) ppm.

^{19}F NMR (376 MHz, $CDCl_3$) δ –162.6 (m, 2F), –165.3 (m, 2F) ppm.

^{13}C NMR (150 MHz, $CDCl_3$) δ 138.2, 135.4 (d, J = 249 Hz), 135.0 (d, J = 238 Hz), 123.5, 115.1 ppm.

Methyl 6,7,8,9-tetrafluorodibenzo[*b*,*e*][1,4]dioxine-2-carboxylate (**4.19**)

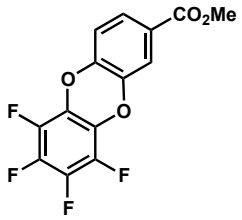

H_2SO_4 (one drop) was added to a mixture of 3,4-dihydroxybenzoic acid (0.92 g, 6.00 mmol) in MeOH (20 mL) maintained under N_2. The ensuing mixture was then heated at reflux. After 16 h, the mixture was concentrated under reduced pressure and MeCN (20 mL) added. Hexafluorobenzene (1.10 g, 6.00 mmol) and K_2CO_3 (4.15g, 30.0 mmol) were added to the ensuing magnetically stirred mixture which was then heated at reflux. After 16 h, the reaction mixture was cooled and NaCl (30 mL of a saturated aqueous solution) and EtOAc (30 mL) were added and phases separated. The aqueous phase was then further extracted with EtOAc (3 x 20 mL) and organic fractions were combined, dried ($MgSO_4$), filtered, and concentrated under reduced pressure. The ensuing solid was then recrystallised from EtOAc and triturated (Et_2O) to provide the previously unreported compound (300 mg, 12% yield) as a colourless solid.

^{1}H NMR (600 MHz, $CDCl_3$) δ 7.74 (dd, J = 8, 2 Hz, 1H), 7.68 (d, J = 2 Hz, 1H), 7.03 (d, J = 9 Hz, 1H), 3.93 (s, 3H) ppm.

^{13}C NMR (150 MHz, $CDCl_3$) δ 165.2, 143.8, 139.8, 137.7, 136.7, 136.0, 128.7, 128.5, 127.6, 127.2, 118.4, 116.9, 52.4, 30.9 ppm.

^{19}F NMR (564 MHz, $CDCl_3$) δ –161.8 (m, 2F), –164.0 (m, 1F), –164.5 (m, 1F) ppm.

IR (NaCl) 1722, 1700, 1521, 1506, 1443, 1305, 1020 cm^{-1}.

EIMS (*m*/*z*, relative intensity) 314 (M^+, 75), 283 (100), 255 (44).

2,3,4,5,6-Pentafluoro-*N*-methoxy-*N*-methylbenzamide (**4.22**)

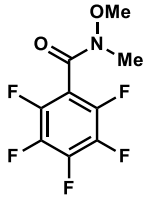

Thionyl chloride (1631mg, 13.7 mmol) was slowly added to 2,3,4,5,6-pentafluorobenzoic acid (500 mg, 2.36 mmol) at 0 °C. The resulting reaction mixture was heated at 90 °C. After 16 h,

the mixture was cooled and solvent removed under reduced pressure. The resulting grey solid (660 mg, 2.86 mmol) was used in the next step without further purification. *N*-*O*-dimethylhydroxylamine hydrochloride (335 mg, 3.44 mmol) was added to a CH_2Cl_2 solution (7.5 mL) containing triethylamine (1397 μL, 10.0 mmol) before 2,3,4,5,6-pentafluorobenzoyl chloride (660 mg, 2.86 mmol) was slowly added in portions. The resulting reaction mixture was magnetically stirred at ambient temperature. After 16 h, CH_2Cl_2 (10 mL) and water (5 mL) were added. The phases were separated and the aqueous phase extracted with CH_2Cl_2 (2 x 10 mL). The combined organic fractions were dried ($MgSO_4$), filtered and concentrated under reduced pressure. The resulting residue was subjected to flash chromatography on silica gel (0–30% EtOAc/hexane elution) to afford the previously reported compound (141 mg, 19% over two steps) as a colourless solid.[35]

^{1}H NMR (400 MHz, $CDCl_3$) δ 3.60 (s, 3H), 3.42 (s, 3H) ppm.

^{19}F NMR (376 MHz, $CDCl_3$) δ –140.7 (m, 2F), –152.1 (t, *J* = 20.5 Hz, 1F), –160.6 (m, 2F) ppm.

(Perfluorophenyl)methyl 2,3,4,5,6-pentafluorobenzoate (**4.24**)

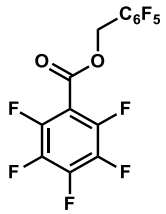

2,3,4,5,6-Pentafluorobenzaldehyde (393 mg, 2.00 mmol), [$RuCl_2$(*p*-cymene)$_2$] (15.3 mg, 50 μmol), triphenylphosphine (26.3 mg, 100 μmol), and sodium formate (40.9 mg, 600 μmol) were combined and dioxane (2 mL) added under an atmosphere of nitrogen. The resulting reaction mixture was heated at 80 °C and magnetically stirred. After 16 h, the reaction mixture was concentrated under reduced pressure and the ensuing residue was subjected to flash chromatography on silica gel (0–20% CH_2Cl_2/hexane elution) to afford the previously reported compound (164 mg, 21% yield) as a colourless solid.[36]

^{1}H NMR (400 MHz, $CDCl_3$) δ 5.49 (s, 2H) ppm.

^{19}F NMR (376 MHz, $CDCl_3$) δ –137.8 (m, 2F), –141.8 (m, 2F), –147.7 (tt, *J* = 20.6, 5.2 Hz 1F), –151.8 (tt, *J* = 20.6, 2.5 Hz 1F), –160.4 (m, 2F), –161.5 (m,2F) ppm.

^{13}C NMR (1000 MHz, $CDCl_3$) δ 158.4, 141.8, 108.4 (td, *J* = 17, 4.0 Hz), 107.1 (td, *J* = 15, 4.0 Hz), 55.0 ppm.

Benzyl 2,3,4,5,6-pentafluorobenzoate (**4.27**)

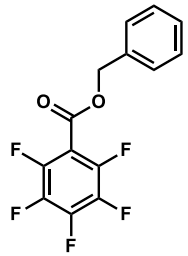

4-(Dimethylamino)pyridine (52 mg, 429 μmol) was added to a magnetically stirred solution of pentafluorobenzoic acid (1.00 g, 4.72 mmol) and benzyl alcohol (444 μL, 4.29 mmol) in CH_2Cl_2 (20 mL) at 0 °C under an atmosphere of N_2. After 5 m, EDCI (1.15 g, 6.00 mmol) and NEt_3 (1.19 mL, 10.7 mmol) were added and the ensuing mixture was warmed to ambient temperature. After 16 h, the reaction mixture was washed with $KHSO_4$ (20 mL of a saturated aqueous solution), $NaHCO_3$ (20 mL of a saturated aqueous solution), and H_2O (20 mL) successively. The organic phase was then dried (Na_2SO_4), filtered, and concentrated under reduced pressure. The ensuing residue was then subjected to chromatography (silica plug contained in a sintered glass funnel: ~3 cm height, 5 cm diameter; 10% EtOAc/hexane elution) to provide the previously reported compound as a colourless oil (455 mg, 32% yield).[37]

^{1}H NMR (400 MHz, $CDCl_3$) δ 7.48–7.36 (complex m, 5H), 5.43 (s, 2H) ppm.

^{19}F NMR (376 MHz, $CDCl_3$) δ –137.8 (m, 2F), –148.4 (t, J = 21 Hz, 1F), –160.3 (m, 2F) ppm.

Furan-2-ylmethyl 2,3,4,5,6-pentafluorobenzoate (**4.29**)

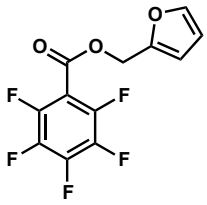

4-(Dimethylamino)pyridine (52 mg, 429 μmol) was added to a magnetically stirred solution of pentafluorobenzoic acid (1.00 g, 4.72 mmol) and furfuryl alcohol (371 μL, 4.29 mmol) in CH_2Cl_2 (20 mL) at 0 °C under an atmosphere of N_2. After 5 m, EDCI (1.15 g, 6.00 mmol) and NEt_3 (1.19 mL, 10.7 mmol) were added and the ensuing mixture was warmed to ambient temperature. After 16 h, the reaction mixture was washed with $KHSO_4$ (20 mL of a saturated aqueous solution), $NaHCO_3$ (20 mL of a saturated aqueous solution), and H_2O (20 mL) successively. The organic phase was then dried (Na_2SO_4), filtered, and concentrated under reduced pressure. The ensuing residue was then subjected to chromatography (silica plug

contained in a sintered glass funnel: ~3 cm height, 5 cm diameter; 10% EtOAc/hexane elution) to provide the previously unreported compound as a colourless oil (521 mg, 38% yield).

^{1}H NMR (400 MHz, $CDCl_3$) δ 7.48 (dd, J = 1.8, 0.6 Hz, 1H), 6.54 (d, J = 3.2 Hz, 1H), 6.42 (dd, J = 3.3, 1.8 Hz, 1H), 5.38 (s, 2H) ppm.

^{19}F NMR (376 MHz, $CDCl_3$) δ –137.8 (m, 2F), –148.3 (t, J = 21 Hz, 1F), –160.3 (m, 2F) ppm.

^{13}C NMR (150 MHz, $CDCl_3$) δ 158.7, 148.1, 145.5 (d, J = 256 Hz), 143.8, 143.3 (d, J = 262 Hz), 137.7 (d, J = 253 Hz), 111.7, 110.7, 107.9 (td, J = 16, 3.9 Hz), 60.0 ppm.

IR (NaCl) 1739, 1501, 1391, 1298, 1192, 951 cm^{-1}.

EIMS (m/z, relative intensity) 292 (M^+, 15), 195 (15), 81 (100).

Prop-2-yn-1-yl 2,3,4,5,6-pentafluorobenzoate (**4.31**)

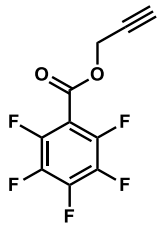

4-(Dimethylamino)pyridine (52 mg, 429 μmol) was added to a magnetically stirred solution of pentafluorobenzoic acid (1.00 g, 4.72 mmol) and propargyl alcohol (250 μL, 4.29 mmol) in CH_2Cl_2 (20 mL) at 0 °C under an atmosphere of N_2. After 5 m, EDCI (1.15 g, 6.00 mmol) and NEt_3 (1.19 mL, 10.7 mmol) were added and the ensuing mixture was warmed to ambient temperature. After 16 h, the reaction mixture was washed with $KHSO_4$ (20 mL of a saturated aqueous solution), $NaHCO_3$ (20 mL of a saturated aqueous solution), and H_2O (20 mL) successively. The organic phase was then dried (Na_2SO_4), filtered, and concentrated under reduced pressure. The ensuing residue was then subjected to chromatography (silica plug contained in a sintered glass funnel: ~3 cm height, 5 cm diameter; 10% EtOAc/hexane elution) to provide the previously reported compound as a colourless oil (521 mg, 38% yield).[38]

^{1}H NMR (400 MHz, $CDCl_3$) δ 4.99 (d, J = 2.5 Hz, 2H), 2.60 (t, J = 2.5Hz, 1H) ppm.

^{19}F NMR (376 MHz, $CDCl_3$) δ –137.4 (m, 2F), –147.5 (t, J = 20 Hz, 1F), –160.1 (m, 2F) ppm.

^{13}C NMR (150 MHz, $CDCl_3$) δ 158.3, 145.6 (d, J = 258 Hz), 143.5 (d, J = 259Hz), 137.7 (d, J = 255 Hz), 107.4 (d, J = 15, 4 Hz), 76.2, 53.9 ppm.

_N_-(4-((dicyclohexylamino)methyl)-2,3,5,6-tetrafluorophenyl)acetamide (4.32)

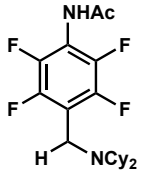

This compound was prepared according to General Procedure 6. Reaction between *N*-(pentafluorophenyl)acetamide (500 μmol) and Cy_2NMe. The ensuing residue obtained from the reaction mixture was subjected to flash column chromatography (silica gel, 0–30% EtOAc/hexane elution; 1% NEt_3 was also present in the eluent) to provide the previously unreported compound as a colourless solid (115 mg, 57% yield).

^{1}H NMR (600 MHz, $CDCl_3$) δ 7.11 (bs, 1H), 3.85 (s, 2H), 2.46 (t, J = 11.8 Hz, 2H), 2.25 (s, 3H), 1.76 (complex m, 8H), 1.61 (d, J = 12.9 Hz, 2H), 1.36 (m, 4H), 1.22 (m, 4H), 1.08 (m, 2H) ppm.

^{19}F NMR (564 MHz, $CDCl_3$) δ –144.3 (s, 2F), –147.0 (s, 2F) ppm.

^{13}C NMR (150 MHz, $CDCl_3$) δ 168.3, 145.6 (d, J = 249 Hz), 141.9 (d, J = 249 Hz), 118.8, 114.4, 57.7, 37.8, 31.8, 26.6, 26.2 ppm.

IR (NaCl) 2929, 2853, 2362, 2339, 1684, 1499, 1477, 1296, 1272, 1033, 891, 668 cm^{-1}.

HRESIMS $[M + H]^+$ Found 401.2205. $C_{21}H_{29}F_4N_2O$ requires 401.2211.

_N_-(4-(1-(Dicyclohexylamino)propyl)-2,3,5,6-tetrafluorophenyl)acetamide (4.33)

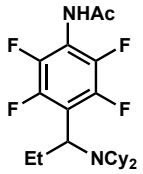

This compound was prepared according to General Procedure 6. Reaction between *N*-(pentafluorophenyl)acetamide (395 μmol) and Cy_2NPr. The ensuing residue obtained from the reaction mixture was subjected to flash column chromatography (silica gel, 0–30% EtOAc/hexane elution; 1% NEt_3 was present in the eluent) to provide the previously unreported compound as a colourless solid (32 mg, 19% yield).

^{1}H NMR (600 MHz, $CDCl_3$) δ 7.07 (bs, 1H), 4.33 (dd, J = 9.2, 6.2, 1H), 2.86 (t, J = 11.5 Hz, 2H), 2.24 (s, 3H), 2.01 (m, 1H), 1.86 (m, 1H), 1.78 (d, J = 11.1 Hz, 2H), 1.68 (t, J = 14.4 Hz, 4H), 1.59 (d, J = 12.2 Hz, 2H), 1.46 (qd, J = 12.2, 3.1 Hz, 2H), 1.37–1.17 (complex m, 8H), 1.05 (qt, J = 12.8, 3.5 Hz, 2H), 0.81 (t, J = 7.3 Hz, 3H) ppm.

^{19}F NMR (564 MHz, $CDCl_3$) δ –140.9 (s, 2F), –146.4 (s, 2F) ppm.

^{13}C NMR (150 MHz, $CDCl_3$) δ 168.2, 145.1 (d, J = 245 Hz), 142.2 (d, J = 249 Hz), 123.3, 113.7, 55.5, 53.7, 34.1, 33.6, 26.9, 26.8, 26.3, 26.0, 11.8 ppm.

IR (NaCl) 3251, 2929, 2853, 1683, 1646, 1520, 1476, 1453, 1371, 1272, 1182, 1134, 1117, 1098, 986, 892, 735 cm^{-1}.

EIMS (*m*/z, relative intensity) 428 (M^+, 1), 181 (8), 138 (100), 56 (50).

_N_-(4-(1-(Diethylamino)propyl)-2,3,5,6-tetrafluorophenyl)acetamide (**4.34**)

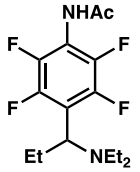

This compound was prepared according to General Procedure 6. Reaction between *N*-(perfluorophenyl)acetamide (500 μmol) and triethylamine {$Gd(OTf)_3$ not added}. *Title compound* **4.34** was formed in 66% yield (average of two experiments) as determined via ^{19}F NMR spectroscopy with the aid of a calibrated internal standard. The ensuing residue obtained from the reaction mixture was subjected to flash column chromatography (silica gel, 0–50% EtOAc/ hexane elution; 1% NEt_3 was present in the eluent) to provide a sample of the previously unreported compound as a colourless solid.

^{1}H NMR (400 MHz, $CDCl_3$) δ 7.25 (bs, 1H), 4.43 (q, J = 7.1 Hz, 1H), 2.72 (sextet, J = 7.2 Hz, 2H), 2.38 (sextet, J = 6.5 Hz, 2H), 2.25 (s, 3H), 1.55 (d, J = 7.3 Hz, 3H), 1.06 (t, J = 6.7 Hz, 6H) ppm.

^{19}F NMR (376 MHz, $CDCl_3$) δ –140.3 (s, 2F), –146.0 (s, 2F) ppm.

^{13}C NMR (150 MHz, $CDCl_3$) δ 168.2, 145.4 (d, J = 246 Hz), 142.3 (d, J = 251 Hz), 118.9, 114.9, 51.4, 43.4, 29.7, 23.0, 17.2, 12.5 ppm.

IR (NaCl) 3254, 2975, 2938, 1684, 1646, 1496, 1472, 1373, 1275, 1102, 982, 944 cm^{-1}.

HRESIMS $[M + H]^+$ Found 307.1424. $C_{14}H_{19}F_4N_2O$ requires 307.1428.

***N*-(2,3,5,6-tetrafluoro-4-((hexadecyl(methyl)amino)methyl)phenyl)acetamide (4.35)**

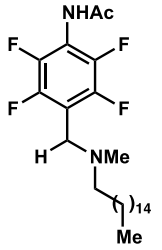

This compound was prepared according to General Procedure 6. Reaction between *N*-(pentafluorophenyl)acetamide (500 μmol) and *N*,*N*-dimethylhexadecan-1-amine. *Title compound* **4.35** was formed in 21% yield (average of two experiments) as determined via ^{19}F NMR spectroscopy with the aid of a calibrated internal standard. The ensuing residue obtained from the reaction mixture was subjected to flash column chromatography (silica gel, 0–30% EtOAc/ hexane elution; 1% NEt_3 was present in the eluent) to provide a sample of the previously unreported compound (+ co-eluting starting material **4.3**) as a colourless solid.

^{1}H NMR (600 MHz, $CDCl_3$) δ 7.17 (bs, 1H), 3.72 (s, 2H), 2.42 (t, J = 7.5 Hz, 2H), 2.25 (s, 6H), 1.53 (t, J = 6.6 Hz, 2H), 1.28 (s, 24H), 0.90 (t, J = 7.1 Hz, 3H) ppm.

^{19}F NMR (564 MHz, $CDCl_3$) δ –139.5, (s, 0.35F), –142.3 (s, 1.65F), –145.7 (s, 0.3F), –146.1 (s, 1.7F) ppm; 4 signals observed (rotamers present).

^{13}C NMR (150 MHz, $CDCl_3$) δ 168.3, 145.5 (d, J = 247 Hz), 142.1 (d, J = 250 Hz), 115.4, 111.8, 61.0, 57.2, 48.1, 41.8, 41.5, 31.9, 29.69, 29.67, 29.66, 29.63, 29.61, 29.56, 29.47, 29.44, 29.36, 27.3, 22.7, 14.1 ppm.

***N*-(2,3,5,6-Tetrafluoro-4-(1-methylpyrrolidin-2-yl)phenyl)acetamide (4.36)**

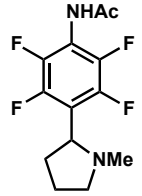

This compound was prepared according to General Procedure 6. Reaction between *N*-(pentafluorophenyl)acetamide (500 μmol) and *N*-methylpyrrolidine. *Title compound* **4.36** was formed in 26% yield (average of two experiments) as determined via ^{19}F NMR spectroscopy with the aid of a calibrated internal standard. The ensuing residue obtained from the reaction mixture was subjected to flash column chromatography (silica gel, 0–60% EtOAc/ hexane

elution; 1% NEt_3 was present in the eluent) to provide a sample of the previously unreported compound as a colourless solid.

^1H NMR (600 MHz, $CDCl_3$) δ 7.65 (bs, 1H), 3.66 (t, J = 8.3 Hz, 1H), 3.22 (t, J = 8.3 Hz, 1H), 2.31 (q, J = 8.8 Hz, 1H), 2.27 (s, 3H), 2.24–2.16 (complex m, 4H), 2.14–2.06 (complex m, 2H), 1.88 (m, 1H) ppm.

^{19}F NMR (564 MHz, $CDCl_3$) δ –143.5 (s, 2F), –146.4 (s, 2F) ppm.

^{13}C NMR (150 MHz, $CDCl_3$) δ 168.8, 145.5 (d, J = 249 Hz), 142.4 (d, J = 249 Hz), 119.3, 115.5 (t, J = 14 Hz), 60.4, 57.3, 40.8, 30.7, 23.6 ppm.

IR (NaCl) 3257, 2975, 2792, 1684, 1525, 1501, 1478, 1373, 1277, 1034, 1002, 985, 937 cm^{-1}.

EIMS (*m*/*z*, relative intensity) 290 (M^+, 25), 84 (100).

_N_-(4-(1-Ethylpyrrolidin-2-yl)-2,3,5,6-tetrafluorophenyl)acetamide (**4.37**)

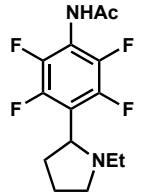

This compound was prepared according to General Procedure 6. Reaction between *N*-(pentafluorophenyl)acetamide (500 μmol) and *N*-ethylpyrrolidine. *Title compound* **4.37** was formed in 34% yield (average of two experiments) as determined via ^{19}F NMR spectroscopy with the aid of a calibrated internal standard. The ensuing residue obtained from the reaction mixture was subjected to flash column chromatography (silica gel, 0–60% EtOAc/ hexane elution; 1% NEt_3 was present in the eluent) to provide a sample of the previously unreported compound (+ co-eluting starting material **4.3**) as a colourless solid.

^1H NMR (600 MHz, $CDCl_3$) δ 7.67 (bs, 1H), 3.81 (t, J = 7.6 Hz, 1H), 3.29 (t, J = 7.6 Hz, 1H), 2.60 (m, 1H), 2.31-2.13 (complex m, 6H), 2.07 (m, 2H), 1.87 (m, 1H), 1.02 (t, J = 7.3 Hz, 3H) ppm.

^{19}F NMR (564 MHz, $CDCl_3$) δ –143.3 (s, 2F), –146.7 (s, 2F) ppm.

^{13}C NMR (150 MHz, $CDCl_3$) δ 169.0, 145.4 (d, J = 247 Hz), 142.2 (d, J = 250 Hz), 120.3, 114.6 (t, J = 14 Hz), 58.9, 53.5, 48.6, 30.6, 23.4, 13.4 ppm.

IR (NaCl) 3254, 3218, 1684, 1652, 1540, 1506, 1471, 1370, 1276, 1149, 1090, 1000, 984, 923 cm^{-1}.

EIMS (*m*/*z*, relative intensity) 304 (M^+, 15), 289 (100), 218 (55), 178 (35), 98 (60).

N-(4-(1-Decylpyrrolidin-2-yl)-2,3,5,6-tetrafluorophenyl)acetamide (4.38)

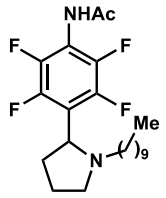

This compound was prepared according to General Procedure 6. Reaction between *N*-(pentafluorophenyl)acetamide (500 μmol) and *N*-decylpyrrolidine. *Title compound* **4.38** was formed in 50% yield (average of two experiments) as determined via ^{19}F NMR spectroscopy with the aid of a calibrated internal standard. The ensuing residue obtained from the reaction mixture was subjected to flash column chromatography (silica gel, 10–60% EtOAc/ hexane elution; 1% NEt_3 was present in the eluent) to provide a sample of the previously unreported compound as a colourless solid.

^{1}H NMR (600 MHz, $CDCl_3$) δ 7.01 (bs, 1H), 3.70 (t, J = 7.6 Hz, 1H), 3.20 (t, J = 8.2 Hz, 1H), 2.39 (m, 1H), 2.21–2.04 (complex m, 6H), 1.97 (m, 2H), 1.77 (d, J = 9.1 Hz, 1H), 1.31 (quin, J = 6.7 Hz, 2H), 1.23–1.07 (complex m, 14H), 0.80 (t, J = 7.5 Hz, 3H) ppm.

^{19}F NMR (564 MHz, $CDCl_3$) δ –143.2 (s, 2F), –146.8 (s, 2F) ppm.

^{13}C NMR (150 MHz, $CDCl_3$) δ 168.3, 145.5 (d, J = 249 Hz), 142.2 (d, J = 250 Hz), 120.6, 114.5, 59.2, 54.9, 53.9, 31.9, 30.7, 29.57, 29.56, 29.4, 29.3, 28.6, 27.4, 23.5, 22.7, 14.1 ppm.

IR (NaCl) 3225, 2927, 2855, 2793, 1683, 1652, 1531, 1501, 1475, 1456, 1277, 1147, 1093, 997, 983 cm^{-1}.

EIMS (*m*/*z*, relative intensity) 416 (M^+, 2), 289 (100), 218 (24), 178 (14).

N-(2,3,5,6-Tetrafluoro-4-(1-isopropylpyrrolidin-2-yl)phenyl)acetamide (4.39)

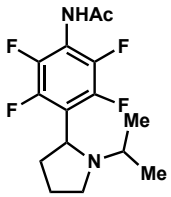

This compound was prepared according to General Procedure 6. Reaction between *N*-(pentafluorophenyl)acetamide (400 μmol) and *N*-isopropylpyrrolidine. *Title compound* **4.39** was formed in 17% yield (average of two experiments) as determined via ^{19}F NMR spectroscopy with the aid of a calibrated internal standard. The ensuing residue obtained from the reaction mixture was subjected to flash column chromatography (silica gel, 30–60%

EtOAc/ hexane elution; 1% NEt_3 was present in the eluent) to provide a sample of the previously unreported compound (+ co-eluting starting material **4.3**) as a colourless solid.

^{1}H NMR (600 MHz, $CDCl_3$) δ 7.73 (bs, 1H), 4.20 (t, J = 6.9 Hz, 1H), 3.10 (t, J = 8.3 Hz, 1H), 2.79 (quin, J = 6.5 Hz, 1H), 2.60 (q, J = 7.9 Hz, 1H), 2.25-2.13 (complex m, 4H), 2.02 (m, 2H), 1.82 (m, 1H), 1.02 (d, J = 6.6 Hz, 3H), 0.96 (d, J = 6.3 Hz, 3H) ppm.

^{19}F NMR (564 MHz, $CDCl_3$) δ –143.6 (s, 2F), –146.8 (s, 2F) ppm.

^{13}C NMR (150 MHz, $CDCl_3$) δ 169.0, 145.3 (d, J = 247 Hz), 142.3 (d, J = 250 Hz), 121.6, 114.5 (t, J = 14 Hz), 54.5, 50.0, 47.4, 31.6, 23.8, 21.5, 16.0 ppm.

IR (NaCl) 3242, 2970, 2937, 1684, 1521, 1501, 1476, 1456, 1277, 992,cm^{-1}.

EIMS (*m*/z, relative intensity) 318 (M^+, 10), 303 (100), 218 (70), 178 (20).

_N_-(4-(((2-(Dimethylamino)ethyl)(methyl)amino)methyl)-2,3,5,6-tetrafluorophenyl)acetamide (**4.40**)

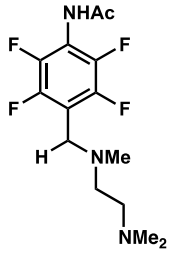

This compound was prepared according to General Procedure 6. Reaction between *N*-(pentafluorophenyl)acetamide (500 μmol) and TMEDA {$Gd(OTf)_3$ not added}. *Title compound* **4.40** was formed in 67% yield (average of two experiments) as determined via ^{19}F NMR spectroscopy with the aid of a calibrated internal standard. The ensuing residue obtained from the reaction mixture was dissolved in CH_2Cl_2 (10 mL) and HCl (10 mL of a 2 M aqueous solution) was added. The aqueous phase was washed with CH_2Cl_2 (3x 10 mL) then treated with K_2CO_3 (saturated aqueous solution) until pH >7. The aqueous phase was then extracted with CH_2Cl_2 (3x 10 mL) to provide a sample of the previously unreported compound as a pale yellow solid.

^{1}H NMR (600 MHz, $CDCl_3$) δ 8.39 (bs, 1H), 3.65 (s, 2H), 2.49 (t, J = 7.0 Hz, 2H), 2.42 (t, J = 6.3 Hz, 2H), 2.21 (s, 6H), 2.16 (s, 3H), 2.12 (s, 3H) ppm.

^{19}F NMR (564 MHz, $CDCl_3$) δ –142.7 (s, 2F), –145.9 (s, 2F) ppm.

^{13}C NMR (150 MHz, $CDCl_3$) δ 169.1, 145.4 (d, J = 245 Hz), 142.2 (d, J = 250 Hz), 115.9 (t, J = 14 Hz), 113.8 (t, J = 18 Hz), 57.0, 54.5, 48.4, 45.5, 41.5, 22.7 ppm.

IR (NaCl) 3200, 2951, 2826, 1700, 1481, 1371, 1295, 1276, 1136, 1124, 1026, 910 cm^{-1}.

EIMS (*m*/*z*, relative intensity) 321 (M^+, 1), 263 (11), 178 (20), 58 (100).

_N_-(4-(((3-(Dimethylamino)propyl)(methyl)amino)methyl)-2,3,5,6-tetrafluorophenyl)acetamide (**4.41**)

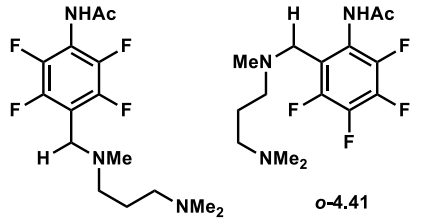

p-4.41 *o*-4.41

These compounds were prepared according to General Procedure 6. Reaction between *N*-(pentafluorophenyl)acetamide (500 μmol) and *N*,*N*,*N*′,*N*′-tetramethylpropane-1,3-diamine {$Gd(OTf)_3$ not added}. Compound ***p*-4.41** was formed in 60% yield (average of two experiments) and compound ***o*-4.41** was formed in 6% yield (average of two experiments) as determined via ^{19}F NMR spectroscopy with the aid of a calibrated internal standard. The ensuing residue obtained from the reaction mixture was dissolved in CH_2Cl_2 (10 mL) and HCl (10 mL of a 2 M aqueous solution) was added. The aqueous phase was washed with CH_2Cl_2 (3x 10 mL) then treated with K_2CO_3 (saturated aqueous solution) until pH >7. The aqueous phase was then extracted with CH_2Cl_2 (3 x 10 mL) to provide a sample of the previously unreported compound ***p*-4.41** (which contained traces of compound ***o*-4.41**) as a pale yellow solid.

^{1}H NMR (600 MHz, $CDCl_3$) δ 8.50 (bs, 1H), 3.66 (s, 1.5H), 3.60 (s, 0.5H) 2.41 (t, J = 7.3 Hz, 2H), 2.31 (t, J = 7.7 Hz, 2H), 2.22 (s, 6H), 2.19 (s, 6H), 1.67 (t, J = 7.4 Hz, 2H) ppm; 8 signals observed (rotamers present).

^{19}F NMR (564 MHz, $CDCl_3$) δ –142.9 (s, 1.5F), –143.3 (s, 0.5F) –146.1 (s, 1.5F), –146.3 (s, 0.5F) ppm; 4 signals observed (rotamers present).

^{13}C NMR (150 MHz, $CDCl_3$) δ 169.0, 145.4 (d, J = 246 Hz), 142.2 (d, J = 251 Hz), 115.8 (t, J = 14 Hz), 114.3 (t, J = 17 Hz), 57.6, 55.1, 48.0, 45.3, 41.5, 25.4, 22.7 ppm.

IR (NaCl) 3205, 2450, 2793, 1688, 1527, 1483, 1371, 1295, 1277, 1124, 1029, 910 cm^{-1}.

EIMS (*m*/z, relative intensity) 335 (M^+, 1), 263 (5), 178 (25), 115 (30), 58 (100).

_N_-(4-(((2-(Dimethylamino)butyl)(methyl)amino)methyl)-2,3,5,6-tetrafluorophenyl)acetamide (**4.42**)

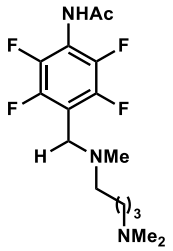

***p*-4.42**

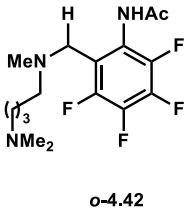

***o*-4.42**

These compounds were prepared according to General Procedure 6. Reaction between *N*-(pentafluorophenyl)acetamide (500 μmol) and *N*,*N*,*N*′,*N*′-tetramethylbutane-1,4-diamine {$Gd(OTf)_3$ not added}. Compound ***p*-4.42** was formed in 45% yield (average of two experiments) and compound ***o*-4.42** was formed in 3% yield (average of two experiments) as determined via ^{19}F NMR spectroscopy with the aid of a calibrated internal standard. The ensuing residue obtained from the reaction mixture was dissolved in CH_2Cl_2 (10 mL) and HCl (10 mL of a 2 M aqueous solution) was added. The aqueous phase was washed with CH_2Cl_2 (3x 10 mL) then treated with K_2CO_3 (saturated aqueous solution) until pH >7. The aqueous phase was then extracted with CH_2Cl_2 (3 x 10 mL) to provide a sample of the previously unreported compound ***p*-4.42** (which contained traces of compound ***o*-4.42**) as a pale yellow solid.

^1H NMR (600 MHz, $CDCl_3$) δ 8.25 (bs, 1H), 3.67 (s, 2H), 2.40 (t, J = 6.5 Hz, 2H), 2.31 (m, 2H), 2.24 (s, 3H), 2.21 (s, 6H), 2.19 (s, 3H), 1.50 (m, 4H) ppm.

^{19}F NMR (564 MHz, $CDCl_3$) δ –139.8 (s, 0.7H), –142.8 (s, 1.3F), –145.6 (s, 0.7F), –146.1 (s, 1.4F) ppm; 4 signals observed (rotamers present).

^{13}C NMR (150 MHz, $CDCl_3$) δ 168.8, 145.5 (d, J = 247 Hz), 142.2 (d, J = 250 Hz), 115.6, 114.5, 60.8, 59.5, 59.4, 56.8, 48.1, 45.3, 45.1, 41.8, 41.5, 28.8, 25.2, 25.0, 22.8 ppm.

IR (NaCl) 3199, 2947, 2865, 1680, 1516, 1501, 1371, 1275, 1126, 1029, 909 cm^{-1}.

EIMS (*m*/z, relative intensity) 349 (M^+, 1), 284 (6), 221 (10), 71 (100).

***N*-(4-(((2-(Dimethylamino)hexyl)(methyl)amino)methyl)-2,3,5,6-tetrafluorophenyl)acetamide** (**4.43**)

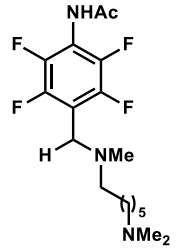

p-**4.43**

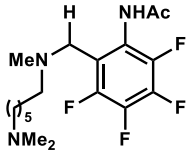

o-**4.43**

These compounds were prepared according to General Procedure 6. Reaction between *N*-(pentafluorophenyl)acetamide (500 μmol) and *N*,*N*,*N*′,*N*′-tetramethylhexane-1,6-diamine {$Gd(OTf)_3$ not added}. Compound ***p*-4.43** was formed in 65% yield (average of two experiments) and compound ***o*-4.43** was formed in 7% yield (average of two experiments) as determined via ^{19}F NMR spectroscopy with the aid of a calibrated internal standard. The ensuing residue obtained from the reaction mixture was dissolved in CH_2Cl_2 (10 mL) and HCl (10 mL of a 2 M aqueous solution) was added. The aqueous phase was washed with CH_2Cl_2 (3 x 10 mL) then treated with K_2CO_3 (saturated aqueous solution) until pH >7. The aqueous phase was then extracted with CH_2Cl_2 (3 x 10 mL) to provide a sample of the previously unreported compound ***p*-4.43** (which contained traces of compound ***o*-4.43**) as a pale yellow solid.

^1H NMR (600 MHz, $CDCl_3$) δ 8.15 (bs, 1H), 3.68 (s, 2H), 2.39 (t, J = 7.4 Hz, 2H), 2.29 (m, 2H), 2.27 (s, 6H), 2.24 (s, 3H), 2.23 (s, 3H), 1.46 (m, 4H), 1.29 (m, 4H) ppm.

^{19}F NMR (564 MHz, $CDCl_3$) δ –142.8 (s, 2F), –146.2 (s, 2F) ppm.

^{13}C NMR (150 MHz, $CDCl_3$) δ 168.7, 145.5 (d, J = 247 Hz), 142.3 (d, J = 250 Hz), 115.7 (t, J = 16 Hz), 114.8 (t, J = 17 Hz), 59.6, 56.7, 48.3, 45.1, 41.9, 27.33, 27.29, 27.2, 27.1 ppm.

IR (NaCl) 3209, 2939, 2859, 1679, 1525, 1476, 1448, 1274, 1030 cm^{-1}.

EIMS (*m*/*z*, relative intensity) 377 (M^+, 1), 178 (26), 157 (12), 126 (19), 112 (38) 58 (100).

***N*-(4-(1-(Diisopropylamino)ethyl)-2,3,5,6-tetrafluorophenyl)nonanamide** (**4.44**)

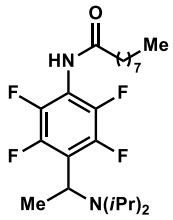

This compound was prepared according to General Procedure 6. Reaction between *N*-(pentafluorophenyl)nonanamide (500 μmol) and *i*Pr$_2$NEt. Title compound **4.44** was formed in 63% yield (average of two experiments) as determined via ^{19}F NMR spectroscopy with the aid of a calibrated internal standard. The ensuing residue obtained from the reaction mixture was subjected to flash column chromatography (silica gel, 0–30% EtOAc/ hexane elution; 1% NEt$_3$ was present in the eluent) to provide a sample of the previously unreported compound (+ co-eluting starting material) as a colourless solid.

^{1}H NMR (400 MHz, CDCl$_3$) δ 7.12 (bs, 1H), 4.65 (q, J = 7.2 Hz, 1H), 3.36 (sept, J = 6.7 Hz, 2H), 2.43 (t, J = 7.2 Hz, 2H), 1.73 (quin, J = 7.4 Hz, 3H), 1.51 (d, J = 7.1 Hz, 3H), 1.30 (complex m, 15 H), 1.12 (d, J = 6.6 Hz, 6H), 0.94 (d, J = 6.6 Hz, 6H), 0.90 (t, J = 6.6 Hz, 5H) ppm; 44 protons observed (starting material present).

^{19}F NMR (376 MHz, CDCl$_3$) δ –142.3 (d, J = 12 Hz, 2F), –146.6 (d, J = 22 Hz, 2F) ppm.

^{13}C NMR (150 MHz, CDCl$_3$) δ 171.9, 145.0 (d, J = 241 Hz), 142.3 (d, J = 253 Hz), 124.5, 113.8 (t, J = 14 Hz), 46.1, 45.8, 31.9, 29.4, 29.3, 29.2, 25.6, 22.81, 22.76, 22.6, 19.8, 14.2 ppm.

HRESIMS Found [M + H]$^+$, 433.2840. $C_{23}H_{37}F_4N_2O$ requires 433.2837.

N*-(4-(1-(Diisopropylamino)ethyl)-2,3,5,6-tetrafluorophenyl)-2-phenylacetamide** (p*-4.45**) **&** ***N*-(2-(1-(Diisopropylamino)ethyl)-3,4,5,6-tetrafluorophenyl)-2-phenylacetamide** (***o*-4.45**)

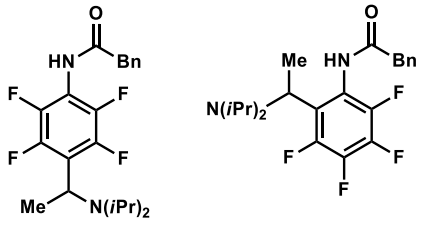

***p*-4.45** ***o*-4.45**

These compounds were prepared according to General Procedure 6. Reaction between *N*-(pentafluorophenyl)-2-phenylacetamide (500 μmol) and *i*Pr$_2$NEt . Compound ***p*-4.45** was formed in 80% yield (average of two experiments) and compound ***o*-4.45** was formed in 5%

yield (average of two experiments) as determined via ^{19}F NMR spectroscopy with the aid of a calibrated internal standard. The ensuing residue obtained from the reaction mixture was subjected to flash column chromatography (silica gel, 0–30% EtOAc/ hexane elution; 1% NEt_3 was present in the eluent) to provide the previously unreported compound ***p*-4.45** as a colourless solid (which contained traces of compound ***o*-4.45**).

^1H NMR (600 MHz, $CDCl_3$) δ 7.31–7.21 (complex m, 5H), 6.94 (bs, 1H), 4.54 (q, J = 7.1 Hz, 1H), 3.69 (s, 2H), 3.25 (sept, J = 6.7 Hz, 2H), 1.39 (d, J = 7.5 Hz, 3H), 1.01 (d, J = 7.0 Hz, 6H), 0.82 (d, J = 7.0 Hz, 6H) ppm.

^{19}F NMR (564 MHz, $CDCl_3$) δ –124.8 (s, 0.13F), –135.9 (d, J = 22Hz, 0.13F), –141.0 (d, J = 20 Hz, 0.13F), –142.2 (d, J = 13 Hz, 2F), –146.5 (d, J = 24 Hz, 2F), –164.3 (td, J = 21, 8.4 Hz, 0.12F) ppm.

^{13}C NMR (150 MHz, $CDCl_3$) δ 169.5, 144.8 (d, J = 243 Hz), 142.2 (d, J = 250 Hz), 134.0, 129.4, 129.2, 127.8, 124.6 (t, J = 17 Hz), 113.6 (t, J = 15 Hz), 45.9, 45.6, 43.4, 22.7, 22.4, 19.6 ppm.

IR (NaCl) 2927, 2854, 1733, 1514, 1450, 1357, 1287, 1163, 1092, 996 cm^{-1}.

HRESIMS $[M + H]^+$ Found 411.2045. $C_{22}H_{27}F_4N_2O$ requires 411.2060.

_N_-(4-(1-(Diisopropylamino)ethyl)-2,3,5,6-tetrafluorophenyl)-2-(4-fluorophenyl)acetamide (4.46)

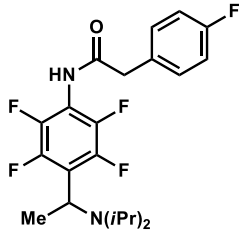

This compound was prepared according to General Procedure 6. Reaction between 2-(4-fluorophenyl)-*N*-(pentafluorophenyl)acetamide (500 μmol) and iPr$_2$NEt. Title compound **4.46** was formed in 86% yield (average of two experiments) as determined via ^{19}F NMR spectroscopy with the aid of a calibrated internal standard. The ensuing residue obtained from the reaction mixture was subjected to flash column chromatography (silica gel, 0–20% EtOAc/ hexane elution; 1% NEt_3 was present in the eluent) to provide a sample of the previously unreported compound as a colourless solid.

^1H NMR (600 MHz, $CDCl_3$) δ 7.34 (t, J = 5.7 Hz, 2H), 7.09 (t, J = 8.8 Hz, 2H), 6.92 (bs, 1H), 4.65 (q, J = 8.0 Hz, 1H), 3.78 (s, 2H), 3.35 (sept, J = 7.0 Hz. 2H), 1.50 (d, J = 6.8 Hz, 3H), 1.11 (d, J = 6.8 Hz, 6H), 0.92 (d, J = 6.8 Hz, 6H) ppm.

^{19}F NMR (564 MHz, $CDCl_3$) δ –114.4 (s, 1F), –142.1 (s, 2F), –146.5 (d, J = 13 Hz, 2F) ppm.

^{13}C NMR (150 MHz, $CDCl_3$) δ 169.2, 163.2, 161.5, 144.8 (d, J = 245 Hz), 142.3 (d, J = 250 Hz), 131.1 (d, J = 8 Hz), 129.7 (d, J = 3 Hz), 124.8 (t, J = 16 Hz), 116.1 (d, J = 21 Hz), 113.4 (t, J = 15 Hz), 46.0, 45.7, 42.5, 22.7, 22.4, 19.6 ppm.

IR (NaCl) 3245, 2971, 2936, 1675, 1648, 1511, 1476, 1197, 1228, 1158, 1005, 948, 839 cm^{-1}.

EIMS (*m*/z, relative intensity) 428 (M^+, 3), 413 (20), 192 (83), 109 (50), 86 (100).

_N_-(4-(1-(Diisopropylamino)ethyl)-2,3,5,6-tetrafluorophenyl)pent-4-enamide (**4.47**)

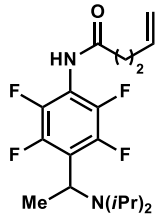

This compound was prepared according to General Procedure 6. Reaction between *N*-(pentafluorophenyl)pent-4-enamide (500 μmol) and *i*Pr$_2$NEt. *Title compound* **4.47** was formed in 64% yield (average of two experiments) as determined via ^{19}F NMR spectroscopy with the aid of a calibrated internal standard. The ensuing residue obtained from the reaction mixture was subjected to flash column chromatography (silica gel, 0–30% EtOAc/ hexane elution; 1% NEt_3 was present in the eluent) to provide a sample of the previously unreported compound as a colourless solid.

^{1}H NMR (600 MHz, $CDCl_3$) δ 7.04 (bs, 1H), 5.82 (m, 1H), 5.07 (d, J = 17 Hz, 1H), 5.01 (d, J = 9.8 Hz, 1H), 4.56 (q, J = 7.3 Hz, 1H), 3.28 (sept, J = 6.7 Hz, 2H), 2.51–2.40 (complex m, 4H), 1.42 (d, J = 7.4 Hz, 3H), 1.03 (d, J = 6.8 Hz, 6H), 0.86 (d, J = 6.8 Hz, 6H) ppm.

^{19}F NMR (564 MHz, $CDCl_3$) δ –142.2 (bs, 2F), –146.5 (d, J = 24Hz, 2F) ppm.

^{13}C NMR (150 MHz, $CDCl_3$) δ 170.5, 144.8 (d, J = 245 Hz), 142.1 (d, J = 250 Hz), 136.4, 124.5 (t, J = 16 Hz), 116.3, 113.6 (t, J = 14 Hz), 46.0, 45.7, 35.5, 29.3, 22.7, 22.4, 19.7 ppm.

IR (neat) 2971, 1671, 1524, 1476, 1399, 1363, 1290, 1212, 1152, 1084, 1004, 944, 914 cm^{-1}.

HRESIMS $[M + H]^+$ Found 375.2055. $C_{19}H_{27}F_4N_2O$ requires 375.2054.

***N*-(4-(1-(Diisopropylamino)ethyl)-2,3,5,6-tetrafluorophenyl)benzamide (4.48)**

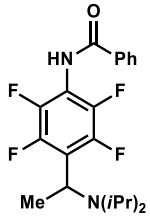

This compound was prepared according to General Procedure 6. Reaction between *N*-(pentafluorophenyl)benzamide (557 μmol) and *i*Pr$_2$NEt. The ensuing residue obtained from the reaction mixture was subjected to flash column chromatography (silica gel, 0–10% EtOAc/hexane elution; 1% NEt$_3$ was also present in the eluent) to provide the previously unreported compound as a colourless solid (102 mg, 46% yield).

^{1}H NMR (600 MHz, CDCl$_3$) δ 7.81 (d, J = 7.7 Hz, 2H), 7.62 (bs, 1H), 7.49 (t, J = 7.3 Hz, 1H), 7.39 (t, J = 7.7 Hz, 2H), 4.78 (q, J = 6.4 Hz, 1H), 3.28 (sept, J = 6.7 Hz, 2H), 1.43 (d, J = 7.3 Hz, 3H), 1.03 (d, J = 6.6 Hz, 6H), 0.86 (d, J = 6.6 Hz, 6H) ppm.

^{19}F NMR (564 MHz, CDCl$_3$) δ –142.1 (d, J = 21 Hz, 2F), –146.3 (d, J = 21 Hz, 2F) ppm.

^{13}C NMR (150 MHz, CDCl$_3$) δ 165.7, 144.9 (d, J = 245 Hz), 142.3 (d, J = 251 Hz), 132.8, 132.6, 128.8, 127.7, 124.4 (t, J = 17 Hz), 114.0 (t, J = 15 Hz), 16.0, 45.7, 22.7, 19.7 ppm.

IR (neat) 3299, 2968, 1672, 1466, 972 cm^{-1}.

HRESIMS [M + H]$^+$ Found 397.1900. $C_{21}H_{25}F_4N_2O$ requires 397.1898.

***N*-(4-(1-(Diisopropylamino)ethyl)-2,3,5,6-tetrafluorophenyl)-3,5-bis(trifluoromethyl)benzamide (4.49)**

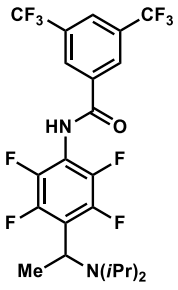

This compound was prepared according to General Procedure 6. Reaction with *N*-(Pentafluorophenyl)-3,5-bis(trifluoromethyl)benzamide (40 μmol). *Title compound* **4.49** was formed in 25% yield (average of two experiments) as determined via ^{19}F NMR spectroscopy with the aid of a calibrated internal standard.

^{19}F NMR (564 MHz, CDCl$_3$) δ –63.5 (s, 6F), –140.1 (quin, J = 11 Hz, 2F), –145.8 (m, 2F) ppm.

EIMS (*m*/z, relative intensity) 532 (M^+, 3), 517 (27), 432 (19), 241 (68), 213 (14), 86 (100).

HREIMS [M^+] Found 532.1580. $C_{23}H_{22}F_{10}N_2O$ requires 532.1572.

tert-Butyl (4-(1-(diisopropylamino)ethyl)-2,3,5,6-tetrafluorophenyl)carbamate (**4.50**)

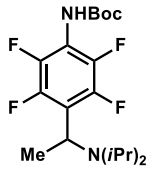

This compound was prepared according to General Procedure 6. Reaction between *tert*-butyl (pentafluorophenyl)carbamate (326 μmol) and *i*Pr$_2$NEt. The ensuing residue obtained from the reaction mixture was subjected to flash column chromatography (silica gel, 0–15% EtOAc/hexane elution; 1% NEt$_3$ was present in the eluent) to provide the previously unreported compound as a colourless solid (110 mg, 86% yield).

^{1}H NMR (600 MHz, CDCl$_3$) δ 6.00 (bs, 1H), 4.65 (q, J = 7.2 Hz, 1H), 3.37 (sept, J = 6.6 Hz, 2H), 1.53 (s, 9H), 1.51 (d, J = 7.3 Hz, 3H), 1.12 (d, J = 6.5 Hz, 6H), 0.95 (d, J = 6.9 Hz, 6H) ppm.

^{19}F NMR (564 MHz, CDCl$_3$) δ –142.5 (dd, J = 22.4, 9.1 Hz, 2F), –148.1 (dd, J = 22.4, 9.6 Hz, 2F) ppm.

^{13}C NMR (150 MHz, CDCl$_3$) δ 152.3, 144.8 (d, J = 244 Hz), 142.2 (d, J = 249 Hz), 123.6 (t, J = 18Hz), 114.5 (t, J = 16 Hz), 81.9, 45.9, 45.6, 28.1, 22.6, 22.5, 19.7 ppm.

IR (neat) 3272, 2972, 1711, 1524, 1475, 1298, 1154, 960, 951, 858 cm^{-1}.

HRESIMS [M + H]$^+$ Found 393.2157. $C_{19}H_{29}F_4N_2O_2$ requires 393.2160.

4-(1-(Diisopropylamino)ethyl)-2,3,5,6-tetrafluorophenylamine (***p*-4.51**)

& 2-(1-(Diisopropylamino)ethyl)-3,4,5,6-tetrafluorophenylamine (***o*-4.51**)

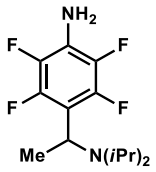

***p*-4.51**

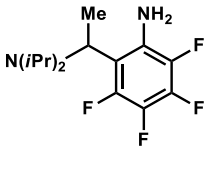

***o*-4.51**

These compounds were prepared according to General Procedure 6. Reaction between pentafluoroaniline (500 μmol) and *i*Pr$_2$NEt. The ensuing residue obtained from the reaction mixture was subjected to flash column chromatography (silica gel, 0–15% EtOAc/ hexane

elution; 1% NEt_3 was present in the eluent) to provide the previously unreported compounds as a colourless oil (90 mg, 1.4:1 mixture of ***p*-4.51** : ***o*-4.51**, 62% yield).

4-(1-(Diisopropylamino)ethyl)-2,3,5,6-tetrafluorophenylamine (***p*-4.51**)

^{1}H NMR (600 MHz, $CDCl_3$) δ 4.46 (q, J = 7.3 Hz, 1H), 3.75 (bs, 2H), 3.25 (sept, J = 6.6 Hz, 2H), 1.39 (d, J = 7.2 Hz, 3H), 1.02 (d, J = 6.7 Hz, 6H), 0.85 (d, J = 6.8 Hz, 6H) ppm.

^{19}F NMR (564 MHz, $CDCl_3$) δ –144.1 (d, J = 22 Hz, 2F), –162.4 (d, J = 23 Hz, 2F) ppm.

HRESIMS $[M + H]^+$ Found 293.1634. $C_{14}H_{21}F_4N_2$ requires 293.1635.

***N*-Isopropyl-*N*-(1-(2,3,5,6-tetrafluoro-4-(4-methoxyphenoxy)phenyl)ethyl)propan-2-amine** (**4.52**)

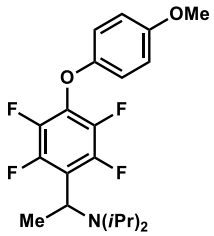

This compound was prepared according to General Procedure 6. Reaction between 1,2,3,4,5-pentafluoro-6-(4-methoxyphenoxy)benzene (400 μmol) and iPr$_2$NEt. *Title compound* **4.52** was formed in 28% yield (average of two experiments) as determined via ^{19}F NMR spectroscopy with the aid of a calibrated internal standard. The ensuing residue obtained from the reaction mixture was subjected to flash column chromatography (silica gel, 0–30% EtOAc/ hexane elution; 1% NEt_3 was present in the eluent) to provide a sample of the previously unreported compound (+ co-eluting starting material) as a colourless solid.

^{1}H NMR (600 MHz, $CDCl_3$) δ 6.85 (m, 2H), 6.77 (m, 2H), 4.57 (q, J = 7.4 Hz, 1H), 3.70 (s, 3H), 3.28 (sept, J = 6.8 Hz, 2H), 2.45 (d, J = 7.4 Hz, 3H), 1.04 (d, J = 6.8 Hz, 6H), 0.87 (d, J = 6.8 Hz, 6H) ppm.

^{19}F NMR (564 MHz, $CDCl_3$) δ –142.6 (d, J = 22 Hz, 2F), –156.5 (d, J = 24 Hz, 2F) ppm.

^{13}C NMR (150 MHz, $CDCl_3$) δ 157.8, 151.4, 145.2 (d, J = 246 Hz), 141.5 (d, J = 253 Hz), 132.2 (t, J = 13 Hz), 121.9 (t, J = 17 Hz), 55.7, 45.9, 45.7, 22.7, 22.4, 19.8 ppm.

HRESIMS $[M + H]^+$ Found 400.1890. $C_{21}H_{25}F_4NO_2$ requires 400.1894.

***N*-Isopropyl-*N*-(1-(1,3,4-trifluorodibenzo[*b*,*e*][1,4]dioxin-2-yl)ethyl)propan-2-amine (*p*-4.53)**

& *N*-Isopropyl-*N*-(1-(2,3,4-trifluorodibenzo[*b*,*e*][1,4]dioxin-1-yl)ethyl)propan-2-amine (*m*-4.53)

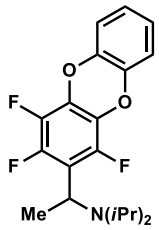

p-4.53

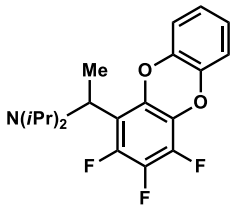

o-4.53

These compounds were prepared according to General Procedure 6. Reaction between 1,2,3,4-tetrafluorodibenzo[*b*,*e*][1,4]dioxine (400 μmol) and *i*Pr$_2$NEt. Compound ***p*-4.53** was formed in 48% yield (average of two experiments) and compound ***m*-4.53** was formed in 9% yield (average of two experiments) as determined via ^{19}F NMR spectroscopy with the aid of a calibrated internal standard. The ensuing residue obtained from the reaction mixture was subjected to flash column chromatography (silica gel, 0–15% EtOAc/ hexane elution; 1% NEt$_3$ was present in the eluent) to provide a sample of the previously unreported compound ***p*-4.53** (which contained traces of compound ***m*-4.53**) as a colourless solid.

^{1}H NMR (600 MHz, CDCl$_3$) δ 6.90–6.81 (m, 4H), 4.58 (q, J = 7.3 Hz, 1H), 3.37 (sept, J = 6.8 Hz, 2H), 1.50 (d, J = 7.0 Hz, 3H), 1.12 (d, J = 6.7 Hz, 6H), 0.97 (d, J = 6.6 Hz, 6H) ppm.

^{19}F NMR (564 MHz, CDCl$_3$) δ –141.2 (d, J = 9.5 Hz, 1F), –144.2 (d, J = 23 Hz, 1F),–163.9 (dd, J = 23, 9.8 Hz, 1F) ppm.

^{13}C NMR (150 MHz, CDCl$_3$) δ 145.5 (d, J = 237 Hz), 144.7 (d, J = 242 Hz), 141.0 (d, J = 62 Hz), 138.7 (d, J = 250 Hz), 136.9 (J = 250 Hz), 131.0 (t, J = 4.9 Hz), 124.8 (d, J = 34 Hz), 119.3 (td, J = 17, 2.6 Hz), 116.8 (d, J = 11 Hz), 45.7, 45.6, 22.9, 22.5, 20.0 ppm; 14 signals observed.

HRESIMS $[M + H]^+$ Found 366.1670. $C_{20}H_{23}F_3NO_2$ requires 366.1675.

Methyl 8-(1-(diisopropylamino)ethyl)-6,7,9-trifluorodibenzo[*b*,*e*][1,4]dioxine-2-carboxylate (**4.54**)

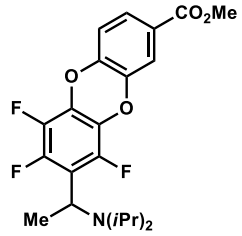

This compound was prepared according to General Procedure 6. Reaction between methyl 6,7,8,9-tetrafluorodibenzo[*b*,*e*][1,4]dioxine-2-carboxylate (500 μmol) and *i*Pr$_2$NEt. *Title compound* **4.54** was formed in 71% yield (average of two experiments) as determined via ^{19}F NMR spectroscopy with the aid of a calibrated internal standard. The ensuing residue obtained from the reaction mixture was subjected to flash column chromatography (silica gel, 0–10% EtOAc/ hexane elution; 1% NEt$_3$ was present in the eluent) to provide a sample of the previously unreported compound as a colourless solid.

^{1}H NMR (600 MHz, CDCl$_3$) δ 7.70–7.67 (m, 1H), 7.65–7.63 (m, 1H), 7.02–6.97 (m, 1H), 4.58 (qd, J = 7.20, 2.00 Hz, 1H), 3.91 (s, 3H), 3.36 (sept, J = 6.69 Hz, 2H), 1.50 (d, J = 7.2 Hz, 3H), 1.12 (d, J = 6.7 Hz, 6H), 0.97 (d, J = 6.8 Hz, 6H) ppm.

^{19}F NMR (564 MHz, CDCl$_3$) δ –141.3 (d, J = 29 Hz, 1F), –144.3 (dd, J = 223, 22 Hz, 1F), –164.4 (t, J = 26 Hz, 1F) ppm.

^{13}C NMR (150 MHz, CDCl$_3$) δ 165.4, 145.0 (d, J = 244 Hz), 144.4, 143.9 (d, J = 244 Hz), 140.5, 136.3 (d, J = 249 Hz), 130.3 (dt, J = 12.7, 4.8 Hz), 127.1, 126.8, 119.8 (td, J = 17, 2.5 Hz), 118.3, 117.1 (dd, J = 233, 16 Hz), 116.7, 52.3, 45.7, 45.6, 22.7, 22.5, 19.9 ppm.

HRESIMS $[M + H]^+$ Found 424.1729. $C_{22}H_{25}F_3NO_4$ requires 424.1730.

(8-(1-(Diisopropylamino)ethyl)-6,7,9-trifluorodibenzo[*b*,*e*][1,4]dioxin-2-yl)methanol (***p*-4.55**)

(9-(1-(Diisopropylamino)ethyl)-6,7,8-trifluorodibenzo[*b*,*e*][1,4]dioxin-2-yl)methanol (***m*-4.55**)

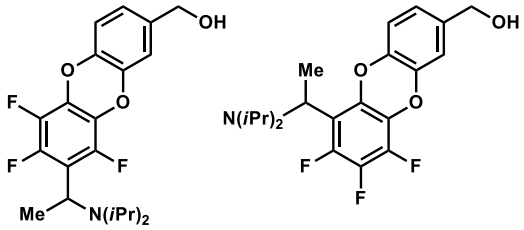

***p*-4.55** ***o*-4.55**

These compounds were prepared according to General Procedure 6. Reaction between (6,7,8,9-tetrafluorodibenzo[*b*,*e*][1,4]dioxin-2-yl)methanol (500 μmol) and *i*Pr$_2$NEt. Compound ***p*-4.55** was formed in 53% yield (average of two experiments) and compound ***m*-4.55** was formed in 9% yield (average of two experiments) as determined via ^{19}F NMR spectroscopy with the aid of a calibrated internal standard. The ensuing residue obtained from the reaction mixture was subjected to flash column chromatography (silica gel, 0–30% EtOAc/ hexane elution; 1% NEt$_3$ was present in the eluent) to provide a sample of the previously unreported compound ***p*-4.55** (which contained traces of compound ***m*-4.55**) as a colourless solid.

^{1}H NMR (600 MHz, CDCl$_3$) δ 7.01–6.86 (complex m, 3H), 4.62–4.55 (complex m, 3H), 3.36 (sept, J = 6.4 Hz, 2H), 2.15 (bs, 1H), 1.50 (d, J = 7.0 Hz, 3H), 1.12 (d, J = 6.7 Hz, 6H), 0.97 (d, J = 6.7 Hz, 6H) ppm.

^{19}F NMR (564 MHz, CDCl$_3$) δ –141.1 (dd, J = 31, 9 Hz, 1F), –144.1 (dd, J = 23, 11 Hz, 1F), –163.8 (qd, J = 21, 9 Hz, 1F) ppm.

^{13}C NMR (150 MHz, CDCl$_3$) δ 144.7 (d, J = 242 Hz), 144.0 (d, J = 243 Hz), 140.7, 140.2, 140.0, 139.6, 138.1, 137.9, 136.3, (d, J = 247 Hz), 130.8 (m), 128.1 (dt, J = 18, 4 Hz), 123.0 (d, J = 36 Hz), 119.3 (t, J = 17 Hz), 116.1 (dd, J = 209, 10 Hz), 64.2, 45.63, 45.61, 22.7, 22.5, 20.0 ppm.

IR (NaCl) 3326, 2970, 2873, 1700, 1654, 1596, 1481, 1279, 1214, 1150, 1114, 1005, 988 cm^{-1}.

EIMS (*m*/*z*, relative intensity) 395 (M$^+$, 6), 380 (28), 295 (65), 86 (100).

1,2,3,4,5-Pentafluorobenzene (**4.56**)

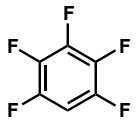

This compound was prepared according to General Procedure 7. Reaction with 1,2,3,4,5,6-hexafluorobenzene (500 μmol). Title compound **4.56** was formed in 85% yield (average of two experiments) as determined via ^{19}F NMR spectroscopy with the aid of a calibrated internal standard. This compound is known.[39]

^{19}F NMR (564 MHz, $CDCl_3$) δ –139.6 (quin, J = 11 Hz, 2F), –155.1 (t, J = 20 Hz, 1F), –163.2 (m, 2H) ppm.

EIMS (*m*/*z*, relative intensity) 168 (M^+, 13), 154 (14), 114 (63), 86 (100).

HREIMS [M^+] Found 168.0002. C_6HF_5 requires 167.9998.

1,2,4,5-Tetrafluoro-3-(trifluoromethyl)benzene (**4.57**)

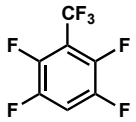

This compound was prepared according to General Procedure 7. Reaction with 1,2,3,4,5-pentafluoro-6-(trifluoromethyl)benzene (500 μmol). Title compound **4.57** was formed in 65% yield (average of two experiments) as determined via ^{19}F NMR spectroscopy with the aid of a calibrated internal standard. This compound is known.[38]

^{19}F NMR (564 MHz, $CDCl_3$) δ –57.0 (t, J = 23 Hz, 3F), –137.5 (m, 2H), –141.8 (m, 2H) ppm.

EIMS (*m*/*z*, relative intensity) 218 (M^+, 14), 189 (14), 114 (54), 86 (100).

HREIMS [M^+] Found, 217.9969. C_7HF_7 requires 217.9966.

1-(2,3,5,6-Tetrafluorophenyl)ethenone (**4.58**)

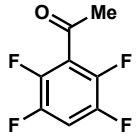

This compound was prepared according to General Procedure 7. Reaction with 1-(pentafluorophenyl)ethanone (500 μmol. Title compound **4.58** was formed in 60% yield

(average of two experiments) as determined via ^{19}F NMR spectroscopy with the aid of a calibrated internal standard. This compound is known.[38]

^{19}F NMR (564 MHz, $CDCl_3$) δ –138.8 (quin, J = 10 Hz, 2F), –143.2 (m, 2F) ppm.

EIMS (*m*/*z*, relative intensity) 192 (M^+, 41), 177 (100), 149 (59), 99 (43), 43 (86).

HREIMS [M^+] Found 192.0194. $C_8H_4F_4O$ requires 192.0198.

Methyl 2,3,5,6-tetrafluorobenzoate (**4.59**)

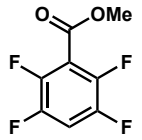

This compound was prepared according to General Procedure 7. Reaction with methyl 2,3,4,5,6-pentafluorobenzoate (500 μmol). Title compound **4.59** was formed in 83% yield (average of two experiments) as determined via ^{19}F NMR spectroscopy with the aid of a calibrated internal standard. This compound is known.[38]

^{19}F NMR (564 MHz, $CDCl_3$) δ –138.7 (m, 2F), –140.9 (m, 2F) ppm.

EIMS (*m*/*z*, relative intensity) 208 (M^+, 24), 177 (100), 149 (54), 99 (32).

HREIMS [M^+] Found 208.0142. $C_8H_4F_4O_2$ requires 208.0147.

2,3,5,6-Tetrafluoro-*N*-methylbenzamide (**4.60**)

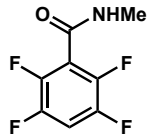

This compound was prepared according to General Procedure 7. Reaction with 2,3,4,5,6-pentafluoro-*N*-methoxy-*N*-methylbenzamide (500 μmol). *Title compound* **4.60** was formed in 27% yield (average of two experiments) as determined via ^{19}F NMR spectroscopy with the aid of a calibrated internal standard.

^{19}F NMR (564 MHz, $CDCl_3$) δ –139.2 (quin, J = 10 Hz, 2F), –143.2 (m, 2F) ppm.

EIMS (*m*/*z*, relative intensity) 207 (M^+, 32), 188 (46), 177 (100), 149 (65), 99 (46), 58 (35).

HREIMS [M^+] Found 207.0301. $C_8H_5F_4N_1O_1$ requires 207.0307.

Phenyl 2,3,5,6-tetrafluorobenzoate (**4.61**)

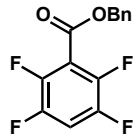

This compound was prepared according to General Procedure 7. Reaction with phenyl 2,3,4,5,6-pentafluorobenzoate (500 μmol). The ensuing residue obtained from the reaction mixture was subjected to flash column chromatography (silica gel, 0–10% EtOAc/hexane elution) to provide the previously unreported compound (70 mg, 49% yield) as a colourless solid.

^{1}H NMR (600 MHz, $CDCl_3$) δ 7.47 (m, 2H), 7.44–7.37 (complex m, 3H), 7.22 (quin, J = 8.3 Hz, 1H), 5.45 (s, 2H) ppm.

^{19}F NMR (564 MHz, $CDCl_3$) δ –137.4 (m, 2F), –139.2 (m, 2F) ppm.

^{13}C NMR (150 MHz, $CDCl_3$) δ 159.5, 145.8 (d, J = 250 Hz), 144.6 (d, J = 257 Hz), 134.6, 128.72, 128.70, 128.4, 113.6 (t, J = 16 Hz), 108.8 (t, J = 22 Hz), 68.4 ppm.

IR (NaCl) 1739, 1501, 1456, 1391, 1297, 1192, 951 cm^{-1}.

EIMS (*m*/*z*, relative intensity) 284 (M^+, 30), 177 (40), 149 (13), 91 (100).

(Pentafluorophenyl)methyl 2,3,5,6-tetrafluorobenzoate (**4.62**)

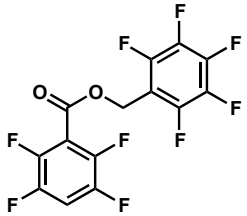

This compound was prepared according to General Procedure 7. Reaction with (pentafluorophenyl)methyl 2,3,4,5,6-pentafluorobenzoate (500 μmol). *Title compound* **4.62** was formed in 35% yield (average of two experiments) as determined via ^{19}F NMR spectroscopy with the aid of a calibrated internal standard. The ensuing residue obtained from the reaction mixture was subjected to flash column chromatography (silica gel, 0–10% EtOAc/ hexane elution) to provide a sample of the previously unreported compound as a colourless oil.

^{1}H NMR (600 MHz, $CDCl_3$) δ 7.16 (quin, J = 8.0 Hz, 1H), 5.43 (s, 2H) ppm.

^{19}F NMR (564 MHz, $CDCl_3$) δ –137.0 (m, 2F), –138.8 (m, 2F), –141.4 (dd, J = 21, 7 Hz, 2F), –151.3 (t, J = 20 Hz, 1F), –161.1 (m, 2F) ppm.

^{13}C NMR (150 MHz, $CDCl_3$) δ 160.0, 145.9 (d, J = 250 Hz), 145.8 (d, J = 252 Hz), 144.5 (dt, J = 258, 4 Hz), 142.3 (d, J = 257 Hz), 137.5 (d, J = 253 Hz), 112.5 (t, J = 16 Hz), 109.3 (t, J = 23 Hz), 108.3 (td, J = 17, 4 Hz), 55.0 ppm.

IR (NaCl) 1748, 1525, 1506, 1313, 1295, 1190, 1133, 1059, 969, 939, 712 cm^{-1}.

EIMS (*m*/z, relative intensity) 374 (M^+, 22), 181 (100), 149 (22), 99 (27).

HREIMS [M^+] Found 374.0000. $C_{14}H_3F_9O_2$ requires 373.9989.

Prop-2-yn-1-yl 2,3,5,6-tetrafluorobenzoate (**4.63**)

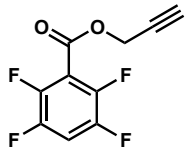

This compound was prepared according to General Procedure 7. Reaction with prop-2-yn-1-yl 2,3,4,5,6-pentafluorobenzoate (500 μmol). *Title compound* **4.63** was formed in 43% yield (average of two experiments) as determined via ^{19}F NMR spectroscopy with the aid of a calibrated internal standard. The ensuing residue obtained from the reaction mixture was subjected to flash column chromatography (silica gel, 0–10% EtOAc/ hexane elution) to provide a sample of the previously unreported compound (+ co-eluting starting material) as a colourless solid.

^{1}H NMR (600 MHz, $CDCl_3$) δ 7.25 (quin, J = 8.0 Hz, 1H), 4.98 (d, J = 2.74, 2H), 2.59 (t, J = 2.5 Hz, 1H) ppm.

^{19}F NMR (564 MHz, $CDCl_3$) δ –137.3 (m, 2F), –138.9 (m, 2F) ppm.

^{13}C NMR (150 MHz, $CDCl_3$) δ 158.9, 145.9 (d, J = 251 Hz), 144.7 (d, J = 259 Hz), 112.7 (t, J = 16 Hz), 109.2 (t, J = 22 Hz), 76.1, 76.0, 53.8 ppm.

EIMS (*m*/z, relative intensity) 232 (M^+, 10), 177 (100), 149 (30), 99 (25).

Furan-2-ylmethyl 2,3,5,6-tetrafluorobenzoate (**4.64**)

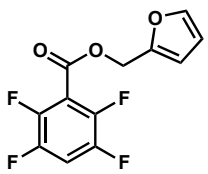

This compound was prepared according to General Procedure 7. Reaction with furan-2-ylmethyl 2,3,4,5,6-pentafluorobenzoate (500 μmol). *Title compound* **4.64** was formed in 48%

yield (average of two experiments) as determined via ^{19}F NMR spectroscopy with the aid of a calibrated internal standard. The ensuing residue obtained from the reaction mixture was subjected to flash column chromatography (silica gel, 0–10% EtOAc/ hexane elution) to provide a sample of the previously unreported compound (+ co-eluting starting material) as a colourless solid.

^{1}H NMR (600 MHz, $CDCl_3$) δ 7.48 (d, J = 1.8 Hz, 1H), 7.21 (quin, J = 8.1 Hz, 1H), 6.54 (t, J = 2.2 Hz, 1H), 6.42 (dd, J = 3.2, 1.9 Hz, 1H), 5.38 (s, 2H) ppm.

^{19}F NMR (564 MHz, $CDCl_3$) δ –137.4 (m, 2F), –139.2 (m, 2F) ppm.

^{13}C NMR (150 MHz, $CDCl_3$) δ 159.3, 148.2, 145.9 (d, J = 250 Hz), 144.5 (d, J = 260 Hz), 143.8, 113.3 (t, J = 16 Hz), 111.6, 110.7, 108.8 (t, J = 22 Hz), 59.9 ppm.

EIMS (m/z, relative intensity) 274 (M^+, 20), 177 (15), 81 (100).

_N_-Methyl-_N_-(2,3,5,6-tetrafluorophenyl)acetamide (4.65)

& _N_-(4-(1-(Diisopropylamino)ethyl)-2,3,5,6-tetrafluorophenyl)-_N_-methylacetamide (_p_-4.65*) & _N_-(2-(1-(Diisopropylamino)ethyl)-3,4,5,6-tetrafluorophenyl)-_N_-methylacetamide (_o_-4.65*)

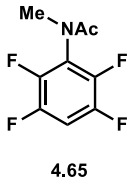

4.65

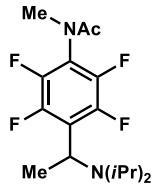

p-4.65*

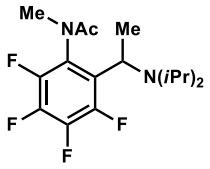

o-4.65*

This compound was prepared according to General Procedure 7. Reaction with *N*-methyl-*N*-(pentafluorophenyl)acetamide (500 μmol). The ensuing residue obtained from the reaction mixture was subjected to flash column chromatography (silica gel, 0–20% EtOAc/hexane elution; 1% NEt_3 was present in the eluent) to provide hydrodefluorination product **4.65** as a colourless solid (49 mg, 44% yield) and a colourless solid (17 mg, 10% yield; 3.7:1 mixture of ***p*-4.65*** and ***o*-4.65***).

_N_-Methyl-_N_-(2,3,5,6-tetrafluorophenyl)acetamide (4.65)

^{1}H NMR (600 MHz, $CDCl_3$) δ 7.07(quin, J = 8.8 Hz, 0.8H), 6.98 (quin, J = 8.8 Hz, 0.2H), 3.29 (s, 0.5H), 3.16 (s, 2.5H), 2.25 (s, 0.5H), 1.86 (s, 2.5H) ppm; 6 signals observed (rotamers present).

^{19}F NMR (564 MHz, $CDCl_3$) δ –137.3 (quin, J = 10 Hz, 1.7F), –139.0 (quin, J = 10 Hz, 0.3F), –145.5 (m, 0.3F), –146.2 (m, 1.7F) ppm; 4 signals observed (rotamers present).

^{13}C NMR (150 MHz, $CDCl_3$) δ 170.5, 170.1, 146.1 (d, J = 248 Hz), 143.3 (d, J = 250 Hz), 124.0 (t, J = 15 Hz), 106.0 (t, J = 22 Hz), 105.0 (t, J = 22 Hz), 38.4, 35.7, 21.5, 21.1 ppm; 11 signals observed (rotamers present).

HRESIMS $[M + H]^+$ Found 222.0539. $C_9H_8F_4NO$ requires 222.0537.

N*-(4-(1-(Diisopropylamino)ethyl)-2,3,5,6-tetrafluorophenyl)-*N*-methylacetamide** (p*-4.65***) & ***N*-(2-(1-(diisopropylamino)ethyl)-3,4,5,6-tetrafluorophenyl)-*N*-methylacetamide** (***o*-4.65***)

HRESIMS $[M + H]^+$ Found 349.1898. $C_{17}H_{25}F_4N_2O$ requires 349.1898.

1,2,4,5-Tetrafluoro-3-vinylbenzene (**4.66**)

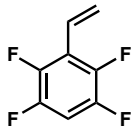

This compound was prepared according to General Procedure 7. Reaction with 1,2,3,4,5-pentafluoro-6-vinylbenzene (500 μmol). *Title compound* **4.66** was formed in 14% yield (average of two experiments) as determined via ^{19}F NMR spectroscopy with the aid of a calibrated internal standard.

^{19}F NMR (564 MHz, $CDCl_3$) δ –141.4 (quin, J = 11 Hz, 2F), –146.2 (m, 2F) ppm.

EIMS (*m*/*z*, relative intensity) 176 (M^+, 3), 132 (14), 90 (100), 43 (19).

HREIMS $[M^+]$ Found 176.0244. $C_8H_4F_4$ requires 176.0249.

4,5,7-Trifluoro-3-(pentafluorophenyl)-2-phenylbenzofuran (**4.67**)

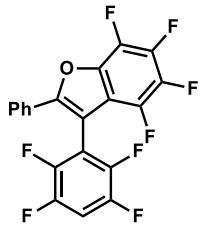

This compound was prepared according to General Procedure 7. Reaction with 4,5,6,7-tetrafluoro-3-(pentafluorophenyl)-2-phenylbenzofuran (100 μmol) (this reaction was performed in a 2:1 MeCN/ DMF solution). *Title compound* **4.67** was formed in 24% yield (average of two experiments) as determined via ^{19}F NMR spectroscopy with the aid of a calibrated internal standard.

^{19}F NMR (564 MHz, $CDCl_3$) δ –137.7 (m, 2F), –138.3 (m, 2F), –152.1 (m, 1F), –159.8 (t, J = 20 Hz, 1F), –161.2 (t, J = 19 Hz, 1F), –162.7 (t, J = 20 Hz, 1F) ppm.

EIMS (*m*/*z*, relative intensity) 414 (M^+, 100), 394 (50), 197 (20).

tert-Butyl (2,3,5,6-tetrafluoro-4-(1-methylpyrrolidin-2-yl)phenyl)carbamate (**4.69**)

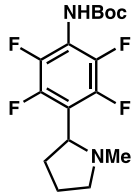

This compound was prepared according to General Procedure 6. Reaction between *tert*-butyl (pentafluorophenyl)carbamate (1 mmol) and *N*-methylpyrrolidine. *Title compound* **4.69** was formed in 31% yield (average of two experiments) as determined via ^{19}F NMR spectroscopy with the aid of a calibrated internal standard. The ensuing residue obtained from the reaction mixture was subjected to flash column chromatography (silica gel, 0–30% EtOAc/ hexane elution; 1% NEt_3 was present in the eluent) to provide a sample of the previously unreported compound as a colourless solid.

^{1}H NMR (600 MHz, $CDCl_3$) δ 6.42 (bs, 1H), 3.66 (dd, J = 9.0, 7.3 Hz, 1H), 3.26 (t, J = 7.6 Hz, 1H), 2.32–2.26 (complex m, 4H), 2.19 (m, 1H), 2.12 (m, 2H), 1.88 (dd, J = 15.7, 9.8 Hz, 1H), 1.52 (s, 9H) ppm.

^{19}F NMR (564 MHz, $CDCl_3$) δ –144.0 (dd, J = 21, 9 Hz, 2F), –147.9 (dd, J = 22, 11 Hz, 2F) ppm.

^{13}C NMR (150 MHz, $CDCl_3$) δ 152.3, 145.5 (d, J = 247 Hz), 142.2 (d, J = 249 Hz), 118.5 (t, J = 14 Hz), 115.8 (t, J = 14 Hz), 82.0, 60.3, 57.3, 40.9, 30.7, 28.1, 23.7 ppm.

IR (NaCl) 3279, 2979, 2734, 1713, 1653, 1520, 1501, 1481, 1368, 1303, 1248, 1159, 974 cm^{-1}.

EIMS (*m*/*z*, relative intensity) 348 (M^+, 15), 291 (8), 247 (7), 57 (100).

***N*-(2,3,5,6-Tetrafluorophenyl)acetamide** (**4.71**)

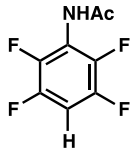

This compound was prepared according to General Procedure 6. Reaction between *N*-(4-bromo-2,3,5,6-tetrafluorophenyl)acetamide (472 μmol) and *i*Pr_2NEt. *Title compound* **4.71** was

formed in 54% yield (average of two experiments) as determined via ^{19}F NMR spectroscopy with the aid of a calibrated internal standard. The ensuing residue obtained from the reaction mixture was subjected to flash column chromatography (silica gel, 0–30% EtOAc/ hexane elution; 1% NEt_3 was present in the eluent) to provide a sample of the previously unreported compound as a colourless solid.

^1H NMR (600 MHz, $CDCl_3$) δ 7.68 (bs, 1H), 7.00 (quin, J = 8.3 Hz, 1H), 2.23 (s, 3H) ppm.

^{19}F NMR (564 MHz, $CDCl_3$) δ –139.2 (s, 2F), –145.5 (s, 2F) ppm.

^{13}C NMR (150 MHz, $CDCl_3$) δ 168.9, 145.9 (d, J = 247 Hz), 142.2 (d, J = 248 Hz), 116.8 (t, J = 13 Hz), 103.9 (t, J = 23 Hz), 22.8 ppm.

EIMS (*m*/*z*, relative intensity) 207 (M^+, 2), 165 (100), 137 (12).

_N_-(4-(1-(Diethylamino)ethyl)-2,3,5,6-tetrafluorophenyl)acetamide (4.34) & _N_-(4-Ethyl-2,3,5,6-tetrafluorophenyl)acetamide (4.73)

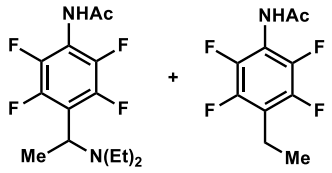

4.34 **4.73**

These compounds were prepared according to General Procedure 6. Reaction between *N*-(pentafluorophenyl)acetamide (500 μmol) and triethylamine. *Title compounds* **4.34** and **4.73** were formed in 15% and 15% yield respectively (average of two experiments) as determined via ^{19}F NMR spectroscopy with the aid of a calibrated internal standard. The ensuing residue obtained from the reaction mixture was subjected to flash column chromatography (silica gel, 0–50% EtOAc/ hexane elution; 1% NEt_3 was present in the eluent) to provide samples of the previously unreported compounds as colourless solids.

_N_-(4-(1-(Diethylamino)ethyl)-2,3,5,6-tetrafluorophenyl)acetamide (4.34)

^1H NMR (600 MHz, $CDCl_3$) δ 7.04 (bs, 1H), 4.47 (bs, 1H), 2.77 (bs, 2H), 2.44 (bs, 2H), 2.27 (s, 3H), 1.59 (bs, 3 H), 1.10 (bs, 6H) ppm.

^{19}F NMR (564 MHz, $CDCl_3$) δ –140.2 (s, 2F), –146.1 (s, 2F) ppm.

^{13}C NMR (150 MHz, $CDCl_3$) δ 168.2, 145.4 (d, J = 246 Hz), 142.3 (d, J = 252 Hz), 118.9, 114.9, 51.4, 43.4, 29.7, 23.0, 17.2, 12.6 ppm.

HRESIMS $[M + H]^+$ Found 307.1424. $C_{14}H_{19}F_4N_2O_1$ requires 307.1428.

***N*-(4-Ethyl-2,3,5,6-tetrafluorophenyl)acetamide** (**4.73**)

^{1}H NMR (600 MHz, $CDCl_3$) δ 7.06 (bs, 1H), 2.77 (q, J = 7.6 Hz, 2H), 2.25 (s, 3H), 1.24 (t, J = 7.6 Hz, 3H) ppm.

^{19}F NMR (564 MHz, $CDCl_3$) δ –146.1 (s, 2F), –147.0 (s, 2F) ppm.

^{13}C NMR (150 MHz, $CDCl_3$) δ 168.5, 144.8 (d, J = 244 Hz), 142.3 (d, J = 247 Hz), 120.5, 113.5, 23.0, 16.3, 13.8 ppm.

HRESIMS $[M + Na]^+$ Found 258.0511. $C_{10}H_9F_4N_1O_1Na_1$ requires 258.0512.

***N*-(4-(1-(Dipropylamino)propyl)-2,3,5,6-tetrafluorophenyl)acetamide** (**4.74**) & ***N*-(2,3,5,6-Tetrafluoro-4-propylphenyl)acetamide** (**4.75**)

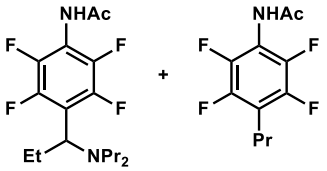

4.74 **4.75**

These compounds were prepared according to General Procedure 6. Reaction between *N*-(pentafluorophenyl)acetamide (500 μmol) and tripropylamine. *Title compounds* **4.74** and **4.75** were formed in 17% and 14% yield respectively (average of two experiments) as determined via ^{19}F NMR spectroscopy with the aid of a calibrated internal standard. The ensuing residue obtained from the reaction mixture was subjected to flash column chromatography (silica gel, 0–50% EtOAc/ hexane elution; 1% NEt_3 was present in the eluent) to provide samples of the previously unreported compounds as colourless solids.

***N*-(4-(1-(Dipropylamino)propyl)-2,3,5,6-tetrafluorophenyl)acetamide** (**4.74**)

^{1}H NMR (600 MHz, $CDCl_3$) δ 6.89 (bs, 1H), 4.06 (t, J = 7.2 Hz, 1H), 2.45 (m, 2H), 2.17 (s, 3H), 2.03 (m, 2H), 1.97 (m, 1H), 1.81 (quin, J = 6.7 Hz, 1H), 1.38 (quin, J = 7.0 Hz, 4H), 0.85 (t, J = 7.4 Hz, 3H), 0.80 (t, J = 7.3 Hz, 6H) ppm.

^{19}F NMR (564 MHz, $CDCl_3$) δ –139.1 (s, 2F), –146.0 (s, 2F) ppm.

^{13}C NMR (150 MHz, $CDCl_3$) δ 168.1, 145.5 (d, J = 245 Hz), 142.2 (d, J = 252 Hz), 117.1, 114.4, 58.5, 51.9, 24.2, 23.1, 21.5, 11.86, 11.78 ppm.

HRESIMS $[M + H]^+$ Found 348.1827. $C_{17}H_{24}F_4N_2O$ requires 348.1825.

***N*-(2,3,5,6-Tetrafluoro-4-propylphenyl)acetamide** (**4.75**)

^{1}H NMR (600 MHz, $CDCl_3$) 6.87 (bs, 1H), 2.62 (t, *J* = 7.6 Hz, 2H), 2.16 (s, 3H), 1.56 (sextet, *J* = 7.5 Hz, 2H), 0.90 (t, *J* = 7.4 Hz, 3H) ppm.

^{19}F NMR (564 MHz, $CDCl_3$) δ –145.1 (s, 2F), –147.0 (s, 2F) ppm.

^{13}C NMR (150 MHz, $CDCl_3$) δ 168.3, 145.0 (d, *J* = 245 Hz), 142.3 (d, *J* = 248 Hz), 119.0, 113.5, 24.6, 23.0, 22.5, 13.6 ppm.

HRESIMS $[M + H]^+$ Found 249.0771. $C_{11}H_{12}F_4NO$ requires 249.0777.

***N*-(4-(1-(Dibutylamino)butyl)-2,3,5,6-tetrafluorophenyl)acetamide** (**4.76**) **&** ***N*-(4-Butyl-2,3,5,6-tetrafluorophenyl)acetamide** (**4.77**)

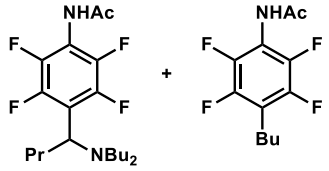

4.76 **4.77**

These compounds were prepared according to General Procedure 6. Reaction between *N*-(pentafluorophenyl)acetamide (500 μmol) and tributylamine. *Title compounds* **4.76** and **4.77** were formed in 29% and 17% yield respectively (average of two experiments) as determined via ^{19}F NMR spectroscopy with the aid of a calibrated internal standard. The ensuing residue obtained from the reaction mixture was subjected to flash column chromatography (silica gel, 0–40% EtOAc/ hexane elution; 1% NEt_3 was present in the eluent) to provide samples of the previously unreported compounds as colourless solids.

***N*-(4-(1-(Dibutylamino)butyl)-2,3,5,6-tetrafluorophenyl)acetamide** (**4.76**)

^{1}H NMR (600 MHz, $CDCl_3$) δ 6.87 (bs, 1H), 4.02 (t, *J* = 7.1 Hz, 1H), 2.44 (m, 2H), 2.19 (s, 3H), 2.00 (m, 2H), 1.87 (m, 1H), 1.76 (m, 1H), 1.33 (complex m, 10H), 0.89 (t, *J* = 7.5 Hz, 3H), 0.83 (t, *J* = 7.3 Hz, 6H) ppm.

^{19}F NMR (564 MHz, $CDCl_3$) δ –139.0 (s, 2F), –145.8 (s, 2F) ppm.

^{13}C NMR (150 MHz, $CDCl_3$) δ 168.2, 145.4 (d, *J* = 244 Hz), 142.3 (d, *J* = 250 Hz), 116.8, 114.2, 58.9, 51.4, 24.4, 23.1, 21.4, 20.3, 11.88, 11.80 ppm.

HRESIMS $[M + H]^+$ Found 390.2301. $C_{20}H_{31}F_4N_2O$ requires 390.2294.

***N*-(4-Butyl-2,3,5,6-tetrafluorophenyl)acetamide** (**4.77**)

^{1}H NMR (600 MHz, $CDCl_3$) 6.94 (bs, 1H), 2.64 (t, J = 7.4 Hz, 2H), 2.14 (s, 3H), 1.78 (quin, J = 6.9 Hz, 2H), 1.48 (sextet, J = 7.6 Hz, 2H), 0.88 (t, J = 7.5 Hz, 3H) ppm.

^{19}F NMR (564 MHz, $CDCl_3$) δ –145.0 (s, 2F), –146.9 (s, 2F) ppm.

^{13}C NMR (150 MHz, $CDCl_3$) δ 168.2, 144.8 (d, J = 242 Hz), 142.5 (d, J = 246 Hz), 118.6, 112.7, 24.6, 23.0, 22.8, 22.6, 13.4 ppm.

HRESIMS $[M + H]^+$ Found 2463.0937. $C_{12}H_{14}F_4NO$ requires 263.0933.

6.4 References

(1) W. C. Still,; M. Kahn; A. Mitra, *J. Org. Chem.* **1978**, *43*, 2923–2925.

(2) G. M. Sheldrick, *Acta. Cryst.* **2015**, *71*, 3–8.

(3) O. V. Dolomanov; L. J. Bourhis; R. J. Gildea; J. A. K. Howard; H. Puschmann, *J. Appl. Cryst.* **2009**, *42*, 339–341.

(4) G. A. Crosby; J. N. Demas, *J. Phys. Chem.* **1971**, *75*, 991–1024.

(5) K. Nakamaru, *Bull. Chem. Soc. Jpn.* **1982**, *55*, 2697–2705.

(6) J. Frey; T. Kraus; V. Heitz; J.-P. Sauvage, *Chem. Eur. J.* **2007**, *13*, 7584–7594.

(7) D. Milstein; J. K. Stille, *J. Am. Chem. Soc.* **1979**, *101*, 4992–4998.

(8) M. Pirtsch; S. Paria; T. Matsuno; H. Isobe; O. Reiser, *Chem. Eur. J.* **2012**, *18*, 7336–7340.

(9) Q. Zhang; J. Chen; Y. Cheng; L. Wang; D. Ma; X. Jing; F. Wang, *J. Mater. Chem.* **2004**, *14*, 895–900.

(10) D. G. Cuttell; S.-M. Kuang; P. E. Fanwick; D. R. McMillin; R. A. Walton, *J. Am. Chem. Soc.* **2002**, *124*, 6–7.

(11) E. Mejía; S.-P. Luo; M. Karnahl; A. Friedrich; S. Tschierlei; A.-E. Surkus; H. Junge; S. Gladiali; S. Lochbrunner; M. Beller, *Chem. Eur. J.* **2013**, *19*, 15972–15978.

(12) H. C. Guo; R. H. Zheng; H. J. Jiang, *Org. Prep. And Proc.* **2012**, *44*, 392–396.

(13) X.-G. Liu; W. Sun, *Eur. J. Inorg. Chem.* **2013**, 4732–4742.

(14) S. H. Shin; N. Y. Sim, Preparation of quinoxaline derivatives for organic electroluminescent devices, *KR 2016117823*, 11 Oct 2016.

(15) P. S. Gribanov; Y. D. Golenko; M. A. Topchiy; L. I. Minaeva; A. F. Asachenko; M. S. Nechaev, *Eur. J. Org. Chem.* **2018**, 120–125.

(16) Y. Zhang; Z. Lu; A. Desai; W. D. Wulff, *Org. Lett.* **2008**, *10*, 5429–5432.

(17) V. Diemer; H. Chaumeil; A. Defoin; A. Fort; A. Boeglin; C. Carré, *Eur. J. Org. Chem.* **2008**, 1767–1776.

(18) A. J. Pallenberg; K. S. Koenig; D. M. Barnhart, *Inorg. Chem.* **1995**, *34*, 2833–2840.

(19) V. Kalsani; M. Schmittel; A. Listorti; G. Accorsi; N. Armaroli, *Inorg. Chem.* **2006**, *45*, 2061–2067.

(20) J. R. Kirchhoff; R. E. Gamache Jr.; M. W. Blaskie; A. A. Del Pagio; R. K. Lengel; D. R. McMillin, *Inorg. Chem.* **1983**, *22*, 2380–2384.

(21) S.-P. Luo; E. Mejía; A. Friedrich; A. Pazidis; H. Junge; A.-E. Surkus; R. Jackstell; S. Denurra; S. Gladiali; S. Lochbrunner; M. Beller, *Angew. Chem., Int. Ed.* **2013**, *52*, 419–423.

(22) D. B. Bagal; G. Kachkovskyi; M. Knorn; T. Rawner; B. M. Bhanage; O. Reiser, *Angew. Chem., Int. Ed.* **2015**, *54*, 6999–7002.

(23) X. Ju; D. Li; W. Li; W. Yu; F. Bian, *Adv. Synth. Catal.* **2012**, *354*, 3561–3567.

(24) J. Tang; G. Grampp; Y. Liu; B.-X. Wang; F.-F. Tao; L.-J. Wang; X.-Z. Liang; H.-Q. Xiao; Y.-M. Shen, *J. Org. Chem.* **2015**, *80*, 2724–2732.

(25) X.-L. Long; J.-D. Guo; T. Lei; B. Chen; C.-H. Tung; L.-Z. Wu, *Org. Lett.* **2018**, *20*, 2916–2920.

(26) D. S. Sharada; A. H. Shinde; S. M. Patel; S. Vidyacharan, *J. Org. Chem.* **2016**, *81*, 6463–6471.

(27) M. Wada; T. Murata; H. Oikawa; H. Oguri, *Org. Biomol. Chem.* **2014**, *12*, 298–306.

(28) Q. Qin; S. Yu, *Org. Lett.* **2015**, *17*, 1894–1897.

(29) B. Xing; C. Ni; J. Hu, *Angew. Chem., Int. Ed.* **2018**, *57*, 9896–9900.

(30) M. Jia; H. Zhang; Y. Lin; D. Chen; Y. Chen; Y. Xia, *Org. Biomol. Chem.* **2018**, *16*, 3615–3624.

(31) M. B. Khaled; R. K. El Mokadem; J. D. Weaver III, *J. Am. Chem. Soc.* **2017**, *139*, 13092–13101.

(32) H.-X. Dai; A. F. Stepan; M. S. Plummer; Y.-H. Zhang; J.-Q. Yu, *J. Am. Chem. Soc.* **2011**, *133*, 7222–7228.

(33) S. Xie; Y. Zhang; O. Ramström; M. Yan. *Chem. Sci.* **2016**, *7*, 713–718.

(34) T. Iwasaki; A. Fukuoka; X. Min; W. Yokoyama; H. Kuniyasu; N. Kambe, *Org. Lett.* **2016**, *18*, 4868–4871.

(35) Y. A. Getmanenko; M. Fonari; C. Risko; B. Sandhu; E. Galán; L. Zhu; P. Tongwa; D. K. Hwang; S. Singh; H. Wang; S. P. Tiwari; Y.-L. Loo; J.-L. Brédas; B. Kippelen; T. Timofeeva; S. R. Marder, *J. Mater. Chem. C* **2013**, *1*, 1467–1481.

(36) M.-O. Simon; S. Darses, *Adv. Synth. Catal.* **2010**, *352*, 305–308.

(37) B. Lu; F. Zhu; H.-M. Sun; Q. Shen, *Org. Lett.* **2017**, *19*, 1132–1135.

(38) N. N. Solodukhin; N. E. Borisova; A. V. Churakov; K. V. Zaitsev, *J. Fluorine Chem.* **2016**, *187*, 15–23.

(39) S. M. Senaweera; A. Singh; J. D. Weaver, *J. Am. Chem. Soc*. **2014**, *136*, 3002–3005.

A.1 X-Ray Crystallographic Information

A.1.1 ORTEP representation of complex 2.1

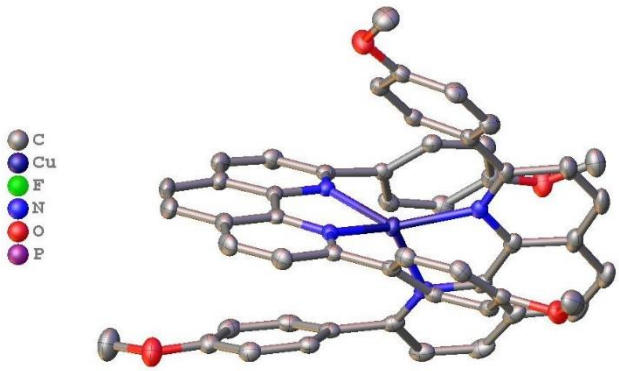

Figure A.1.1: ORTEP representation of complex **2.1**. Thermal ellipsoids are drawn at the 50% probability level. Hexafluorophosphate ions, hydrogens atoms and disorder have been omitted for clarity.

A.1.2 ORTEP representation of complex 2.6

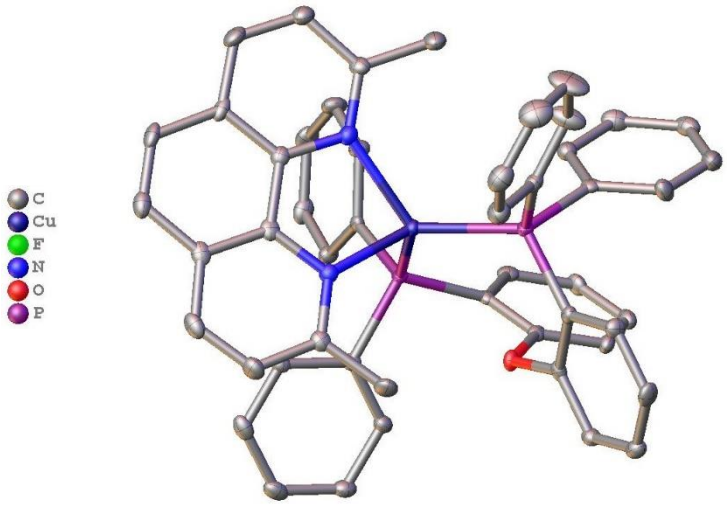

Figure A.1.2: ORTEP representation of complex **2.6**. Thermal ellipsoids are drawn at the 50% probability level. One of two complete CuL_2 residues was chosen to display. Hexafluorophosphate ions, hydrogens atoms and solvent molecules have been omitted for clarity.

A.1.3 ORTEP representation of complex 2.7

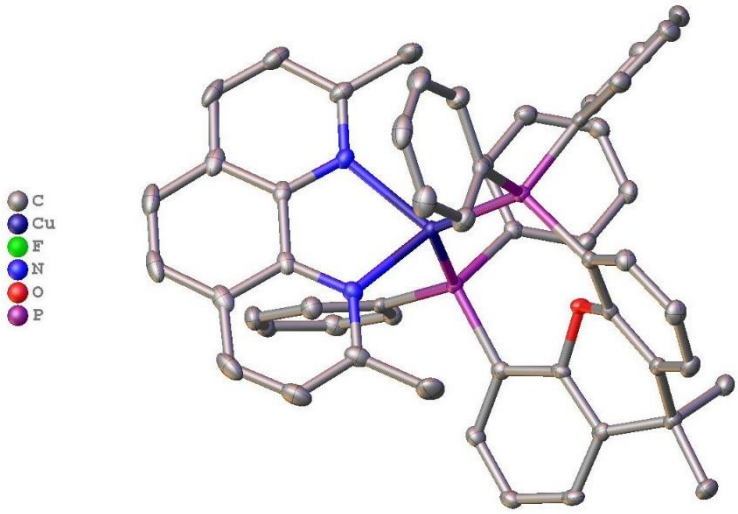

Figure A.1.3: ORTEP representation of complex **2.7**. Thermal ellipsoids are drawn at the 50% probability level. Hexafluorophosphate ions, hydrogens atoms and disorder have been omitted for clarity.

A.1.4 ORTEP representation of complex 2.34

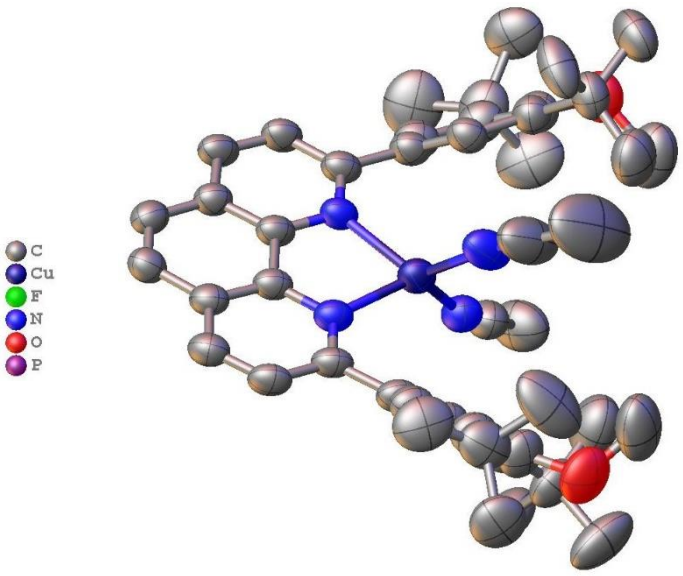

Figure A.1.4: ORTEP representation of complex **2.34**. Thermal ellipsoids are drawn at the 50% probability level. One of three residues containing a complete $CuL(MeCN)_2$ unit was chosen to be displayed. Hexafluorophosphate ions and hydrogens atoms have been omitted for clarity.

A.1.5 ORTEP representation of complex 2.35

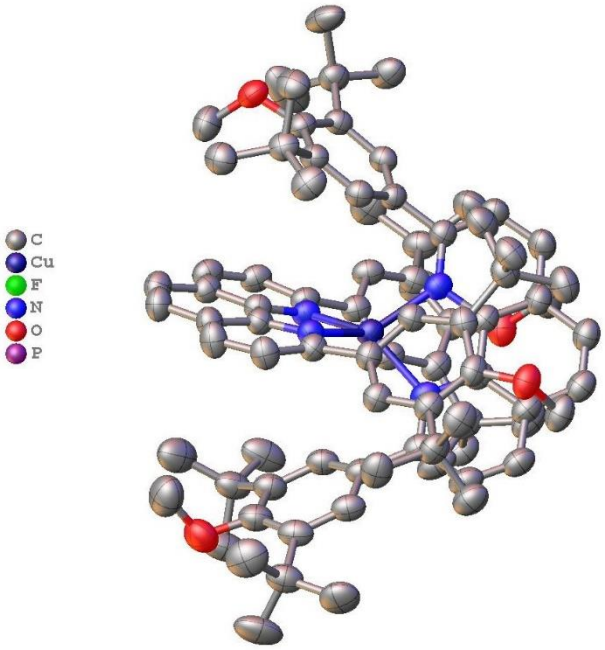

Figure A.1.5: ORTEP representation of complex **2.35**. Thermal ellipsoids are drawn at the 50% probability level. The residue containing a complete CuL_2 unit was chosen to be displayed. Hexafluorophosphate ions, hydrogens atoms, solvent molecules and disorder have been omitted for clarity.

A.1.6 ORTEP representation of complex 2.40

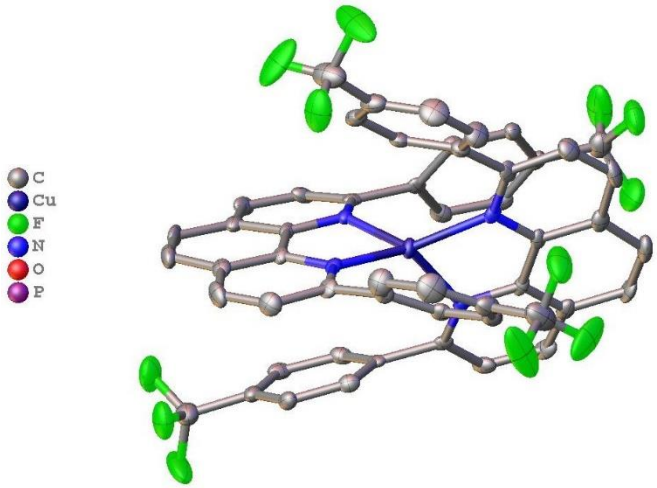

Figure A.1.6: ORTEP representation of complex **2.40**. Thermal ellipsoids are drawn at the 50% probability level. Hexafluorophosphate ions, hydrogens atoms and disorder have been omitted for clarity.

A.1.7 ORTEP representation of complex 2.42

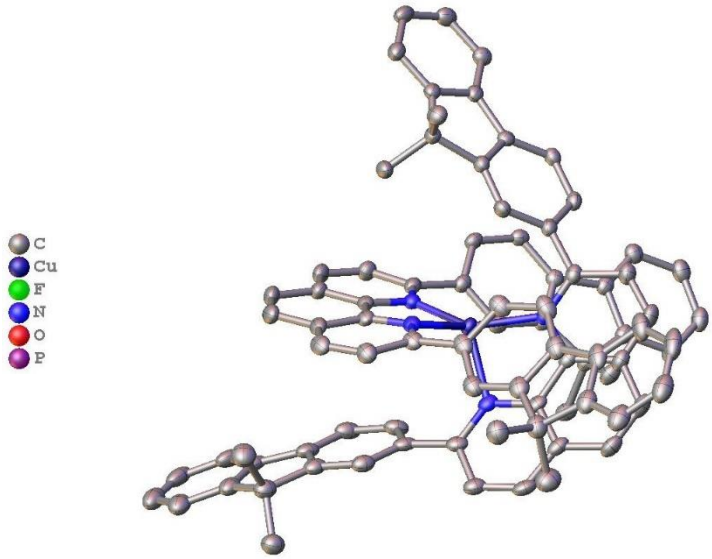

Figure A.1.7: ORTEP representation of complex **2.42**. Thermal ellipsoids are drawn at the 50% probability level. Hexafluorophosphate ions, hydrogens atoms, solvent molecules and disorder have been omitted for clarity.

A.1.8 ORTEP representation of complex 2.49

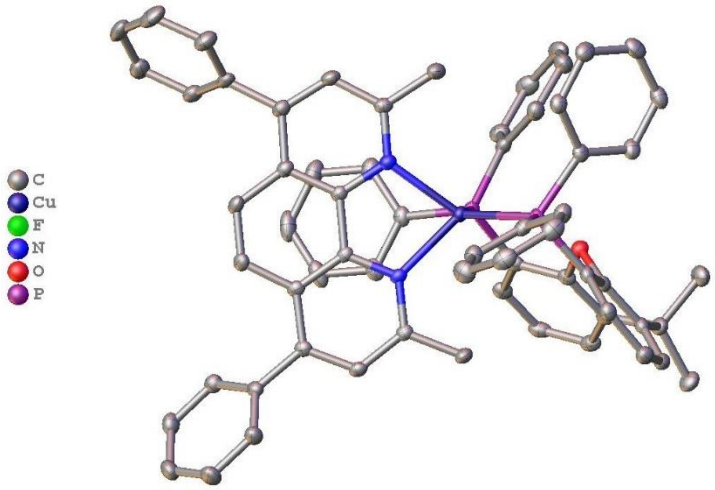

Figure A.1.8: ORTEP representation of complex **2.49**. Thermal ellipsoids are drawn at the 50% probability level. Hexafluorophosphate ions, hydrogens atoms, solvent molecules and disorder have been omitted for clarity.

A.2 Publications

The following list details the publications that have resulted from research performed during the candidature of the Doctor of Philosophy.

Publications Resulting from Research Described in this Thesis:

Peer-Reviewed Journals:

1. A. Olding; **T. P. Nicholls**; A. C. Bissember,
   Recent Applications of [Cu(dap)$_2$]Cl in Visible Light-Mediated Photoredox Catalysis,
   Australian Journal of Chemistry **2018**, *71*, 547–548.

2. **T. P. Nicholls**; J. C. Robertson; M. G. Gardiner; A. C. Bissember,
   Identifying the Potential of Pulsed LED Irradiation in Synthesis: Copper-Photocatalysed C–F Functionalisation,
   Chemical Communications **2018**, *54*, 4589–4592.

3. **T. P. Nicholls**; D. Leonori; A. C. Bissember,
Applications of Visible Light Photoredox Catalysis to the Synthesis of Natural Products and Related Compounds,
Natural Product Reports **2016**, *33*, 1248–1254.

4. **T. P. Nicholls**; G. E. Constable; J. C. Robertson; M. G. Gardiner; A. C. Bissember,
Brønsted Acid Cocatalysis in Copper(I)-Photocatalyzed α-Amino C–H Bond Functionalization,
ACS Catalysis **2016**, *6*, 451–457.

Publications Resulting from Research Not Described in this Thesis:

Peer-Reviewed Journals:

1. **T. P. Nicholls**; L. C. Henderson; A. C. Bissember,
Brønsted Acid-Mediated Radical Processes in Organic Synthesis,
Australian Journal of Chemistry **2015**, *68*, 1791–1795.

Book Chapters:

1. '**Seven-Membered Rings**' A. G. Meyer; J. A. Smith; C. Hyland; C. C. Williams; A. C. Bissember; T. P. Nicholls, In *Progress in Heterocyclic Chemistry, Vol. 28*; G. W. Gribble, J. A. Joule, Eds.; Elsevier: Amsterdam, 2016.

All six articles listed in Appendix A.2 have been removed for copyright or proprietary reasons.